UNIVERSITY OF SURREY LIBRARY

AUTHOR
F.M. TURNER

TITLE
Care of Patients fitted with an External Fixation Device

I agree that the above thesis/dissertation shall be available for reading in accordance with the regulations governing the use of University of Surrey theses.

Author's Signature

USER'S DECLARATION

I undertake not to reproduce any portion of, or to use any information derived from, this thesis without first obtaining the permission, in writing, of the Librarian of the University of Surrey

DATE	SIGNATURE	ADDRESS
6.3.86		

All rights reserved

INFORMATION TO ALL USERS
The quality of this reproduction is dependent upon the quality of the copy submitted.

In the unlikely event that the author did not send a complete manuscript and there are missing pages, these will be noted. Also, if material had to be removed, a note will indicate the deletion.

Published by ProQuest LLC (2017). Copyright of the Dissertation is held by the Author.

All rights reserved.
This work is protected against unauthorized copying under Title 17, United States Code
Microform Edition © ProQuest LLC.

ProQuest LLC.
789 East Eisenhower Parkway
P.O. Box 1346
Ann Arbor, MI 48106 - 1346

UNIVERSITY OF SURREY

REGULATIONS FOR HIGHER DEGREES: COPYRIGHT

Preamble

Dissemination of knowledge is one of the objects of the University. Therefore Members of the University and others who submit theses/dissertations for higher degrees are expected to relinquish to the University certain rights of reproduction and distribution.

Moreover, it is recognised that applicants owe a duty to their Departments of study, the Academic Staff and sponsoring bodies for their respective contributions to the research. Within the limits of these requirements, the author's copyright is safeguarded.

REGULATIONS

1. When submitting a thesis/dissertation for the purposes of a higher degree the applicant shall sign an irrevocable authority in prescribed form appointing the Librarian his attorney with the right to reproduce the thesis/dissertation by photocopy or in microfilm and to distribute copies to those institutions or persons who in the Librarian's opinion require them for academic (as distinct from commercial) purposes.

2. The Librarian in consultation with the appropriate Department of study or sponsoring body shall have the right to refuse to provide copies, or to impose such conditions as he thinks fit on the provision of copies, with the object of safeguarding the applicant's copyright and the interests of the University and the sponsoring body.

3. These Regulations are subject to requirements of any body under whose sponsorship the research project giving rise to the thesis/dissertation is carried on.

1284315 (5918431)

Sc18

CARE OF PATIENTS FITTED WITH AN EXTERNAL FIXATION DEVICE

by

Fiona M. Turner, M.C.S.P., Cert. Ed., Dip. T.P., Dip. Biomech.

A dissertation submitted for the degree of Master of Philosophy at the University of Surrey

1982

5918431

C O N T E N T S

ACKNOWLEDGEMENTS

I should like to express my thanks to C. Wyn-Jones who initiated this project and to Dr. J.G. Wielogorski as my supervisor for his continual support and encouragement throughout this work.

The extensive help given to me by Professor I. Allinson in the theoretical analysis was invaluable and my thanks also to Dr. J. Taylor for his help in some computing and analytical detail.

Considerable assistance was given by Mr. S. McCall in the experimental work and the understanding of strain gauge technology. I should also like to express my thanks to all those who provided technical help in the manufacture of specimens, in particular Mr. Hardicott and to W.W. Howard (Southampton) who donated the Greenheart.

There were many who gave help and advice during this project but in particular I am grateful to Dr. P. Richards, who has provided a continual critique of this report.

Finally, I express my gratitude to the D.H.S.S. for generous financial support, and to my husband for his total support during my trials and tribulations.

SUMMARY

Severe lower limb fractures may be stabilized by an External Fixation Device such as the DENHAM BAR, which is a single-sided Fixator. The feasibility of detecting healing in tibial shaft fractures using this device as a transducer was investigated. The Bar was instrumented with strain gauges and calibrated in two modes to determine its reliability as a transducer. Further experimentation was carried out on a Bone / Fixator configuration to determine the limits of detectable strain in the Bar which results from firstly, a complete break, and secondly, when the bone is fully healed.

The experimental work was fraught with practical difficulties and the results indicated that the bar did not behave as a reliable transducer. This suggested that direct instrumentation of the bar is not a suitable technique for clinical application. A lack of response from the strain gauges was found when the bar was in situ with fully healed bone indicating that the device behaved as a redundant structure at this stage.

The Denham Bar is, however, a clinically popular device but subject to wide variation in its application. Using the device as a basis for a theoretical analysis, strain energy techniques were employed to determine whether intermediary stages of healing could be detected by related changes in the level of strain. The extent of this analysis indicated that as healing bone reaches 10 - 15% of normal strength changes in the level of healing are not detectable by the bar. The motion at the fracture site, that the device permits, was also determined from a further analysis using Beam Deflection techniques. These

results were compared with an analysis of the same configuration using the PRIME STRESS PROGRAM. A number of Fixator and Physiological variables were identified, which were then selected for further analysis by the Prime Stress program to determine their relative importance and contribution to overall stiffness.

From this final investigation the maximum and minimum criteria for stability were established. The analysis included a consideration of healing bone and the changes in fracture site motion which occur as the strength of CALLUS (Healing bone) approaches that of normal bone.

CHAPTER ONE: INTRODUCTION

Traditional methods for assessing the healing following fracture of long bones are based upon radiological and a variety of less easily classified criteria which fall under the somewhat vague title 'clinical'. The most important clinical tests centre around movement (or rather lack of it) in the region of the break point. This is taken as an indication of the strength of 'callus' (the callus being the material which makes the initial union between fractured bone ends). Measurements tend to be qualitative, somewhat subjective and are fraught with problems of interpretation. Thus, for example, pain free motion is unsatisfactory as pain and non-union (non-healing) of broken bones do not always coincide (Matthews et al, 1974).

It is obvious that prognosis and patient care could be considerably improved if an accurate quantitative, mechanically based measure of fracture stability (movement lack) could be found. This was the aim of this project.

The initial research proposal was for the continuation of work on the detection of healing begun at the University of Surrey on a newly designed bilateral "external fixator", the "Sayegh Frame" (Sayegh, 1979). As this frame has not found popular clinical use however, the subsequent proposal submitted by Dr. J. Wielogorski and Mr. C. Wyn-Jones suggested that the work continued using the "Denham Bar", which is clinically popular. This device is a single-sided external fixator which is connected to the antero-medial aspect of the tibia by six or more transfixing pins. It was envisaged that the bar, instrumented with strain gauges, could be used as a transducer

for the detection of motion at the fracture site. As the strength characteristics of regenerating bone change with time, the assumption was that the relative motion of the two fracture ends would also diminish. This would result in a reduction of bar deformation and the levels of strain.

Finding the correct experimental approach posed a number of problems. Initial experiments were planned to find the best instrumentation of the Denham bar for the deformation envisaged. As the availability of fresh cadaveric material was limited, it was decided that a substitute material with consistent physical properties in the range covered by bone, the hardwood "Greenheart" would be used in these pilot experiments. As will be seen in Chapter Four, these experiments showed the bar to be unreliable as a transducer and the deformation initially too small to satisfactorily record changes in the level of strain which would be likely to occur during healing. A subsequent theoretical analysis also revealed that the later stages of healing (i.e. when the callus is approximately 10 - 15% of the strength of normal bone) could not be monitored by an instrumentated bar.

By this stage a considerable portion of the time available for the project had elapsed and the following course of action was decided upon.

Although the Denham Bar is a popular device, considerable variability in its application had been observed, and the time for removal was found to be based upon subjective findings. Within the University of Surrey a computer simulation, the PRIME STRESS PROGRAM, was available, which it was felt could be used for the three-dimensional

analysis of a system (a SPACE FRAME) involving different configurations of bone, transfixing pins and Denham Bar. The application of this program with the input of data on physiological and anatomical variables should give quantitative information about the range of motion that is permitted at the fracture site. The physiological variables included the likely changes in the mechanical properties of callus and the effect upon fracture site motion.

Until now, bio-engineers have followed the sensible, but not proven idea, that "stiffness is best" with little consideration of the changes in physiological demands during healing. It was felt that, with an improved understanding of a fixator, suitably compared with theories of bone healing, the requirements of an ideal fixator could be defined.

CHAPTER TWO

2.A.1 PART A: INTRODUCTION TO ENGINEERING CONCEPTS AND THE PROPERTIES OF MATERIALS RELEVANT TO THIS STUDY

All solids subjected to an externally applied load or force, deform. The deformation which results from a compressive load, applied through the long axis of a body, e.g. a bone, results in a decrease in length and an increase in breadth (Figure 1a,b) Conversely a tensile axial load will elongate the bone and reduce its breadth (Figure 1c).

The ratio of

$$\frac{\text{change in length}}{\text{original length}} = \text{STRAIN}$$

may be expressed as

$$\frac{l}{L} = \text{unit strain} = \varepsilon$$

and $$\varepsilon \times 10^{-6} = \text{micro strain}$$

Strain may be detected by small resistive elements called STRAIN GAUGES. These are bonded to the surface of a body or member and undergo the same deformation as the surface. A change in resistance (R) occurs since

$$R \propto \frac{L}{A}$$ where L = length of wire, A = cross-sectional area

This may be measured by connection to a Wheatstone Bridge. It is the application of this technique which will be presented in the

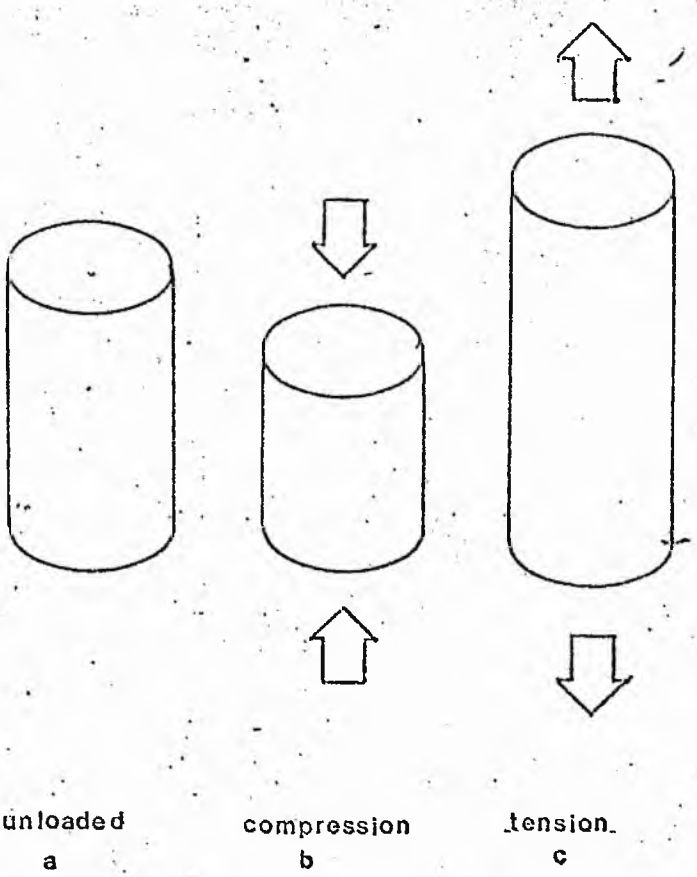

fig.1.

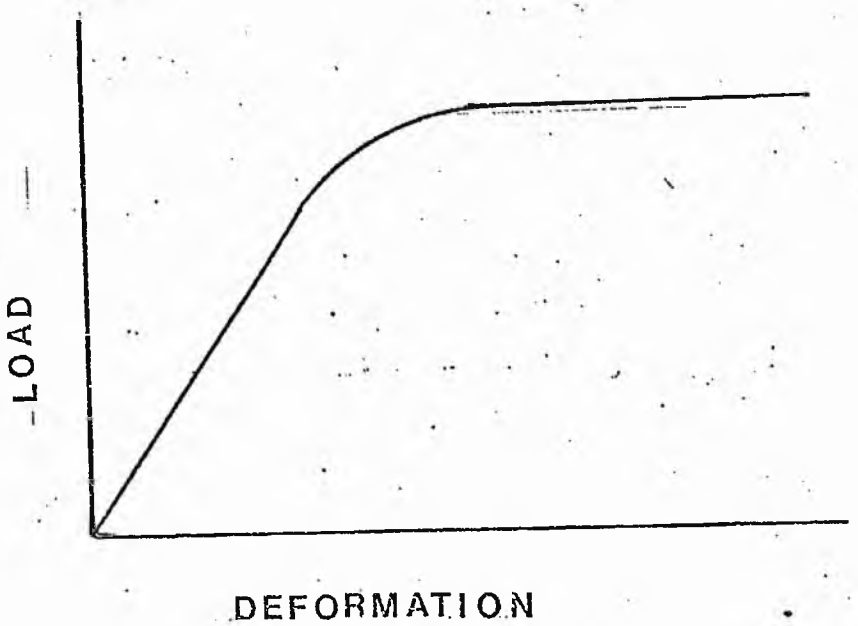

fig.2

experimental work in Chapter Four.

2.A.2 If the deformation of a body is measured and plotted as a LOAD-DEFORMATION curve then certain characteristics emerge. With repeated loading and unloading a linear relationship is observed between load and deformation, and no permanent deformation of the member occurs. (Fig. 2) If the load per unit area is excessive then permanent deformation takes place and failure may occur. The STRESS or load per unit area may then be calculated where

$$\text{STRESS} = \frac{\text{FORCE}}{\text{AREA}} \quad \text{or}$$

$$\sigma = \frac{F}{A} \quad \text{where}$$

F = mass x acceleration due to gravity

= x kg x 9.81 = X Newtons

The ratio of $\frac{\text{STRESS}}{\text{STRAIN}}$ determines the Young's Modulus of Elasticity (E) where

$$E = \frac{\sigma}{\varepsilon}$$

e.g., E for steel 200 GN/M^2, E (Bone) 20 GN/M^2

A member may also be loaded in TORSION where twisting occurs due to the external moment or TORQUE (T) and

T = Force x Perpendicular distance to the line of action of the force.

SHEAR STRAIN (γ) is the angular deformation that results from torsion, e.g. in Figure 3, when line AB twists through γ to AC, RA

rotates through Θ to RC:

therefore $L = R\Theta$

and SHEAR STRAIN (γ) may be expressed as

$$\gamma = \frac{R\Theta}{L}$$

The modulus of elasticity in torsion is known as the MODULUS OF RIGIDITY (G) where

$$G = \frac{\text{SHEAR STRESS}}{\text{SHEAR STRAIN}}$$

SHEAR STRESS is usually expressed as τ but the relationship $\tau = \frac{F}{A}$ is similar to the expression for stress where $\sigma = \frac{F}{A}$.

2.A.3 For any given material (Shigley 1976) the relationship between the modulus of elasticity (E) and the modulus of rigidity is established by the formula

$$G = \frac{E}{2(1+\nu)} = \frac{\text{MODULUS OF ELASTICITY}}{2(1 + \text{POISSON'S RATIO})}$$

where $\nu = \frac{\text{lateral strain}}{\text{axial strain}}$

For ISOTROPIC materials, which have the same properties in all directions, the values for E and G are equal in all directions. Bone is however ANISOTROPIC since its properties are not the same in all directions and the stiffness of the material is dependant upon the direction of loading.

Frankel and Burstein (1971) and Burstein and Reilly (1976) demonstrated that human cortical bone is weakest in shear and strongest

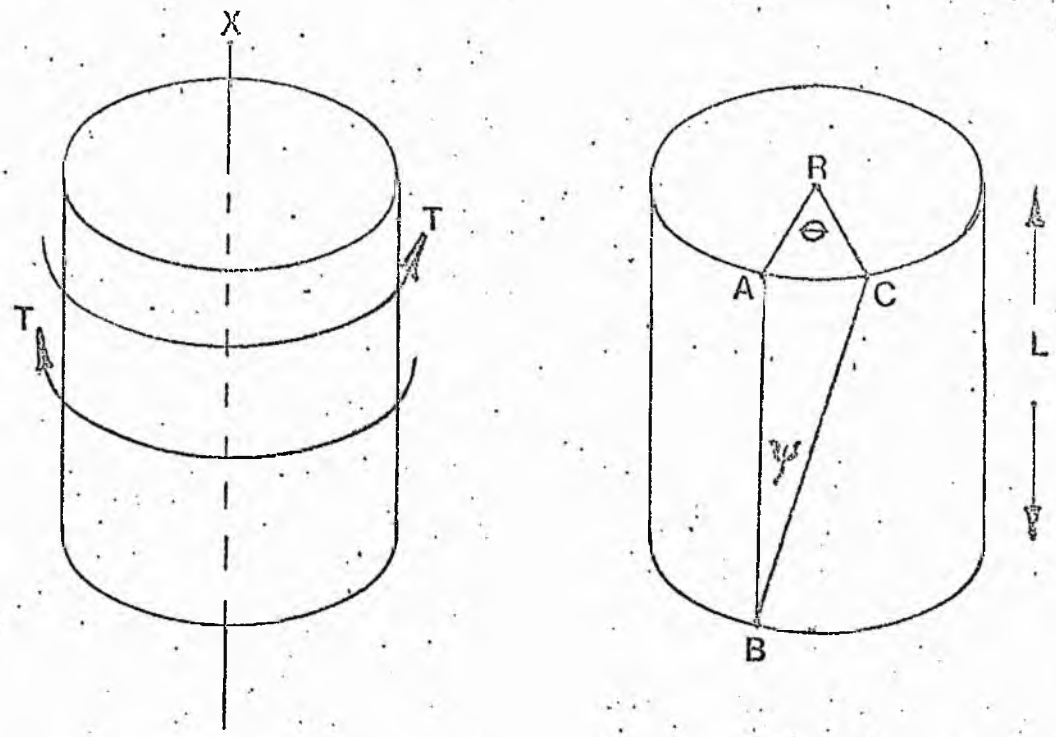

fig.3 Torsion in a solid rod

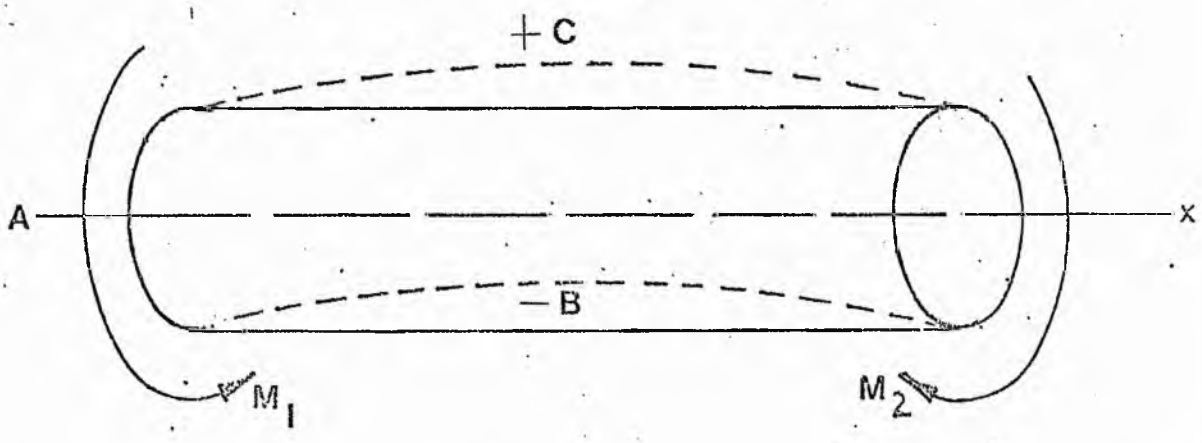

fig 4

Greenheart (Ocotea rodiaei) is a botanical hardwood which is exported principally from British Guiana. It is very heavy and weighs about 72 lbs per cubic foot. The grain is straight, often free from knots but difficult to work since it has a tendency to split. Microscopically it has a diffuse porous structure. The timber is air seasoned, very durable and has been traditionally used for dock and lock gates.

The specimens of timber used in this work were supplied by W.W. Howard, timber merchants, Southampton.

in compression. The following table is a comparison of the values for the elastic moduli of materials used in this work.

TABLE 1

MATERIAL	TYPE	YOUNG MODULUS (E) N/mm^2	MODULUS OF RIGIDITY (G)
Stainless Steel	316,316L	200,000	87,000
Aluminium	-	10,000	3,745
Tibial Cortex	Range of Values (WET - BONE)	18,999 - 28,996	5,500
Greenheart	12% Moisture Content	25,507	12,616
	43% Moisture Content	20,475	11,926
Fibrocartilage	WET (Human Annulus Fibrosis)	72.5	-
Hyaline Cartilage	WET	490	-
Polymethyl Methacrylate	-	2,000	-

Maximum values for the mechanical properties of tibial cortex are found in the 20-29 age group with an average reduction of all properties by 17% in the 70-79 years age group (Yamada 1970).

2.A.4 If a beam is subjected to bending by two equal bending moments (M_1 and M_2) Figure 4, maximal tensile stresses will occur at the convex surface at C and maximal compressive stresses on the concave surface at B.

The magnitude of the stress is proportional to the distance from the NEUTRAL AXIS (AX) which is the axis along which no change in length due to bending occurs. The ability of that member to withstand deformation, i.e. the strength, is however dependant upon additional factors to the elastic moduli (E + G) of the material. The distribution of material away from the neutral axis is known as the SECOND MOMENT OF AREA (I). This concept may be understood by considering bending of a ruler in which two equal bending moments (M_1 and M_2) are applied firstly about the transverse axis z - z (Figure 5a), then secondly about the vertical axis y - y (Figure 5b). The second moment of area is greater in (b) than in (a), and a corresponding increase in resistance to bending will occur in (b). The derived formula for the second moments of area are related to the cross-sectional shape of the structure, i.e. a circle, square etc., and standard formulae used in this work may be found in Appendix 5.2

The equivalent factor in torsion is the POLAR SECOND MOMENT of area (J). For a solid circular member such as the DENHAM Bar the value for J may be derived using the formula

$$J = \frac{\pi D^4}{32}$$

If the TORQUE (T), the radius and the length are known a theoretical value for strain may be determined, then compared with experimental levels of strain where

$$\text{maximum shear stress} = \frac{\text{TORQUE X RADIUS}}{\text{Polar Second Moment of Area}}$$

$$\text{therefore} \quad \tau = \frac{T\,r}{J}$$

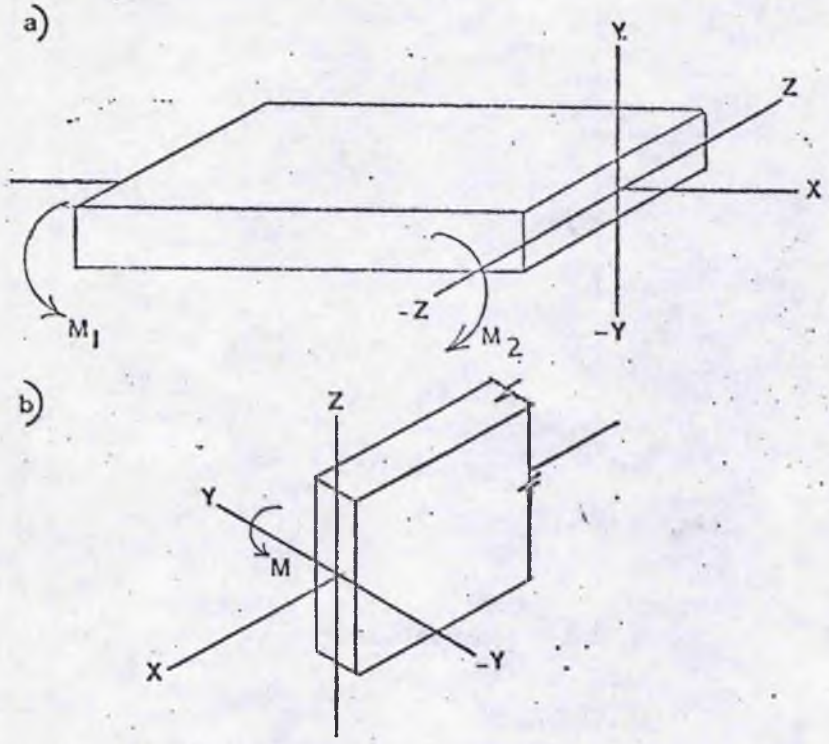

fig 5

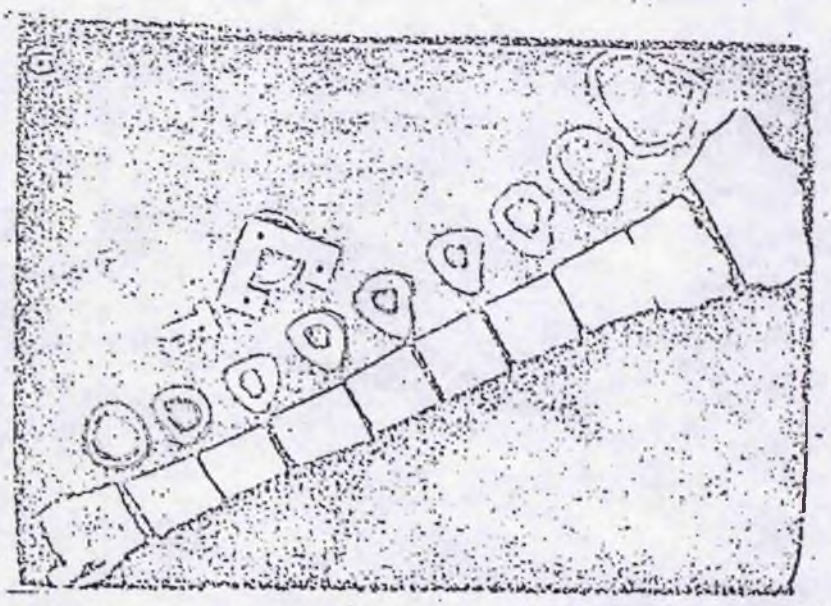

fig. 6 Tibial Cross-sections

From Evans 1951

and $G = \frac{\tau}{\gamma} = \frac{\text{shear stress}}{\text{shear strain}}$

therefore $\gamma = \frac{\tau}{G}$

where G = MODULUS OF RIGIDTY

For theoretical work the values for Second Moment of Area and Polar Moments of Area of uniform cross-sections may be derived using appropriate Standard Formulae (Appendix 1A). The non-uniformity of bone, e.g. Tibia, is however apparent from cross-sections of this bone taken at intervals along its length (Figure 6). As a result standard formulae for area, second moments of area and polar moments of area are not directly applicable. This has inevitably presented some problems in the application of basic engineering theory to the representation of bone dimensions in theoretical work. Cadaveric bone also presents a range of mechanical properties which very according to the moisture content of the bone and other physiological factors particular to the individual from whom the specimen was removed. (Evans and Lebow 1951, Dempster abd Liddicoat 1952, Dempster and Coleman 1960).

In this work a substitute material for bone was used in the experiments which reduced the number of variables and yet maintained a relationship with human tibia.

2.A.5 The use of bone models in experimental and theoretical work

Previous workers have experimented with a variety of substitute materials for bone.

Evans et al (1979) used 45 mm square timber for the analysis of a

single-sided fixator and suggested that comparable results with experiments using bone could be obtained. It was not clear however which type of wood was used, or that the moisture content of the wood at the time of the experiments was established. The elastic moduli of hard-woods such as Oak and Greenheart differ greatly from softwoods such as Pine and a range of 7.5 GN/M^2 is quoted for different types of Pine with 12% moisture content. The moisute content of wood and bone influence the mechanical behaviour of these materials and lower values of the elastic moduli for "wet" bone or wood with 43% moisture content are found (see Table 1).

Kempson (1979) (personal communication) in a comparative study of external fixators, in a fixator / bone configuration, repeated the experiments replacing bone with metal tubing, and found that the stiffest configuration occurred with metal tubing. Karlström & Olerud (1977) in the analysis of a quadrilateral fixator used synthetic bone, but encountered difficulties in the precise measurement of the material properties. It was found that the stiffness characteristics of the synthetic material resembled bone in bending but large differences occurred in torsion. Karlström attributed these differences to the variations in the cross-section between the synthetic bone and the cadaveric material.

Since there was insufficient data from these previous workers to construct a comparative bone model in the author's experimental work, a simple bone model using Greenheart was designed. This hardwood was found to have similar values of Young's Modulus to human tibial cortex. The diemnsions of this model and the data for bone in the theoretical analyses (using the PRIME STRESS PROGRAM) was based upon a consideration of anatomical data and the cortical profiles presented by two groups of

workers (Piezali, Hight and Nagel 1980, and Miller and Purkey 1980). These profiles had been compiled by various computer programs using mathematical techniques of integration with data derived from measurements of tibial cortices. (see Part B).

2.A.6 The Prime Stress Program

Primes' version of STRESS (i.e. STRuctural Engineering System Solver) was obtainable at the University of Surrey for the analysis of framed structures. The program is written in Fortran IV language and computes forces, reactions, moments, three-dimensional displacements, temperature changes and distortions in structures composed of prismatic slender members. The program uses a right-handed orthoganol Cartesian co-ordinate system and suggests the use of S.I. units. The orientation of each member in the structure to be analysed is defined relative to this system but the description of the shape of each member (Member Properties) is defined by the local co-ordinate system. The local x axis of each member is the longitudinal axis of that member (Figure 7) and is independant of the spatial orientation of the member. For further reference material the reader is referred to the Bibliography at the end of this work. The terms used in the Reference Manual (Prime Users Manual 3.2) employ conventional engineering terminology. Some difficulty was however encountered in the interpretation of "Shear Area" AY/AZ with respect to local member properties. The interpretation of the method for determining this data will be described more fully in Chapter Five which discusses the work carried out with the Prime Stress Program.

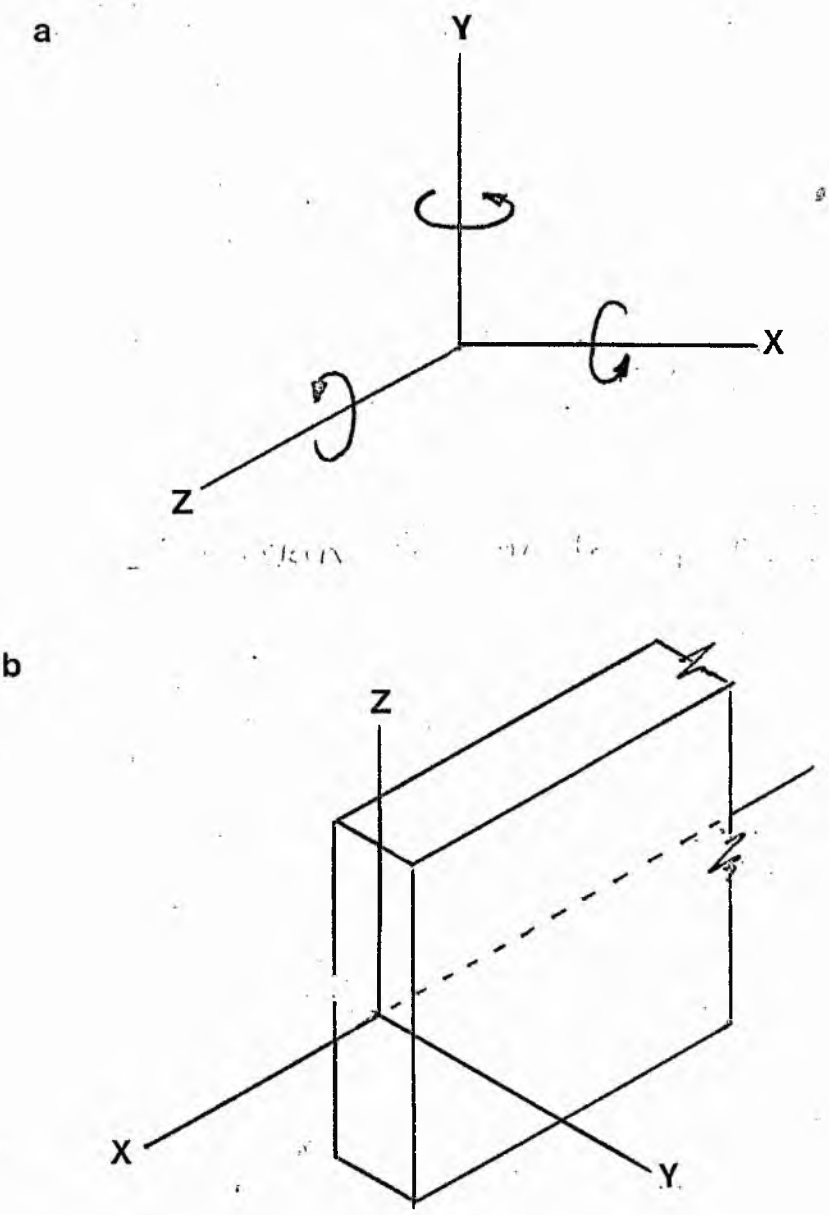

fig 7 a) Cartesian co-ordinate system

b) Local member co-ordinates

PART B: THE TIBIA AND FIBULA

2.B.1 Shape and dimensions of the bone

The tibia consists of an assymetrical shaft and an expanded proximal end formed by the medial and lateral condyles articulating with the femur. The proximal end slopes slightly downwards from the anterior midline to the protuberance of the tibial tubercle (Figure 8). The bone is generally triangular in cross-section (see Figure 6 Part A) tapering distally with subsequent developmental external rotation of 20 degrees (Lanyon and Bourn 1979).

Cortical profiles demonstrating the change in area and second moments of area along the bone length, have been presented by two independant groups of workers in 1980, Piezali et al and Miller and Purkey. Piezali's work was based upon the program developed by Thomson in 1971 and Miller and Purkey compiled comparable cortical profiles from a computer program (SCADS) by Piotrowski and Kellman (1973, 1978). Piezali et al derived data for Thomson's program by selecting co-ordinates at 1" intervals of the bone length from only two pairs of bones. Miller and Purkey however, obtained similar profiles from 9 pairs of bone but excluded the proximal and distal 20% of the bone length in their calculations. From their work Miller and Purkey found that significant differences occurred in pairs of bones from different individuals, but the profiles of geometric distribution were none-the-less comparable. They isolated such characteristics as height, weight and sex of the individual as more important in determining these geometric differences than the overall length of the bone. They did however find that there was no significant right-left bias, thus negating any notion that pedal dominance contributes to bone size.

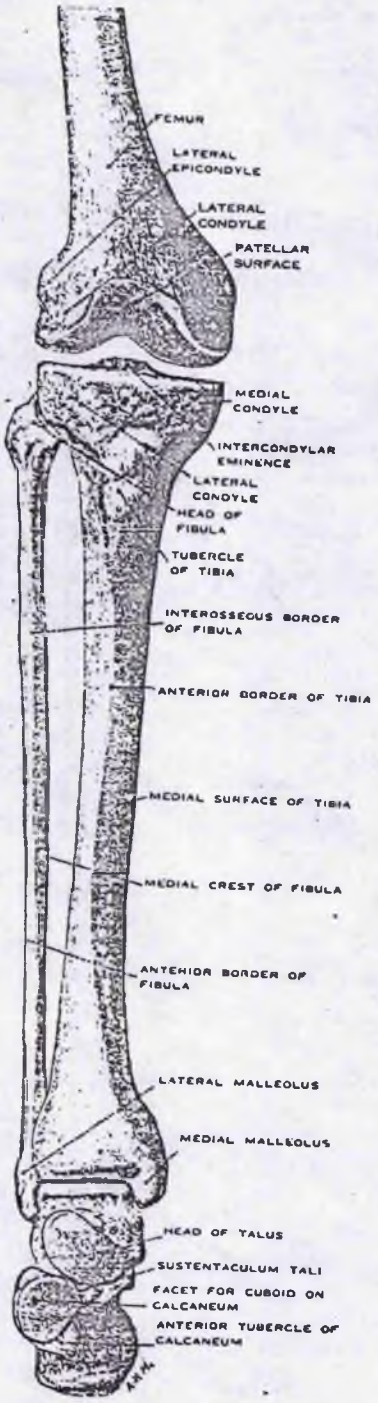

fig.8 The Tibia & Fibula (right leg)

Reproduced from Surface & Radiological Anatomy (1976)

The findings of Miller and Purkey also demonstrated that the outward appearance of bone does not mirror the thickness of the cortex. This is evident, for example, in the proximal expanded section of the tibia in the region of the tibial plateau (Figure 9). It was demonstrated by both teams that gross cortical area and the values for Polar moments of area (J) are variable along the length of bone (Figure 10). Miller and Purkey however suggested that the values for polar moments of area, derived from standard formulae for circular tubes, are exaggerated. They felt that more realistic profiles could be obtained using the "Membrane Analogy", a technique for the analysis of non-uniform members, (Den Hartog 1953). The effective "J" value was therefore calculated (Figure 11) and these values are used in this work as the data source for the polar moments of area (J) in the analysis by the Prime Stress Program (Chapter Five). Miller and Purkey also point out that the minimum value for I (second moments of area) and J is found at approximately 70% of the bone length (Figure 12) which they relate to the earlier findings of Frankel and Burstein in 1965 that torsional fractures are most likely to occur at this level. The application of the dimensional data to my own work, presented by these two groups, Piezali et al and Miller and Purkey (op. cit.), is described more fully in the experimental work in Chapter Four, and the analytical work in Chapter Five.

Anthropometric data (Davis 1979, personal communication) compared favourably with measurements of tibial length taken by the author in which an average length of 42 cm was found. This was obtained by measuring the distance between the medial tibial condyle and the horizontal line at the level of the ankle joint. In this work the location of any landmarks, e.g. fracture site, were expressed in millimetres from the proximal end of the bone, but represented a percentage of bone length.

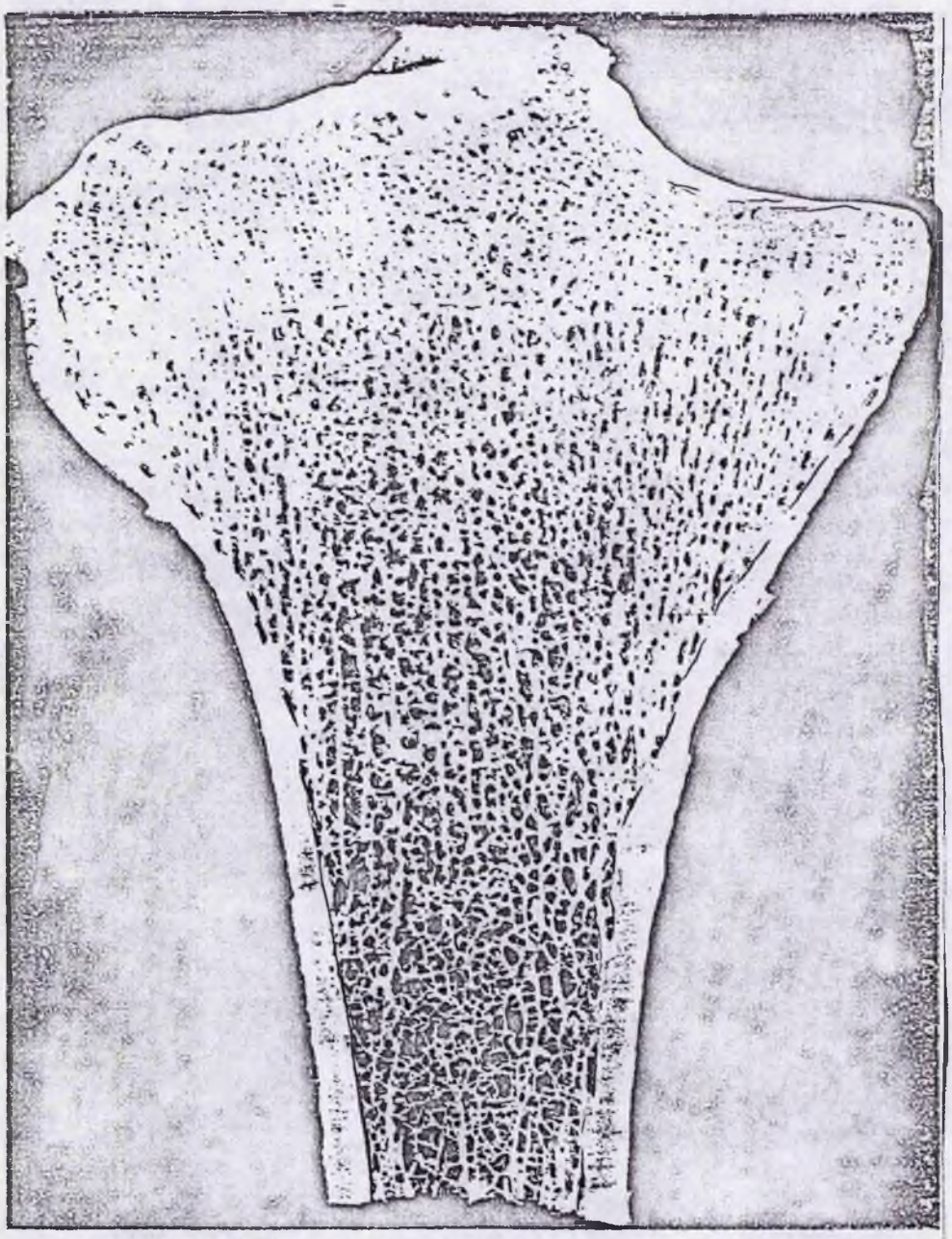

Fig. 1. Midfrontal section of the normal proximal tibia. Knee joint obtained from a 22-year-old male autopsy specimen with no previous history of joint disease.

fig 9

Reproduced from Hayes et al 1978

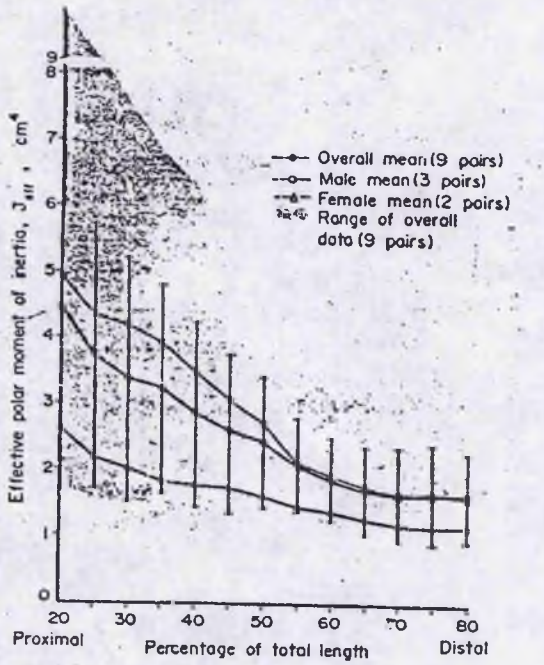

Fig. 10. Effective polar moment, J_{eff}, vs percentage of bone length measuring from proximal (20%) to distal (80%). Error bars represent ± 1 S.D. from overall mean (9 pairs).

fig11 from (Miller & Purkey 1980)

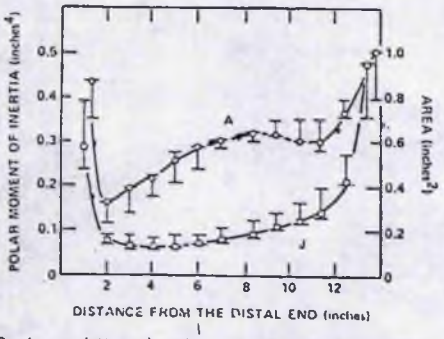

Fig. 3. Areas (A) and polar moments of inertia (J) along the tibial axis.

fig10 from (Piezali et al 1980)

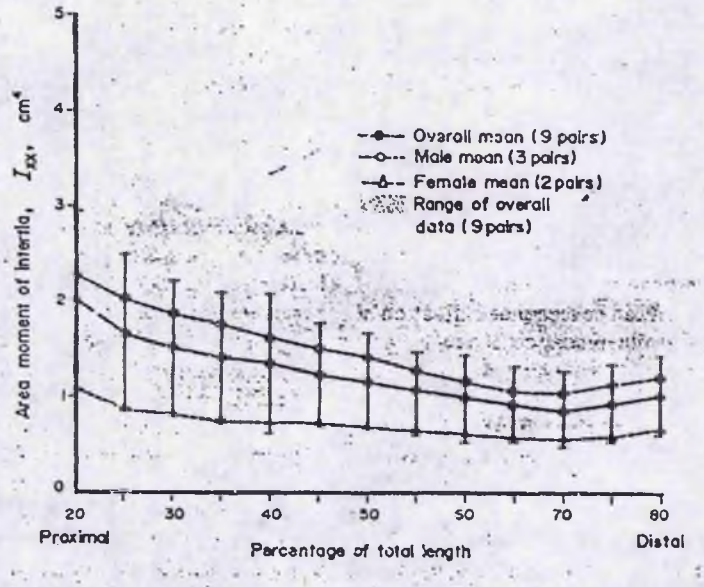

Area moment of inertia, I_{xx} vs percentage of bone length measuring from proximal (20%) to distal (80%). Error bars represent ± 1 S.D. from overall mean (9 pairs).

Fig. 12 from **Miller & Purkey 1980)**

2.B.2 The distribution of muscle attachments and forces generated by their activity

The tibia is deficient in muscle attachments over the anterio-medial border and the distal quarter of the bone shaft (Figure 13). The proximal section tends to give attachment to those muscles which act upon the knee and the remaining sections of the shaft give direct attachment to the three muscles which act upon the foot (Flexor Digitorum Longus, Tibialis Anterior and Posterior). The fibula however gives rise to extensive muscular attachment to the remaining muscles which act upon the foot (Figures 13 and 14). From a consideration of the anatomical details alone, a severe unstable fracture of the mid-shaft of the tibia and fibula is more likely to cause extensive muscular dysfunction while similar fractures located more distally are likely to cause ligamentous disruption or damage. Mechanical function of the foot is enhanced by the containment of tendons within the flexor and extensor retinaculae, and it follows that disruption of the retinaculae is likely to hinder full restoration of function. The extent of damage to muscle and soft tissue at the time of fracture should therefore be considered in the rehabilitation of patients.

Normal movement occurs as a result of complimentary agonist and antagonistic muscle action. This synergic activity of muscles acting upon a limb at any given time must therefore be considered before analysing the effects of forces due to individual muscle activity.

The analysis of these forces is based upon four principal criteria (Frankel and Nordin 1980).

1. The identification of structures involved in the production of forces by consideration of the local anatomy.

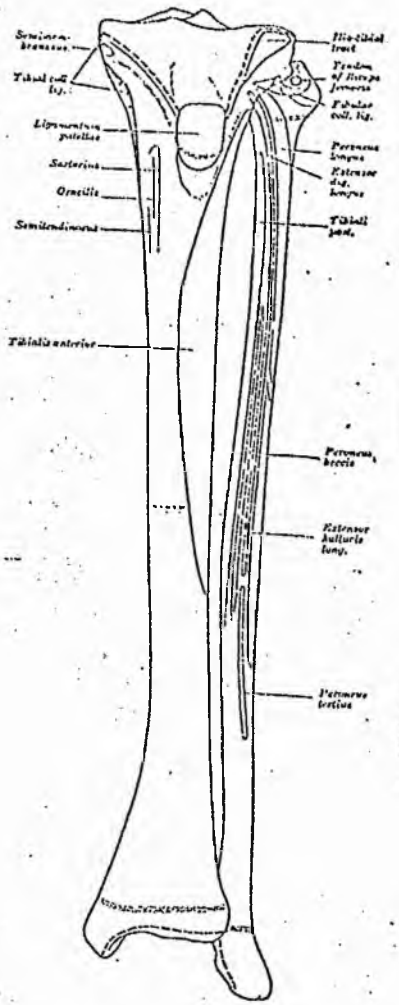

Anterior view (13)

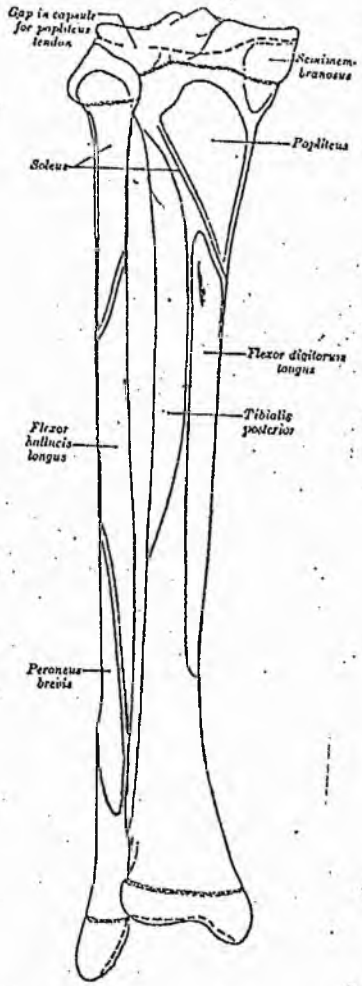

Posterior view (14)

Figures 13,14-The left Tibia and Fibula (from Gray's Anatomy)

2. The angular acceleration of the moving body part which may be measured by light goniometry or photographically and correlated with time.
3. The mass moment of inertia of the moving body part which can be obtained from anthropometric charts (Drillis et al 1964).
4. The torque (T) about the joint where T = force x perpendicular distance from the centre of motion (measured radiographically) and T = mass moment of inertia x angular acceleration. Since T, mass moment of inertia, angular acceleration and the perpendicular distance from the centre of motion can be determined, then the force can be calculated.

Extensive analysis of muscle forces has been carried out (Winter 1980, Nissan 1980, Seireg and Arvikar 1975) and a comparative survey of some theoretical models predicting muscle forces is presented by Patriarco (1981). Seireg and Arvikar's work correlated well with electromyographic studies and a comprehensive analysis of lower limb forces during normal walking is presented e.g. Figure 15. Although considerable work has been undertaken to quantify lower limb joint forces (Rydell 1965, Morrison 1968, 1970 and Paul 1967) there appears to be little experimental evidence which quantifies the load sharing components of bone and muscle during normal activity. Siereg and Arvikar's computation of forces generated by individual muscles of the lower leg is listed below in Table 2. These forces were calculated for 15%, 39% and 53% of the walking cycle corresponding to the flat floor, midstance and push-off phases of walking (Figure 16).

If the direction, magnitude and point of application of the force are known then the effects of that force applied to the tibia may be assessed by vectoral resolution of that force into the vertical and

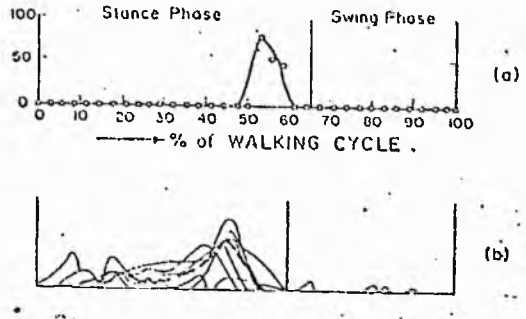

(a) Theoretical results for the tibialis posterior. EMG response from the tibialis posterior during normal level walking.

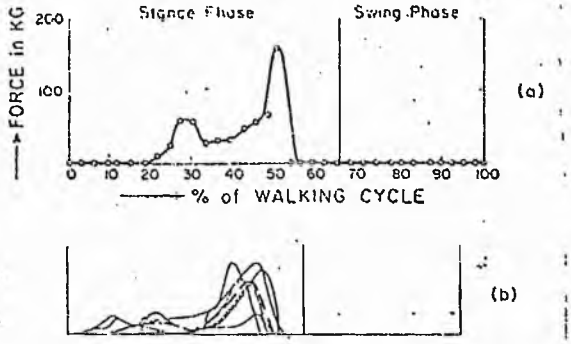

(a) Theoretical result for the flexor digitorum longus. (b) EMG response from the flexor digitorum longus during normal level walking.

fig 15 (Seireg & Arvikar 1975)

Muscular load sharing during walking

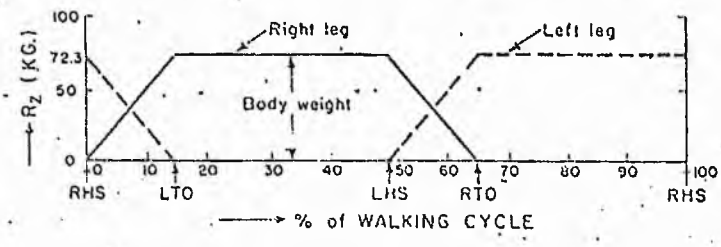

Simplified ground reaction R_z during quasi-static walking. (RHS: right heel strike; LTO: left toe off; LHS: left heel strike; RTO: right toe off.)

fig 16 (from Seireg & Arvikar 1975)

horizontal components (Figure 17). Figure 17 represents a fractured limb with rigid fixation at the knee and an actively contracting gastro-enemious (F), then the horizontal component (H) results in compressive axial loading of the bone and the vertical component (V) will tend to displace the distal fragment vertically so that compression and rotation of the distal section will occur when the calf muscle contracts.

TABLE 2

	Force in Newtons		SEIREG & ARVIKAR
	Percentage of gait cycle		
	15%	39%	53%
Calf	0	1692	26.5
Quadriceps	767	0	0
Hamstrings	1532.3	1147	1048
Tibialis Anterior	484	0	0
Tibialis Posterior	0	0	0
Ext. Dig. Long.	400	0	26.5
Flex. Hall. Long.	0	0	0
Peronei.	0	0	0
Ext. Hall.	0	888	117.7
Flex. Dig. Long.	0	347.3	0

2.B.3 The load bearing axis of the leg and the forces transmitted through the knee and ankle joints during static and dynamic activity.

The tibia is the principal load carrying bone of the lower leg

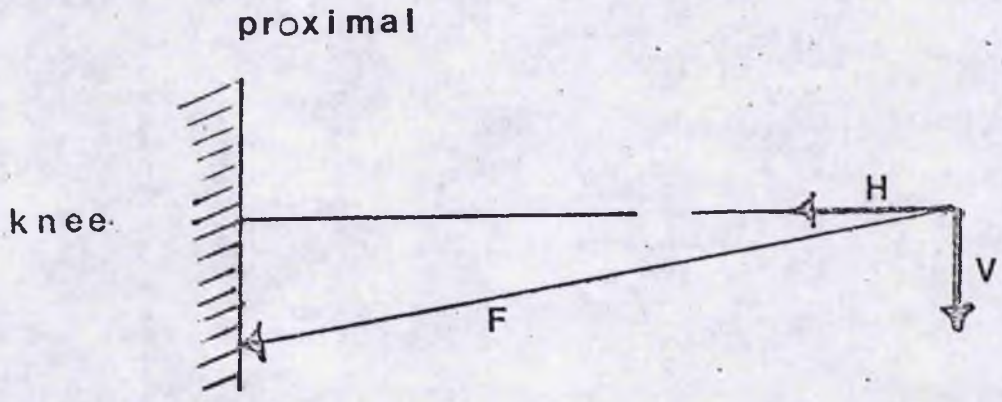

fig 17

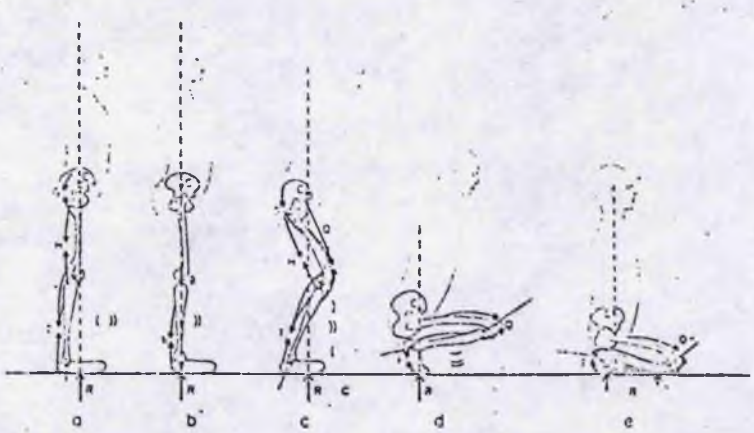

Fig. 1[8]. Selected body positions in the AP (antero-posterior) plane, giving examples of static analyses. a) Military bearing with hyperextended knee joints. b) An approximate axial loading of the lower extremity. c) Standing with flexed knee joints. d) and e) Kneeling positions. T represents the m. triceps surae; s the m. soleus; F the dorsal foot muscles; H the hamstrings muscles; Q the m. quadriceps femoris and G the m. gluteus maximus.

fig 18 (Ljunggren 1980)

although Lambert (1971) suggested that the fibula does take a small component of the load. In the normal erect posture a line from the centre of gravity of the body extends through the anterior portion of the sacral vertebrae, passing 5 cm or less behind the line joining the hip joints (Basmaijan 1967). This line then descends vertically in the midline to a point anterior to the line joining the centre of the knee joints from which it descends in the midline, anterior to the line joining the ankle joint. This assumes a normal erect adult posture although variations do occur (Figure 18). The centre of joint pressure in the knee tends to be located in the medial joint compartment immediately following heel strike (Morrison 1968, Harrington 1976) (Figure 19). Morrison (1968) and Paul (1974) have shown that maximum loading of the knee joint (up to four times body weight) occurs during the stance phase only and that the very small loading during the swing phase is due entirely to gravitational and inertial effects. Morrison (op. cit.) has postulated that loading is lower in the less fit, the aged and pathological states. Harrington (op. cit.) suggests that in certain abnormal gaits (e.g. a Trendelenburg gait), the centre of the joint pressure is transferred from the medial to the lateral knee compartment.

During normal load bearing activity it is doubtful whether direct axial loading of the tibia occurs as synergic muscle activity causes continual anterior-posterior motion and direct axial loading would only be transient. It has been suggested by experimental work with strain gauges bonded directly to the surface of bone that the functionally loaded tibia is continually subjected to bending since tensile and compressive strains have been recorded on opposing surfaces of the bone (Lanyon and Bourn 1979).

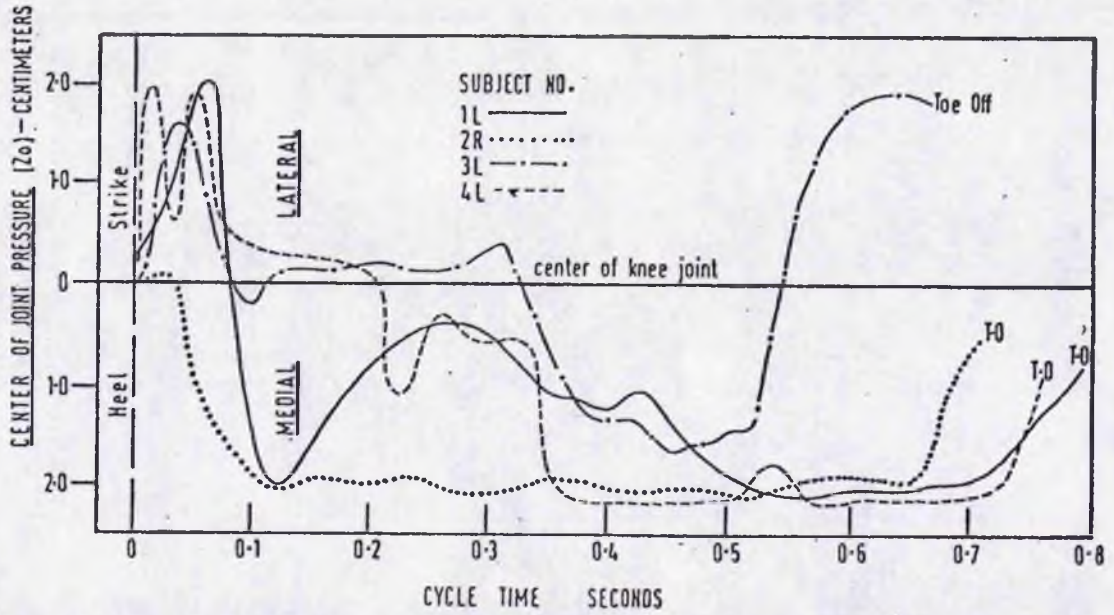

Variation of centre of joint pressure. The centre of joint pressure tends to be located in the medial joint compartment during weight bearing in normal individuals.

fig 19

(reproduced from Harrington 1976)

2.B.4 The distribution of mass in the lower leg and foot

In a biomechanical analysis it is necessary to know the total weight of each limb section involved in the analysis and the point at which the resultant gravitational force is acting upon that limb. The study of body mass is ancient, with investigations recorded as early as 3000 B.C. but Drillis (1964) summarised results from work produced over the past century. Unlike the mechanical properties of bone, the mass of a limb is independent of age or sex (Bernstein 1936) and it is apparent from clinical experience that mass may not necessarily be an indication of muscle bulk or strength. The work of Harless (1860), and Bernstein (Figure 20) suggests that the total weight of the lower leg (shank) and foot is less than half the weight of the thigh. This would however not appear to be true from the work of Fischer (1906), Dempster (1955) and Davis (Figure 21) (personal communication). Drillis suggests that the popular belief that the mass centre of all segments is located at approximately 45% of the total segment length measured from the proximal end, is untrue. He suggests that the mass distribution of the body and the centre of gravity of all segments is related to body build. The anthropometric data used in this work is based upon the standard anthropometry of males with a mean height of 170 cm and a total body mass of 75 kg (Davis 1979 personal communication).

2.B.5 The mechanical properties of the tibial cortex

Whole bone consists of cortical and cancellous bone with a porosity (or bone occupied by non-oseous material) of 5 - 30% for cortical bone and 30 - 90% for cancellous bone (Frankel and Nordin 1980).

TABLE 7. BODY SEGMENT AS PER CENT OF TOTAL BODY MASS (= 100.00)

Segment	Bernstein (Living Subjects)			Fischer
	76 Males	76 Females	Average	3 Male Cadavers
Upper arms	5.31	5.20	5.26	6.72
Forearms	3.64	3.64	3.64	4.56
Hands	1.31	1.10	1.26	1.68
Thighs	24.33	25.78	25.11	23.16
Shanks	9.41	9.68	9.49	10.54
Feet	2.92	2.58	2.75	3.66

TABLE 6. BODY SEGMENT MASS AS PER CENT OF TOTAL MASS (MALES ONLY)

Segment	Investigator			
	Harless	Braune and Fischer	Bernstein	Dempster
Head, neck, and trunk less limbs	53.42	49.68	52.98	56.50
Upper arms	6.48	6.72	5.31	5.30
Forearms	3.62	4.56	3.64	3.10
Hands	1.68	1.68	1.41	1.20
Thighs	22.36	23.16	24.43	19.30
Shanks	8.78	10.54	9.31	9.00
Feet	3.66	3.66	2.92	2.80

fig 20

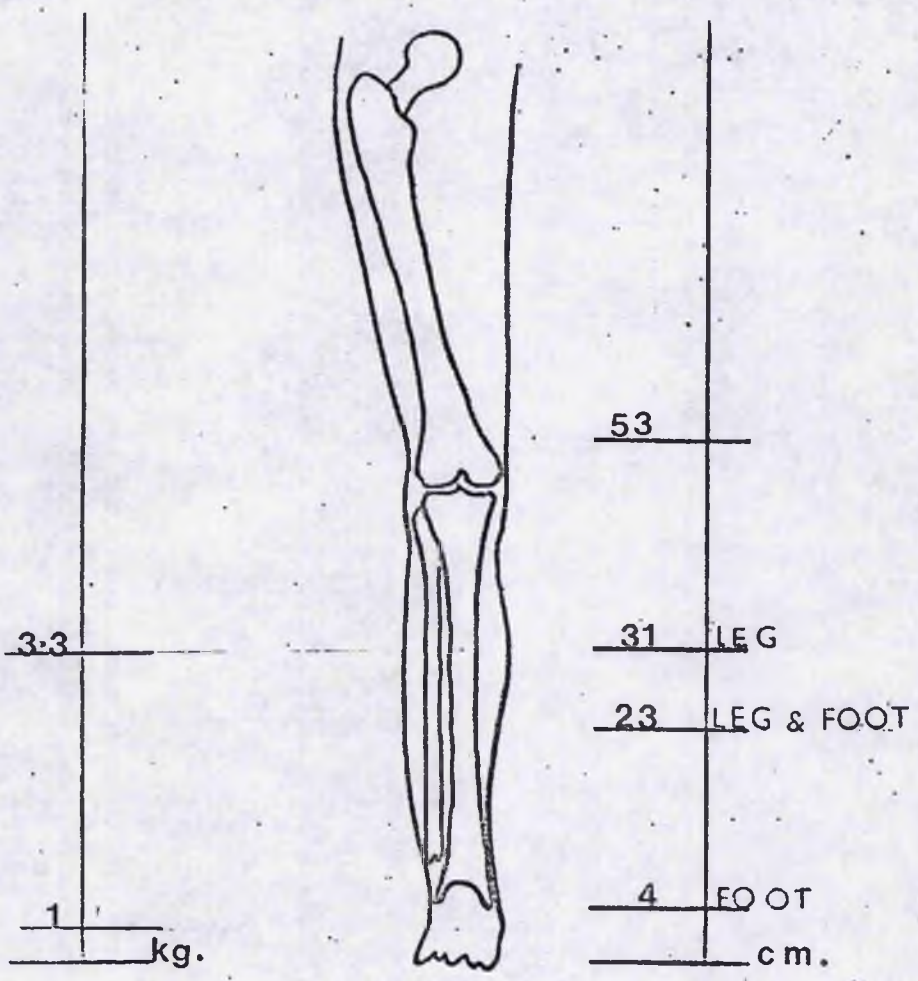

mass of limb parts

height of centre of gravity from the ground

fig 21 Anthropometric data (Davis 1979)

The strength of whole bone largely depends however upon the second moments of area and the elastic moduli of compact bone. Evans (1957) and Yamada (1970) reviewed extensively the mechanical properties of compact bone and Evans defined a number of factors which influence the stress-strain relationship. These were defined as the moisture content, the preservation technique (e.g. chemical treatment or air drying), the shape of the cross-sectional area, the direction of application of force with respect to the long axis of the bone or the collaginous fibres and the age, health, sex and race of the subject, from whom the specimen was obtained. Burstein and Reilly (1976) also suggested that significant differences occur in osteoparotic or cortico-steroid treated individuals.

The range of values for Youngs modulus of human tibia presented by various workers extends from 18 GN/M^2 - 35.3 GN/M^2. Swanson and Freeman (1977) suggest a mean value of 20 GN/M^2 while Yamada (op cit) suggests 18 GN/M^2 for wet tibial cortical bone. Burstein and Reilly (1976) and Yamada also suggest that tibial cortical bone is stiffer than femoral cortical bone. Rauber (1876) first demonstrated the visco-elastic behaviour of bone which is dependent upon the duration of the load applied to the bone. Brief intermittent loading shows rapid and complete recovery of deformation, whereas sustained loading produces two phases of activity in which an initial instantaneous deformation is followed by a gradual time dependent deformation.

The value for torsional rigidity (G) of tibial cortex has not been clearly defined although considerable data has been presented for the ultimate limits of failure in torsion, which Yamada (1970) suggests is five sevenths of the limit for femoral cortex. The tibia, relative

to the femur, appears therefore to be stiffer in bending but weaker in torsion.

2.B.6 Stability of the tibia and fibula

During flexion of the knee the normal range of motion in the anterio - posterior plane is 140°. Rotation of the tibia about the femoral condlyes is complicated by additional transverse and axial rotation. The transverse rotation is maximal at 30° flexion and 0° in full extension with 30° internal rotation and 45° external rotation when the knee is flexed to 90° (Figure 22). At 30° flexion, Piezali Seering et al (1978) suggest that the medial collaterial ligament aids flexion by displacing the medial memcius and reducing the resistance to motion. The results from their work also suggest that the collateral ligaments are more important in the control of transverse tibial motion than previously acknowledged. The traditional view is that bony apposition prevented motion, but they suggest that lateral tibial motion is resisted by the medial collateral and posterior cruciate while medial displacement is resisted by the lateral ligament and the anterior cruciate. Maximal rotation of 11° in the frontal plane during walking has been recorded by Kettelcamp et al (1970). The medial femoral condyle is approximately 17 mm longer than the lateral condyle and normal motion of the tibia about the femoral condyles occurs as a spiralling lateral motion of the tibia about femoral polycentric radii. The knee is therefore additionally stabilized in full extension by this "screw-home" mechanism (Frankel and Nordin 1980).

Stability of the fibula is maintained by the ligaments of the superior and inferior tibio fibular syndesmosis (Johnson et al, Grays Anatomy 1958), the talo-fibular ligaments and the interosseous membrane. The interosseous

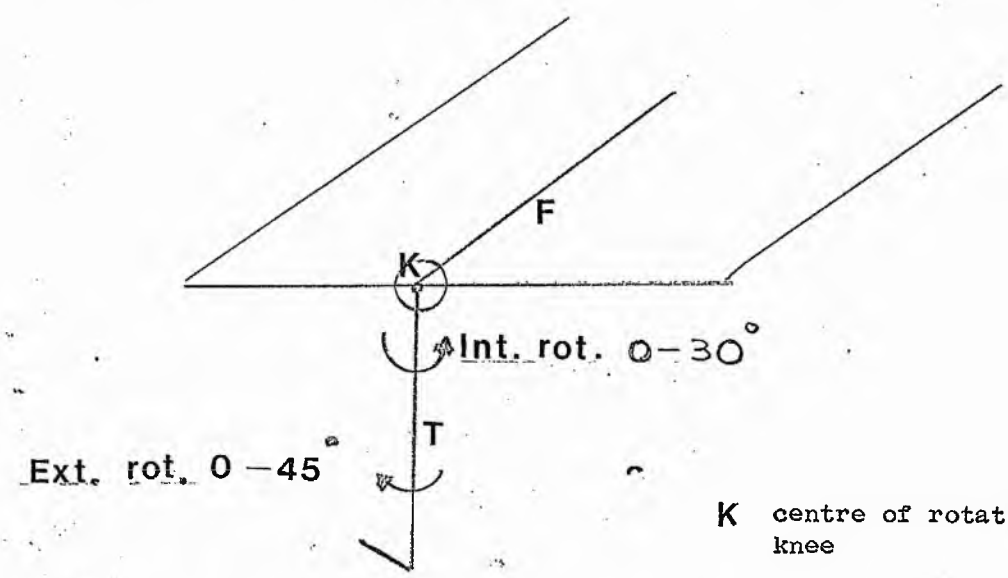

Figure 22: Thigh fully supported knee in 90° flexion.

membrane is tightly attached to the inter osseous border of the tibia and fibula blending with the upper edge of the distal tibio-fibula ligament. It is approximately 75μm thick passing downwards and laterally from proximal to distal at an approximate angle of 20° (Figure 23).

Sarmiento (1974) carried out experimental work to determine the role of an intact interosseous membrane upon fracture site stability and deduced that the membrane, although capable of elongating 120 per cent before failure, had a peak load carrying capacity at 50 per cent elongation. Displacement of the fracture, supported externally with a cast brace and an intact membrane, was minimal, whereas experiments repeated with disruption of the membrane caused extensive displacement at the fracture site. Further work by Sarmiento suggested that fractures of the tibia and fibula at one level were less likely to cause a disruption of the membrane than fractures at differing levels. From a consideration of the cross-section of the tibia, fibula and interosseous membrane (Figure 23) the configuration may be viewed as an I-beam in which maximal strength of the lower limb is gained by the remote distribution of mass away from the central interconnecting member (the interosseous membrane).

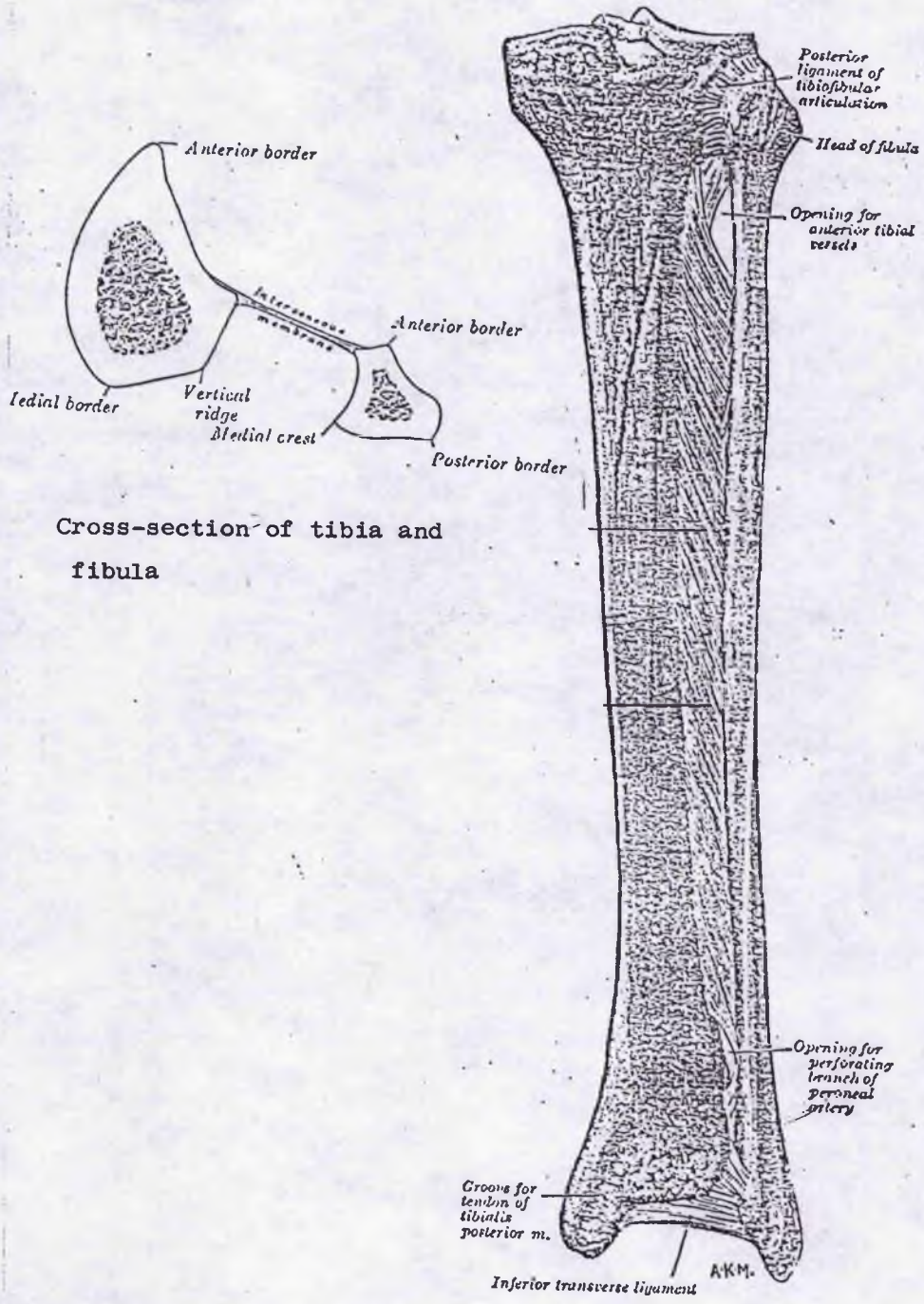

Cross-section of tibia and fibula

fig 23 The right Tibia and Fibula (posterior view)

from Hamilton & Simon (1976)

2.C.1 PART C: THE PROCESS OF FRACTURE HEALING

The traditional view that healing of a fracture occurs in progressive stages of clot formation, inflammatory response and organization of the clot into a fibro-cartiliaginous matrix which is later converted into woven bone, forms the basis for the understanding of fracture repair. The process of healing is however complex and not fully understood. The hypotheses conflict and until such time that these views are firmly contradicted they contribute to the understanding of fracture repair.

In the case of patients fitted with an external fixation device such as the Denham Bar, the rate of fracture repair and the mechanical state of the callus are at present evaluated by radiological and manual tests of stability (see 2.C.5) which give qualitative rather than quantitative information about the strength of healing bone. Clinically the Denham Bar has been found to allow greater motion at the fracture site than other devices which are now used (see Part D, Chapter 2) successfully for the treatment of severe lower limb fractures. Earlier designs, e.g. the Anderson frame and Stader splint were found to give rise to complications, resulting in non-union, and their use is now discontinued. Clearly the management of patients fitted with an external fixation device should be carried out with an understanding of the process of fracture repair and the factors which enhance or restrict the response.

2.C.2 The production of bone, or calcification may occur extra-skeletally e.g., in myositis ossificans, but the repair of bone is thought to be an

extension of the normal ossification processes that occur during development and maturation of the skeleton. Ossification may occur by a single process of INTRAMEMBRANOUS OSSIFICATION or by the two-fold process of INTRAMEMBRANOUS and ENDOCHONDRAL ossification (Williams and Warwick, 1980, Grays Anatomy). Intramembranous ossification occurs with the direct transformation of mesenchymal or primitive cells into bone and generally occurs without the production of any callus (Ketenjian 1978). It has been found that in rigidly immobilized fractures the process of repair is by intramembranous ossification. Endochodral ossification, on the other hand, occurs in fractures which are less rigidly immobilized. In this case bone formation occurs in the epiphyseal growth plates of developing young bones (Bloom and Fawcett, 1975).

The traditional view of fracture repair presented by Weinman and Sicher (1955) suggests six clearly defined stages of healing although in reality these stages may merge.

1. Clotting of the maematoma
2. Organization of the clot
3. The reparative stage with formation of the fibrous collar
4. Formation of primary bone callus
5. Formation of secondary bone callus
6. Functional reconstruction of the bone.

McGibbin (1978) has reviewed concisely the processes that are involved in fracture repair which I feel eliminates conflicting terminology. McGibbin describes four different healing processes:

a) The Primary Callus response
b) External bridging callus
c) Late medullary callus
d) Primary cortical healing.

The healing of a fracture will therefore be described as follows:

A. The initial response to injury

B. The primary callus response

C. The formation of external bridging callus

D. Late medullary callus

E. Primary cortical healing

F. The process of remodelling.

A. The initial response to injury

The initial local response to a fractured bone is a simultaneous activation of localised bleeding and haematoma formation with an associated acute inflammatory response of surrounding soft tissue (Rhine-lander 1974). As a result of the inflammatory response vasodilatation, oedema, exudation of plasma and phagocytic cells occurs, followed by removal of necrotic tissue (Lindholm et al, 1969). Bone deprived of nutrition usually necroses back to the level of viable circulation (Johnson 1980) but resorption may not necessarily occur (Schenk and Willeneger, 1967).

McGibbon (op. cit.) suggests that the first evidence of cell division occurs within eight hours of injury. This is first seen in the periosteum, extends throughout the whole length of bone, but finally localises around the fracture site within a few days. Cellular activity has also been noted in the surrounding soft tissues. Cells in the bone ends at the fracture site have not been found to be activated although Schenk and Willeneger (1967) suggest that osteoclasts may ream out tunnels in dead bone.

B. The primary callus response

The invasion of the clot by fibro-vascular tissue is rapid and begins within the first few hours of injury. Collagen is laid down and the matrix of subsequent woven bone, the PRIMARY CALLUS may be produced in the sub-periosteal space within six days.

Within the inner layer of the periosteum, the CAMBIAL LAYER, and on the free surfaces of the bone (endosteal and periosteal) are spindle-shaped cells similar to fibroblasts. These are the precursor cells of osteoblasts and are known as OSTEOPROGENATOR cells. Primary callus is produced directly from osteoprogenator cells, and the callus may be detected radiologically within two weeks of injury (Johnson, 1980).

This stage appears to be a fundamental response of bone to injury and occurs independantly of environmental factors. The process does not continue indefinitely, and it has been found by Phillips and McKenna (1976) that formation of a firm callus collar is dependant upon the early contact of regenerating callus surfaces. The factors which trigger the activity of the mesenchymal cells are unknown but prostoglandins are amongst the substances implicated (Falkoner et al, 1980).

C. The formation of the external bridging callus

An external bridging callus is formed when fixation of a fracture allows some mobility at the fracture site. The formation of bone is dependent upon an adequate blood supply. If this is insufficient cartilage will tend to form rather than bone, and Brighton and Krebs (1972) found that cartilage tends to predominate in regions of low oxygen

tension. Eventually however the cartilage differentiates into bone from centres of ossification by the process of endochondral ossification. This process is not yet fully understood and a sequential transition from one type of cell to another has not yet been fully demonstrated (Ketenjian, 1978), but Ketenjian localises early callus formation to the mitochondrial granules which increase in this stage. The production of callus in both the Primary callus response and in External bridging callus is temporal. The latter may eventually proceed to fibrous non-union.

D. The formation of late medullary callus

This form of repair would appear to be best suited to conditions of stability rather than mobility. The callus appears as replacement tissue where bone is partially deficient, e.g. pin holes. The term medullary callus is slightly confusing in that medullary callus arises predominantly from the cavity of a long bone but it is the general term for replacement osseous material. The structure of medullary callus is similar to external callus although McGibbon suggests that cartilage formation is less prominent. Unlike external callus however, the differentiating activity of this tissue from cartilage to bone may continue for months. McGibbon again points out that little is known about the factors which stimulate the continuing activity of this tissue.

E. Primary bone healing

In contrast to the previously described types of repair tissue necrotic bone at the fracture site may not always be resorbed (Schenk and Willeneger, 1967). Recanalization of new Haversian systems may occur by osteoclasts reaming out a tunnel in the dead bone with eventual

vascularisation and the subsequent transport of osteoblasts to create new osteons. As the osteoblasts break across the junction between the necrotic bone ends Primary bone union is established. This process is clearly dependent upon firm apposition of the bone surfaces prior to union. McGibbin summarises the characteristics of these four processes in Table 3:-

Type of healing	Speed	Ability to bridge gaps	Tolerance of movement	Tolerance of total rigidity	Importance of external soft tissues
Primary callus response	++++	+	++++	++++	—
External bridging callus	+++	+++	+++	—	++++
Late medullary callus	++	++++ (slow)	++	+++	—
Primary cortical	+	—	—	++++	—

Radiologically, detection of primary bone (cortical) healing is often difficult since there is no visible sign of callus formation (Weisser 1964) and this type of healing is often associated with rigid external fixation.

F. The phase of remodelling

Remodelling and repair is a continual process which becomes disrupted during healing and recommences when firm union of the bone is established. (For further reading refer to the bibliography at the end of this text).

2.C.3 FACTORS WHICH INFLUENCE HEALING

From the brief review of fracture healing presented in the preceding pages it is clear that healing is dependent upon a number of intrinsic and extrinsic factors. These will be discussed in the light of current knowledge.

INTRINSIC FACTORS

1. Vascularity of the fracture bed

The concept that reliable bone healing is dependent upon an intact vascular bed is well established. The work of Trueta in 1968 and Bloom and Fawcett (1975) suggests one possible explanation. Trueta showed that osteoprogenator cells are also derived from the vascular endothelium and Bloom and Fawcett suggest that developing bone matrix tends to orientate equidistantly from the neighbouring vessels in the Primary callus.

There is also evidence that motion at the fracture site enhances bone deposition (e.g., in the production of external bridging callus). It is not clear however whether these beneficial effects are due to the actual motion or to the local increase in circulation due to muscle activity.

2. The role of the periosteum

The periosteum is absent from the articular surface of long bones and in young bones this tissue tends to be thick and vascular. It modifies during life to become much thinner and less vascular. Although the precursor cells to osteoblasts, the osteoprogenator cells have been observed in the innermost layer of the periosteum, the CAMBIAL LAYER, (Young 1962) and their osteogenic potential defined, recent work by Houghton and Rooker (1979) which supports earlier work by Crilly (1972), suggests that division of the periosteum, either total or complete, stimulates longitudinal growth of the bone. Houghton and Rooker accept Crilly's idea that this may have been due to the

mechanical release of the periosteal restraint upon the growth plate. Conversely Mulholland and Pritchard (1959) found that if a segment of bone is removed and the periosteal tube remains, successful regeneration of new bone takes place.

3. A minimal fracture gap

It was shown by Phillips and McKenna in 1976 that rapid involution of the advancing callus collar occurs if firm contact is not established within two weeks from the time of fracture. Hoaglund and States (1967) found from clinical retrospective studies that union was prolonged if less than fifty per cent apposition between the bone ends is maintained and that the shortest healing times occurred in spiral fractures. Although contact and compression between opposing bone surfaces enhance healing it would appear that in the presence of a fracture gap, healing is dependent upon:

(a) The level at which callus is forming, i.e. the distance between two advancing "collars" of callus

(b) the rate of growth of the callus.

4. Mechanical influences and the bioelectric potential of bone

Bioelectric potentials are resting potentials in the millivolt range, not related to movement, muscle activity or stress, and thought to be present in all living tissues (Lake et al, 1978). Hastings (1980) presented the hypothesis that bone belongs to a group of materials which exhibit ferro-electric properties with orientation of dipoles into specific order. (Domains).

These dipoles re-arrange in response to mechanical load with the formation of an electric field. The generation of an electrical charge in response to mechanical loads (the Piezo-electric effect) has been demonstrated by a number of other workers (Fukada and Yasuda, 1957, and Bassett et al, 1971) but there is increasing evidence to suggest that the domain orientation of the dipoles is related to the architecture of the bone.

Bassett, Pawluk and Becker (1964) showed that electro-negativity favours bone formation and Rybicki (1977) demonstrated that the optimal level of mechanical stress produces the highest degree of healing. McGibbon (op.cit) suggests that Wolf's Law which states that "normal bone mass is dependant upon the levels of functional loading" may be explained as a self-regulating feedback mechanism where the stresses and strains in long bones modify the electrical environment of bone cells. Lanyon and Bourn (1979) have shown that opposing surfaces of the tibia are continually under bending during walking and running. These workers recorded compressive and tensile strains on opposing tibial surfaces by the bonding of strain gauges to the surface of human bone. No reference in the literature could be found demonstrating the in-vivo recording of electrical activity in healing bone and there are obvious practical limitations in a human study of this kind.

5. The role of the soft tissues

Lindholm et al in 1979 found that, in response to injury of the bone, an inflammatory response is set up in the surrounding soft tissues. This is also accompanied by an increase in cell division. Ham and Harris (1971) pointed out that injured muscles produce more prostoglandins

than fractured bones and recent work by Dekel et al (1981) have found some evidence to suggest that prostaglandins which are powerful vasodilatators, have a profound effect on bone metabolism. The soft tissue surrounding the fracture may therefore be more important in the production of localised hyperaemia than traditionally thought, which has been suggested by McGibbon.

6. The age of the individual

Developmental ossification of the Tibia is usually complete by the end of the teens, and Hoaglund and States (1967) confirmed the general principle that fractures of the Tibial shaft unite earlier in children than in adults.

Nutritional deficiencies or pathological states tend to have a higher incidence in the elderly and clinical trials are currently being conducted in some hospitals to determine the effect of high vitamin, protein and mineral salt diets upon the elderly orthopaedic patient (Grimes, 1979).

2.C.4 EXTRINSIC FACTORS AFFECTING HEALING

Extrinsic factors are those factors which may be influenced by external means and may be described as follows:

1. Stability at the fracture site
2. The application of compression across the fracture site
3. Functional loading and activity
4. Infection
5. Nutrition
6. Severity of the initial injury

1. Stability at the fracture site

Stability at the fracture site is determined by the efficiency of the supporting system and/or the strength characteristics of healing bone. From the review of the processes involved in healing it is clear that the formation and type of callus produced is dependent upon the relative stability of the part (see Table 3). Uthoff and Duboe (1971) demonstrated that continuation of rigid fixation induces osteoperosis and the canellization of new bone associated with Primary cortical healing. The mechanical advantages of producing a large callus have been defined by Charnley (1970) and the current view is held that failure to produce a good external callus, minimises the strength characteristics of healing bone.

Optimal healing of bone appears therefore to be dependant upon a degree of motion at the fracture and that conditions of absolute rigidity may impede firm union. Few in-vivo studies have been carried out which quantify the relative motion of the bone ends with the various methods of fracture management (see Part D).

2. The application of compression across the fracture site

There is considerable evidence to suggest that the application of compressive forces through the fracture site stimulates the ossification of cartilage in callus (Yamagishi and Yoshimura, 1955, Hert, et al 1972, Chamay and Schantz, 1972). Hert et al also found that compact bone did not react to continual loading but found that intermittent loading stimulated osteoblastic activity on both the periosteal and endosteal aspects of bone. Chamay and Schantz confirmed this finding

and found that bone atrophied with traction and hypertrophied with compression, particularly when the loading was intermittent. Jankovitch and Bidmuch (1972) found from their studies of vibration on rat bone that high vibration frequencies resulted in destruction of bone and cystic formation whereas an increase in bone weight, volume, density and breaking stress resulted from the application of low vibrating frequencies.

3. Functional loading and activity

Optimal levels and duration of compressive loading for the promotion of bone healing have not been determined from animal experiments or clinical study. The problem of relating any experiments with animals to the human situation is whether a linear relationship can be established between them. Furthermore, the in-vivo situation is complicated by the unknown contribution of muscular contraction upon the total compressive force across the fracture site. The need arises therefore to quantify, by clinical observation, the critical level of functional loading for optimal healing.

4. Infection

If infection occurs the surrounding structures are destroyed by phagocytic and enzyme activity. Infection in the stage of haematoma formation will cause destruction of the clot with consequent delay of union of failure to occur at all. Infection may arise at any stage of the patient's recovery but is more likely to occur if an open wound is present or surgical intervention and open reduction of the fracture has been undertaken. The causes of infection are well documented but

additional causes associated with the use of external fixation are noted below:

(a) Destruction of local blood vessels or nerves resulting in impaired or absent local circulation. (External fixation is a suitable method for the management of compound fractures in which damage to these tissues at the time of injury is likely).

(b) Inadequate débridement of dead bone and soft tissue

(c) Failure to bone graft early where extensive bone loss has occurred. The transfixing pins traverse the medullary cavity and spread of infection from any pin tract infections may seriously impair the deposition of new bone around a healthy bone graft.

(d) Bone is a poor conductor of heat and poor drilling techniques may result in excessive heat production locally, leading to bone necrosis and infection.

5. Nutrition

A deficiency of vitamin C limits the production of collagen and bone matrix with a consequent delay in healing (Bloom and Fawcett, 1975). Vitamin D maintains the normal mineral composition of the adult skeleton but deficiencies of these two vitamins (C + D) can usually be controlled by dietetic means. More serious nutritional disorders which may occur in pathological states such as alcoholism, blood dyscrasias and emboli tend to result in avascular necrosis (Grimes, 1979).

6. The severity of the initial injury

States (1965) concluded that victims of high energy trauma (i.e.

pedestrian and road traffic accidents) tended to heal more slowly than victims of low energy trauma, e.g. falls and torsional injuries. Grimes (1979) reported that open fractures heal more slowly. This was originally thought to be due to the loss of haematoma, but the view is now held that the degree of comminution, periosteal stripping, infection and other related trauma are greater contributing factors to retarded healing. Nicol (1963) reported that joint stiffness is a measure of tissue injury rather than the period of immobilization. It is well established that loss of an effective muscle pump which may be due to joint stiffness contributes to delayed healing and persistant oedema

2.C.5 THE DETECTION OF FRACTURE HEALING

The radiological and clinical criteria for the assessment of fracture healing are reviewed along with other methods that have been investigated by previous workers. These methods are categorised as follows:

A. Radiological

B. Clinical

C. Mechanical

D. Others

A. Radiological

Nicholls et al in 1979 defined the radiological criteris for healing as :

(a) Loss of a fracture line

(b) The appearance of trabeculae across the fracture site

(c) Visible callus

(d) Bony bridging.

Experiments were conducted by Nicholls et al with the participation of 27 physicians who were asked to correlate radiological criteria with the strength characteristics of healing rabbit tibia. Although all physicians correctly identified the weakest bone, the strongest two bones were not isolated and the statistical probability of detecting firm union was slightly better than chance. This confirmed the earlier findings by Hicks in 1971 that the moment of union cannot be timed. Guzelsi and Saha (1981) suggest that bone demineralization of less than thirty per cent is not detectable radiologically. In addition the formation of external callus, which is principally cartilaginous prior to ossification, may be masked by a radiologically visible soft tissue shadow. Matthews et al (1974) found that in some cases where radiological evidence had suggested apparent solid union, clinical instability was detected by pain and a "spongy feel".

To determine healing bi-planar X-rays are usually taken with the patient in the relaxed recumbent position but they do not provide the six degrees of freedom which define the relative motion between the two bone ends at the fracture site. Lippert and Hurtsch (1974) urge that the effectiveness of immobilization and stability at the fracture site can only be assessed under functional loading rather than the recumbent position.

B. The clinical criteria for healing

A reduction in fracture site motion, loss of pain, local tenderness to palpation and movement (active and passive), together with the passage of time have all been described by previous workers as the clinical criteria for the determination of union. The judgement of relative

stability is based upon two variable factors:

i) The magnitude of the applied bending moment which is usually applied first in one plane (antero-posterior) then in another plane (medio-lateral).

ii) The visual and manual sensitivity of the examiner to detect motion and angular deformation. Excessive bending may cause a refracture while an inadequate test may lead to a premature decision to abandon the cast or other means of support. Jernberger (1970) and later Matthews (1974) attempted to determine the magnitude of the applied bending moment that would be used to test for full union of a mid-shaft forearm fracture. Their results showed that examiners with more experience, i.e. senior surgeons,tended to use less force. The technique would therefore appear to be a subjective judgement based upon individual examiners skills and experience.

The perception and depth of pain experienced by a patient may be dependant upon a number of other factors such as ethnic origin and mental state. There is however some clinical evidence that, during the formation of primary callus when the fracture site is filled with fibroblasts and new blood vessels, some degree of motion is possible without pain. Jorgensen (1972) suggests that fibroblasts have great tensile strength but no compression strength so that bending of the fracture site can occur without much pain but shortening and displacement are not tolerated.

C. Mechanical tests of stability

Burny (197.8) defined healing of a fracture as the "recovery of the normal mechanical properties of bone", and various workers have

investigated this approach. The work of Lanyon and Bourn (1979) demonstrated the possibility of detecting maximal strain by bonding strain gauges to the cortical bone surface. Levels of stress and the strength characteristics of bone may then be determined but the application of this technique to healing bone has obvious practical limitations:

a) The technique is invasive with all the associated dangers of infection and possible interference with the development of callus.

b) The anisotropy of bone requires the presence of numerous gauges (Fonseca and De Silva, 1975).

The historic revival of external fixation as a means of treating severe lower limb fractures presented the possibility of detecing mechanical stability of the fracture site. The application of a sensing device in place of or attached to the fixation beam (which is external to the skin) has been investigated by two fundamental approaches:

a) The connection of a micrometer and dial gauge to the fixation beam (Jorgenson, 1972).

b) The instrumentation of the fixation beam with strain gauges (Burny, 1978).

These techniques are therefore non-invasive and afford no additional risk to the patient.

a) Micrometer and dial gauge

The principle of this method is based upon the application of 5 Kgf (measured by a spring balance) applied to the bone distal to the fracture site. The fixation beam (the Hoffman fixator) is replaced by the measuring equipment which consists of a dial gauge and micrometer (Figure 24) where

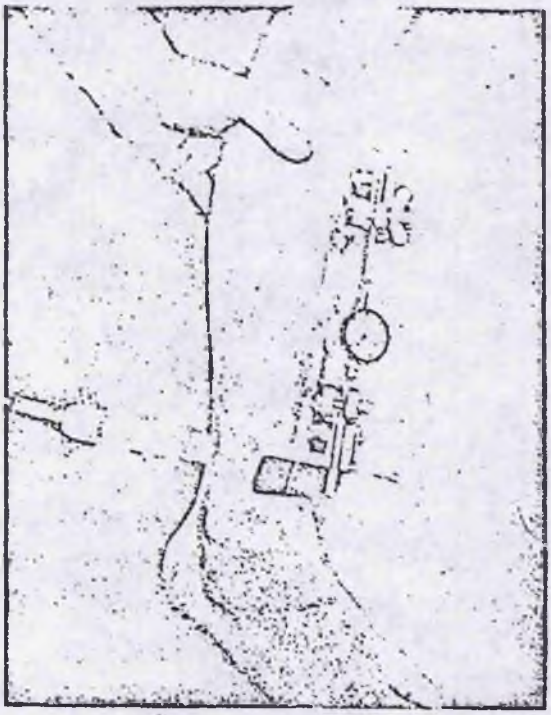

Figure .. A crural fracture loaded by a spring balance in the posterolateral direction

fig 24 (Jorgenson 1972)

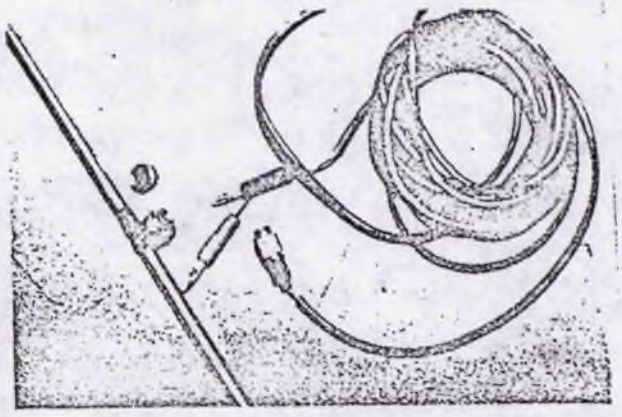

Fixation Beam with incorporated transducer

fig 25 (Burny 1972)

$$\text{the angular deflection at the fracture site} = \frac{\text{micrometer deflection}}{\text{Distance between the bone and the measuring axis}}$$

measured in radians.

The results from Jorgenson's work indicate that an optimum level of total deflection (1^{o}) where

total deflection = bone deflection + fracture site deflection

can be determined and deflection beyond this level may cause a refracture. Jorgensen (1972) concluded from radiological correlation with this finding that the thickness of callus was no indication of strength. Load criteria for fractures with deflections less than 1^{o} could not be established, and Jorgenson found that the ultimate strength of bones from different individuals differed greatly when total deflection was less than 1^{o}.

b) Instrumentation of the fixation beam with strain gauges

Bourgois & Burny (1972) first described this technique for the detection of healing using an instrumented single-sided external fixation device (the Hoffman Bar). This technique is based upon the assumption that any deformation of the bar due to deflection at the fracture site will be detected by the strain gauges and recorded as a change in resistance. Burny investigated two methods:

i. Direct bonding of a single strain gauge to the bar

ii. Replacement of the original bar by a special beam with an incorporated transducer (Figure 25).

Repeated measurements were taken during tests in which patients were asked to perform a simple "straight leg raising" activity. Burny expressed deformation of the bar as a percentsge of healing and maximum deflections were obtained within the first thirty post-operative days. The results from Burny's experimental work, substantiated earlier theoretical findings (Fig. 39, p. 88) that the rapidly decreasing exponential curve obtained during healing becomes asymptotic when the mechanical properties of callus are approximately 25-50% of normal bone. Burny points out that there is a risk of refracture at this level of healing. The levels of experimental strain were not reproduced in Burny's report although data from earlier work with in-vivo instrumentation of canine tibia and internal fixation plates was found (1978).

A direct comparison of my own work with Burny's work could not therefore be made. Burny suggests, from the results of the experimental work that stages of healing (non-union, slow healing or refracture) can be determined from sequential strain gauge recordings. He admits, however that this technique does not provide information about the visco-elastic characteristics of the callus which Jorgenson was able to demonstrate.

Evans and Harris (1980) concluded from experimental work with a single sided fixator, the Oxford device, that direct instrumentation of the fixator beam was feasible but impracticable in the clinical application. A more effective means of determining fracture stability could be investigated by the development of a clamp-on load transducer (Figure 27). The original transducer consisted of two stainless steel half-ring sensing elements mounted at right angles to each other with strain gauges incorporated (Figure 28). This was found to give a linear

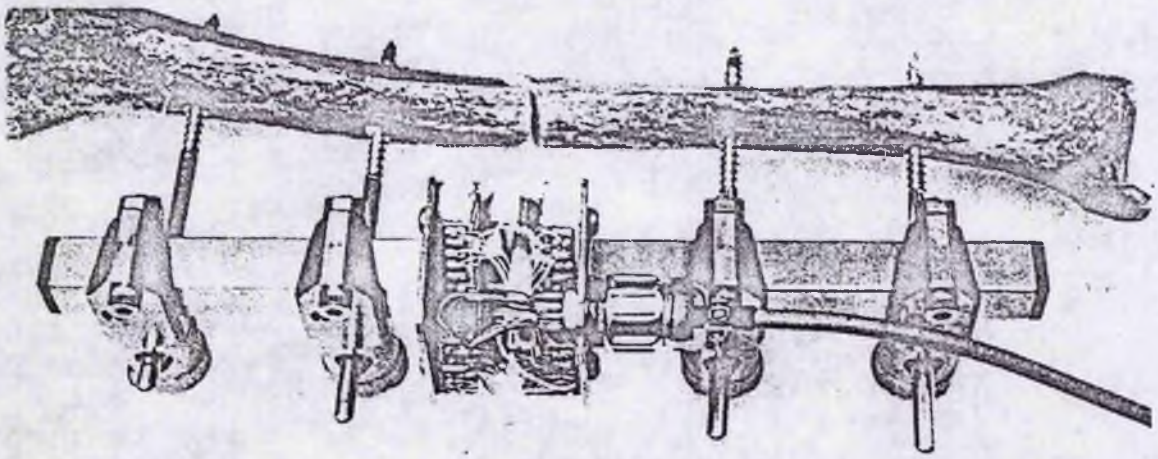

fig 27 The Oxford External Fixator & Load Transducer.

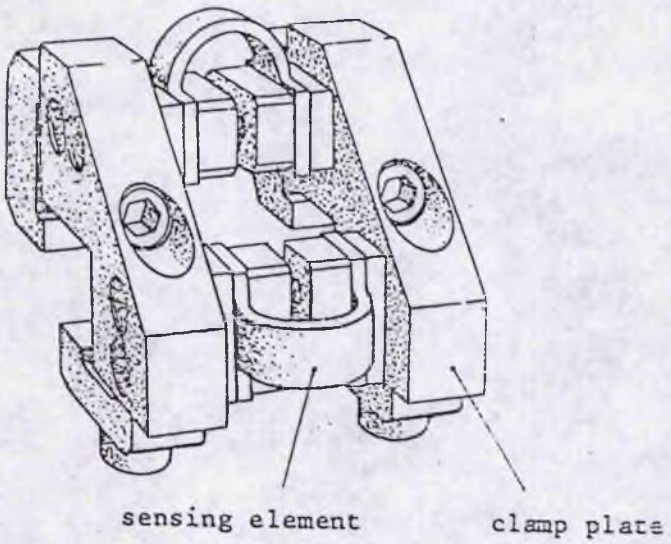

fig 28 The Load Transducer

Figures 27 and 28 reproduced from Evans et al 1978

response but very low levels of strain (below 90 micro-strain) and 5% cross-talk. Modifications to enhance the sensitivity were made to the original transducer by the substitution of a lower modulus material, titanium, as the sensing elements and repositioning of the strain gauges into a full Wheatstone bridge configuration. The modified transducer was calibrated up to 20Nm in bending and 10Nm in torsion, and a linear response up to 300 microstrain and 200 microstrain respectively was observed. Actual levels of microstrain that were recorded from the preliminary clinical trials however are not presented in the graphical data. It is hoped that presentation of data calibrating the device in-vivo will be produced from the clinical trials that are in progress at the time of writing this report.

Further work is also being carried out by this team to measure optically the relative motion at the fracture site. Three mutually perpendicular lateral effect photodetectors are mounted one on each pin and located directly opposite beams transmitted from three light-emitting diodes. This work is in the analytical and experimental stage and data has not yet been published [(Tanner 1981), personal communication.]

My work in this field was originally based upon work begun at the University of Surrey by Sayegh (1978-1979) in which a bilateral external fixation device, the Sayegh frame, was instrumented with strain gauges. This device was found however to be in little use clinically. Since it was envisaged at the outset of my own work that clinical trials would be undertaken, either by myself or subsequent workers, it was felt necessary to continue the investigation utilizing a more popular device. The work of Kempson (1978) who investigated experimentally the relative stability of different types of external fixators, suggested that the

DENHAM BAR was less rigid than the Oxford, Day and Hoffman devices. The Denham Bar, which was selected for my own work, is simple to use, of low cost and an effective means of support for severe low limb fractures.

D. Other methods that have been investigated for the detection of fracture healing

These methods are briefly discussed but not considered to be a routine method of clinical investigation.

a) Ultra-Sound

Brown and Mayor (1976) using a 0.5 MHz pulse transmission ultrasonic device to insonate an animal model, recorded wave changes during the formation of early callus which it is claimed, correlated with ossification not seen radiologically for a further one to two weeks.

b) Thermography

Thermographic trials have been undertaken (St. Mary's Hospital, Paddington) but detection of healing was inconclusive.

c) Photogrammetric method

Lippert and Hirsch (1974) described a method in which skeletal pins were used as markers against a stereometric field. Stereo pictures were then taken using a stroboscope for exposure and the results analysed by a stereocomparator. The results demonstrated that a range of motion is present with different fixation methods, and that changes in limb position

influence the range of fracture site motion. The advantage of this method is that the effects of sustained loading can be observed. It was found by these workers that a time-dependant characteristic of fracture site motion could be observed in healing bone in which a gradual increase in the initial displacement occurs.

d) Radio-nuclide uptake studies

Muheim (1973) using serial 87^{m} strontium demonstrated increased uptake in non-unions but found routine monitoring of fractures inconclusive. Thermography, ultra-sound and radio-active uptake studies do not give information about the mechanical strength of the callus although information may possibly be obtained about the level of active physiology.

PART D: TIBIAL FRACTURES AND THE ROLE OF THE EXTERNAL FIXATION

2.D.1 Severe compound comminuted fractures of the lower limb commonly result from high energy trauma such as road traffic accidents involving motorcyclists and pedestrians (Edge and Denham 1977). Torsional injuries however result from relatively low energy trauma, such as skiing injuries, in which the foot remains fixed and a torsional load is applied about the long axis of the bone during the fall. From the anatomical review presented in Part B of this chapter, it is seen that the weakest section of the tibia occurs at approximately 70% of its length from the proximal end and torsional injuries are most likely to occur at this level. The clinical management of a lower limb fracture is however dependant upon the relative stability between the bone ends. This is influenced by a number of factors:

A. The Direction of Functional Loading

Sayegh (1979) analysed the loading patterns that are imposed upon the lower leg during ordinary daily activities and divided them into six components:

i. Compression / tension.

ii. Antero / postero bending.

iii. Side to side bending.

iv. Antero - poseterior shear.

v. Side to side shear

vi. Axial torque.

If a transverse fracture of both the tibia and fibula is assumed then the deformations that are likely to result are represented in Figure (29). Direct axial loading of the limb, whether in tension or

Axial loading

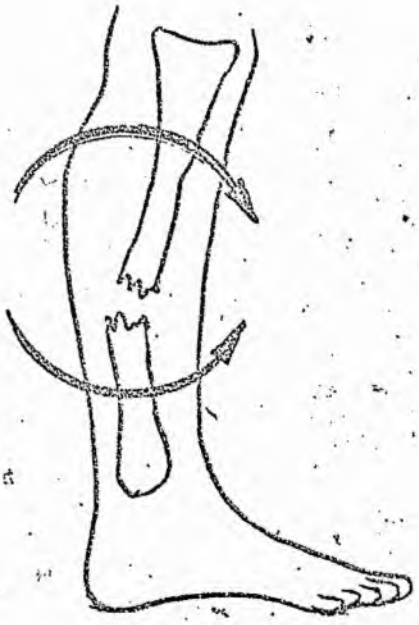

A.P. bending

side to side bending

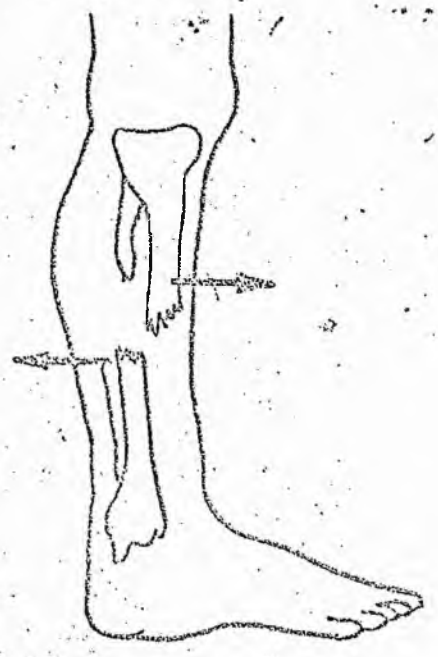

A.P. shear

Medial -Lateral shear

torque

fig. 29 (modified from Sayegh 1979)

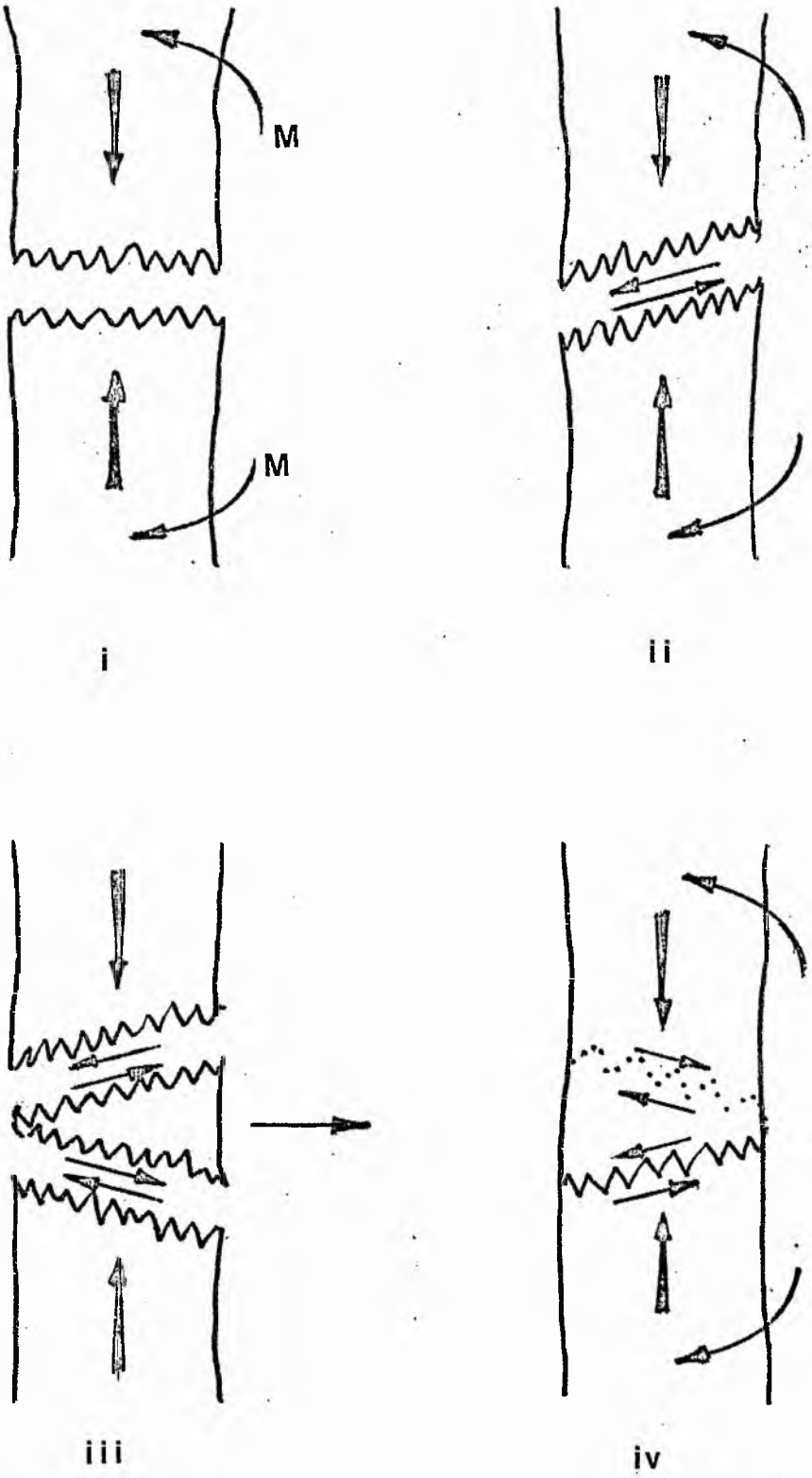

fig 30

in compression is the most stable loading configuration. The compressive component of load is however rarely assumed for any extended period due to the anatomical convexity of the tibia and synergic muscle activity, (see Chapter 2, Part B). The effects of shear, bending and torsion are therefore likely to be present in both weight-bearing and non weight-bearing activities.

B. The Type of Fracture Surface

All fractures are unstable in antero-posterior or lateral bending but the relative stability of the fracture surface may be compared by considering an axial compressive load applied to the leg. The most stable fracture type is a transverse fracture (Figure 30 i.) in which shear effects are minimal in axial loading. Oblique (Figure 30 ii.) or comminuted fractures (Figure 30 iii.) and fractures in which there is extensive bone loss, lack stability. In the latter three fracture types shortening of the limb is likely which may result from premature weight bearing or muscle activity. Spiral fractures (Figure 30 iv.) which result from torsional injuries tend to be more stable if partial integrity of the bone is retained.

C. The Presence of an Intact Fibula

In response to trauma disruption of the fibula may occur at either end of the shaft or at the level of the tibial shaft fracture. The suggestion has been made that the role of the fibula may be to resist torsional loading. This suggests that disruption of the fibula will precede disruption of the tibia under excessive torsional loads. If the fibula is also disrupted any load sharing component of the bone will be forfeited with a consequent loss of stability.

D. Soft Tissue Damage

Sarmiento's work (1974) suggests that the presence of an intact interosseous membrane may prevent excessive permanent displacement of bone fragments (see Chapter 2 Part B.). This experimental work was carried out on a cadaveric fractured fibia in the absence of other soft tissues such as muscles, fascia and skin. The elastic interosseous membrane was found to permit initial displacement of the fracture, when an axial load was applied. This displacement at the fracture site returned, however, to the pre-load position when the load was removed. If the interosseous membrane is removed then the initial displacement remains when the load is removed.

2.D.2 THE PRINCIPLES OF MANAGEMENT FOR FRACTURES OF THE LOWER LIMB

For severe fractures in which there is extensive bone and tissue damage Vidal et al (1979) advocate three fundamental principles of primary treatment.

1) Miniscule surgical débridement to remove all bruised and devascularised bone and soft tissue. Where necessary irrigation should be used to complete the débridement and cleaning.
2) The fracture should be adequately immobilized although distraction may at first be necessary to recover the intial length of the leg.
3) Wounds should be accessible and covered with large dressings to conserve moisture and enhance development of granulation tissue.

Vidal advocates the following three principles for the secondary

managment which he suggests may extend over several months:

a) To obtain eventual union it may be necessary to bridge the osseous gap with cortical grafts or cancellous bone chips.

b) Promote the formation of granulation tissue over the wound.

c) Restore impaired vascularity by micro-surgery techniques using cutaneous-osseous grafts. (These are usually removed from the iliac crest and anastomosed to the edges of the fracture site at viable circulatory channels).

Although less severe fractures may not require preliminary surgery, the following principles of fracture management, advocated by Burny (1978), should be instituted as early as possible:

i) Stable fixation to reduce pain and the risk of continual bleeding at the fracture site.

ii) Restoration of accurate alignment of fragments to ensure interfragmentary contact.

iii) A traumatic reduction to preserve the local vascularity and promote healing.

iv) Functional loading.

Clinical evidence (Dunn 1976) confirms the experimental evidence (see Chapter 2 Part C.) that functional loading coupled with stable external fixation promotes fracture union.

v) Prevent "fracture disease".

This is characterised by loss of normal joint range, stiffness and oedema. Hicks (1971) suggests "fracture disease" may be due to inadequate fracture site fixation rather than muscle inactivity and the immobilization of neighbouring joints.

vi) Restore full functional recovery of the limb and a return to normal gait patterns.

2.D.3 EXTERNAL FIXATION

The concept of an external inter-osseous support system for severe lower limb fractures was first introduced by Lambotte in 1907 (Figure 31) although earlier work on leg lengthening devices had been carried out by Codivilla in 1904. Lambotte's method formed the basis for the development of subsequent fixators by Anderson (1934) and Hoffmann (1938). Anderson, aware of a changing socio-economic climate, understood the need for developing a means of fracture management which promoted restoration of function and at the same time achieved normal alignment of fracture segments. Stader et al (1942) (Figure 32) developed a fixation device, which was based upon the design of a fixator used in the treatment of canine fractures. Johnson and Stowall (1950) conducted a questionnaire survey on the use of external fixation and found that the method had, by that time, fallen into disrepute. The problems encountered were pin tract infections, local necrosis and difficulties in maintaining reduction, immobilization and stability of small metaphyseal fragments (Hierholzer et al 1978). In recent years the Hoffmann device (op cit), a six pin configuration, has been modified to include a compression device (Figure 33). This device has subsequently been used widely in Europe.

In recent years improvements in the design, materials used and instrumentation in conjunction with ideas from various devices for leg lengthening (Rezain 1975) and arthrodesis (Anderson 1945 and Müller 1955) have led to the widespread use of external fixation as a successful method

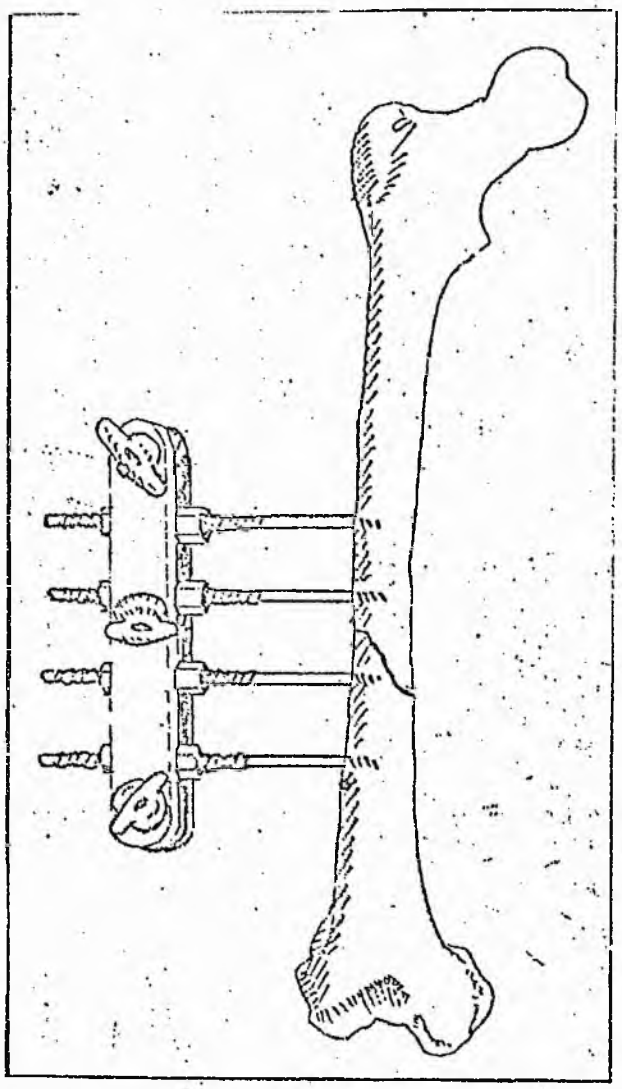

fig. 31 External Fixation
Lambotte (1907)

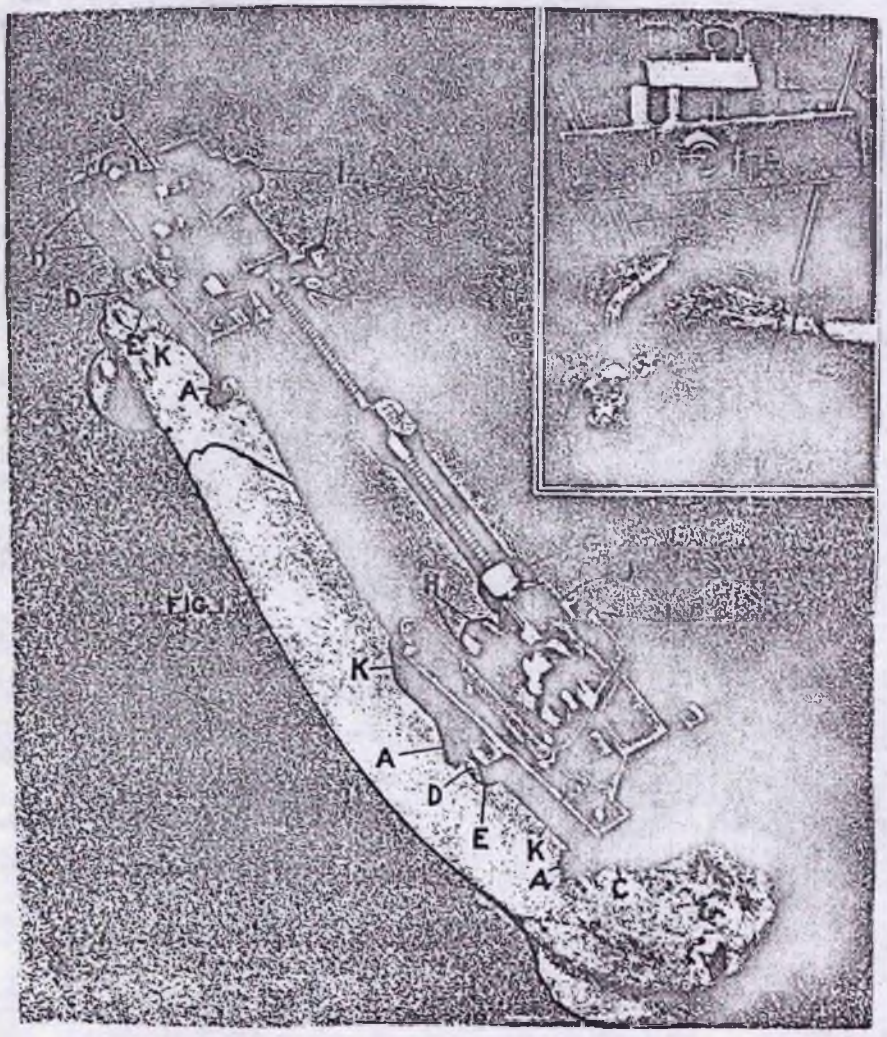

fig 32 **The Stader device**

from Stader 1942

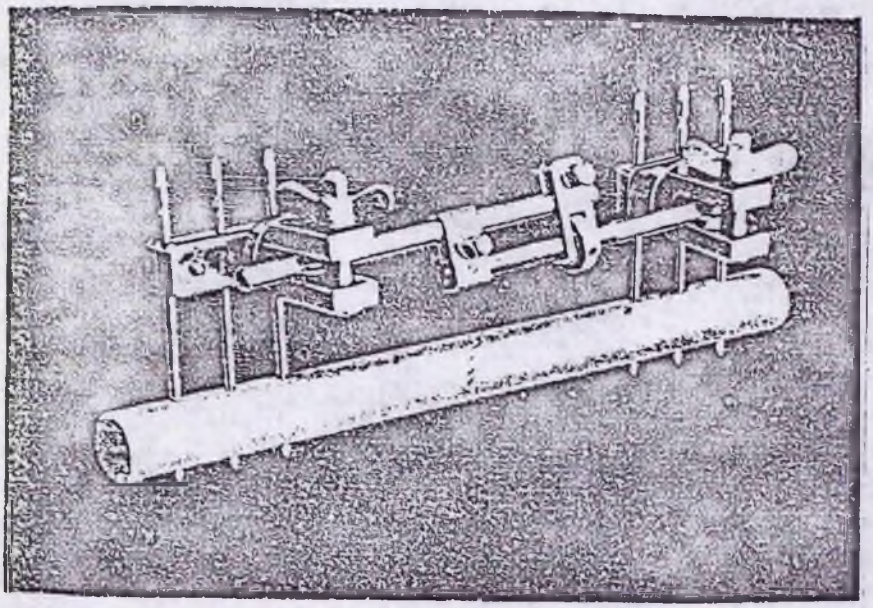

fig. 33 THE HOFFMANN DEVICE

Reproduced from Brooker & Edwards (1979)

TABLE 1. Results of Treatment of Tibial Shaft Fractures

Method	*No. Patients*	*Median Age*	*Fractures*		*Results*			*Average Time to Primary Union (months)*
			Open	*Closed*	*Infected*	*Malunion*	*Nonunion*	
Closed reduction	21	23	8	13	1 (open)	1	1 (closed)	4.6
Lottes nailing	20	29	13	7	0	0	5 (4 open, 1 closed)	5
Screw fixation	13	39	4	9	2 (1 open, 1 closed)	0	2 (1 open, 1 closed)	6.3
External skeletal fixation without compression, open reduction	10	34	8	2	2 (1 open, 1 closed)	1 (open)	3 (3 open)	9
External skeletal fixation without compression, closed reduction	8	36	5	3	0	0	3 (2 open, 1 closed)	6
External skeletal fixation with compression, open reduction	5	28	3	2	0	0	0	3.8
Compression plating	4	24	2	2	0	0	0	3
Noncompression plating	3	45	2	1	0	0	1 (open)	5
Cross-pinning of fracture site	1	16	1	0	0	0	1 (open)	
Total	85		46	39	5 (4 open, 1 closed)	2	16 (12 open, 4 closed)	
Median Age, Percentages		40	54%	46%	5.9%	2.4%	19%	

fig 34 from Dunn (1976)

of managing severe lower limb fractures. Dunn (1976) published the findings from a retrospective case review of displaced tibial shaft fractures between 1960 - 1972, and found that the use of external fixation with compression produced rapid healing times and excellent results. (Figure 34).

2.D.4 CRITERIA FOR THE DESIGN OF AN EXTERNAL FIXATION DEVICE

Sayegh (1979) summarises the commonly held criteria for the design of a fixator as:

1. Simple and easy to maintain.
2. Easy to apply at the time of operation.
3. Able to provide adequate stabilization of the fragment.
4. Freedom to position the fragments in all directions so that an optimum alignment of the fracture can be obtained.
5. Reasonable weight.
6. Allow easy access to soft tissues for re-dressing, grafting and repair.
7. Permit re-positioning of the bone in any one plane.
8. Allow for compression at the fracture site which should also be measurable.
9. Allow early mobilization of the lower limb joints.
10. Allow the patient to walk with partial weight-bearing.
11. May be easily removed when the bones have healed.
12. May be sterilized and re-used.

2.D.5 THE ADVANTAGES AND DISADVANTAGES OF EXTERNAL FIXATION AND THE INDICATIONS FOR ITS USE

The advantages of external fixation have been documented by several workers:

i) The technique does not destroy the medullary circulation. (This may occur with the insertion of intra-medullary nails).

ii) The endosteal elements are not damaged. (Rezaian 1971).

iii) Easy access to the wound allows immediate treatment of any local infection which enclosed methods, e.g. Plaster of Paris, do not readily permit (Wyn-Jones 1978).

iv) For severe fractures in which there is extensive bone loss it is the most suitable means of fixation since the device will prevent shortening yet allow the patient to ambulate non-weight bearing.

v) Rigid support can be maintained indefinitely provided pin tract infections do not occur. The problems of diminishing stability by a poorly fitting plaster cast, due to a reduction of oedema do not arise with external fixation (Burny 1978)(b).

vi) There is less risk of fracture site infection.

vii) Some fixators are designed to have a wide variety of application and the apparent initial high cost may be effectively reduced (e.g. The Ace Fixator).

viii) The risk of amputation is reduced. (Hierholzer et al 1978).

ix) Early active exercise to neighbouring joints is possible.

The disadvanatages attributed to external fixation are as follows:

a) If the device offers a rigidity superior to that of normal bone, functional loading does not take place and non-union may occur.

b) The final success of the fixation method is dependant upon a minimally destructive pin-drilling technique. Excessive heat production during drilling may cause local bone necrosis, subsequent pin tract infections and loosening of the pins. Other factors may, however, cause these infections and loosening of the pins:

i. Cyclic swelling causing motion at the pin hole.

ii. Premature weight-bearing before adequate stability and firm contact of the bone ends has been obtained, may cause large bending moments in the pins leading to their eventual failure.

c) Shortening and angulation at the fracture site may occur if compression of an unstable fracture is permitted or the compressive force is unequal (in a double sided fixator) or excessive.

The indications for the use of external fixation have been described by various authors and those listed below represent the most consistent approach in the treatment of tibial shaft fractures.

Where there is

1. Extensive bone loss, or

2. Severe compound, comminuted fractures in which there is extensive soft tissue damage and mobile free fragments of bone.

3. Infected pseudarthrosis (non-union) and fractures in which there is potential infection (Wyn-Jones 1979).

4. Where early ambulation is essential, e.g. patients with high embolitic risk such as polytraumia (Hiefholzer 1978) or obese inactive individuals.

5. For fractures which are close to the knee or ankle joints (Rezaian 1978).

2.D.6 CLASSIFICATION OF EXTERNAL FIXATORS USED IN THE TREATMENT OF LOWER LIMB FRACTURES AND THEIR RELATIVE ADVANTAGES AND DISADVANTAGES

A number of external fixators are available, both here and abroad, but only those types of fixator which have been used for tibial shaft fractures are reviewed. The particular requirements of an external fixator for these fractures are :

i) the device should be able to withstand cyclical load carrying capacity equal to 75 kg, the standard male weight.

ii) minimal interference with muscle tissue to prevent loss of function.

iii) minimal interference with normal patterns of walking.

Five fundamental types of fixator have been identified (Figures 35) and their biomechanical characteristics which have been investigated by previous workers are briefly reviewed.

TYPE 1, a single sided fixator, is reviewed more extensively at the end of this section, but this device consists of four or more transfixing pins attached to a single rod (Figures 33 and 35). The rod may be either solid or a tube, and is usually made of surgical grade stainless steel. These devices tend to be less rigid than other forms of fixator but the simplicity, low cost and effectiveness have contributed to their popularity.

TYPE 2. Two fixator bars are positioned on the medial and lateral aspects of the tibia, parallel to the long axis of the bone. The bars are held in position by no less than four transfixing pins traversing both cortices of the bone. Minimising the number of pins that are used reduces the possibility of pin tract infections, although stability is enhanced by the use of additional pins (Fischer 1979). Compression may be applied easily in types two and three by the inclusion of telescopic threaded rods (e.g. the Hoffmann device) or a twinbuckle incorporated in each rod (Rezaian 1976). Compression applied evenly prevents angulation of the fracture site. Without compression the stress on the centre pin is increased seventy times. (Fischer 1979).

TYPE 3. This type of device forms a quadrilateral frame with four

type 1

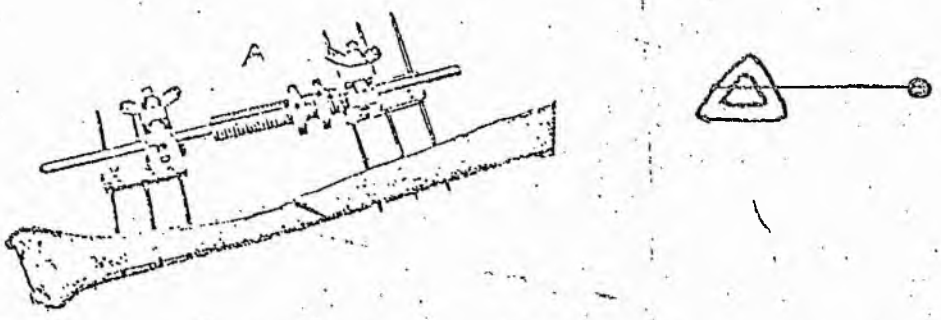

From Brooker & Edwards 1979

type 2

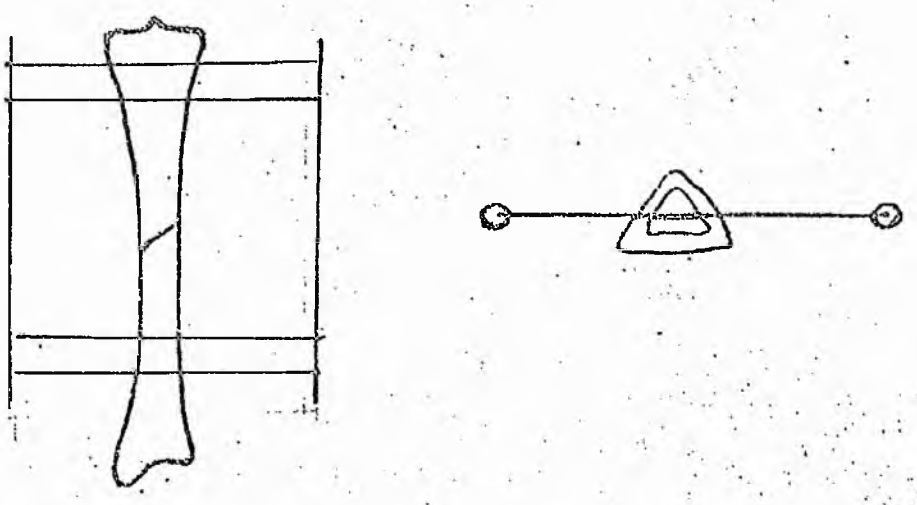

fig. 35. TYPES of EXTERNAL FIXATOR

type 3

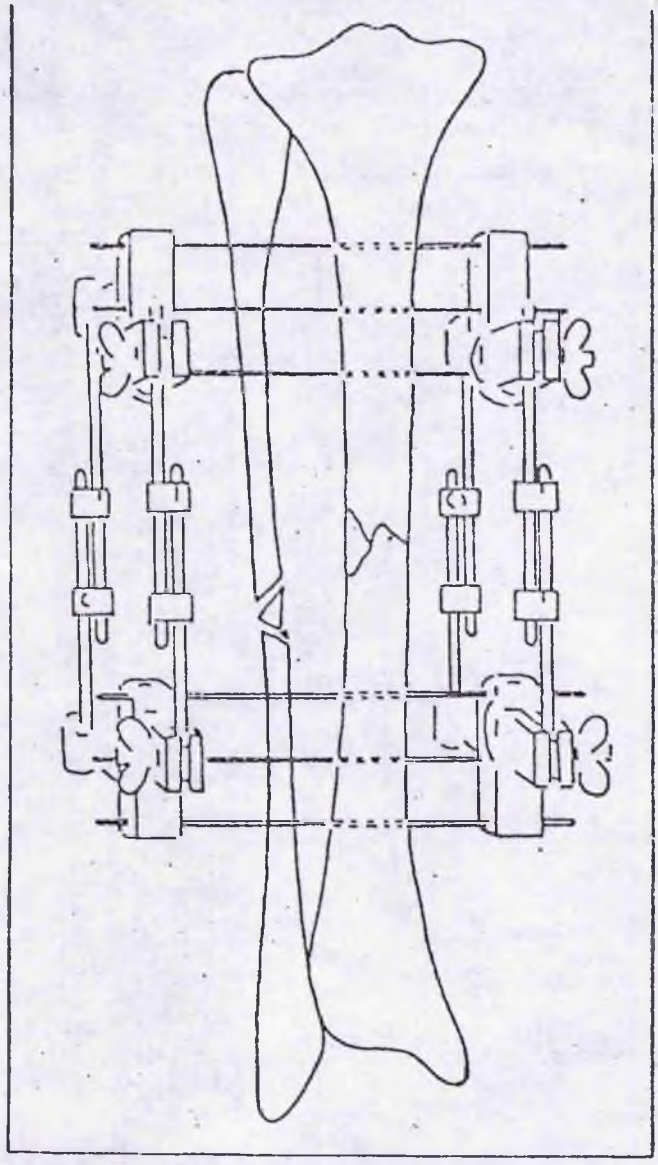

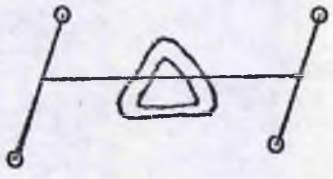

Fig 4. *Schematic drawing of the Hoffmann apparatus mounted as a double-frame system with compression lateral rods. Mounted in this way, the apparatus provides an extremely rigid fixation.*

(from Brooker and Edwards 1979.)

F

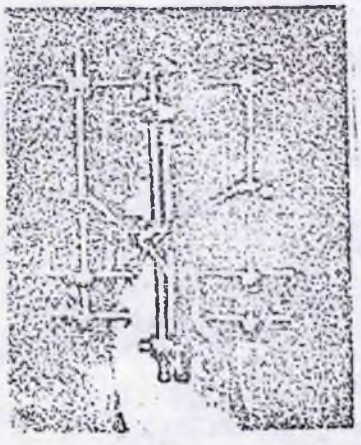

type 4

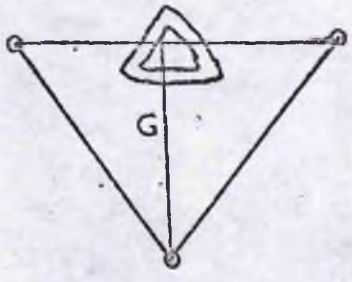

fig 35 cont. (from Hierholzer et al 1978.)

fixator bars, in pairs on the medial and lateral aspects of the tibia. The device is extremely rigid but Fischer (op. cit.) found that it is weakest in antero-posterior bending. The overall stiffness is enhanced by increasing the number of pins and the diameter of each pin. Vidal (1979) advocates however that types two and three offer a rigidity superior to that of normal bone and the indications for their use are limited.

TYPE 4. This triangular configuration employs one or two sets of transfixing pins in conjunction with two or more half-pins stabilizing the third fixator bar (Figure 35). A triangular configuration is generally weaker than a quadrilateral configuration (Fischer 1979), although angulation at the fracture site is minimal. Any weakness due to antero-postero bending may be minimised by the addition of inter-connecting rods (Figures 35 F and G). The advantage of this method is that the use of an excessive number of pins is avoided, but uniform compression is difficult to apply due to fixator assymetry (Fischer op. cit.).

TYPE 5. This device consists of circular rods held in position by two pairs of transfixing pins, one pair proximal to the fracture site and the other distal. The two pins of each pair are perpendicular but in the same horizontal plane (Figure 35 Type 5).

This technique has been used by Dwyer (1973) and in the Volkov-Organesian device (Figure 35). Dwyer suggests that the "Birmingham" device is extremely rigid but the results of clinical trials are not yet available. Although this technique provides extremely rigid fixation of the fracture, direct loading of the bone is minimal. Muscle

type 5

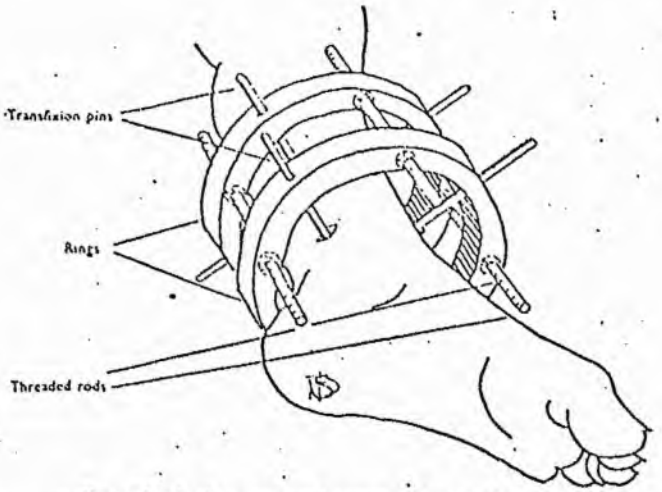

...—East Birmingham external compression device.

from Dwyer (1973)

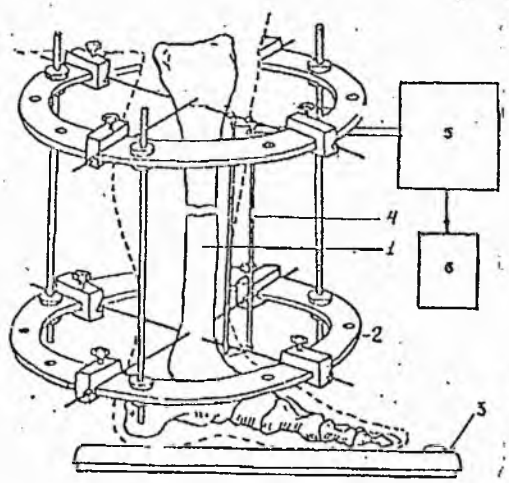

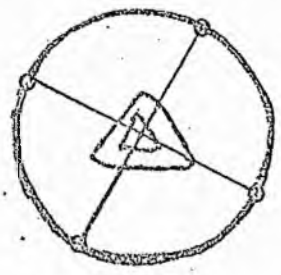

The Volkov–Organesian Device

from Schurov et al (1979)

fig 35 cont

tissue is pierced by the transfixing pins with the inevitable loss of muscle activity and restriction of active joint motion.

TYPE 1 : Single-sided External Fixation Devices

The characteristics of three single-sided fixators, the Hoffmann External Fixator, the Oxford device and the Denham Bar are compared in Table 4.

Kempson (1979 personal communication) conducted a series of experimental studies using both bone and metal tube to determine the relative stiffness of different fixators, The Hughes, AO3, AO2, Oxford, Hoffmann, Day and Denham Bar. From this study the Denham Bar was shown to be the least rigid, particularly in torsion. Further study of the Denham Bar was not, however, carried out to determine the effect of variable configurations upon fixator stiffness.

2.D.7 THE DENHAM BAR

The Denham bar is a stainless steel threaded rod which is usually connected to the tibia by six or more transfixing (Portsmouth) pins. (Figure 36). A keyway is cut along the entire length of the bar along which two aluminium, plastic-coated carriages are free to slide, but may be firmly locked into position by two locknuts at each end of one carriage. The transfixing pins are bonded to the carriages (the latter are notched along their length) by bone cement (polymethyl methacrylate). This technique permits random angulation of the pins but does not allow any further positioning of the pins when the cement has hardened. Edge and Denham (1977), who advocate a 4 cm. gap between the bar and the bone,

TABLE 4

CHARACTERISTIC	HOFFMANN	OXFORD	DENHAM
Fixator Bar	Solid Titanium Rod	16 mm Square steel tube	$\frac{1}{2}$" solid threaded stainless steel bar
Transfixing Pins			
Number of pins	6 or more	4 or more	6 or more
Pin type	Stenmann	Schanz	Portsmouth
Pin Diameter	4 mm	6 mm	4.76 mm
Fixation of Pins to Bar	Pin clamp	Movable clamps for individual adjustment of pins by sliding along the Fixator Bar	Acrylic bonding to movable carriages which can then be locked into position
Adjustment of Angulation	Insertion of pins with a template to ensure parallelism	Considerable manipulation is possible which can then be locked into postion	No restriction on plane or angle of insertion.
Minimal distance between pins	-	26 mm	-
Cost	High (£742 approx.)	Low	Low (£50)
Compression	Telescopic rods	Compression/Distraction device which is attached to the pin clamps on one side of the fracture	Compression springs and lock nuts applied to each end of one carriage
Weight	—	Low	$>$ .8 kg

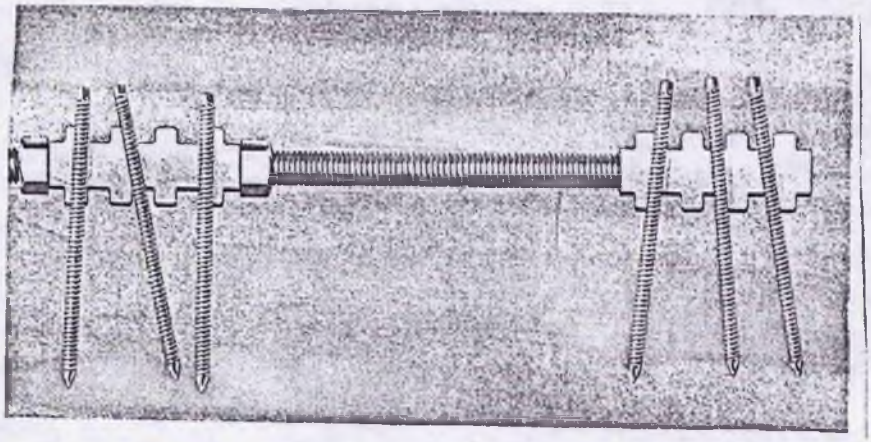

fig 36 THE DENHAM BAR

from Zimmer leaflet 2008

also suggest that random angulation of the pins in the bone reduces the possibility of splitting.

Rotation of the carriage is restricted by the presence of a centrally placed curved filament protruding from its inner surface into the keyway of the bar. Edge and Denham (personal communication) suggest that compression across the fracturesite may be obtained by the interposition of 2 spring washers on either side of one carriage (Figure 37). When the springs are fully compressed a displacement of 2.64 mm occurs.

An additional mechanism has been introduced into the Denham Bar which permits subsequent adjustment of fracture site angulation (The Salford Device).

THE SALFORD DEVICE (Figures 38 a and b).

This mechanism consists of two rods replacing the single bar. These are manipulated by the rotation of four socket head cap screws which clamp the ball end of a universal joint (Figure 38 c).

2.D.8 FACTORS AFFECTING THE STABILITY OF A SINGLE-SIDED FIXATOR

Considerable work has been carried out to determine the optimum pin diameter that can be used without risk of fracture or splitting of the bar in the vicinity of the pin. Ansell and Scales (1968) found that the largest core diameter that can be used without creating a risk of fracture is 2.95 mm although larger diameters are often used (see Table 4). Swanson and Freeman (1970) found that a 3.175 mm hole in bone caused a reduction of bone strength of sixty per cent in bending and thirteen per cent in torsion. Bechtel (1959) concluded that optimum pin diameter should be between 20% - 40% of the bone shaft diameter. Evans et al (1979) (b)

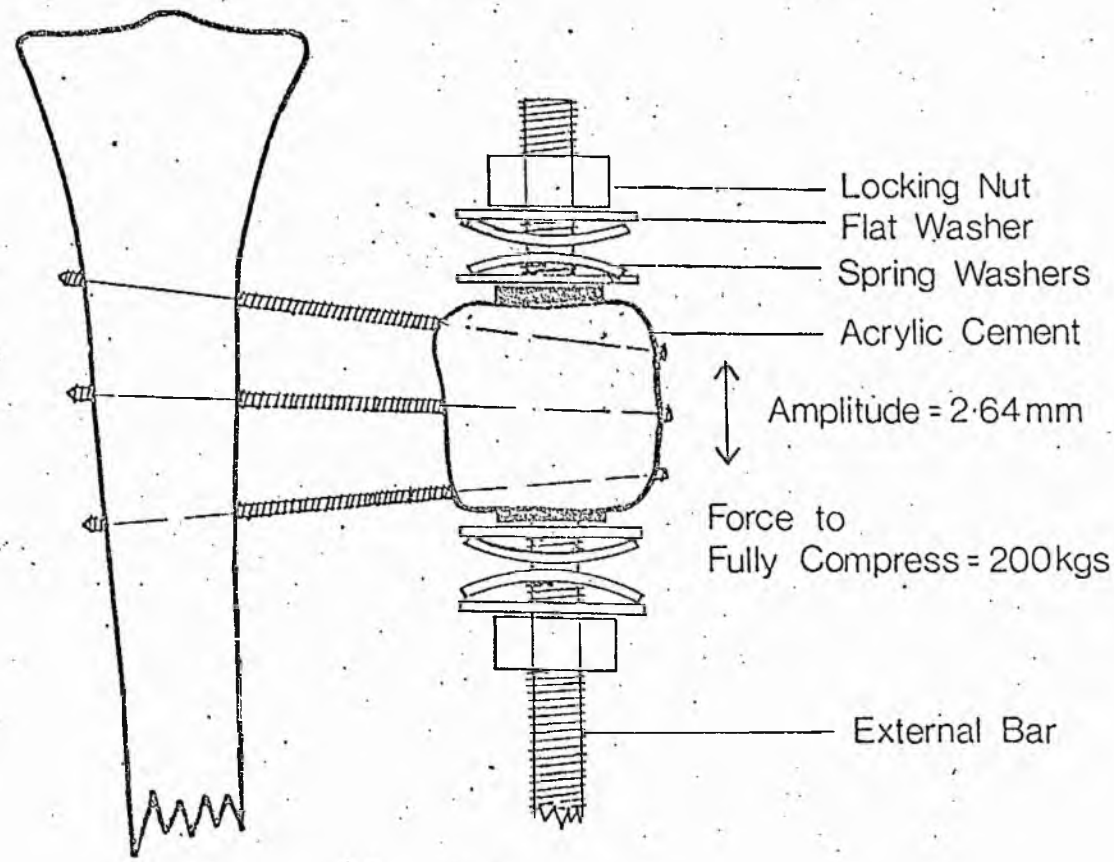

fig 37 The Denham Bar and Spring Washers

From J. Edge (personal communication 1979)

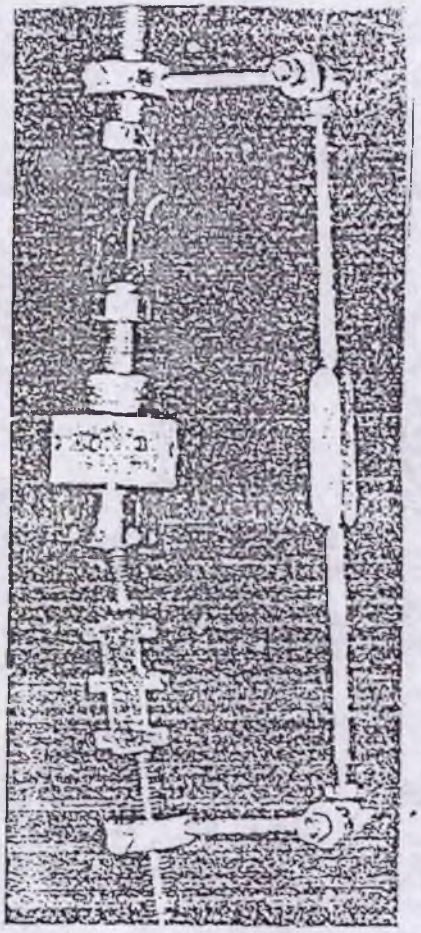

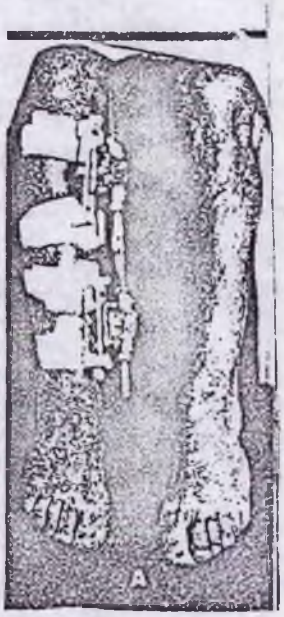

b

The prototype Salford external fixator showing auxi ary angulation adjustment mechanism

a

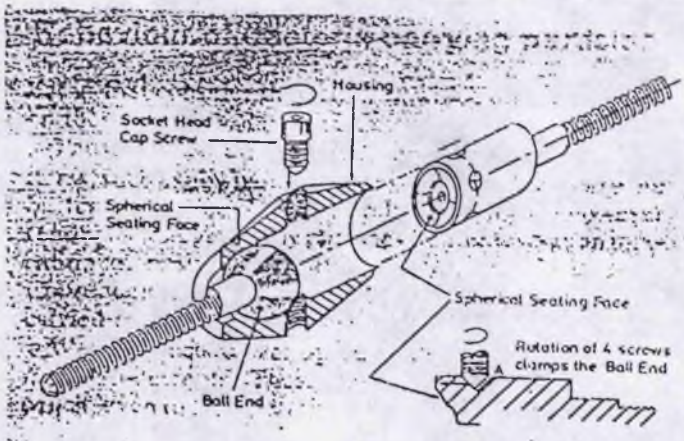

c

Details of Allen screw locking mechanism on the later Salford device

fig 38 From Banks & Dervin (1980)

using the Oxford Fixator, found that stress levels at the screw/bone interface are reduced by one and a half times by using a 6 mm rather than 4 mm Schanz Pin. The Schanz pins differ from the Portsmouth pins in that they are not threaded throughout the entire length. Evans et al also found that fixator sitffness was considerably enhanced by ensuring that the threaded portion of the pin is buried below the cortices so that the main bending load is on the greater diameter of the pin. The safe load carrying capacity of the fixator was found to be inversely proportional to the length of the pin, i.e. the distance between the fixator and the bone.

Tanner (1979) found experimentally that the stiffest pin configuration of a four pin assembly with an Oxford fixator, occurred when the outer two pins were angled to 30^{o} at the fixator with a constant interval between the pins at the bone interface. Burny (1972), however, suggested that the levels of static stress which are likely to cause pin breakage may be reduced by parallel alignment of the pins. Fischer (1979) emphasises however that any factor which governs stiffness should be evaluated in the context of optimal conditions for promoting healing.

2.D.9 THE EFFECT OF PHYSIOLOGICAL VARIABLES UPON OVERALL FIXATOR STIFFNESS

In vitro studies of the mechanical behaviour of screws in bone (Ansell and Scales 1968, Klip and Bosma 1978) have been investigated. Evans et al (1978) using a wood model, suggested that the contribution of 'bone' deflection to overall deflection at the fracture site was minimal (.02 mm bone deflection for 3-4 mm of fracture site deflection). No evidence from the literature could be found to determine the effects of varying bone geometry; fracture site location or muscle activity upon

fixator stiffness.

Burny (1972) evaluated theoretically, using the second theorem of Castigliano, the likely deformations of a fixator bar which would occur as the fracture heals. It was concluded from this analysis that changes in the level of healing can not be detected when the callus is approximately 20 - 50% the normal strength of bone. (See Figure 39).

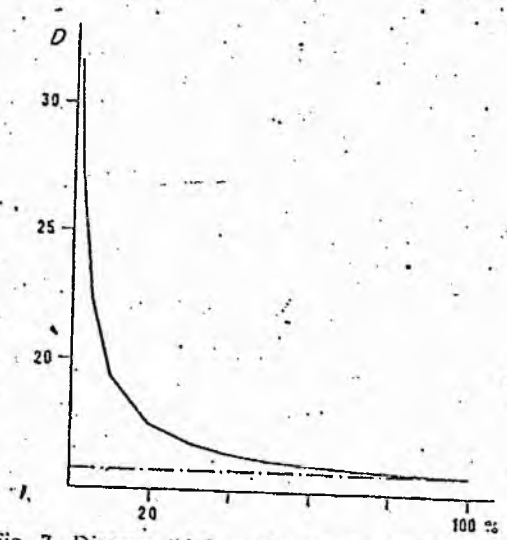

Fig. 7. Diagram "deformation-percentage of healing" obtained in the case of a fracture treated with an osteotaxis.

fig 39 From Bourgeois & Burny 1972

CHAPTER THREE: THEORETICAL ANALYSIS

3.1.1 A theoretical analysis of the bone and fixator was undertaken to determine :

A. The relative motion of the bone ends in a fractured limb supported by an External Fixation device and six transfixing pins.

B. The changes in the residual force applied to the fixator when the limb is functionally loaded during the later stages of healing.

3.2.1 PART A.

The first stage of the analysis considers a fracture of the lower third of the tibia and fibula in which complete disruption of the bones has occurred. To simplify the analytical procedure, the bones are replaced by a single member of uniform cross section and the group of pins proximal to the fracture site are assumed to be attached to the bone by an encastre fixation condition.

The six transfixing pins are assumed to be parallel, coplanar and each pin group is equidistant from the mid-point of the fracture site. (Figure40). The derived data for each bone section, fixator and pins are presented in Appendix 3.1.1. The weight of the pins and the part of the bone proximal to the fracture site is ignored. The forces present are assumed to be due to the mass of the limb distal to the fracture site, the bar, carriages and acrylic bonding (Appendix 3.1.1).

A right-handed Cartesian co-ordinate system is used and the

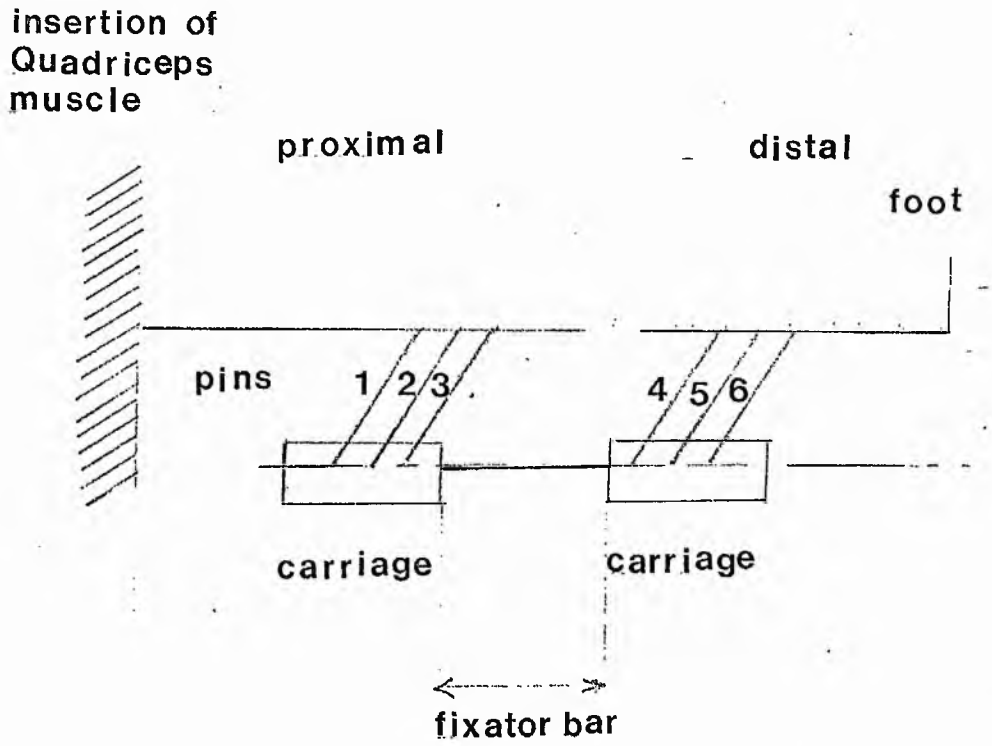

a) Fixator configuration

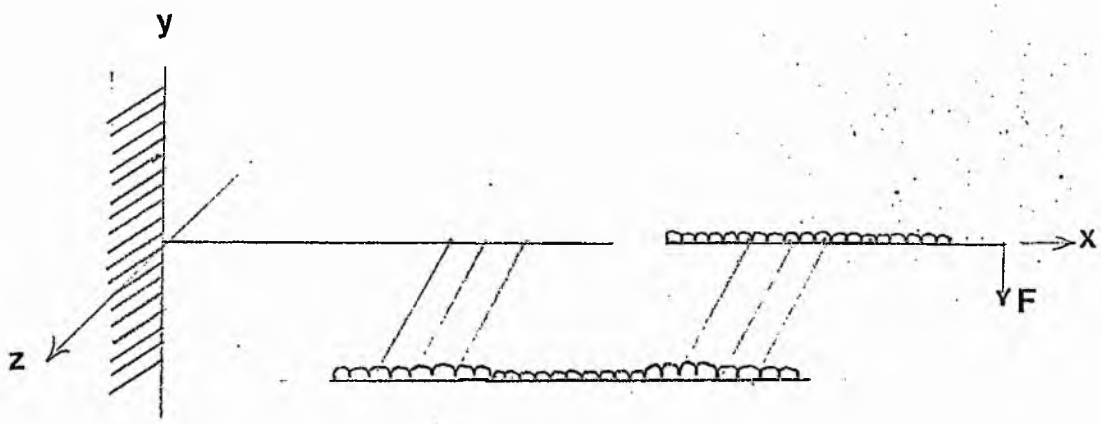

b) loading diagram

fig 40

analysis determines the deflections and rotations occurring in the two groups of pins and fixator bar. The movement occurring at the fracture site, due to the relative motion of the fractured bone ends, is then obtained by vector summation of the individual deflections and rotations.

Using Macaulay's method for calculating beam deflection, the first stage of the analysis considers the deflection (Y_1) and the slope (θ_1) due to bending of the first pin. Further expressions are then derived for the deflection occurring in the remaining two pins of the proximal group.

For the first pin

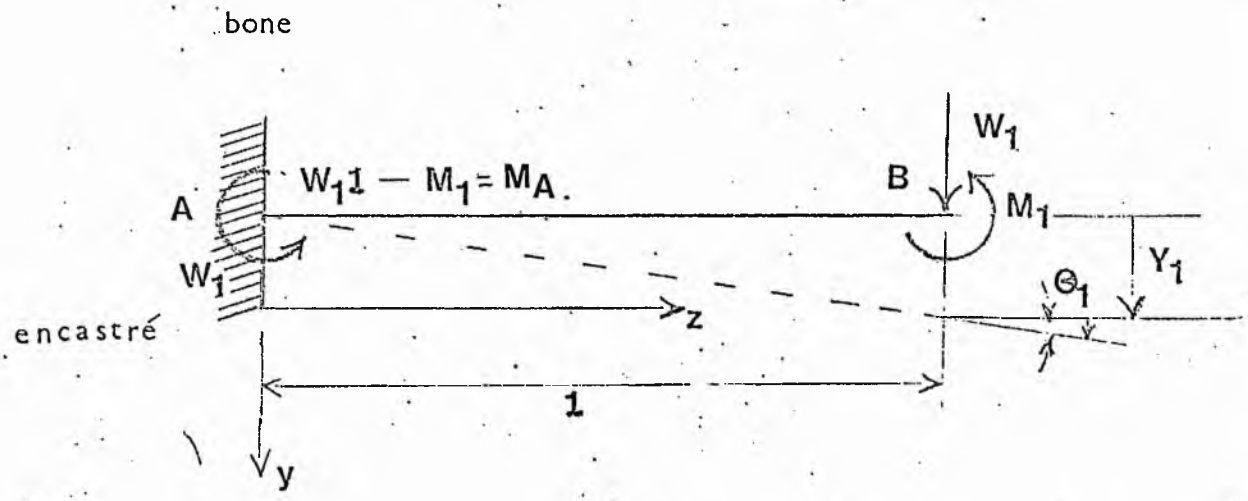

Moments about (A): $M_A + M_1 - W_1 l = 0$

$$\longrightarrow \quad M_A = W_1 l - M_1$$

Using Macaulay's method

$$EI \frac{d^2y}{dz^2} = W_1 z - (W_1 l - M_1)$$

$$EI\frac{dy}{dz} = W_1\frac{z^2}{2} - (W_1 l - M_1)z + A \quad \ldots\ldots\ldots\ldots\ldots \text{(i)}$$

when $z = 0$, $\frac{dy}{dz} = 0$, therefore $A = 0$

$$EI\,y = W_1\frac{z^3}{6} - (W_1 l - M_1)\,z^2/2 + B \quad \ldots\ldots\ldots\text{(ii)}$$

when $z = 0$, $y = 0$, therefore $B = 0$

when $z = l$, $\frac{dy}{dz} = \theta_1$

from (i) $EI\theta_1 = W_1\frac{l^2}{2} - (W_1 l - M_1)l$

$$\longrightarrow \theta_1 = (-W_1\frac{l^2}{2} + M_1 l)\,\frac{1}{EI}$$

$$\longrightarrow \theta_1 = \frac{l}{EI}\,(M_1 - \frac{W_1 l}{2}) \quad \ldots\ldots\ldots\ldots\ldots\ldots\ldots \text{(1)}$$

When $z = l$, $y = Y_1$ (tip deflection)

from (ii) $EIY_1 = W_1\frac{l^3}{6} - (W_1 l - M_1)\,\frac{l^2}{2}$

$$\longrightarrow Y_1 = \frac{l^2}{6EI}\,(3M_1 - 2W_1 l) \quad \ldots\ldots\ldots\ldots\ldots\ldots\ldots \text{(2)}$$

Similarly, $\theta_2 = \frac{l}{EI}\,(M_2 - \frac{W_2 l}{2}) \quad \ldots\ldots\ldots\ldots\ldots\ldots\ldots \text{(3)}$

$$\theta_3 = \frac{l}{EI}\,(M_3 - \frac{W_3 l}{2}) \quad \ldots\ldots\ldots\ldots\ldots\ldots\ldots \text{(4)}$$

$$Y_2 = \frac{l^2}{6EI}\,(3M_2 - 2W_2 l) \quad \ldots\ldots\ldots\ldots\ldots\ldots\ldots \text{(5)}$$

$$Y_3 = \frac{l^2}{6EI}\,(3M_3 - 2W_3 l) \quad \ldots\ldots\ldots\ldots\ldots\ldots\ldots \text{(6)}$$

From equation 1,

$$\frac{EI\theta_1}{l} = M_1 - \frac{W_1 l}{2}$$

$$\longrightarrow M_1 = \frac{EI\theta_1}{l} + \frac{W_1 l}{2} \quad \ldots\ldots\ldots\ldots\ldots\ldots\ldots\ldots\text{(iii)}$$

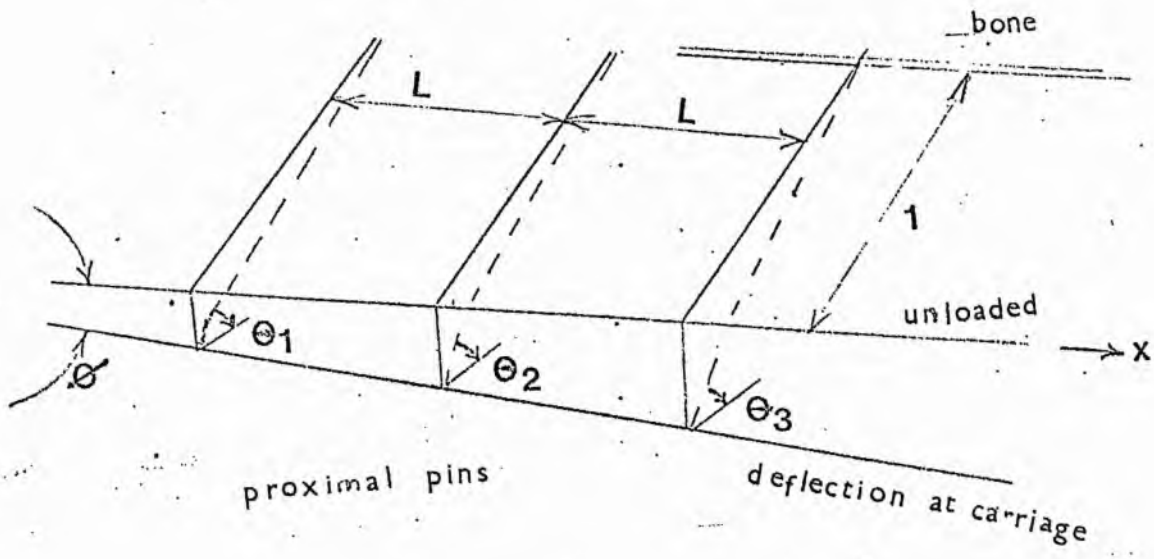

From equation 2,

$$\frac{6EIY_1}{l^2} = 3M_1 - 2W_1 l \quad \text{(assuming a rigid carriage)}$$

$$\longrightarrow 2W_1 l = 3M_1 - \frac{6EIY_1}{l^2}$$

$$\longrightarrow W_1 = \frac{3M_1}{2l} - \frac{3EIY_1}{l^3}$$

$$W_1 = \frac{3}{2l^3}\,(M_1 l^2 - 2EIY_1)$$

$$\text{using (iii)} \longrightarrow W_1 = \frac{3}{2l^3}\left[\left(\frac{EI\Theta_1}{l} + \frac{W_1 l}{2}\right) l^2 - 2EIY_1\right]$$

$$= \frac{3}{2l^3}\left[EI\Theta_1 l + \frac{W_1 l^3}{2} - 2EIY_1\right]$$

$$2W_1 l^3 = 3EI\Theta_1 l + 3W_1 \frac{l^3}{2} - 6EIY_1$$

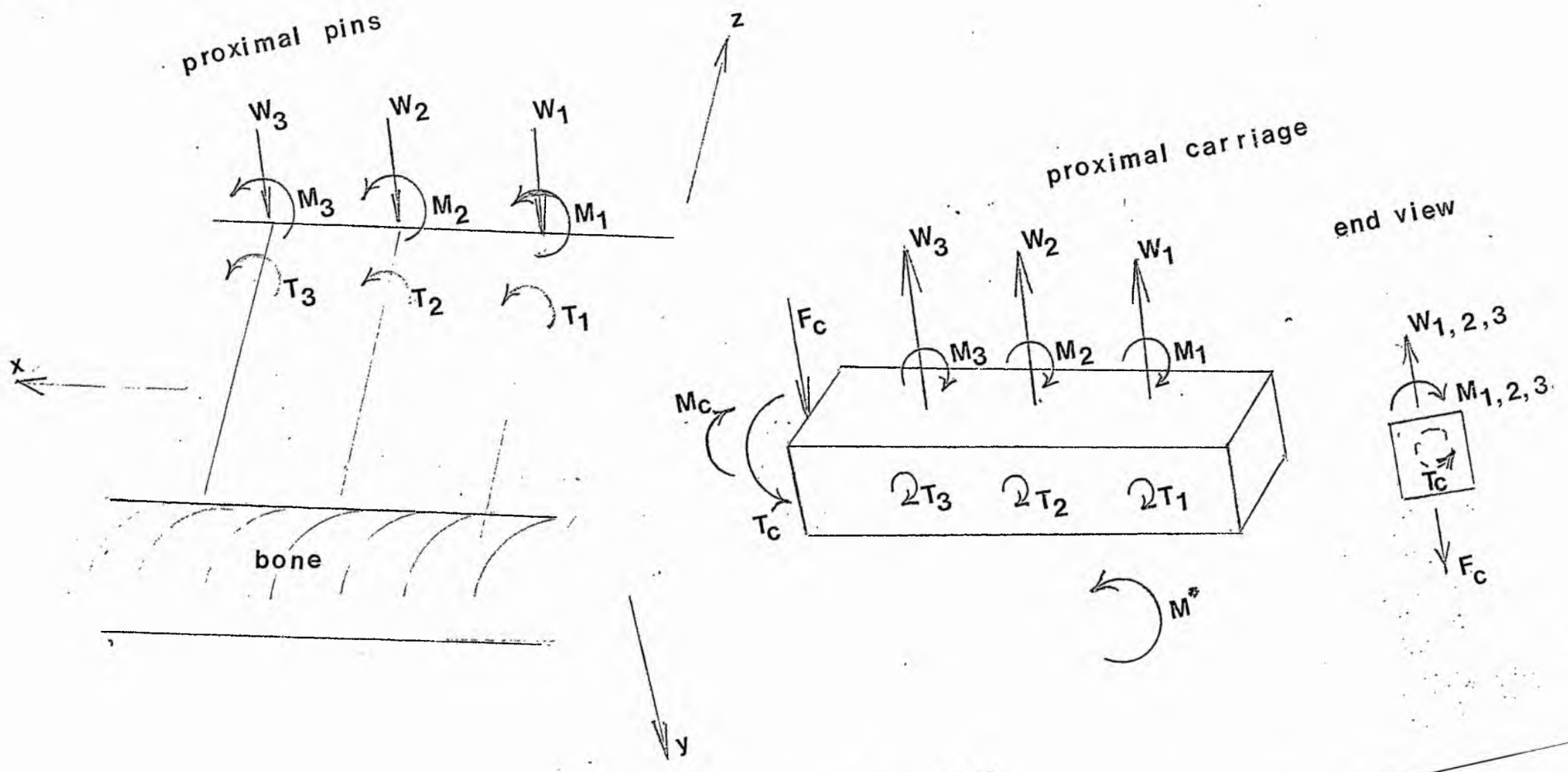

fig 41 Free body diagram

$$4W_1l^3 = 6EI\theta_1l + 3W_1l^3 - 12EIY_1$$

$$W_1l^3 = 6EI\theta_1l - 12EIY_1$$

$$W_1 = \frac{6EI}{l^3}\left[\theta_1l - 2Y_1\right] \quad \text{.....(7)}$$

Similarly $W_2 = \frac{6EI}{l^3}\left[\theta_2l - 2Y_2\right]$

but $Y_2 = Y_1 + \phi L$

therefore $W_2 = \frac{6EI}{l^3}\left[\theta_2l - 2Y_1 - 2\phi L\right]$ .....(8)

and $W_3 = \frac{6EI}{l^3}\left[\theta_3l - 2Y_3\right]$

but $Y_3 = Y_1 + 2\phi L$

$$W_3 = \frac{6EI}{l^3}\left[\theta_3l - 2Y_1 - 4\phi L\right] \quad \text{.....(9)}$$

Considering equilibrium of carriage: (Fig. 41)

Vertical Forces: $Fc = W_1 + W_2 + W_3$ .....(10)

Moments about Carriage Axis: $Tc = M_1 + M_2 + M_3$ ...(11)

Moments about 1st pin: $M^* = T_1 + T_2 + T_3 + W_2L + 2W_3L$

but for rigid carriage $T_1 = T_2 = T_3 = T$

therefore $M^* = 3T + W_2L + 2W_3L$ ..... (12)

Equation (12) $M^* = \frac{3GJ\phi}{l} + \frac{6EI}{l^3}\left[\theta_3l - 2Y_1 - 2\phi L\right] L + \frac{12EI}{l^3}\left[\theta_3l - 2Y_1 - 4\phi L\right] L$

$$M^*l^3 = 3GJ\phi l^2 + 6EI\left[\theta_3l - 2Y_1 - 2\phi L + 2\theta_3l - 4Y_1 - 8\phi L\right] L$$

$$= 3GJ\phi l^2 + 6EI\left[3\theta_3l - 6Y_1 - 10\phi L\right] L$$

$$M^*l^3 = 3GJ\phi l^2 + 18EI\theta_3 lL - 36\,EIY_1 L - 60\phi L^2 \quad \ldots\ldots\ldots (13)$$

Equation (11): using equation (1), $M_1 = \frac{EI\theta_1}{l} + \frac{W_1 l}{2}$

and similarly $M_2 = \frac{EI\theta_2}{l} + \frac{W_2 l}{2}$

and $M_3 = \frac{EI\theta_3}{l} + \frac{W_3 l}{2}$

$$Tc = \frac{EI}{l}(\theta_1 + \theta_2 + \theta_3) + \frac{l}{2}(W_1 + W_2 + W_3)$$

using (7), (8) and (9)

$$= \frac{EI}{l}(\theta_1 + \theta_2 + \theta_3) + \frac{l}{2}\,\frac{6EI}{l^3}\left[\theta_1 l - 2Y_1 + \theta_2 l - 2Y_1 - 2\phi L + \theta_3 l - 2Y_1 - 4\phi L\right]$$

$$= \frac{EI}{l}(\theta_1 + \theta_2 + \theta_3) + \frac{3EI}{l^2}\left[(\theta_1 + \theta_2 + \theta_3)l - 6Y_1 - 6\phi L\right]$$

$$= \left(\frac{EI}{l^2}\right)\left[(\theta_1 + \theta_2 + \theta_3)l + 3(\theta_1 + \theta_2 + \theta_3)l - 18Y_1 - 18\phi L\right]$$

$$= \left(\frac{EI}{l^2}\right)\left[4(\theta_1 - \theta_2 + \theta_3)l - 18\,Y_1 - 18\phi L\right]$$

$$Tc = \frac{2EI}{l^2}\left[2(\theta_1 + \theta_2 + \theta_3)l - 9Y_1 - 9\phi L\right]$$

$$\longrightarrow Tcl^2 = 2EI\ \ 2(\theta_1 + \theta_2 + \theta_3)l - 9Y_1 - 9\phi L \quad \ldots\ldots\ldots\ldots\ldots (14)$$

Equation 10: $Fc = \frac{6EI}{l^3}\left[\theta_1 l - -2Y_1 + \theta_2 l - 2Y_1 - 2\phi L + \theta_3 l - 2Y_1 - 4\phi L\right]$

using (7), (8) and (9)

$$Fcl^3 = 6EI\left[(\theta_1 + \theta_2 + \theta_3)l - 6Y_1 - 6\phi L\right] \quad \ldots(15)$$

(13): $M^*l^3 = 3GJ\phi l^2 + 18\,EI\theta_3 lL - 36EIY_1 L - 60\phi L^2$

(14): $Tcl^2 = 2EI\left[2(\theta_1 + \theta_2 + \theta_3)l - 9Y_1 - 9\phi L\right]$

$$= 6EI\left[2\theta l - 3Y_1 - 3\phi L\right]$$

(15): $Fcl^3 = 6EI\left[(\theta_1 + \theta_2 + \theta_3)l - 6Y_1 - 6\phi L\right]$

$= 18EI\left[\theta l - 2Y_1 - 2\phi L\right]$

(Since carriage is torsionally stiff, assume $\theta_1 = \theta_2 = \theta_3 = \theta$)

Multiply (14) by 2 and subtract from (15) giving,

$$(Fcl - 2Tc)l^2 = 6EI\theta l$$

therefore $\theta = \frac{l}{6EI}(Fcl - 2Tc)$ ..... (16)

(14) $\longrightarrow \frac{Tcl^2}{6EI} = 2\theta l - 3Y_1 - 3\phi L$

$\longrightarrow 3Y_1 = 2\theta l - 3\phi L - \frac{Tcl^2}{6EI}$

$\longrightarrow Y_1 = \frac{2}{3}\theta l - \phi L - \frac{Tcl^2}{18EI}$ .....(iv)

(iv) into (13): $M^*L^3 = 3GJ\phi l^2 + 18EI\theta lL - 36EIL\left[\frac{2}{3}\theta l - \phi L - \frac{Tcl^2}{18EI}\right] - 60\phi L^2$

$\longrightarrow M^*l^3 = 3GJ\phi l^2 + 18EI\theta lL - 24EI\theta lL + 36EI\phi L^2 + 2Tcl^2L - 60\phi L^2$

$\longrightarrow M^*l^3 = \phi\left[3GJl^2 + 36EIL^2 - 60L^2\right] - 6EIlL\theta + 2Tcl^2L$

$\longrightarrow M^*l^3 = 3\phi\left[GJl^2 + 12EIL^2 - 20L^2\right] - 6EIlL\left(\frac{1}{6EI}\right)(Fcl - 2Tc) + 2Tcl^2$

$\longrightarrow \phi = \frac{M^*l^3 + Fcl^3L - 4Tcl^2L}{3\left[GJl^2 + 12EIL^2 - 20L^2\right]}$

$$\phi = \frac{l^2(M^*l + FclL - 4TcL)}{3\left[GJl^2 + 12EIL^2 - 20L^2\right]} \quad \text{.....(17)}$$

Using (iv) $Y_1 = \frac{l^2}{9EI}(Fcl - 2Tc) - \frac{l^2L(M^*l + FclL - 4TcL)}{3\left[GJl^2 + 12EIL^2 - 20L^2\right]} - \frac{Tcl^2}{18EI}$

Therefore $Y_1 = \frac{l^2}{18EI}(2Fcl - 5Tc) - \frac{l^2L(M^*l + FclL - 4TcL)}{3\left[GJl^2 + 12EIL^2 - 20L^2\right]}$ .....(18)

Fixator Bar

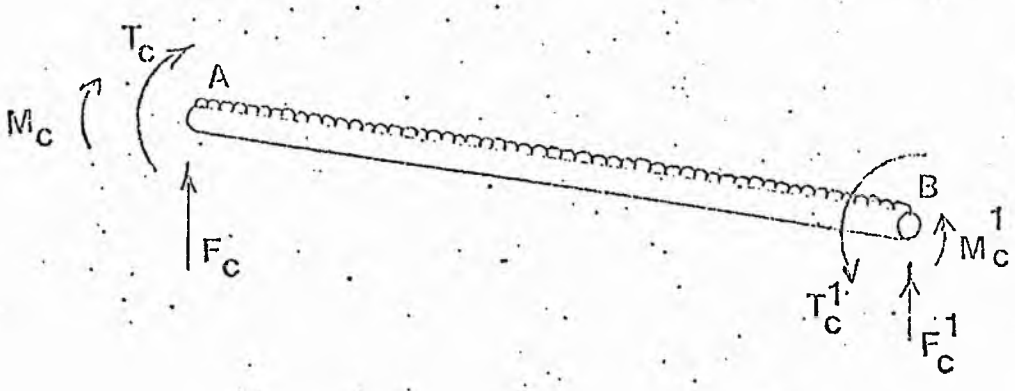

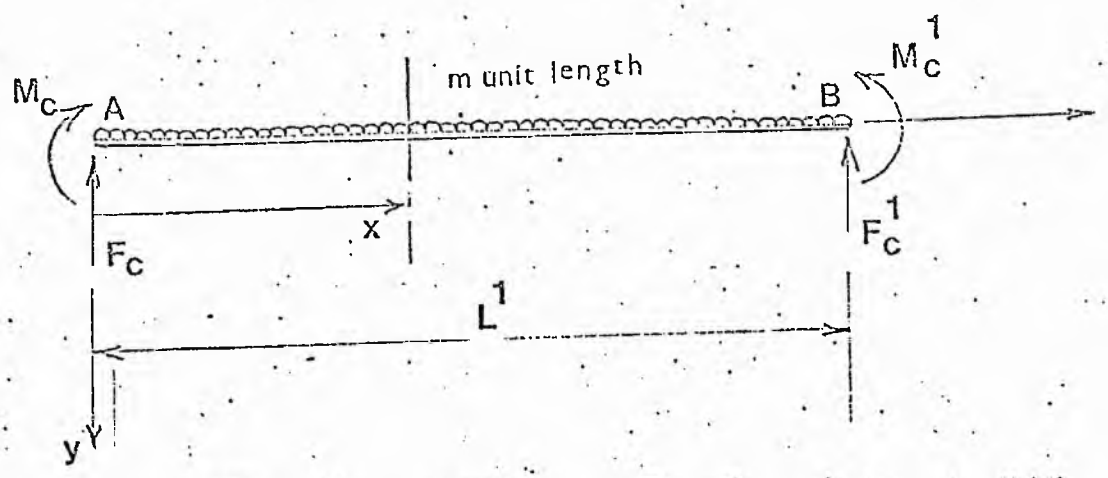

$$M_c^1 = M_c + F_c L^1 + \frac{mL^{1\,2}}{2}$$

$$EIy'' = -M_c + \frac{mx^2}{2} - F_c x$$

$$EIy' = -M_c x + \frac{mx^3}{6} - F_c \frac{x^2}{2} + A$$

$$EIy = -M_c \frac{x^2}{2} + \frac{mx^4}{24} - F_c \frac{x^3}{6} + Ax + B$$

Boundary conditions:

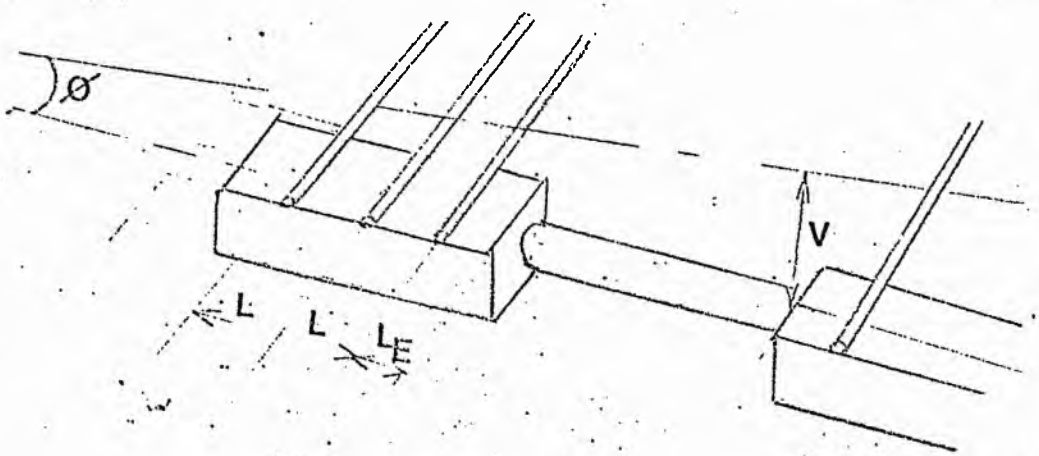

$$y_A = Y_1 + (2L + L_E)\,\emptyset$$

$$y_A = \emptyset$$

therefore $A = EI\emptyset$

and $B = EI(Y_1 + [2L + L_E]\,\emptyset)$

therefore $$y = \frac{1}{EI}\left[-M_c\frac{x^2}{2} + \frac{mx^4}{24} - F_c\frac{x^3}{6}\right] + Y_1 + (2L + L_E + L)\emptyset$$

....(19)

Considering deflection at B:

$$V = \frac{1}{EI}\left[-M_c\frac{L_1^2}{2} + \frac{mL_1^4}{24} - F_c\frac{L_1^3}{6}\right] + Y_1 + (3L + L_E)\emptyset \quad .....(20)$$

Analysis of Distal Area

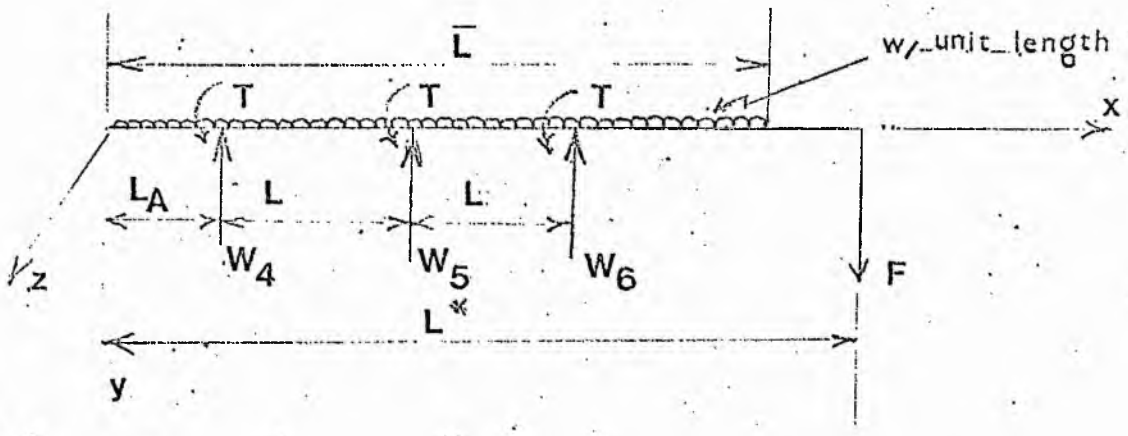

Assumption - leg is relatively very stiff, i.e. bending deformation neglected.

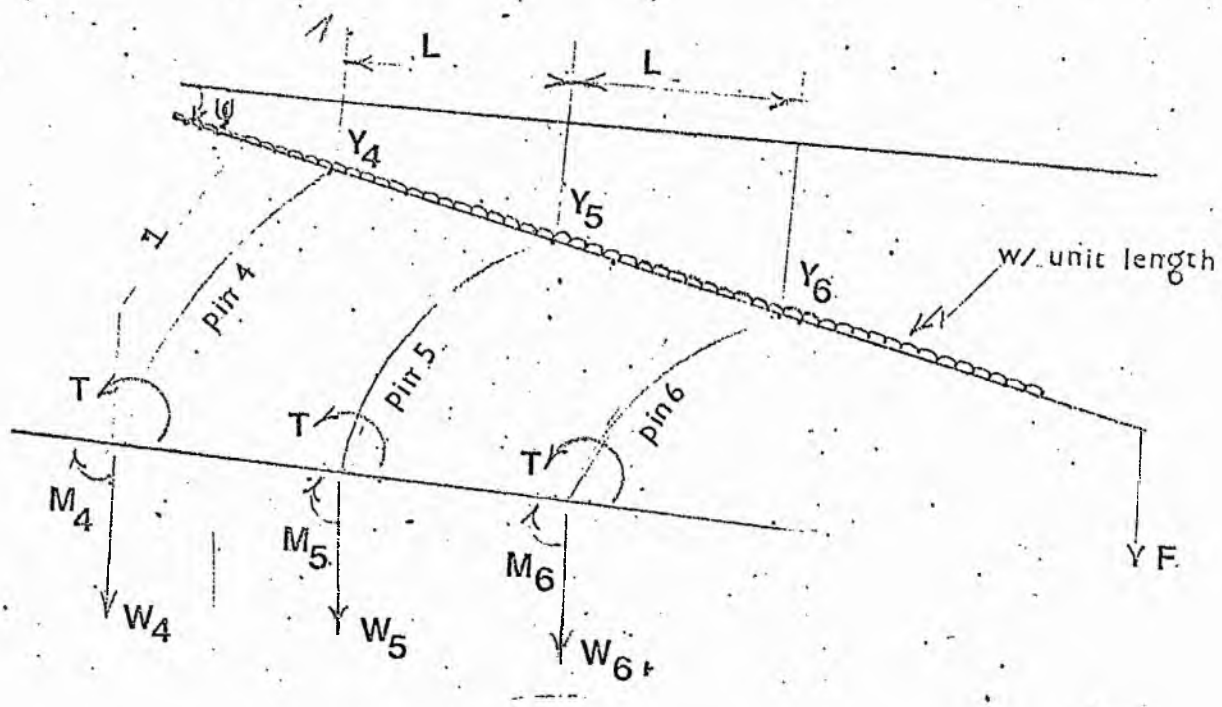

$$Y_5 = Y_4 + L\psi \quad \text{..... (21)}$$

$$Y_6 = Y_4 + 2L\psi \quad \text{..... (22)}$$

consider Pin 4:

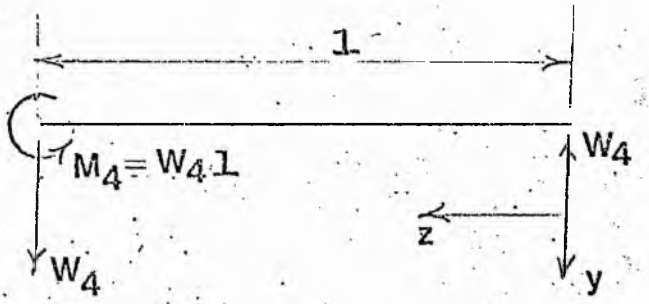

Macauley $EI \frac{d^2y}{dz^2} = W_4 z$

$$EI \frac{dy}{dz} = W_4 \frac{z^2}{2} + A$$

$$EIy = W_4 \frac{z^2}{6} - W_4 \frac{l^2 z}{2} + B$$

therefore $$y = \frac{W_4}{6EI} (z^3 - 3l^2 z + 2l^3)$$

Boundary conditions:

when $z = l, \frac{dy}{dz} = \emptyset$

therefore $$A = - \frac{W_4 l^2}{2}$$

when $z = l , y = \emptyset$

therefore $$B = \frac{W_4 l^3}{3}$$

At tip, $z = \emptyset , Y_4 = \frac{W_4 l^3}{3EI}$ .....(23)

and similarly for Y_5 and Y_6 as functions of W_5 and W_6 respectively.

Equilibrium of Distal Bone

Resolving forces vertically:

$$W_4 + W_5 + W_6 = F + w\bar{L} \quad \text{..... (i)}$$

Moments about 4th pin:

$$F(L - L_A) + \frac{w}{2} (\bar{L} - L_A) = \frac{w}{2} L_A^2 + W_5 L + 2W_6 L + 3T \quad \text{....(ii)}$$

But using (21), (22) and (23)

$$W_4 = \frac{3EIY_4}{l^3} \quad \text{..... (iii)}$$

$$W_5 = \frac{3EIY_5}{l^3} = \frac{3EI}{l^3}(Y_4 + L\psi) \quad \text{.....(iv)}$$

$$W_6 = \frac{3EIY_6}{l^3} = \frac{3EI}{l^3}(Y_4 + 2L\psi) \quad \text{.....(v)}$$

Equilibrium of Distal Carriage

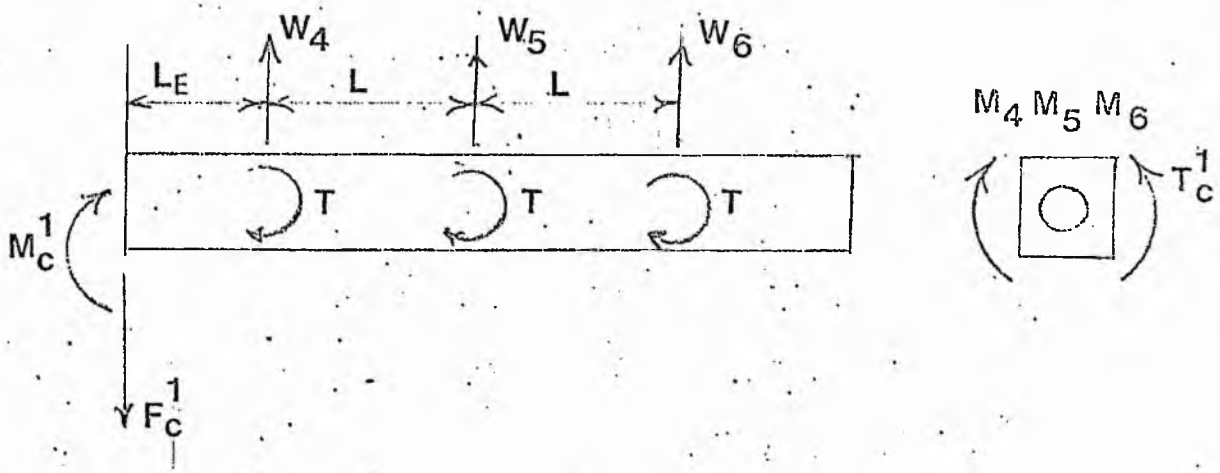

Moments about 4th pin

$$M_c^1 = W_5L + 2W_6L + F_c^1L_E$$

therefore from equations (iii), (iv) and (v)

$$M_c^1 = \frac{3EIL}{l^3}\left[3Y_4 + 5L\psi\right] + F_c^1L_E \quad \text{.....} \quad \text{(vi)}$$

Torques $T_c^1 = M_4 + M_5 + M_6$

$$= l(W_4 + W_5 + W_6)$$

from equations (iii), (iv) and (v)

$$T_c^1 = \frac{9EI}{l^2}(Y_4 + L\psi) \quad \text{.....} \quad (24)$$

Resolving forces vertically:

$$F_c^1 = W_4 + W_5 + W_6$$

$$\longrightarrow F_c^1 = \frac{9EI}{l^3}(Y_4 + L\psi) \quad \ldots\ldots\ldots\ldots\ldots\ldots (25)$$

Now (vi) becomes

$$M_c^1 = \frac{3EIL}{l^3}(3Y_4 + 5L\psi) + \frac{9EIL_E}{l^3}(Y_4 + L\psi) \quad \ldots(26)$$

FIXATOR BAR

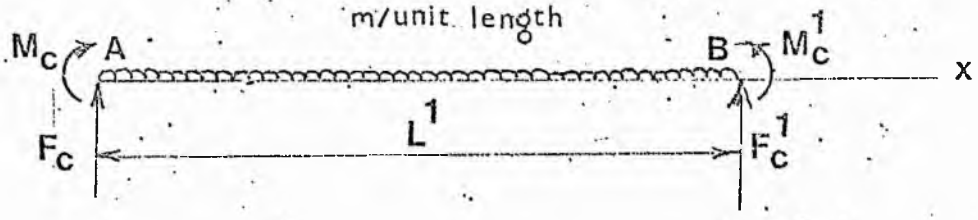

Equilibrium R

$$F_c + F_c^1 = mL^1$$

$$\longrightarrow F_c = mL^1 - \frac{9EI}{l^3}(Y_4 + L\psi) \quad \ldots\ldots\ldots\ldots\ldots\ldots (27)$$

Moments about A

$$M_c = F_c^1 L^1 + M_c^1 - \frac{mL^{1\,2}}{2}$$

$$M_c = \frac{9EIL^1}{l^3}(Y_4 + L\psi) + \frac{3EIL}{l^3}(3Y_4 + 5L\psi) + \frac{9EIL_E}{l^3}(Y_4 + L\psi) - \frac{mL^{1\,2}}{2}$$

$$M_c = \frac{3EI}{l^3}\left[3Y_4L^1 + 3L\psi L^1 + 3Y_4L + 5L^2\psi + 3Y_4L_E + 3L\psi L_E\right] - \frac{mL^{1\,2}}{2}$$

$$\ldots\ldots\ldots (28)$$

and $T_c = T_c^1 = \frac{9EI}{l^3}(Y_4 + L\psi) \quad \ldots\ldots\ldots\ldots\ldots\ldots (29)$

therefore (i) becomes $\frac{9EI}{l^3}(Y_4 + L\psi) = F + w\bar{L}$

$$Y_4 + L\psi = \frac{l^3}{9EI}\left[F + w\bar{L}\right]$$

$$Y_4 = \frac{l^3}{9EI}\left[F + w\bar{L}\right] - L\psi \quad \ldots\ldots\ldots\ldots\ldots\ldots (30)$$

Considering the torsion in the pins,

$$T = \frac{GJ\psi}{l}$$

therefore (ii) becomes

$$F(L - L_A) + \frac{w}{2}(\bar{L}^2 - 2\bar{L}L_A) = W_5L + 2W_6L + \frac{3GJ\psi}{l} \quad \ldots\ldots(vii)$$

let the L.H.S. be $\bar{F}$ i.e.

$$\bar{F} = F(L - L_A) + \frac{w}{2}(\bar{L}^2 - 2\bar{L}L_A) \quad \ldots\ldots\ldots\ldots\ldots(31)$$

(vii) then becomes

$$\bar{F} = W_5L + 2W_6L + \frac{3GJ\psi}{l}$$

$$\rightarrow \bar{F} = \frac{3EIL}{l^3}\left[Y_4 + L\psi + 2Y_4 + 4L\psi\right] + \frac{3GJ\psi}{l}$$

$$\rightarrow \bar{F} = \left[\frac{15EIL^2}{l^3} + \frac{3GJ}{l}\right]\psi + \frac{9EILY_4}{l^3}$$

using equation (30)

$$\bar{F} = \left[\frac{15EIL^2}{l^3} + \frac{3GJ}{l}\right]U + L\left[F + w\bar{L}\right] - \frac{9EIL^2\psi}{l^3}$$

$$\rightarrow \bar{F} = \left[\frac{15EIL^2}{l^3} + \frac{3GJ}{l}\right]U + L\left[F = w\bar{L}\right] - \frac{9EIL^2}{l^3}\psi$$

$$\bar{F} = \frac{3}{l^3}\left(2EIL^2 + GJl^2\right)\psi + L\theta + F + w\bar{L}$$

$$\psi = \frac{\left[\bar{F} - L\theta - (F + w\bar{L})\right] l^3}{3(2EIL^2 + GJl^2)} \qquad \ldots\ldots\ldots\ldots\ldots\ldots (32)$$

Solving for V, ϕ and θ (Appendix 3.1.2.

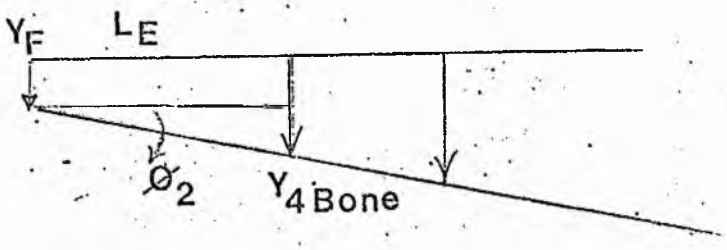

the total deflection at Y_4 Bone

Total $\quad Y_{4B} = V + L_E\phi + Y_4 - \theta l$

and total slope ϕ_2

$$\phi_2 = \phi + \psi = \cdot 046 \text{ Rads} = 2.7^\circ$$

then defelction at the Fracture Site (Y_F)

$$Y_F = Y_{4B} - L_E(\phi_2)$$

$$= 1.73 \text{ mm}$$

and rotation about the x axis (θ)

$$\theta = -\cdot 0068 \text{ Rads}$$

$$= .39^\circ$$

For intermediary values derived from the calculations see Appendix 3.1.2.

3.2.2 PART B.

When healing bone is loaded axially or in bending deflection at the fracture site occurs. Strain Energy techniques are used to determine the residual force transmitted to the fixator when healing bone is subjected to these loading conditions. There is no available data from which the changes in elastic properties of callus can be determined and stages of healing are therefore expressed as a percentage of the values for normal bone.

The analysis considers the effect of:

B.1 Three values of static axial compressive load applied to the bone during the later stages of healing. These are equivalent to partial body weight (37 kg), full body weight (75 kg) and a maximal load of four times body weight.

B.2 The application of bending moments to the bone which result from physiologically applied loads equivalent to the weight of the limb, distal to the fracture site.

B.1. Axial compressive loading of healing bone

The bone / fixator configuration of healing bone (Figure 42) is represented for analytical purposes by Figure (43),

where

MA = bending moments at A

F = applied compressive load

a = length of the pins

b = the distance from the centre of the fracture site to the middle pin

B.1.

Axial compressive loading of healing bone

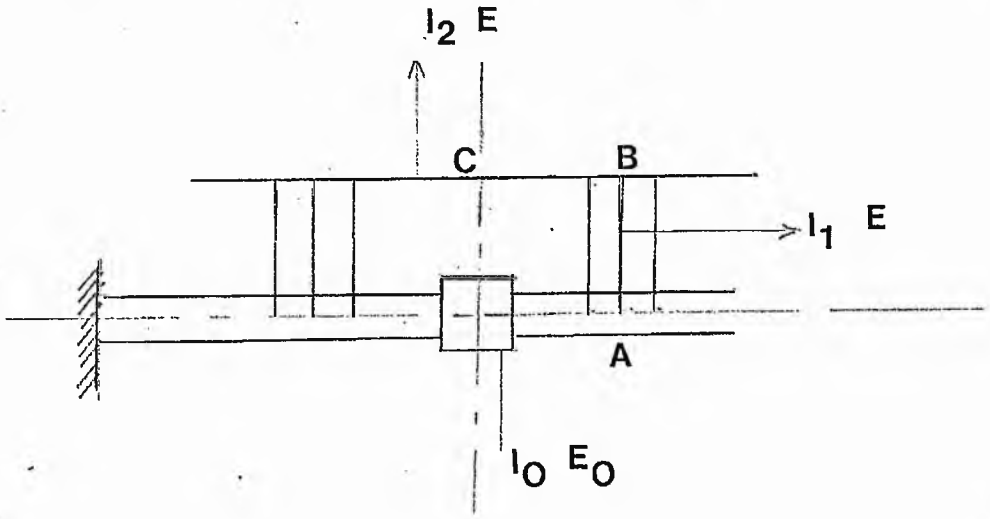

fig.42 Configuration of bone, pins & fixator

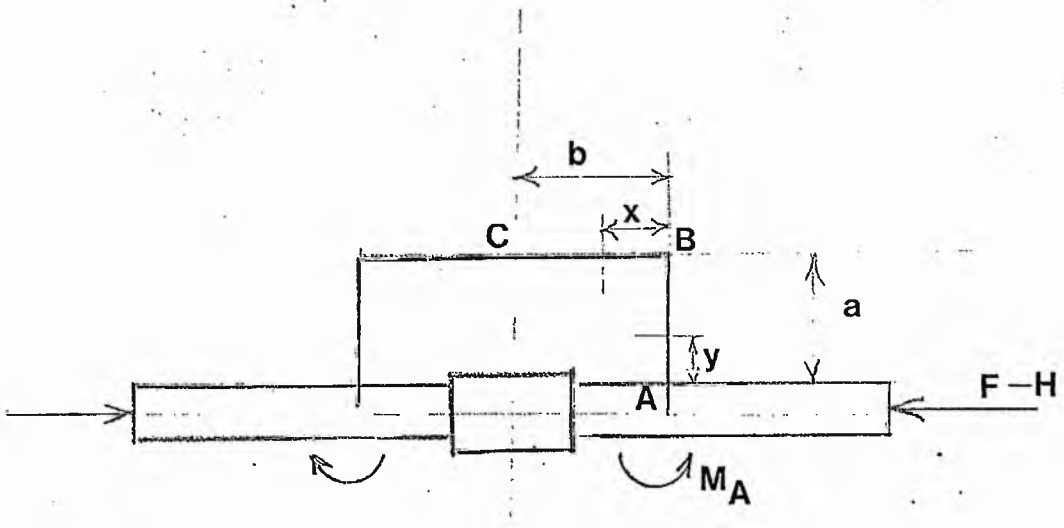

fig 43 Moments & Forces

I_0 = second moment of area of bone

E_0 = Young's modulus of bone

I_2 = second moment of area of the bar

E = Young's modulus of stainless steel

(For the actual values used in the calculation see Appendix 3.2)

The second moment area of each pin group is determined from the middle pin (Figure 44.) where

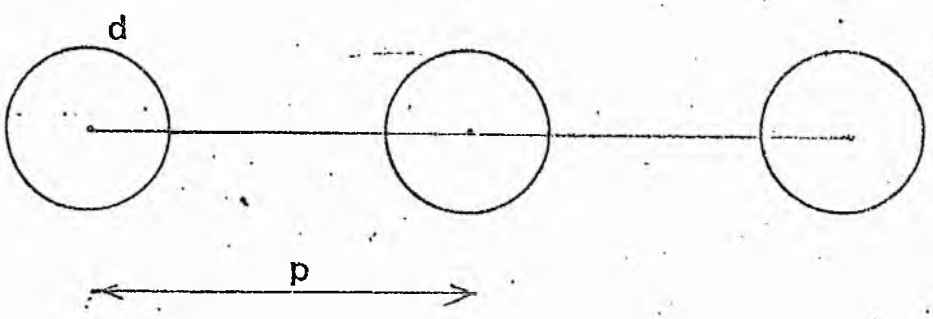

fig. 44

$$\text{the I of each pin} = \frac{d^4}{64} + \frac{d^2}{4} p^2$$

$$= \frac{d^2}{4} \left(\frac{d^2}{16} + p^2\right)$$

$$\text{therefore I of 3 pins} = \frac{d^2}{4} \left[\frac{3d^2}{16} + 2p^2\right]$$

The analysis considers a fracture located in the lower third of the leg. The dimensional data used in the calculations is listed in Appendix 3.2.

From Figure (43)

SECTION	M	$\frac{\partial M}{\partial M_A}$	$\frac{\partial M}{\partial H}$
AB	$M_A - H_y$	1	-y
BC	$M_A - H_a$	1	-a

where Θ_A = Rotation at A and U_A = Displacement at A, applying strain Energy Techniques, then

$$\Theta_A = \int_0^a \frac{H}{EI_1} \frac{\partial M}{\partial M_A} dy + \int_0^a \frac{M}{EI_2} \frac{\partial M}{\partial M_A} dx$$

$$= \frac{1}{EI_1} \int_0^a (M_A - H_y)dy + \frac{1}{EI_2} \int_0^b (M_A - H_a)dx$$

$$= \frac{1}{EI_1} \left[M_A y - \frac{H}{2} y^2 \right]_0^a + \frac{1}{EI_2} \left[M_A x - H_a x \right]_0^b$$

$$= \frac{1}{EI_1} \left[M_A a - \frac{H}{2} a^2 \right] + \frac{1}{EI_2} \left[M_A b - H_a b \right]$$

$$= M_A \left[\frac{a}{EI_1} + \frac{b}{EI_2} \right] - H \frac{a}{2} \left[\frac{a}{EI_1} + \frac{2b}{EI_2} \right] \quad \ldots\ldots\ldots (1)$$

and

$$U_A = \int_0^a \frac{M}{EI_1} \frac{\partial M}{\partial H} dy + \int_0^a \frac{M}{EI_2} \frac{\partial M}{\partial H} dx$$

$$= \frac{1}{EI_1} \int_0^a (M_A - H_y)(-y)dy + \frac{1}{EI_2} \int_0^b (M_A - H_a)(-a)dx$$

$$U_A = \frac{1}{EI_1}\left[-\frac{M_A}{2}y^2 + \frac{H}{3}y^3\right]_0^a + \frac{1}{EI_2}\left[-M_A ax + Ha^2 x\right]_0^b$$

$$= \frac{1}{EI_1}\left[H\frac{a^3}{3} - M_A\frac{a^2}{2}\right] + \frac{1}{EI_2}\left[Ha^2 b - M_A ab\right]$$

$$= -M_A\frac{a}{2}\left[\frac{a}{EI_1} + \frac{2b}{EI_2}\right] + H\frac{a^2}{2}\left[\frac{a}{EI_1} + \frac{3b}{EI_2}\right] \quad \ldots\ldots(2)$$

For Bone (where Strain Energy $= \frac{PL}{AE}$)

then $$U_A = \frac{b(F - H)}{E_0 A^1} \quad \ldots\ldots\ldots\ldots\ldots\ldots\ldots\ldots \quad (3)$$

and $$E_0 I_0 \Theta_A = -Mab$$

therefore $$\Theta_A = \frac{-M_A b}{E_0 I_0} \quad \ldots\ldots\ldots\ldots\ldots\ldots\ldots\ldots \quad (4)$$

therefore from equations (1) + (4)

$$M_A\left[\frac{a}{EI_1} + \frac{b}{EI_2} + \frac{b}{E_0 I_0}\right] = H\frac{a}{2}\left[\frac{a}{EI_1} + \frac{2b}{EI_2}\right]$$

therefore $$H = M_A \frac{1 + \frac{b}{a}\left[\frac{I_1}{I_2} + \frac{EI_1}{E_0 I_0}\right]}{\frac{a}{2}\left[1 + \frac{2b}{a}\frac{I_1}{I_2}\right]} \quad \ldots\ldots\ldots\ldots\ldots(5)$$

and equations (2) + (3) give:

$$F\frac{b}{F_0 A^1} = -M_A\frac{a}{2}\left[\frac{a}{EI_1} + \frac{2b}{EI_2}\right] + H\left[\frac{a^2}{2}\left[\frac{a}{EI_1} + \frac{3b}{EI_2}\right] + \frac{b}{E_0 A}\right]$$

$\ldots\ldots\ldots\ldots$ (6)

Therefore substitution from equation (5) gives solution for M_A from which the Residual Force H may be found.

Solving for M_A and H the results are tabulated in Table 3.1 where F denotes body weight (B.W.). The strain (ε) detectable in the bar is derived from these results (table 3.1) where $\varepsilon = \frac{\sigma}{E}$ and $\sigma = \frac{My}{I}$

TABLE 3.1

F	MaN/M	H(N)	$\varepsilon x10^{-6}$
$\frac{F}{2}$	.04	1.23	3.7
F	.089	2.6	8.8
4xF	.35	10.6	36

It is found that the magnitude of the moments (MA) and residual force (H) are small and the level of strain correspondingly low. A proportional increase in moments, residual force and calculated strain is found in response to peak loads of four times body weight, but the calculated strain from these conditions does not exceed 40 micro-strain (40 $\mu\varepsilon$).

The analysis was then extended to consider the effects of axial loading of the bone during the intermediary stages of healing. Lower values of Young's modulus for bone (E_0) were substituted in equations 5 and 6 (p110) to represent partially healed bone. An applied load of approximately half the standard male weight (37 kg) was assumed for each stage of healing.

These results are tabulated in Table 3.2.

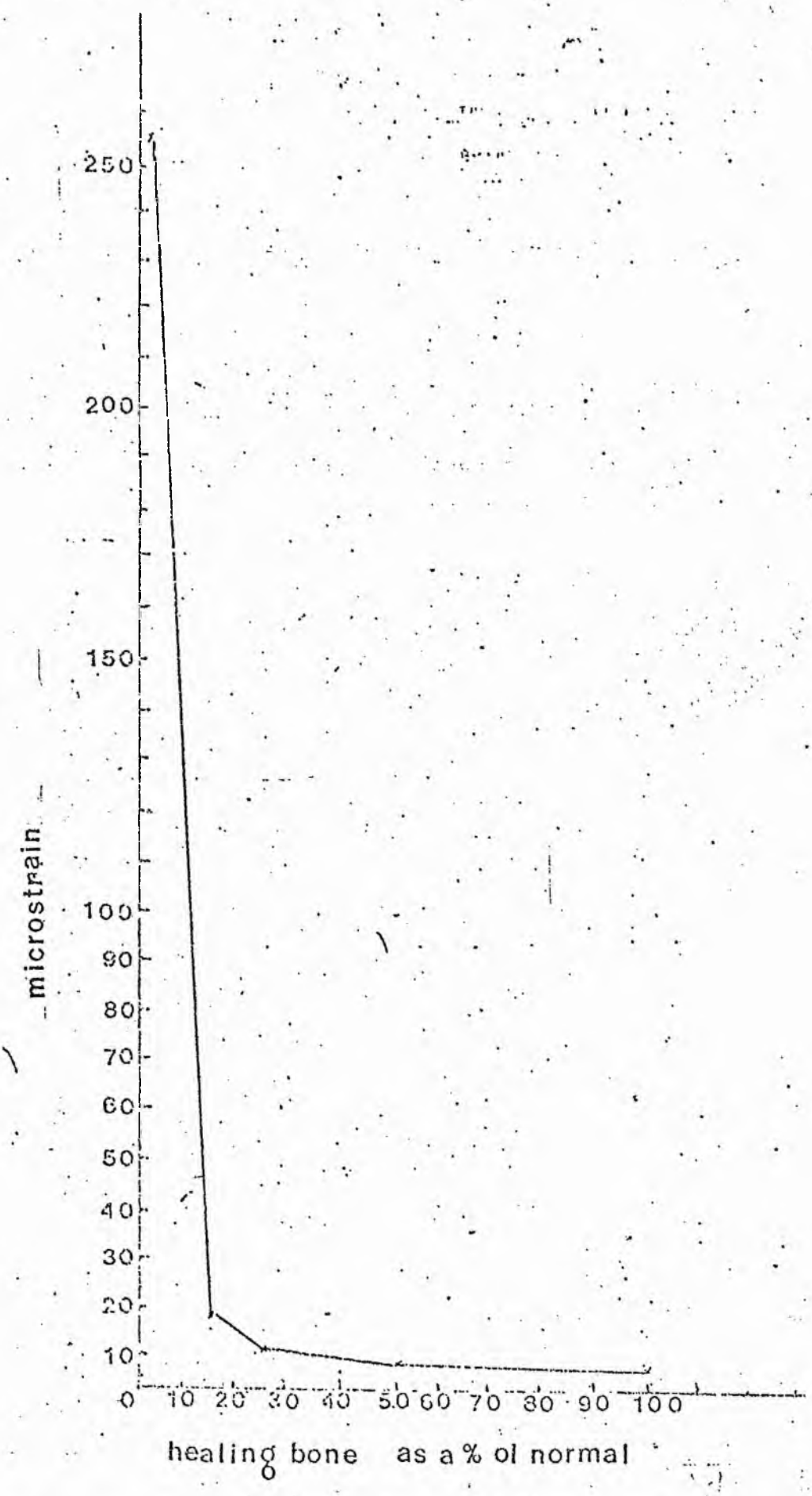

Figure 45: Theoretical limb of strain detectable in the fixator Bar during healing of the bone

TABLE 3.2

% VALUE OF NORMAL BONE	$E(N/M^2)$	M_A	H(NM)	$\mathcal{E} \times 10^{-6}$
NORMAL 100%	25×10^9	.04	1.23	3.7
50%	12.5×10^9	.06	2.19	7.09
25%	6.75×10^9	.07	3.47	11
15%	375×10^7	.03	5.38	18.3
1%	25×10^7	1.1	758.5	255

The graphical presentation of these results, recording calculated values of strain against the change in the material elastic properties of bone during healing is presented in Figure 45. This analysis shows that corresponding changes in the level of strain are small during the later stages of healing (between 15% and 100% of normal values for the Young's Modulus of bone). It can be seen from Figure 45 that rapid decline of the exponential curve occurs between 1 and 25% of the normal values for bone. Between 1 and 15% the magnitude of the residual force increase dramatically indicating loss of stability at the fracture site and a corresponding increase in the level of strain. These findings are later compared, in Chapter 6, with those of healing bone using the Prime Stress Program and the application of these results to patient care are then discussed.

B.2 Healing Bone subjected to Bending

From the previous analysis presented in B.1 consider the application of bending moments (M) where M are the moments due to the weight

of the limb distal to the fracture site. This analysis considers the loading on the distal part of the leg during a non-weight bearing, straight-leg raising activity.

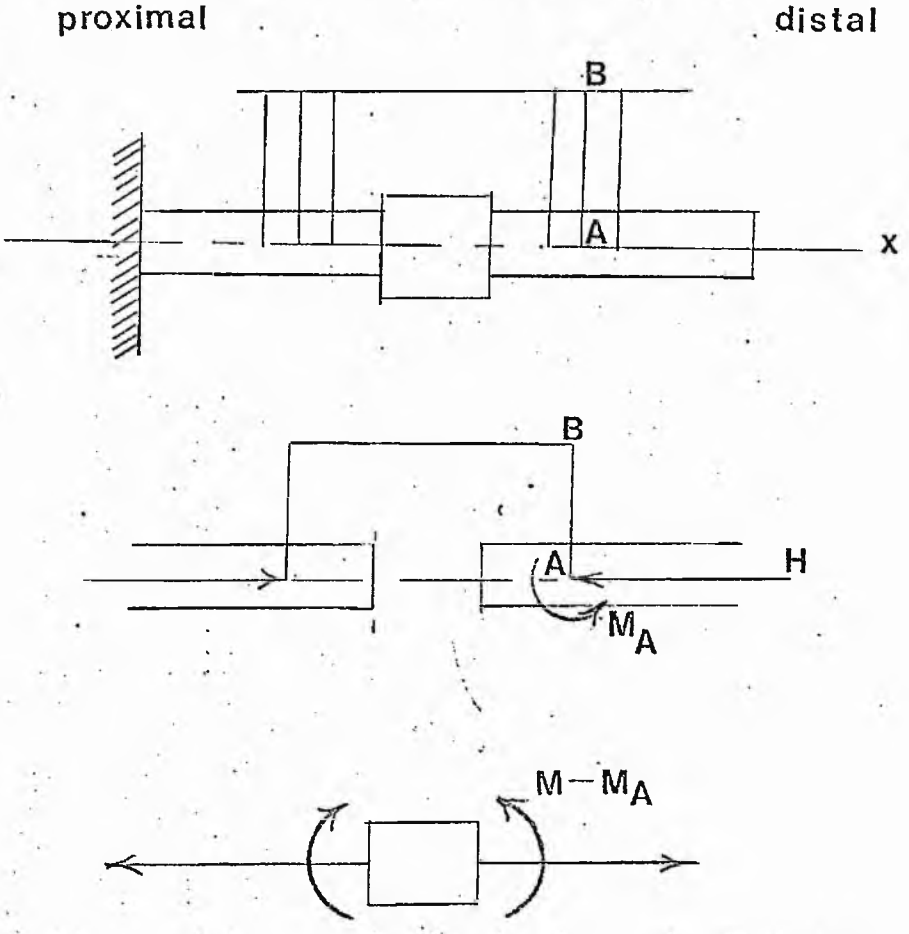

Equation (3) from the previous analysis becomes

$$U_A = \frac{-bH}{E_0 A^1} \quad \ldots\ldots\ldots\ldots\ldots\ldots\ldots\ldots\ldots\ldots \quad (7)$$

and equation (4) becomes

$$E_0 I_0 \Theta_A = (M - M_A)b$$

$$\text{therefore} \quad \Theta_A = \frac{(M - M_A)b}{E_0 I_0} \quad \ldots\ldots\ldots\ldots\ldots\ldots\ldots\ldots\ldots\ldots \quad (8)$$

therefore from equations (2) and (7)

$$\frac{-bH}{E_0 A^1} = -M_A \frac{a}{2}\left[\frac{a}{EI_1} + \frac{2b}{EI_2}\right] + H\frac{a^2}{3}\left[\frac{a}{EI_1} + \frac{3b}{EI_2}\right]$$

solving for M_A

$$\text{therefore} \quad M_A = \frac{H\frac{a^2}{3}\left[\frac{a}{EI_1} + \frac{3b}{E_2I_2}\right] + \frac{b}{E_0}\frac{H}{A^1}}{\frac{a}{2}\left[\frac{a}{EI_1} + \frac{2b}{EI_1}\right]}$$

and equations (1) and (8) gives

$$\frac{(M - M_A)}{E_0I_0} b = M_A\left[\frac{a}{E_1I_1} + \frac{b}{E_2I_2}\right] - H\frac{a}{2}\left[\frac{a}{E_1I_1} + \frac{2b}{E_2I_2}\right]$$

solving for H

$$H = \frac{M_A\left[\frac{a}{EI_1} + \frac{b}{EI_2}\right] - \left[\frac{M - M_A}{E_0 I_0}\right] b}{\frac{a}{2}\left[\frac{a}{EI_1} + \frac{2b}{EI_2}\right]}$$

This analysis again demonstrated little change in the residual force transmitted to the fixator system, during the later stages of healing.

TABLE 3.3

% VALUE OF NORMAL BONE	M_A(Nm)	H(N)
100%	1.9	32.4
50%	1.97	32.8
25%	1.99	33

The magnitude of this force (H) is however greater than the calculated residual force from the previous analysis in which healing bone is loaded

axially with partial body weight (see Table 3.2).

The conclusion was drawn at this stage of the analysis that the fixator bar becomes redundant during the later stages of healing. This justifies the clinical practice of removing the bar before complete consolidation or ossification has occurred.

This analysis is however limited since the dimensional properties of callus, which also change with time, were not considered. Further investigation of the effects of changes in the dimensional and elastic properties of callus was subsequently undertaken in the analysis using the Prime Stress program.

CHAPTER FOUR: THE EXPERIMENTAL WORK

4.1.1 In the proposed experimental work on a bone/fixator configuration it was felt that a standardized approach to testing could be achieved by the design of a simple wood model replicating bone. From a review of the literature it was found that the hardwood Greenheart had some material properties similar to those of tibial cortical bone (see Chapter 2). This observation was confirmed by completing a series of tests on specimens of Greenheart using standard techniques for testing material properties. It was therefore decided to use this wood in the design of a bone model, the diameters of which were determined by the weakest section of the tibia, (see Chapter 2 Part B). From the data presented by Piezali et al (Figure 10) the gross cortical area at this level (approximately 70% of length from the proximal end) was determined by replotting this data as a percentage of length. The total length of the tibia was assumed to be 420 mm. The actual dimensions of the bone model, of uniform cross-section, are detailed in Figure 46

The tube was reamed to a length of 120 mm from the distal end and 270 mm from the proximal end (Figure 46) and "a fracture site" selected at the junction of the middle and lower third of the model.

4.1.2.1 The design of the Denham Bar Transducer

From the analysis in Chapter Three and a consideration of bar deformations resulting from functional loading of a fractured limb (see Chapter 2 Part D) three components of deformation were determined.

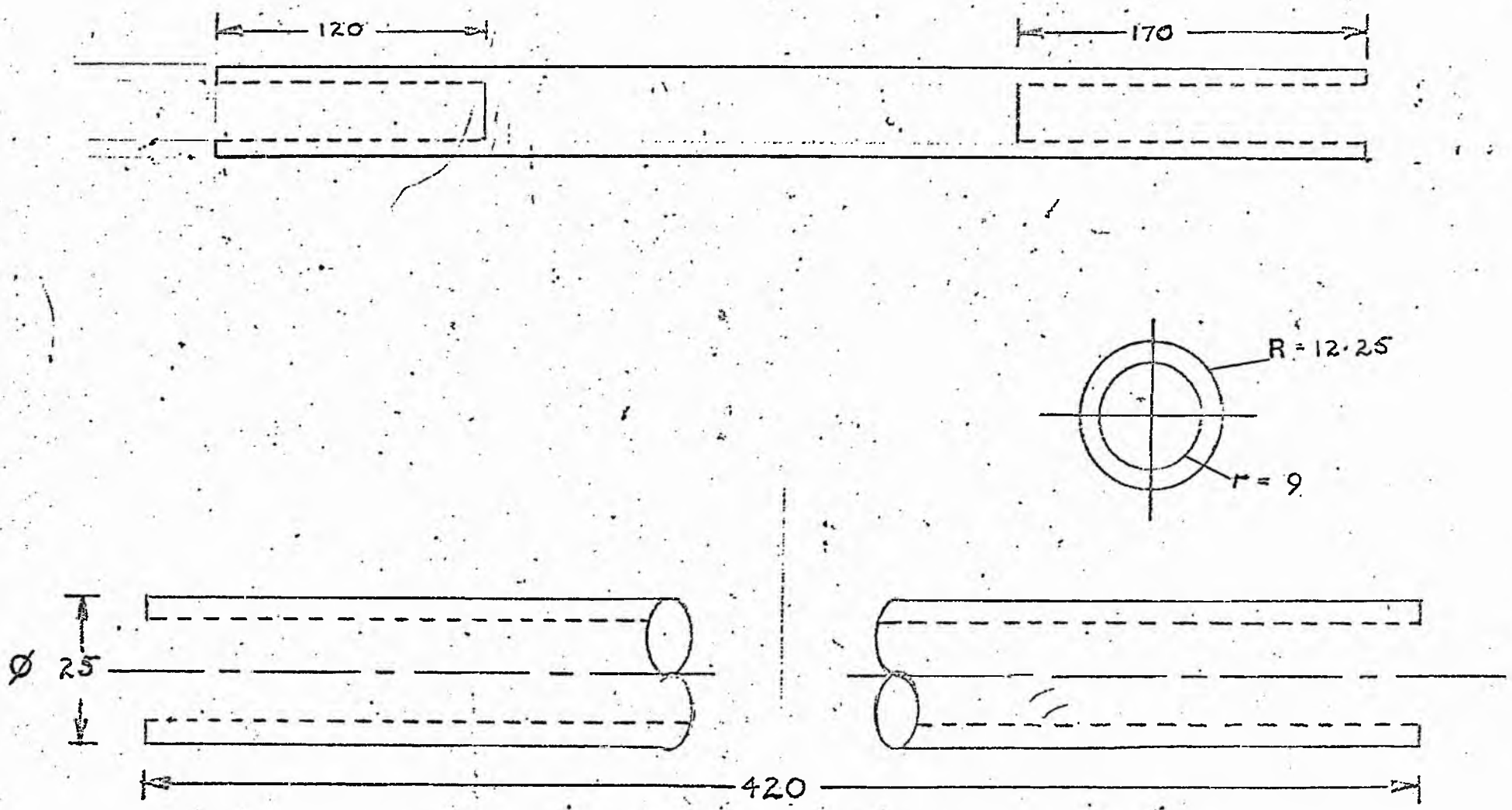

fig. 46 The bone model

These are :

1. Bending
2. Torsion
3. Shear

1. Bending

Bending of the bar in the antero-posterior or medio-lateral direction will arise when bending moments are applied to the bone, e.g. during walking or a straight leg raising activity. As a result tensile strains (positive) will arise on the convex surface of the bar and negative compressive strains on the concave surface. (Fig.47 a)

2. Torsion

Torsion of the bar will result when one section of the fractured limb is fixed while the remaining section rotates about the longitudinal axis of the bone, e.g. in the "non-weight" bearing position when a blanket is pulled across the foot, or in the weight bearing position during the "push-off" phase of walking. Alternatively, as the patient turns to remove items from a locker, the planes of principal stress in torsion are at 45° to the neutral axis of the bar (Figure47b) so that an element A will be subject to tensile strain in one direction and compressive strain in the others.

3. Shear

Shear deformations arise when a horizontal displacement of the fracture ends produces relative displacement of each fragment and the

a) bending

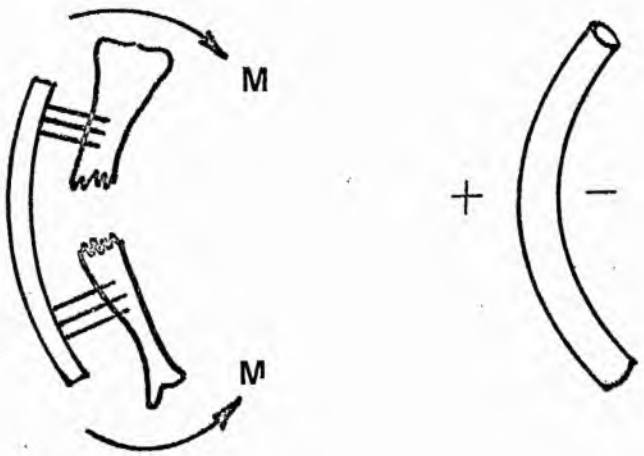

b) torsion

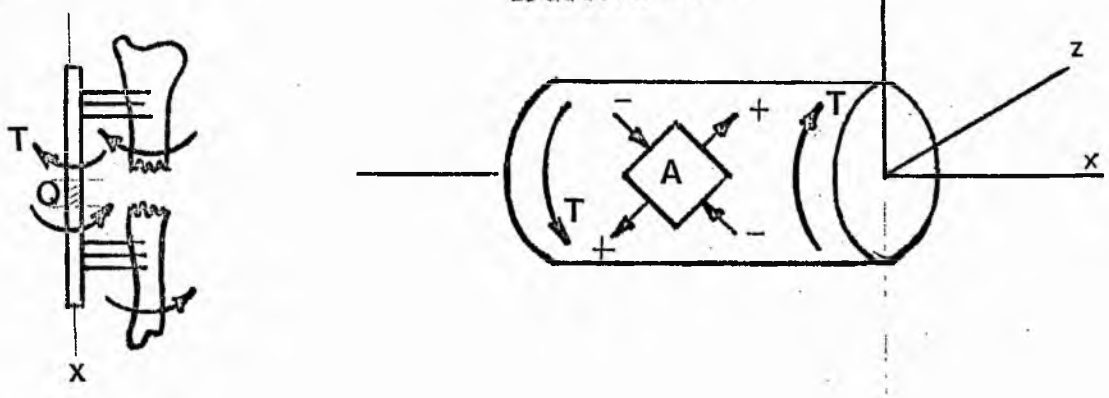

c) shear

fig. 4.7

bar assumes an S-shaped deformation (Figure 4.7c) providing firm fixation at the pin/bone junction is maintained. Consequently tensile strains will occur in the central section of bar and bending at either end. Tensile strains will also arise therefore on the convex surface at V (Figure 4.7c) and compressive strains on the concave surface at (C).

We have seen, however, from the analysis presented in Chapter 3 Part B that simple activities, such as straight leg raising, results in bending and torsion of the bar occurring simultaneously. The magnitude of the strains will therefore be the summation of strain resulting from torsion, bending and shear deformations.

4.1.2.2 The location of the strain gauge

The design of the modified Denham Bar was based upon a model which was obtained from a clinical source (Wyn-Jones 1979). It became apparent that the length of the bar and carriages that are in clinical use may vary. From a discussion with J. Edge (1979) it was also found that the original plastic coating of the carriages (to prevent electrolytic action between two dissimilar metals) was found to be impracticable. (The bar and carriages are re-usable and damage to the plastic coating is often sustained on removal of the pins from the carriages).

In this work the initial criteria to be met by the instrumented device were defined as follows:

1. The instrument should be sufficiently sensitive to record all levels of strain in bending, torsion and shear.
2. Electrically safe for the patient and independant from other electrical sources.

3. Minimal cost.

4. Wires, gauges and leads should not be damaged either on removal of the device, or when the bar is in situ.

5. The bar should be removable to allow normal clinical testing to be conducted.

From observations made on the clinical use of the device it was felt that the most available section of the bar for instrumentation was the middle one. It was concluded from a consideration of the likely bar deformations (4.1.2) that detection of strain would be feasible at this level.

Timoshenko (1965) has shown that high shearing stresses are present in the corners of a key-way. The Denham Bar has a keyway which extends along its entire length thus allowing free passage of the two aluminium carriages. Detection of strain by embedding strain gauges in the floor of the keyway was not therefore considered feasible since some distortion of the signal would occur due to local stresses. A modified bar was then designed with a central section waisted to the depth of the thread and the keyway terminated at this level. Large radii (18.4 mm) were designed for the junctions between the threaded and waisted section (Figure 48). The total length of the modified bar was 294 mm using $\frac{1}{2}$" threaded stainless steel bar. The two carriages were 15 mm square and 70 mm long. Each carriage consisted of a central core equal to the diameter of the threaded section of bar (Figure 48). Excessive rotation was prevented by two Alan keys inserted towards the ends of the carriages in line with the keyway of the fixator bar.

The Strain Gauges

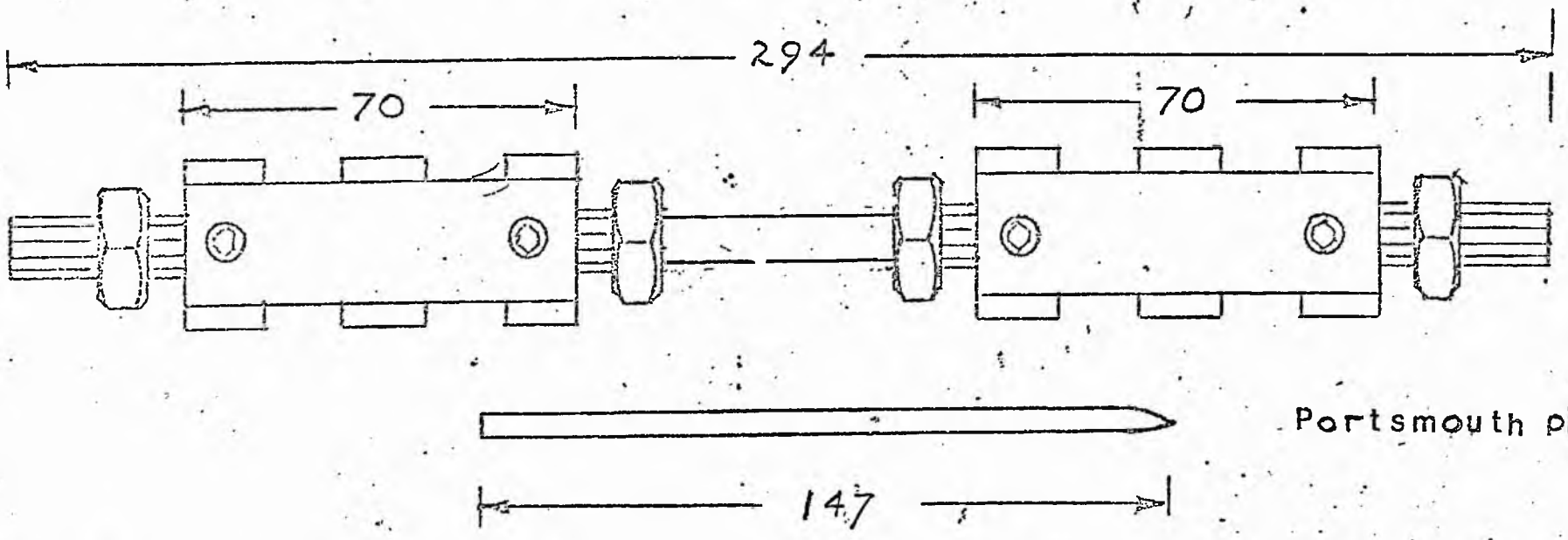

fig 48 The modified bar

Four 1 mm length strain gauges (Gauges 1, 2, 3 and 4) were bonded to the middle of the waisted section of bar, around the circumference, for the detection of bending. They were positioned in two pairs, so that the two gauges of each pair were diametrically opposite (Figure 49). Gauge 3 was in line with the keyway and gauge 2 diametrically opposite forming the first pair. Gauges 1 and 4, the second pair, were located at 90° from the first pair, and again diametrically opposite. Two rosette gauges, with two gauges forming each rosette, for the detection of torsion were oriented at 45° to the long axis of the bar and located diametrically opposite and remote from one end of the waisted section. These four gauges are represented in Figure 49 as gauges 7, 8, 9 and 10. The leads from the torsion gauges were then led to the floor of the keyway at A where they were bonded along its length. The fine leads emerging from the ends were ultimately connected to the recording instruments. Similarly the leads from gauges 1, 2, 3 and 4 were bonded to the floor of the keyway at B (Figure 49).

When the bonding of the gauges and the attachment of the inter-connecting wires had been completed, it was found to be too fragile. It was felt that additional protection of the gauges was required. The whole of the central section was therefore encased in an acrylic jacket (Plate A). This meant, however, that the bar could not be easily removed when in-situ with bone and the transfixing pins.

4.1.3 Recording Instruments

The initial requirements of recording instruments for clinical use are defined as follows:

1. A wide frequency response to cope with dynamic in-vivo loading, e.g. during walking.

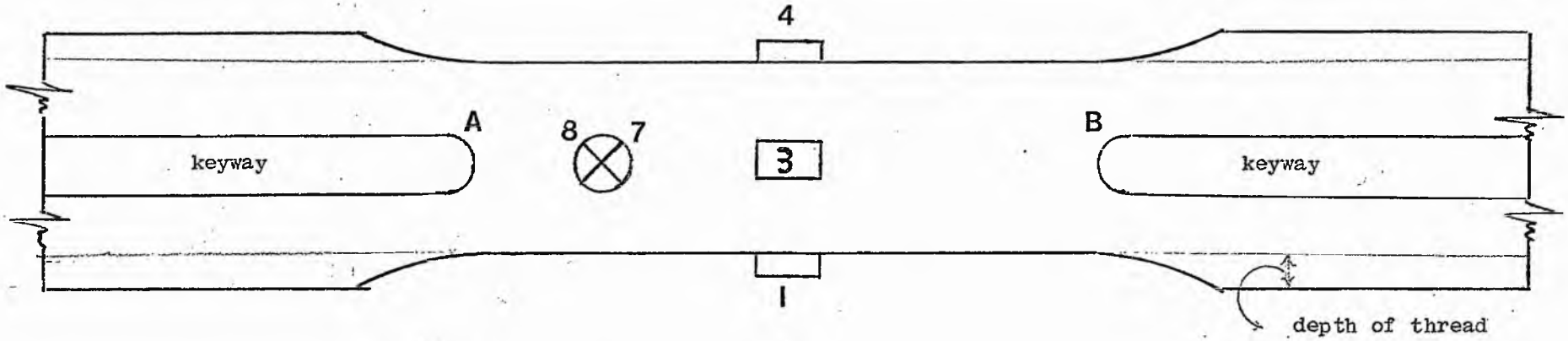

Gauge 3 diametrically opposite 3

Gauges 9 + 10 diamterically opposite 8 + 7

Figure 49: Position of gauges on central section of the modified Denham Bar

PLATE A

2. Portable and light for ease of transportation from bed to bed, or from one hospital to another.

3. Simple to use.

4. Durability.

5. Safe.

6. Insulation from other sources of electrical interference.

Two sources of equipment were considered for the preliminary experimentation:

a) The Dual Channel Gemini bridge amplifier.

b) The Vishay Ten Channel Recorder.

Both systems are transportable and the Gemini has particularly good frequency response at 500 Hz. The main limitation, however, was the maximum use of only two channels. The Vishay has a frequency response of up to 60 Hz, but thereafter the manufacturers recommend connection to a high impedance oscillograph for dynamic strain recording. Gain is constant with the Gemini and sinusoidal movement up to 500 Hz, but the reliability deteriorates with uneven sinusoidal movement, e.g. gait. Beyond 500 Hz a phase lag between the transducer movement and output increases with increasing frequency.

The Vishay output is $\pm$ 1/2 m.a. unfiltered D.C. with sensitivity variable from 80-8000 microstrain and has an accuracy of .1% or 5$\mu\varepsilon$ whichever is the greater.

The advantages of using the Vishay in the preliminary investigation (to determine the feasibility of the Denham Bar Transducer) lay in the ability to detect the level of strain from each gauge. An internal

dummy gauge precludes the use of an additional gauge bonded to an unstrained piece of material (for temperature compensation). It was originally planned to use a full bridge configuration. Following further discussion, however, it was suggested that a 3-wire Quarter Bridge technique should be used since this reduces the temperature-induced lead wire resistance.

Quarter Bridge Three-wire technique

This technique places half of the temperature-induced lead wire resistance change in series with the internal gauges, while the other half is in series with the active gauge R_1 through the two lead wires A and B so that it may be reasoned from Figure 50

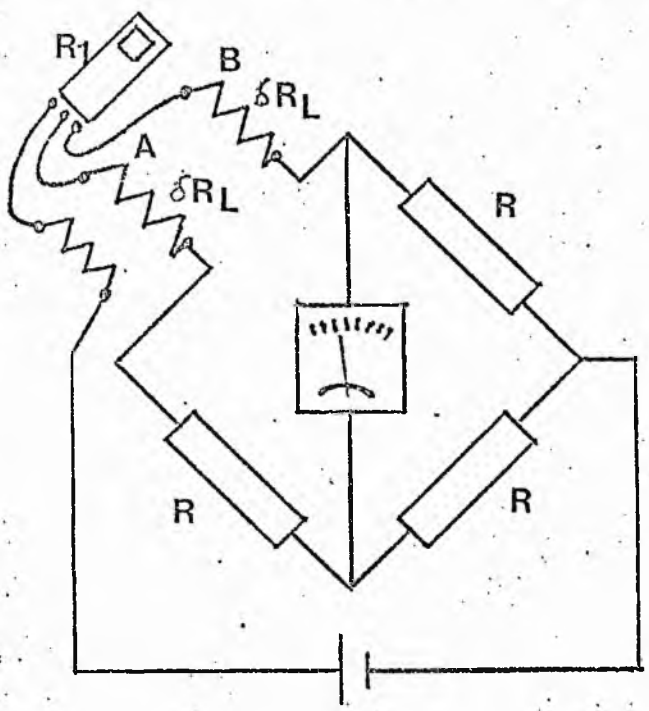

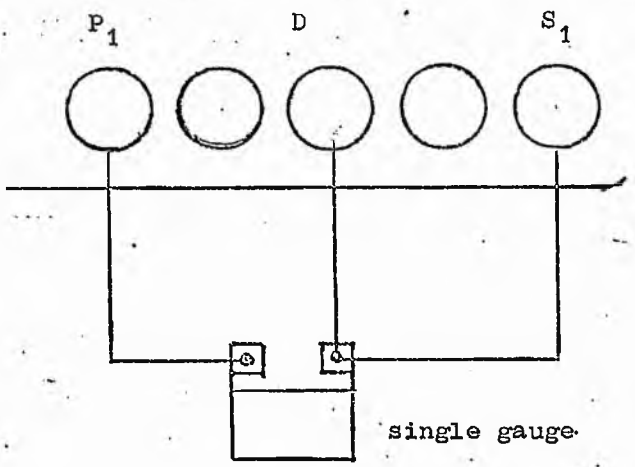

QUARTER BRIDGE WIRING DIAGRAM

fig. 50

that

$$\frac{R + \delta R_L + \delta R_{temp}}{R_1 + \delta R_L + \delta R_{temp}} = \frac{R}{R_1}$$

In the experimental work, the leads from each gauge emerging from the ends of the bar, were connected to the P-350 Digital Strain Indicator according to the wiring diagram (Figure 50) where D is the internal dummy gauge. Since the P-350 Strain Indicator (Plate B) will accept only one input to either a Quarter, Half of Full Bridge, an additional multi-channel Strain Gauge data acquisition system (the SB-1 Switch Box) is required which may be seen in Plate B .

4.2.1 Calibration of the Bar

The Bar was calibrated in torsion using the bench mounted TECQUIPMENT TORSION Testing Machine (SM1/2) and, in tension using the Hounsfield Tensometer (Plate B).

4.2.2 Calibration of the bar in torsion

Two identical alignment jigs were designed to provide rigid fixation of each end of the bar in the torsion apparatus. These jigs (Figure 51) also minimised the damage to the threaded ends of the bar and the leads emerging from the floor of the keyway.

The Design of the Alignment Jigs

The jigs consisted of a length of mild steel, $4\frac{1}{4}$" long and $\frac{3}{4}$" diameter with a central section threaded to within 1" of the tapered end (Figure 51) which inserted into the two-jaw chucks located at either end of the machine mainshaft (Plate C). The two locknuts (Plate C) and the two jigs (Plate C) were carefully screwed on to the bar after first driving the fine lead wires back through the keyway to emerge from the jigs at A and B on the inner side of the locknuts. Clockwise

PLATE B

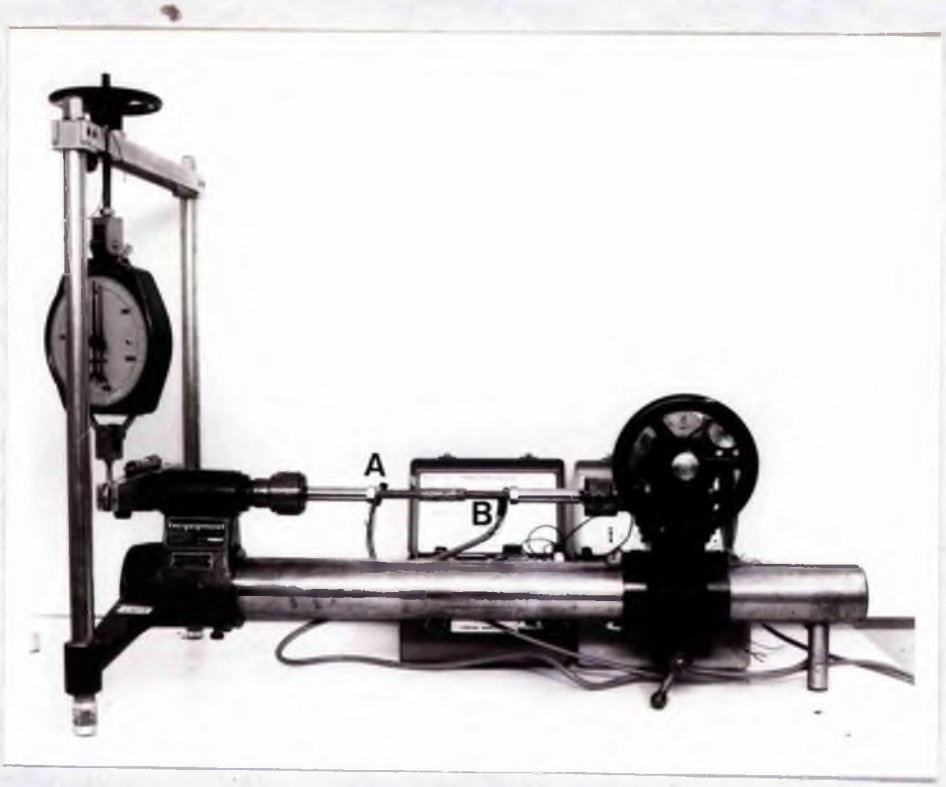

PLATE C

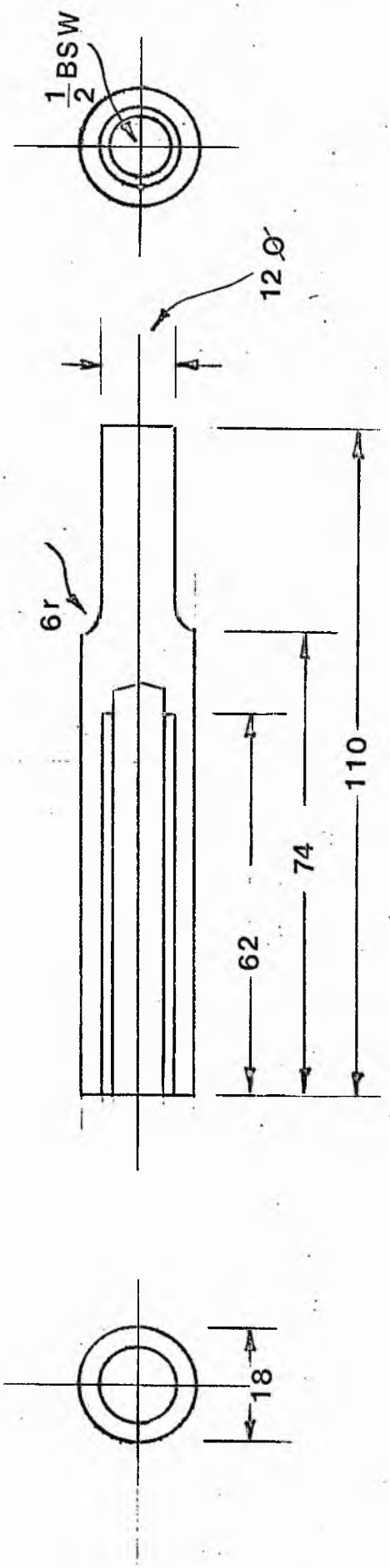

Figure 51 : Alignment jigs

rotation of the jigs, and therefore loosening of the test rig, was prevented by tightening the lock nuts with a spanner against the alignment jigs.

The Testing Procedure

All gauges were connected to the multi-channel recorder and each wired for the quarter bridge three wire technique. The tapered ends of the alignment jigs were inserted horizontally into the two jaw chucks of the machine and firmly locked into position. The Torque Arm and Spring Balance were zeroed in accordance with the Tecquipment No. SM1/2 testing manual. The dial gauge (Plate C) was then zeroed by adjusting the knurled nut at the top right hand side of the gauge, and the initial displacement of the protractor scale noted. The revolution counter and the strain gauges were zeroed with a nil load condition. Incremental loads of 40 mm D_A.N. were applied (NB 1 lb inch = 11.2 mm D_A.N.) and it was noted that up to 160 mm D_A.N, or 1.5° of displacement, that slipping took place. This was counteracted by fixing the hand wheel at each incremental point by firmly supporting the knob on the hand wheel and then taking the readings. Incremental loads of 40 mm D_A.N. were then applied to 900 mm D_AN, then unloaded at 80 mm D_AN decrements. These experiments were repeated four times (Tests 1, 2, 3 and 4) on the same day at ambient room temperature (20°C).

4.2.3 Results of the Torsion Tests

Since the bar was in pure torsion a minimal, non-linear response was noted from gauges 1-4. The level of strain did not exceed $\pm$ 30 $\mu\varepsilon$ and marked drift was found in gauge 4. The drift in this gauge was

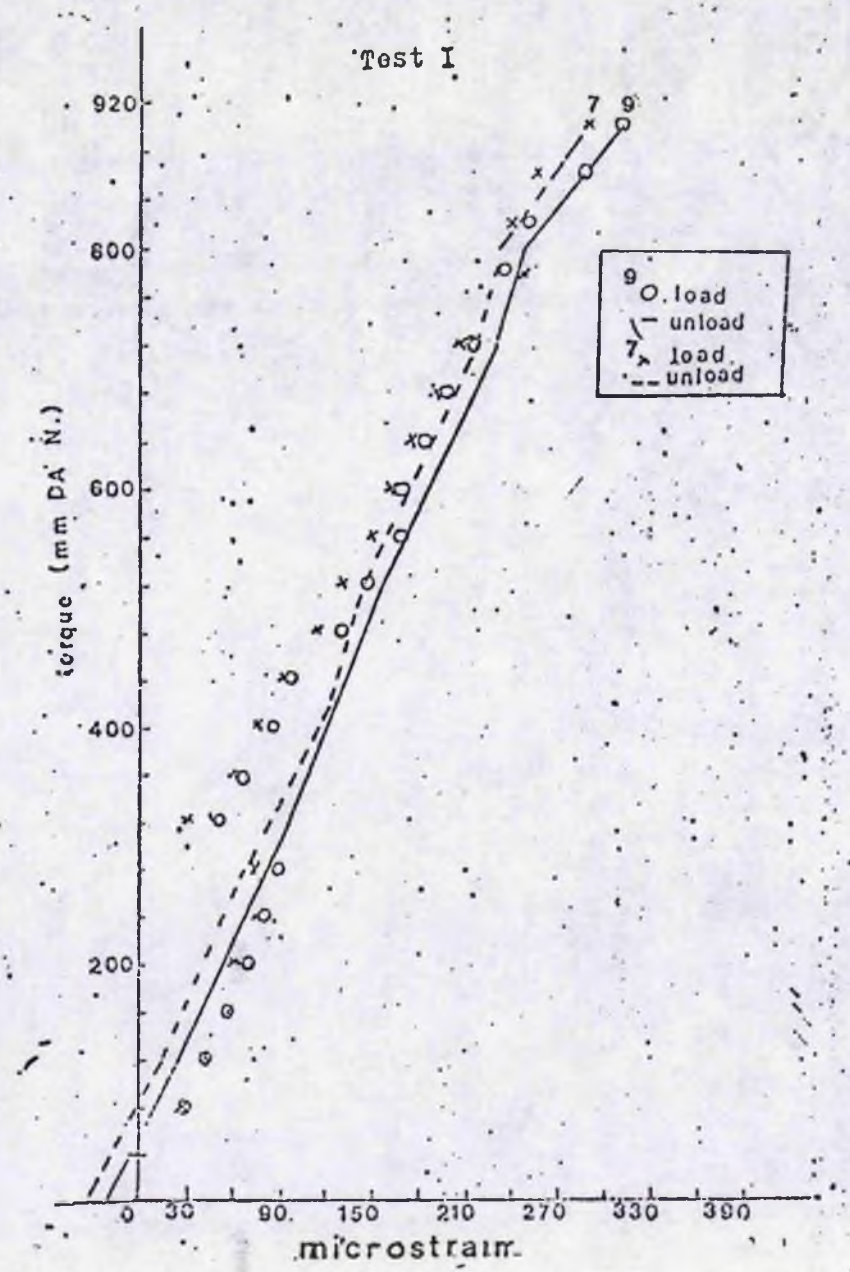

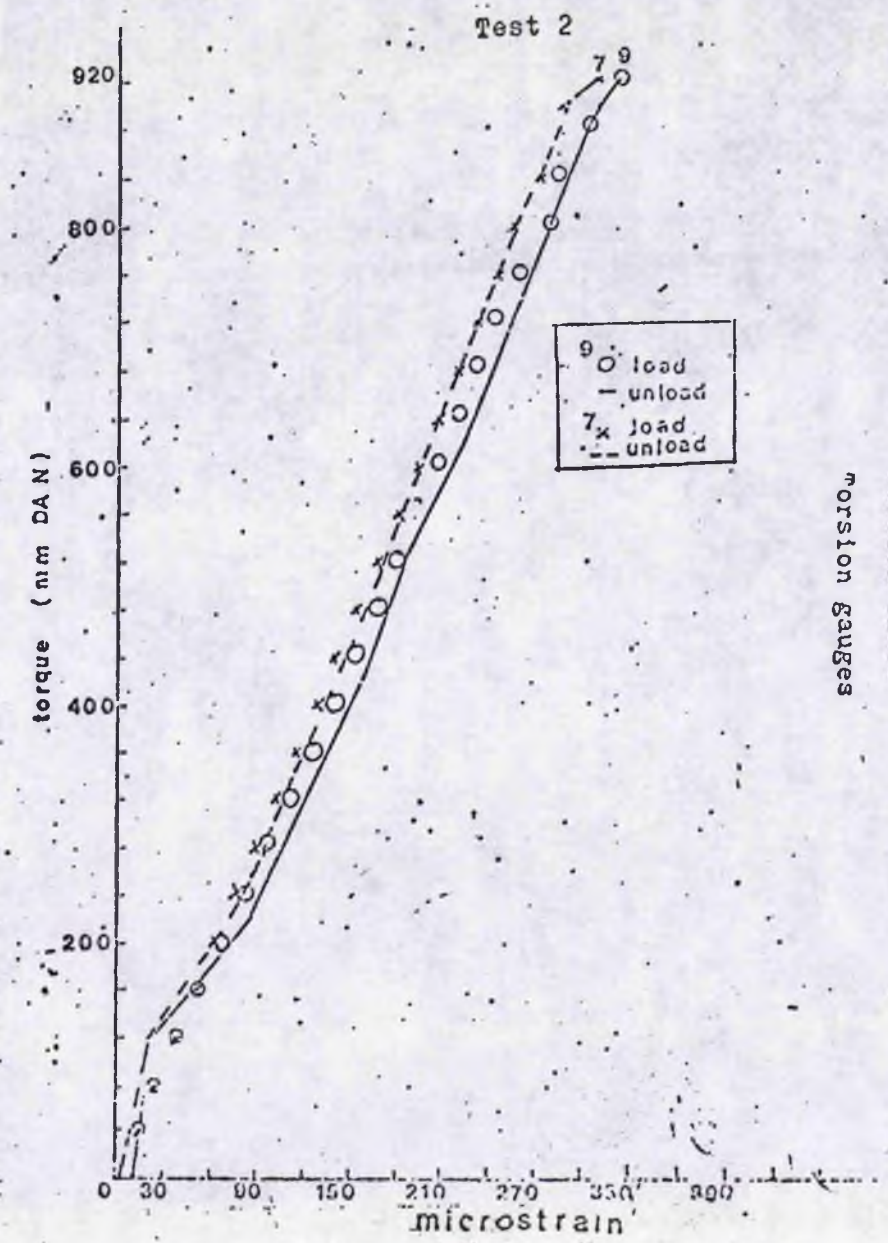

TORSION TESTS

Torsion gauges

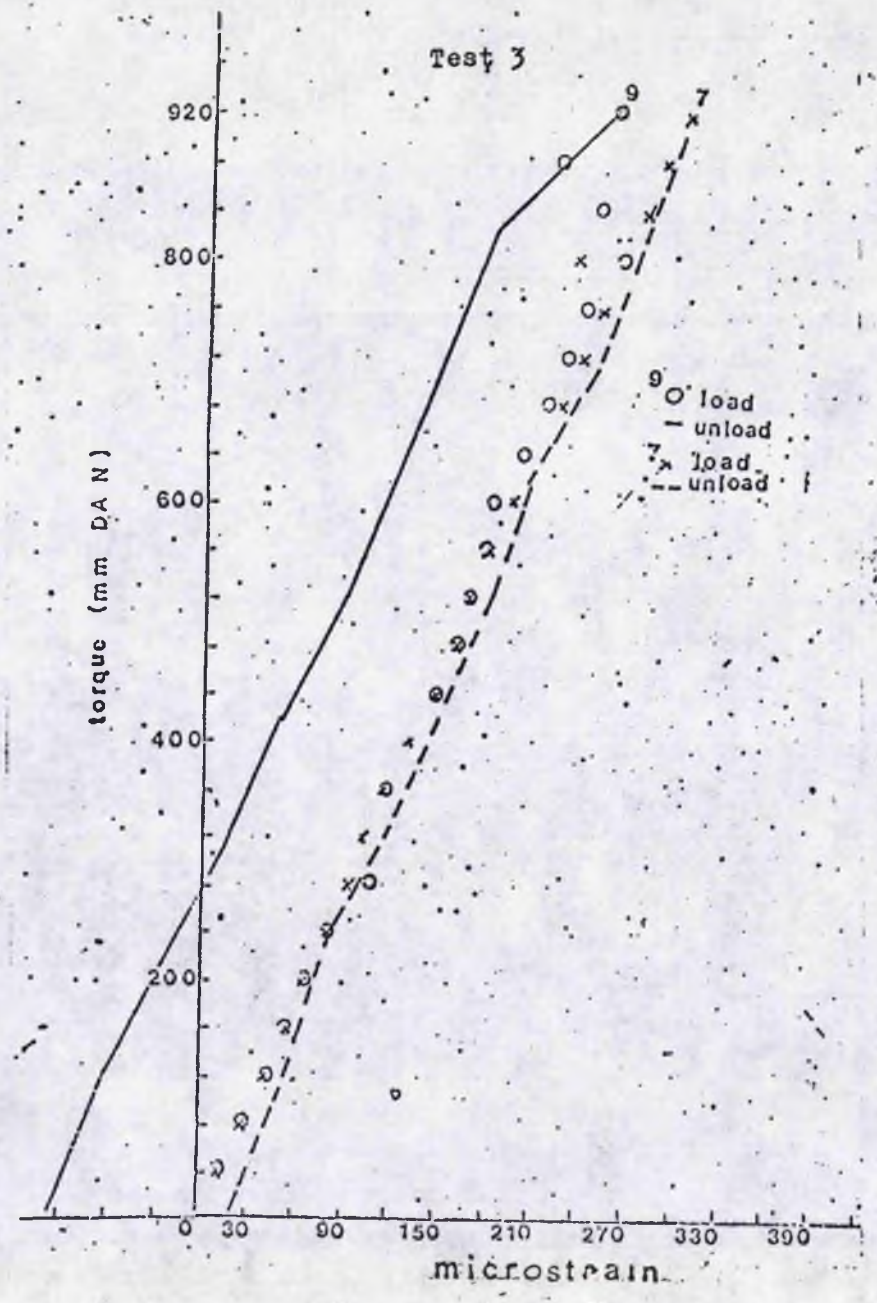

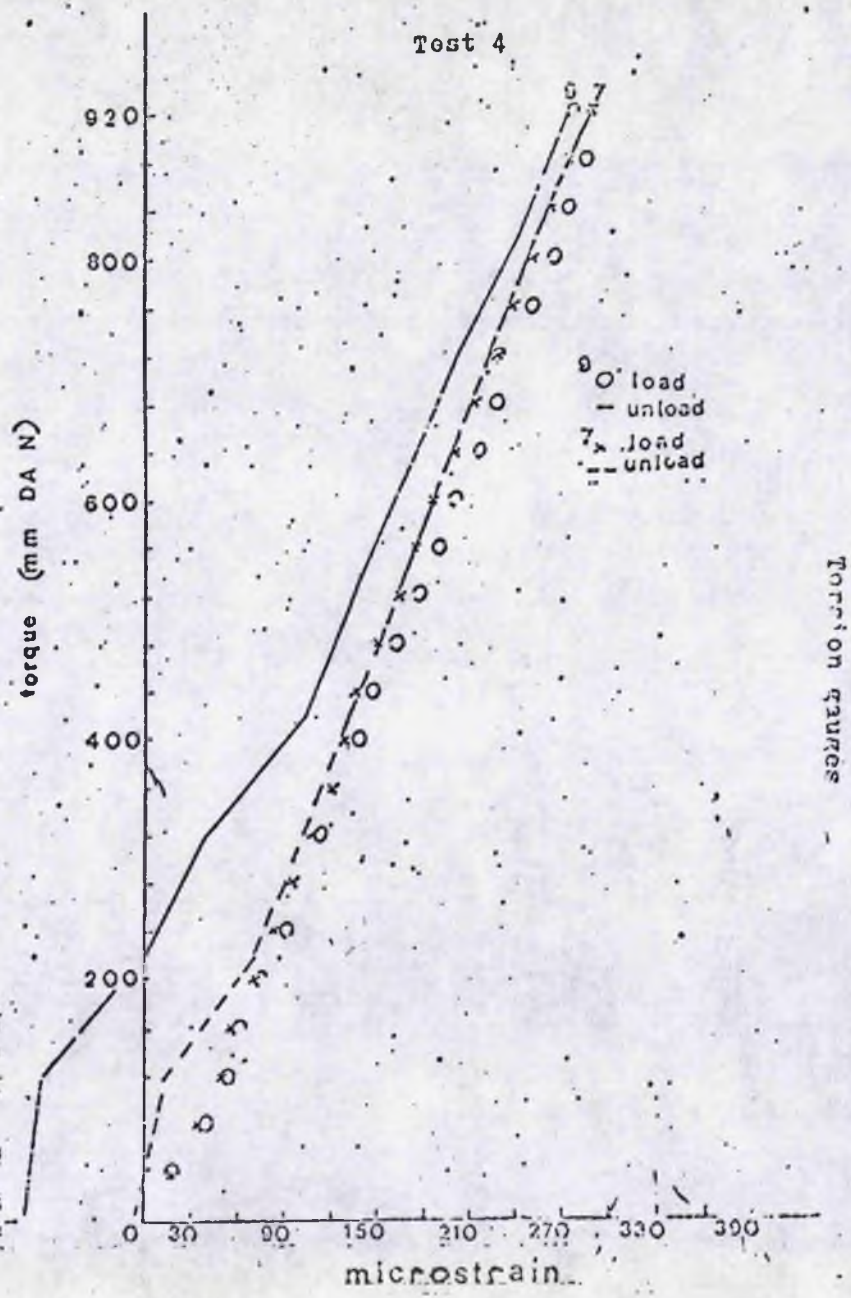

TORSION TESTS.

Torsion figures

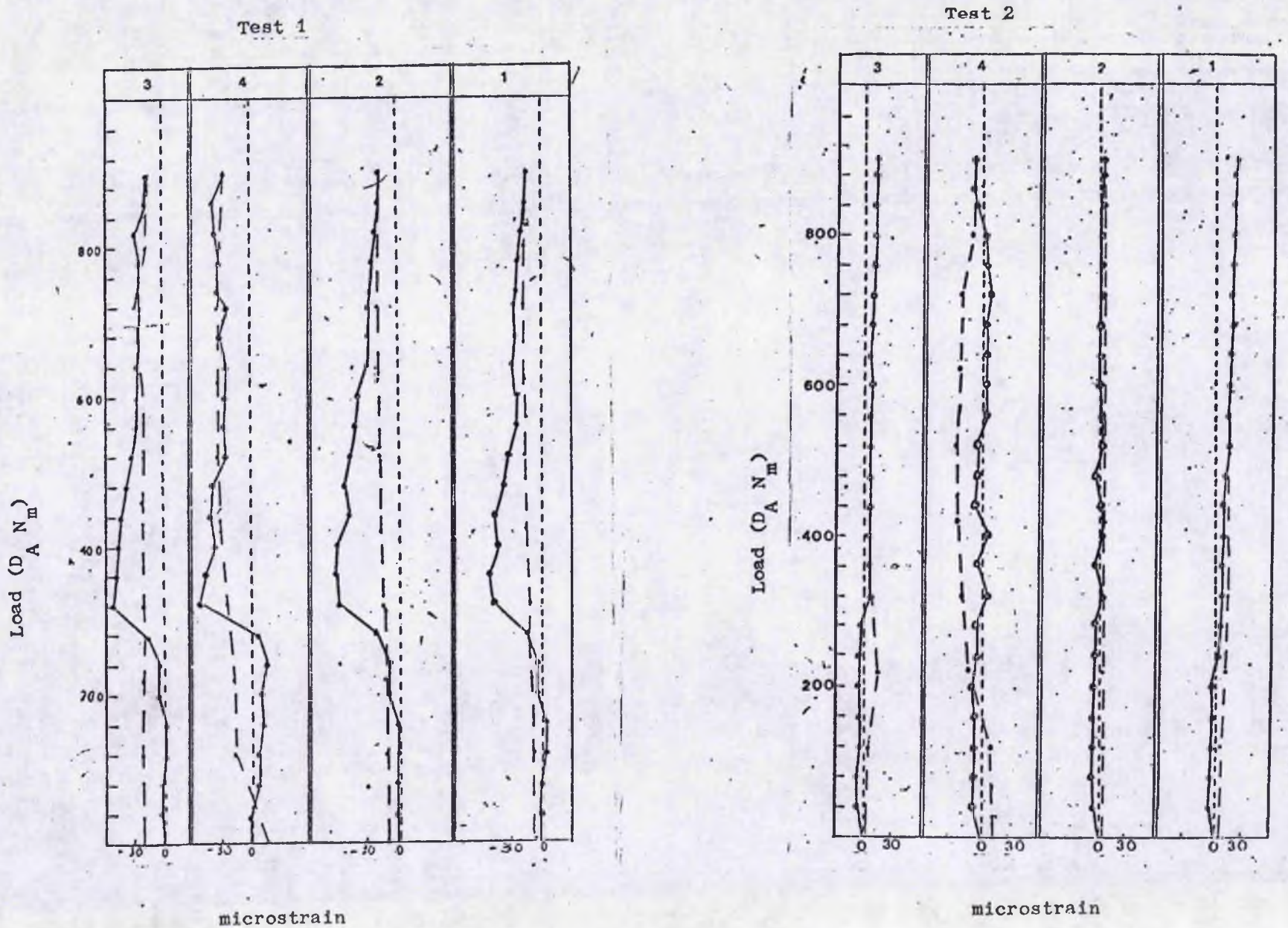

TORSION TESTS (Bending gauges)

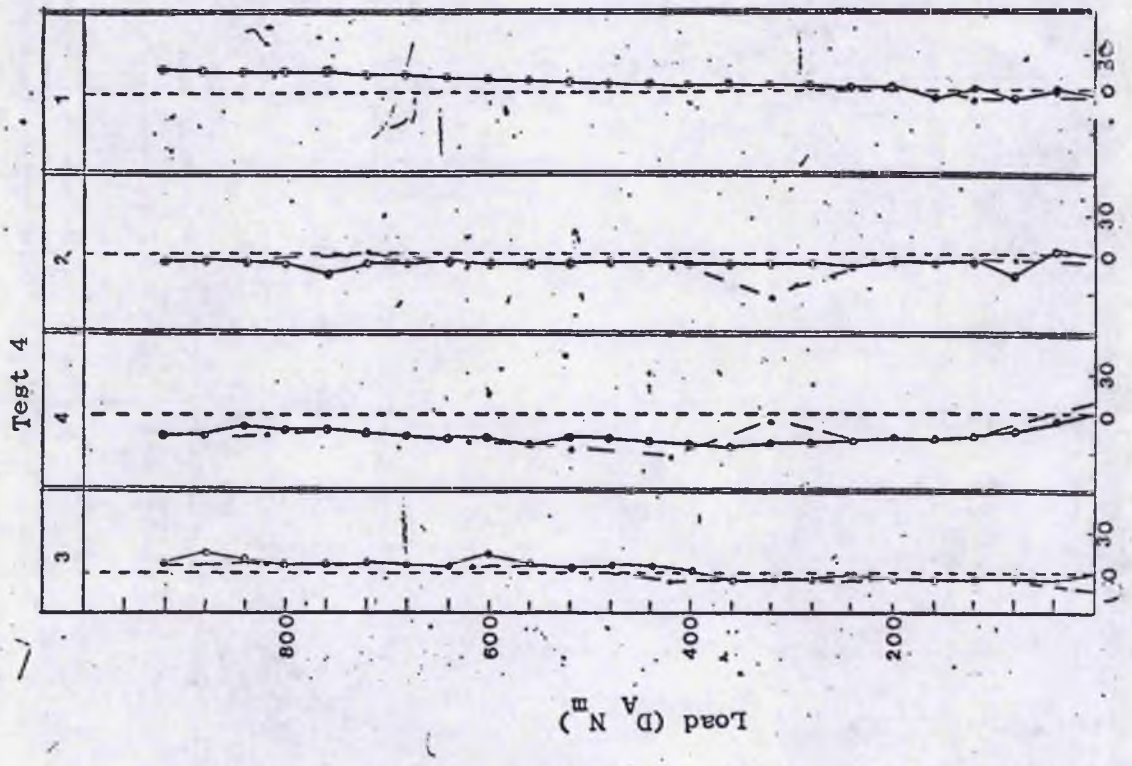
Test 4
1
2
4
3
30
0
30
800
600
400
200
Load (D_A N_m)
microstrain

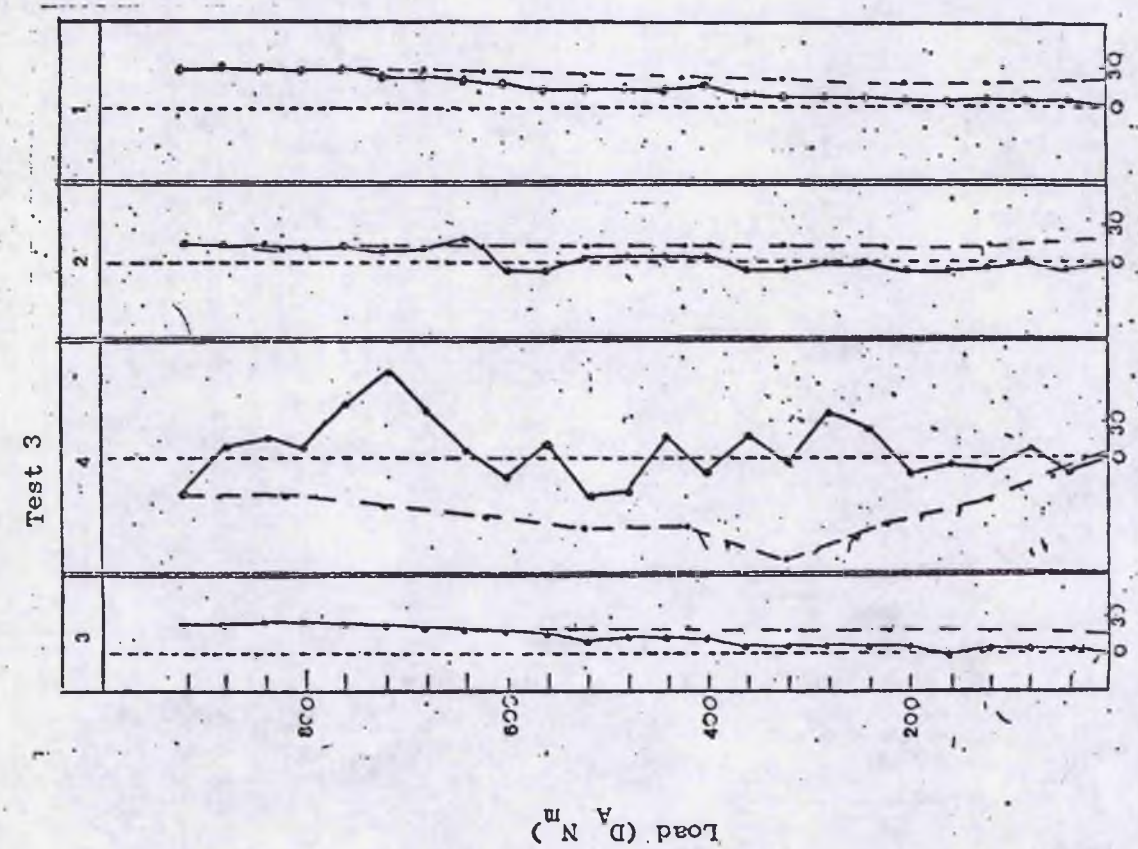
Test 3
1
2
4
3
30
0
30
800
600
400
200
Load (D_A N_m)
microstrain

assumed to be due to disbonding and the low level of strain recorded from all four gauges was thought to be due to random "noise" effects. (Gauges 1-4 were positioned for the detection of any bending strain).

Difficulty was encountered in balancing all four torsion gauges simultaneously and it was found that only two gauges, one from each rosette (gauges 7 and 9) could be balanced at the same time. A linear response and slight hysteresis is observed.

The actual data from the bending and torsion gauges (gauges 1, 2, 3, 4, 7 and 9) is listed in Appendix 4.1.1. and presented graphically on pages 133-136.

4.2.4 Analysis of Data

A calculation of the torque required to produce 100 micro-strain was made using the standard formula for torque in a solid rod where

$$\frac{T}{J} = \frac{G\Theta}{L}$$

where $T = \frac{\tilde{\varsigma} \times \tilde{\wedge} d^3}{16}$ and $G = \frac{\tilde{\varsigma}}{\gamma} = \frac{\text{shear stress}}{\text{shear strain}}$

A core diameter of 9.8 mm and the value of G for steel ($87 \times 10^9 GN/M^2$) was assumed. The torque required to produce 100 microstrain ($\mu\varepsilon$) was found to be 155.7 mm $D_A N$ (13.9 lb inches). The data obtained from the torsion gauges (7 and 9) were plotted graphically recording torque in $mm/D_A N$, against strain. A linear response is observed in Test 2 (page 133) with marked hysteresis in Tests 1, 3 and 4 (pages 133,134). For these tests non-linearity is observed and the slope of the graph was determined by the best fitting line. The modulus of rigidty for the bar was then determined from the slope of each line for both gauges (7 and 9) in all

four tests. The torque per 100 $\mu\varepsilon$ was found to be approximately twice the theoretical value 155.7 mm $D_A N$. The slope of the line was found by the ratio of

$$\frac{\Delta \varepsilon}{\Delta P}$$

to find the strain per unit torque. Where $\Delta \varepsilon$ = change in strain and ΔP = change in torque. The modulus of rigidity could therefore be found where

$$G = \frac{16T}{\pi (d)3} \times \text{unit strain} \quad \text{——— I}$$

These results are tabulated below in Table 4.1. . It can be seen that the value for G was approximately twice the theoretical value of 87 x 10^9 GN/m^2 (column A).

TABLE 4.1.

Test	Gauge	GN/m^2 A	GN/m^2 B	Ratio of $\frac{A}{B}$
1	7	148.3	62.1	.47
2	7	165.6	75.9	.47
3	7	158.7	69	.45
4	7	186.3	82.7	.46
1	9	151.8	75.9	.45
2	9	151.8	69	.45
3	9	172.5	82.8	.48
4	9	172.5	82.8	.48

It was surmised that the acrylic bonding had essentially changed the core diameter of the bar and this increased the torque required to produce a given level of strain. When a bar diameter of 12.5 mm instead

of a core diameter of 9.8 mm was included in equation I of the previous paragraph the value for G (column A) Table 4.1. was effectively halved (Column B) to give a G value within theoretical limits. When this was tested by further theoretical analysis for a bar of composite material the torque produced in the acrylic was very small relative to the torque produced in the steel.

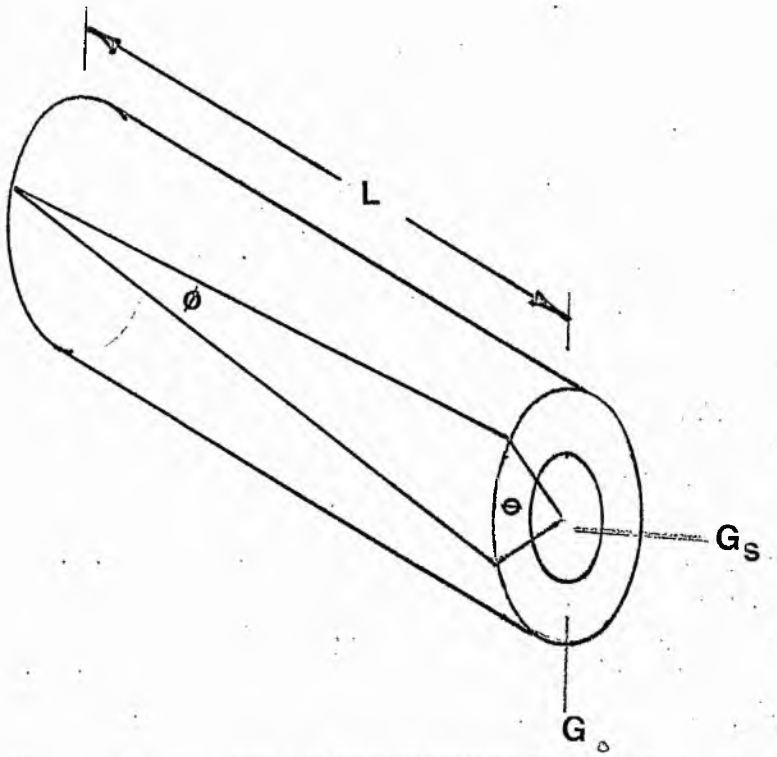

where $\emptyset$ = shear stress

and $G\emptyset = \dfrac{32Td/2}{\pi (D_A^4 - D^4)}$

where D_A = Θ acrylic section, and D = Θ of BAR

(Poissons Ratio ν_S = .28 and ν_A = .38)

At the interface

$$\frac{32\ T_s\ d/2}{\pi (d^4)} = G_s\ \emptyset_1$$

Therefore $$T_s = G_s \phi_1 \frac{\pi d^3}{16}$$

and $$\frac{32 T_A \, d/2}{\pi (D_A^4 - D^4)} = G_A \phi_1$$

therefore

$$\frac{T_s (D_A^4 - D^4)}{T_A D^4} = \frac{G_s}{G_0}$$

therefore $$T_s = \frac{D^4}{D_A^4 - d^4} \times \frac{G_s}{G_A} T_A$$

since $$T = T_A + T_s$$

$$= T_s \left[1 + \frac{T_0}{T_s} \right]$$

therefore $$T = T_s \left[1 + \frac{D_A^4 - D^4}{D^4} \frac{G_A}{G_s} \right]$$

where T = Total Torque obtained from the slope of the line

$= 311.4$ mm $D_A N$

then $T_s = 269$ mm $D_A N$

$T_A = 42$ mm $D_A N$

No further explanation could be found at this time and it was felt that Calibration of the Bar in Torsion was unreliable for transducer purposes, since neither linearity nor repeatability is demonstrated.

4.2.5 Calibration of the Bar in Tension

The alignment jigs used in the Torsion Calibration Test were used

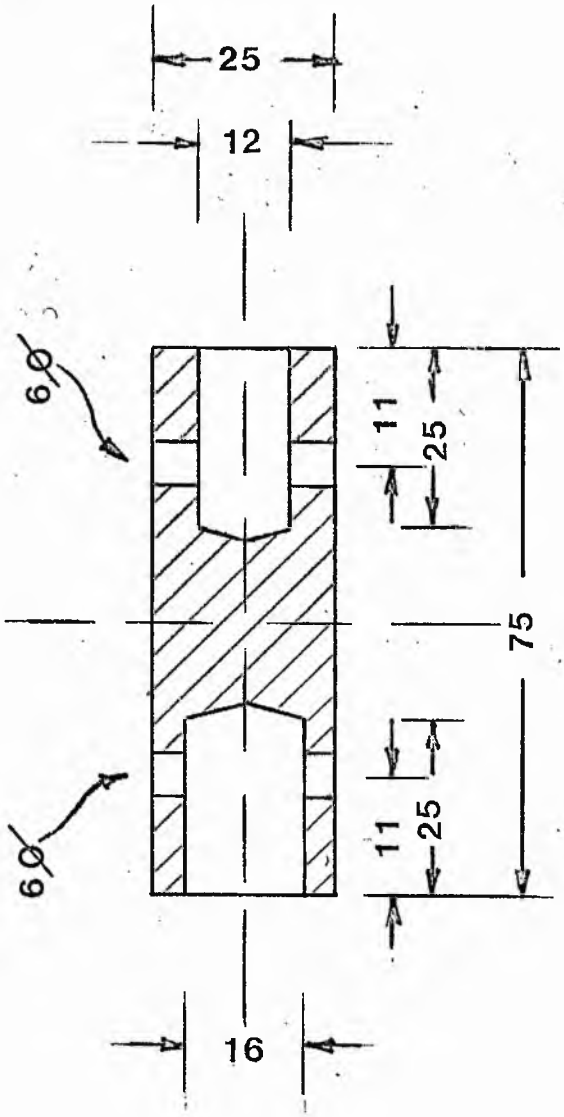

Figure 52: Attachment spigots for tension tests

with slight modification in the tension test using the Hounsfield Tensometer. This was carried out by the addition of 2 short pieces of stainless steel rod (Figure 52) connecting the alignment jig to the testing machine. Holes were bored through the waisted section of each alignment jig and secured in position in the smaller of the two bored holes in the connecting rod (Figure 52). The opposite end was then connected to the multi-axial attachment section of the Hounsfield. The horizontal alignment of the bar, attachment jigs and connecting rod can be viewed in Plate B.

Testing Procedure

Four tests were conducted on the same day at ambient room temperature of 21°C. The gauges were connected to the STRAIN INDICATOR in the manner previously described for the Torsion Tests. A 500 kg force beam was used with a magnification factor of 16 to 1 for the graphical recording. Manual loading was used since an incremental load of 20 kg per increment was considered adequate for the testing procedure and automatic loading does not allow accurate equal incremental tensile loads to be applied. Gauges 1, 2, 3, 4, 7 and 9 were all zeroed under a no-load condition. (Gauges 8 and 10 were not used since they have been found to be defective). Incremental loads of 20 kg f were applied to a limit of 300 kg f. and then unloaded by 40 kg f decrements with readings being taken at each point by zeroing the meter needle and obtaining a digital readout value for strain. Prior to the test a Gauge Factor of 2 had been selected and the test carried out in accordance with the Instruction Manual for the P-350A Strain Indicator. These results are tabulated in Appendix 4.2.1.

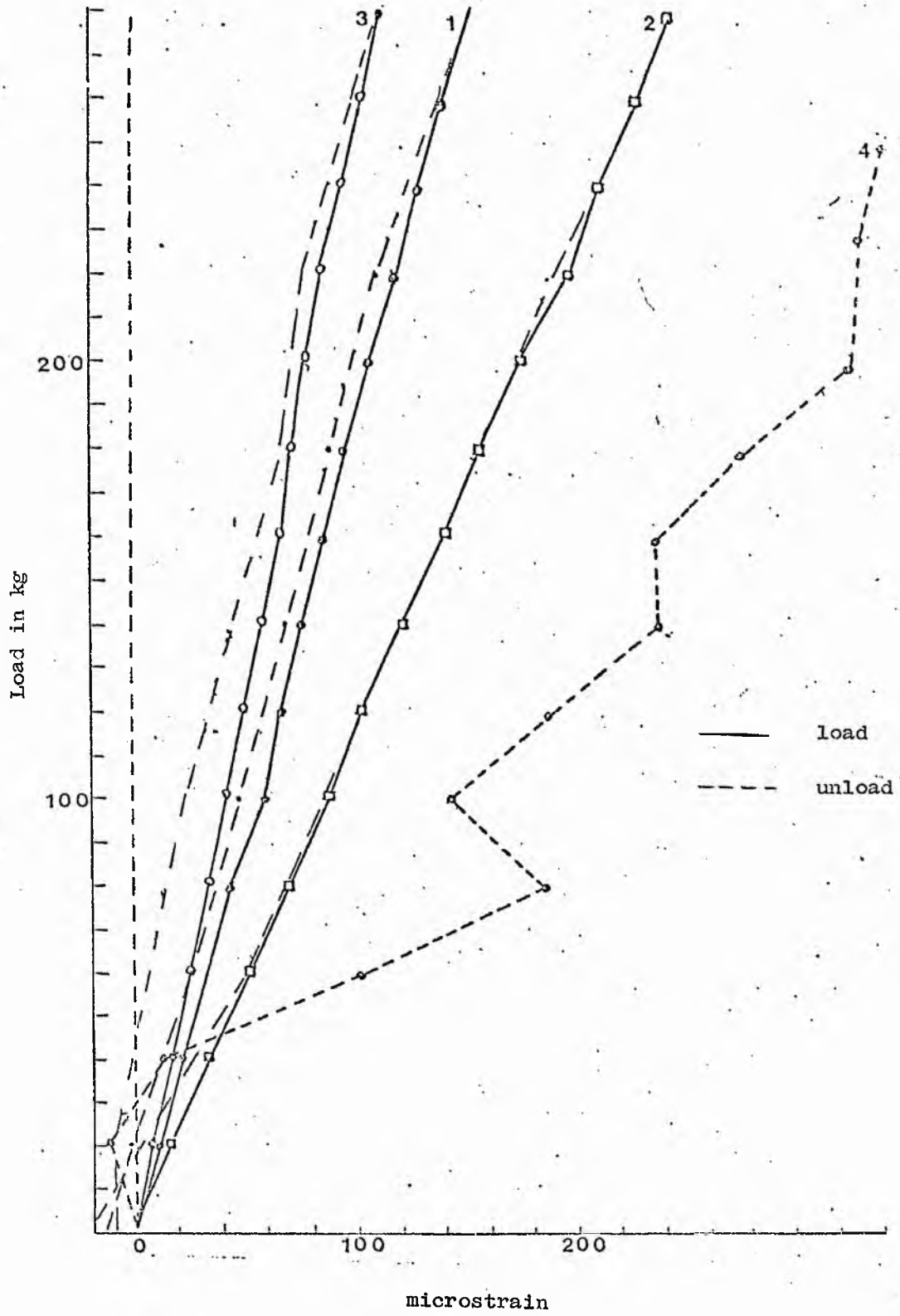

TENSION TEST 1

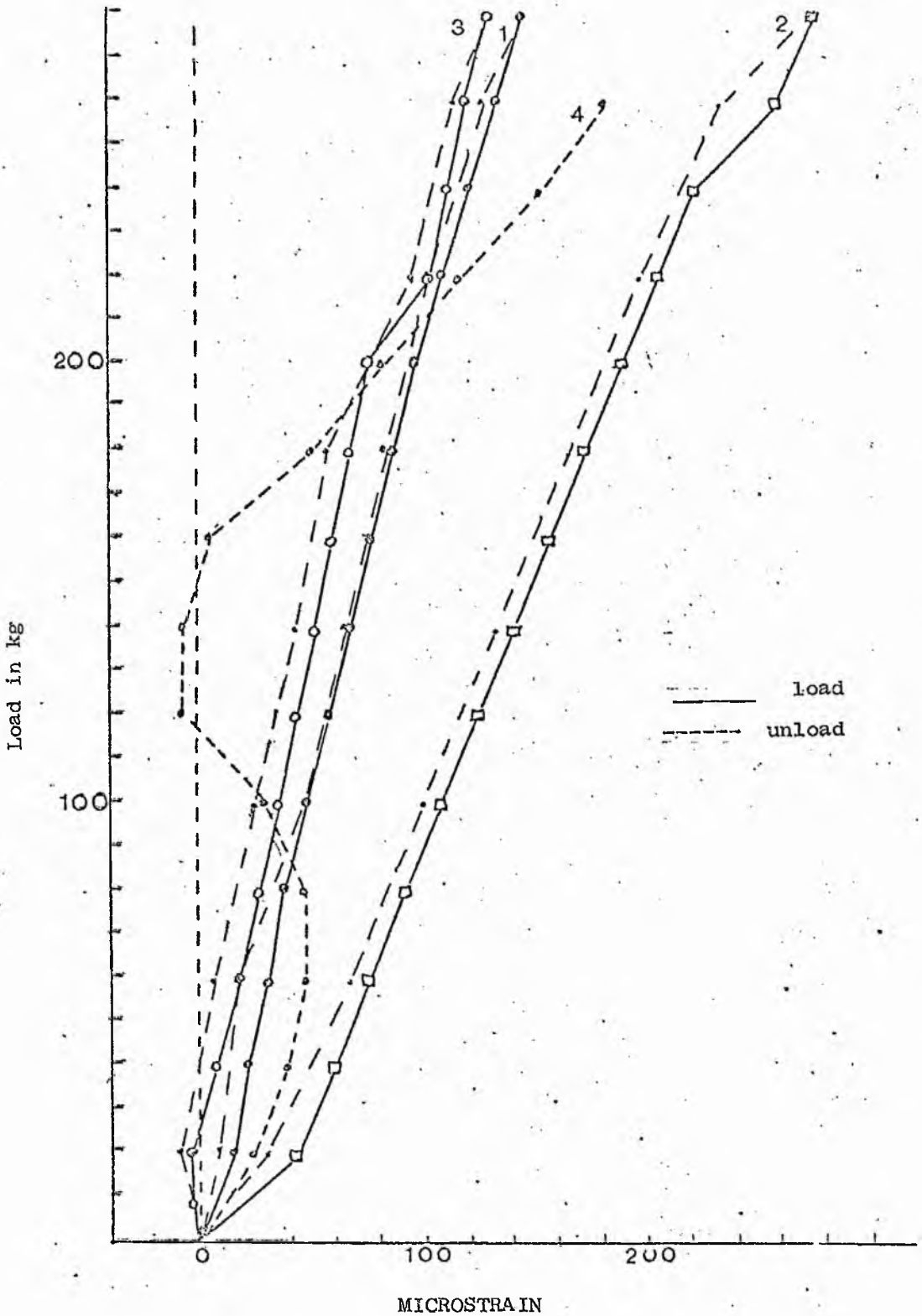

Tension test 2

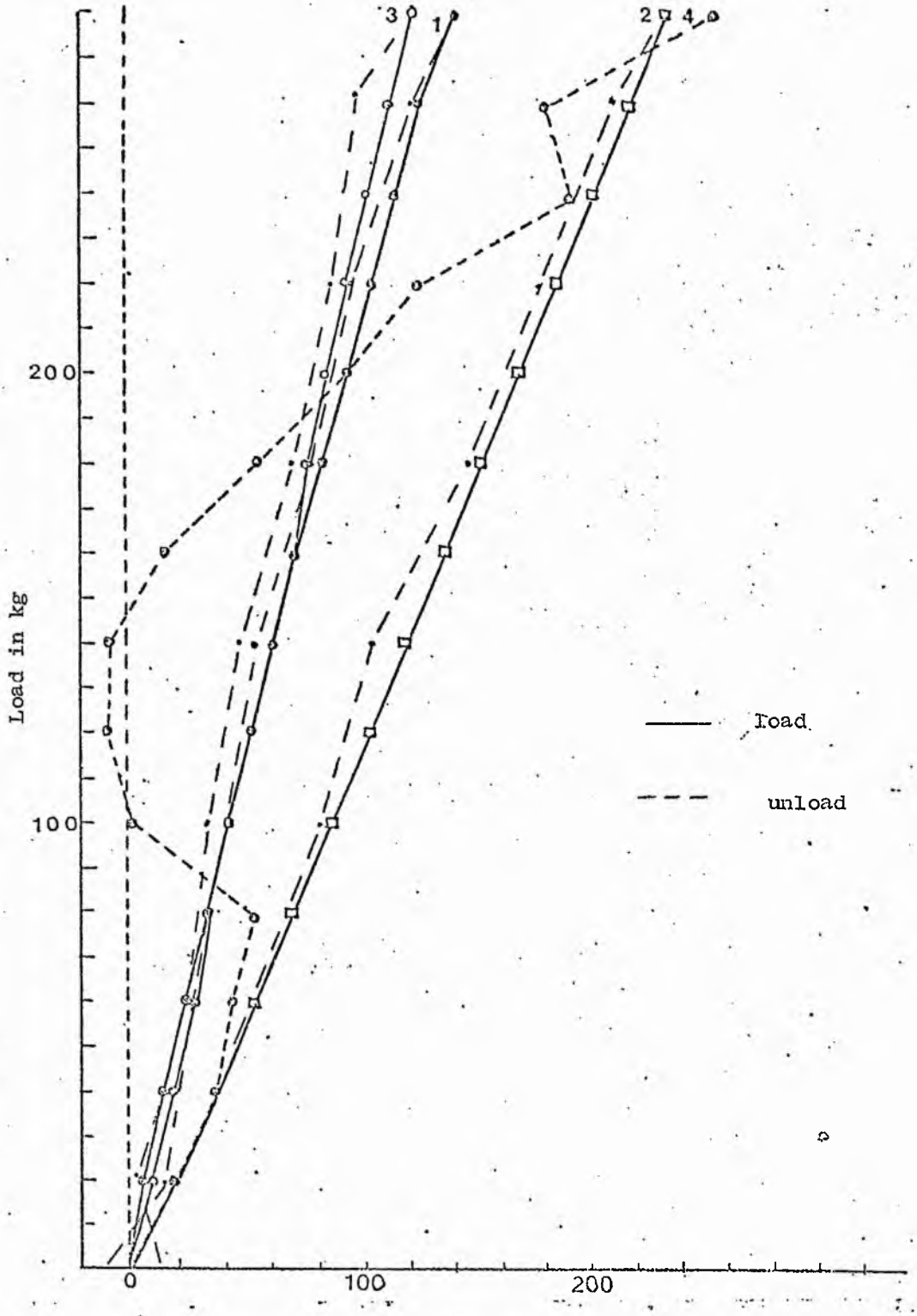

Tension test 3

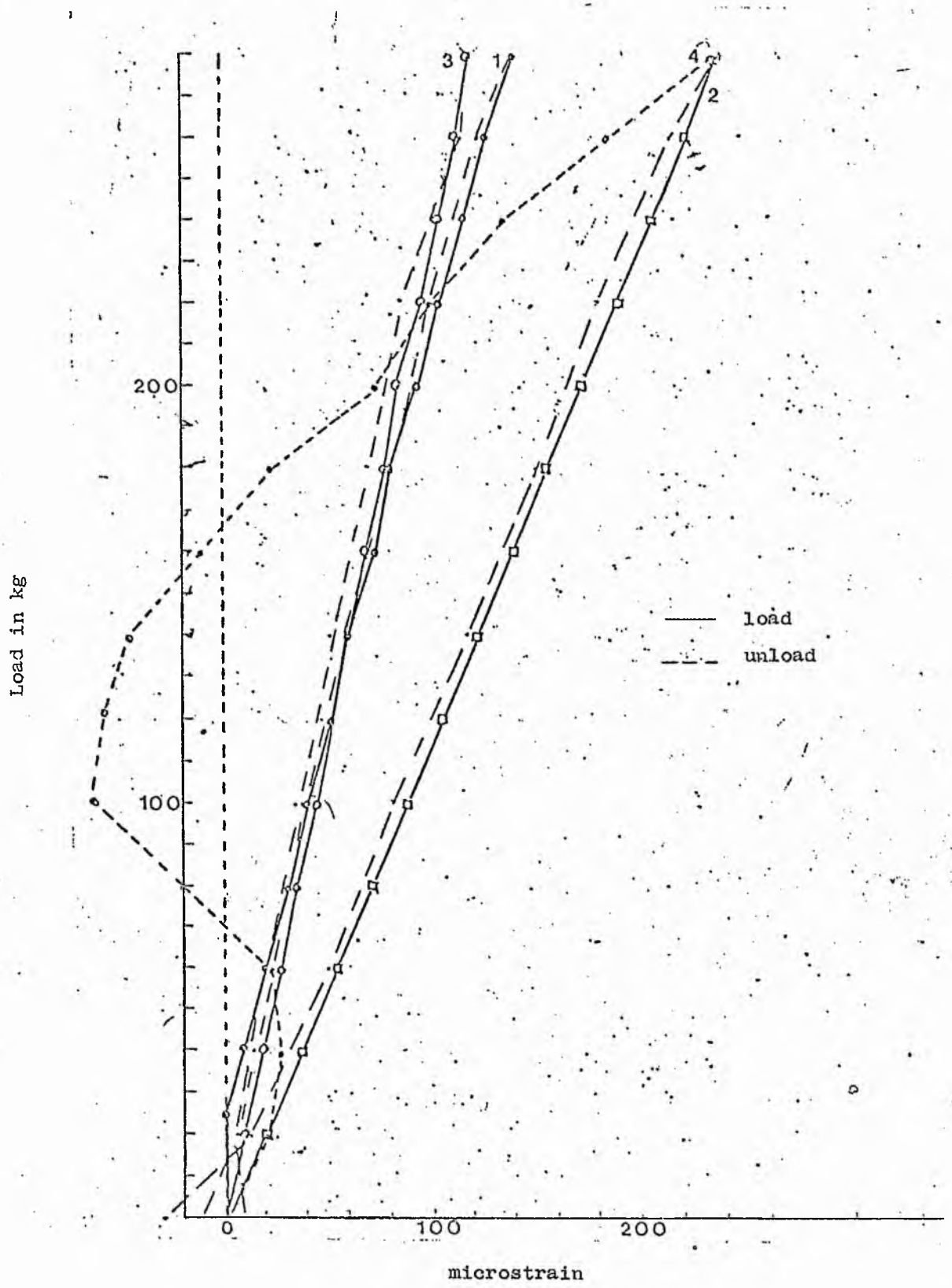

Tension test 4

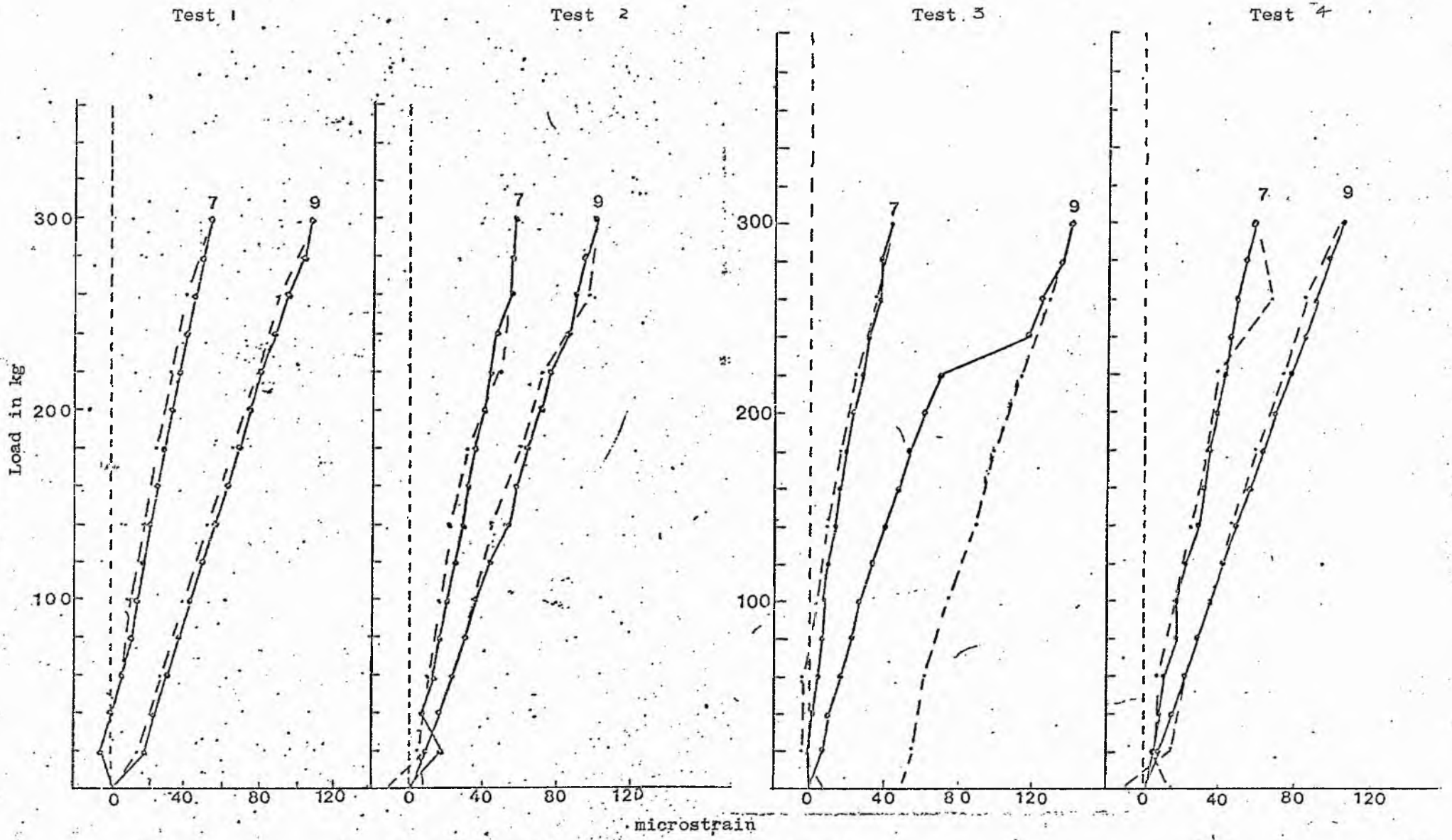

Tension tests : Hounsfield torsion gauges

4.2.6 Analysis of Data for the Tension Tests

Difficulty was encountered in obtaining an initial balance of Gauge 4 simultaneously with the remaining gauges 1, 2 and 3, and marked drift was noted in tests 2, 3 and 4 for this gauge. The data is plotted graphically for gauges 1, 2, 3, 4, 7 and 9, pp. 143-147, recording tensile force (kg f) against strain. The tabulated data is in Appendix

The Torsion Gauges

A linear tensile response is noted in gauges 7 and 9 throughout all tests, but greater levels of strain were recorded in gauge 9. A test performed in Tension should have produced minimal but equal strain of the torsion gauges. Assuming the bar to be correctly aligned in the testing machine, two theories are proposed to account for the differences in magnitude of the strain.

a) Gauge 9 was incorrectly aligned and was therefore recording direct tensile loads rather than any torsional tensile strain.

b) A permanent deformation of the bar existed at the level of attachment of the gauge.

The "Bending" gauges

A linear response was obtained from gauges 1 and 2 in all four tests, but the levels of strain at each incremental load point was not found to be repeatable, and a return to zero load condition produced in gauge 2 - 34 $\mu\varepsilon$ in test 3. At low levels of strain up to + 40 $\mu\varepsilon$ the response in all gauges was non-linear in tests 2 and 4.

The Young's Modulus of the material was determined where

$$E = \frac{\sigma}{\varepsilon} \quad \text{but } \sigma = E\varepsilon = \frac{F}{A}$$

therefore $$E = \frac{F}{A\varepsilon}$$

a unit strain was determined by the ratio $\frac{\Delta \varepsilon}{\Delta P}$ obtained from the slope of the Graph, and the following values for E were obtained for each test (Table 4.2)

TABLE 4.2: Values for Young's modulus derived from TORSION TESTS where ($E = 200 \times 10^9$ GN/m^2) is the anticipated value for stainless steel

Test	Gauge Number 1	2	(E = 200 GN/m^2) 3	Bending eliminated Gauges 3 + 2
1	248	151.8	331.2	241.5
2	269	172.5	310	241
3	276	179.4	276	227
4	262	152	310.5	227

To eliminate stray bending effects the strain may be analysed as follows:

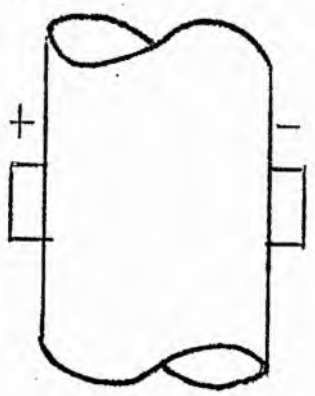

Bending Moment Diagrams

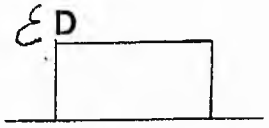

Direct strain εD

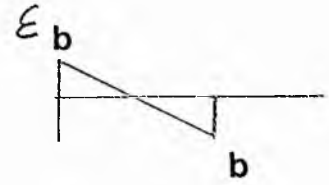

Bending

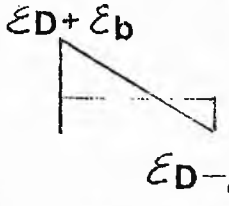

Combined effects

Therefore $\varepsilon_D + \varepsilon_b + \varepsilon_D - \varepsilon_b = 0$

therefore $\frac{2\varepsilon_D}{2} = \varepsilon_D$

and the bending effects are eliminated by summation of the strain in the gauges and dividing by two.

Simultaneously for Young's Modulus

$$\frac{2E}{2} = E$$

and the approximate values derived for the Young's Modulus of the bar are presented in the final column of Table 4.2 where the mean value of 234×10^9 GN/m^2 is obtained and error of 13% from the anticipated value of 200×10^9 GN/m^2 (30×10^6 psi).

The conclusions drawn from the calibration tests are discussed in the final chapter (Chapter 6).

4.3.1 The Bone Model / Fixator Experiments

These experiments were conducted in two stages:

Stage 1: An unfractured specimen representing a fully healed bone.

Stage 2: A fractured specimentrepresenting an unstable fracture of the lower leg. This was simulated by complete disruption of the bone at the junction of the middle and lower third of the leg.

The experiments in Stage II were initially conducted in the early stages of this project, and it was realised from the results obtained that considerably more information about the behaviour of the bone and fixator configuration would be required. In these early experiments all gauges were found to be functioning and levels of strain were recorded from all eight gauges.

4.3.1.1 The Bone Model / Fixator Configuration

The location of the "fracture site" centre was first identified and marked at 247 mm from the proximal end (P) of the model. The two groups of pins were spaced equidistantly from the centre of the fracture site and a minimal distance of 18 mm between the central axis of each pin was established (Plate D). The bone was firmly clamped to the bench and six pin holes were carefully hand-drilled with a 9/64ths drill bit. Care was taken to ensure that both "cortices" were penetrated, but the pins did not protrude excessively from the far cortex. Without alignment jigs parallelism of the pins was difficult to obtain and very slight angulation of the pins occurred.

Two people were required to carry out the bonding of the transfixing

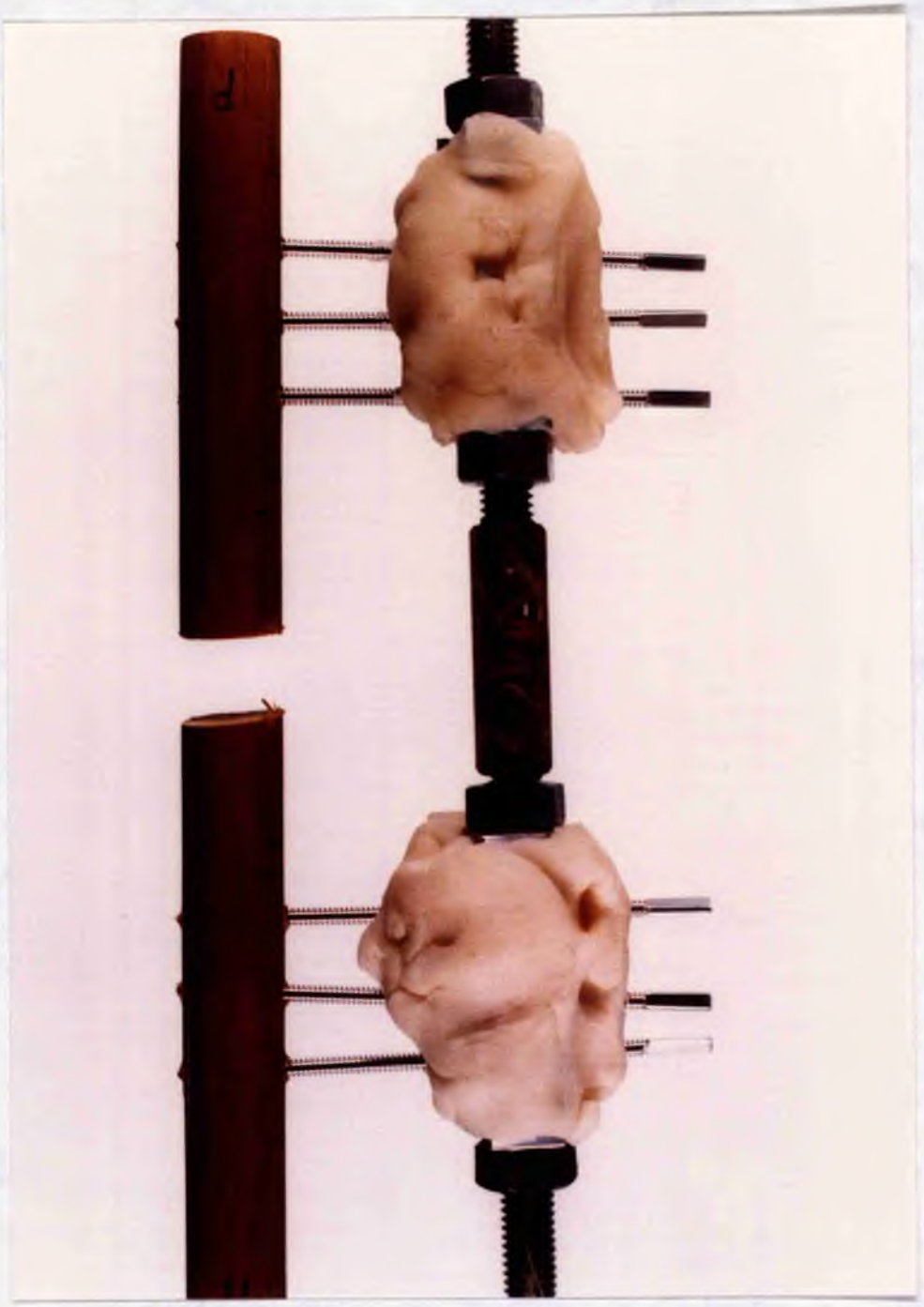

PLATE D

pins to the carriages using bone cement. The cement was mixed in the following proportions by pouring 100 mls of solution, containing 97 mls of Methyl methacrylate monomer and 3 mls of Dimethyl-P-Toluidine, with 90 grams of powder containing 89 grams of Polymethyl Methacrylate and 1 gram Benzoyl Peroxide. The mixture was combined at 20°C and when sufficient heat was produced by the exothermic reaction, the cement was rapidly applied to the pins and carriages. The bar was held parallel to the tibial long axis and intimate bonding between the pins and the carriages obtained. (Plate D). The locknuts were then tightened and the intact "bone" specimen and fixator was then ready for experimental work.

4.3.1.2 Stage I of bone model / fixator experiments

Two series of tests were conducted on the intact bone and fixator applying direct compression to the bone using the Hounsfield Tensometer and then in bending using simple point loading to simulate the weight of the leg distal to the fracture.

Compression Tests

These experiments were designed to determine the levels of strain that can be detected when the fracture is fully healed and the bone is subjected to axially applied physiological loads. These were defined as partial body weight, simulating quiet walking with crutches to full dynamic activity such as ascending stairs or rising from a chair (see Part B Chapter 3).

Prior to these tests and the attachment of the pins and Fixator Bar, the model was subjected to axial compressive loading in the

COMPRESSION CRADLE

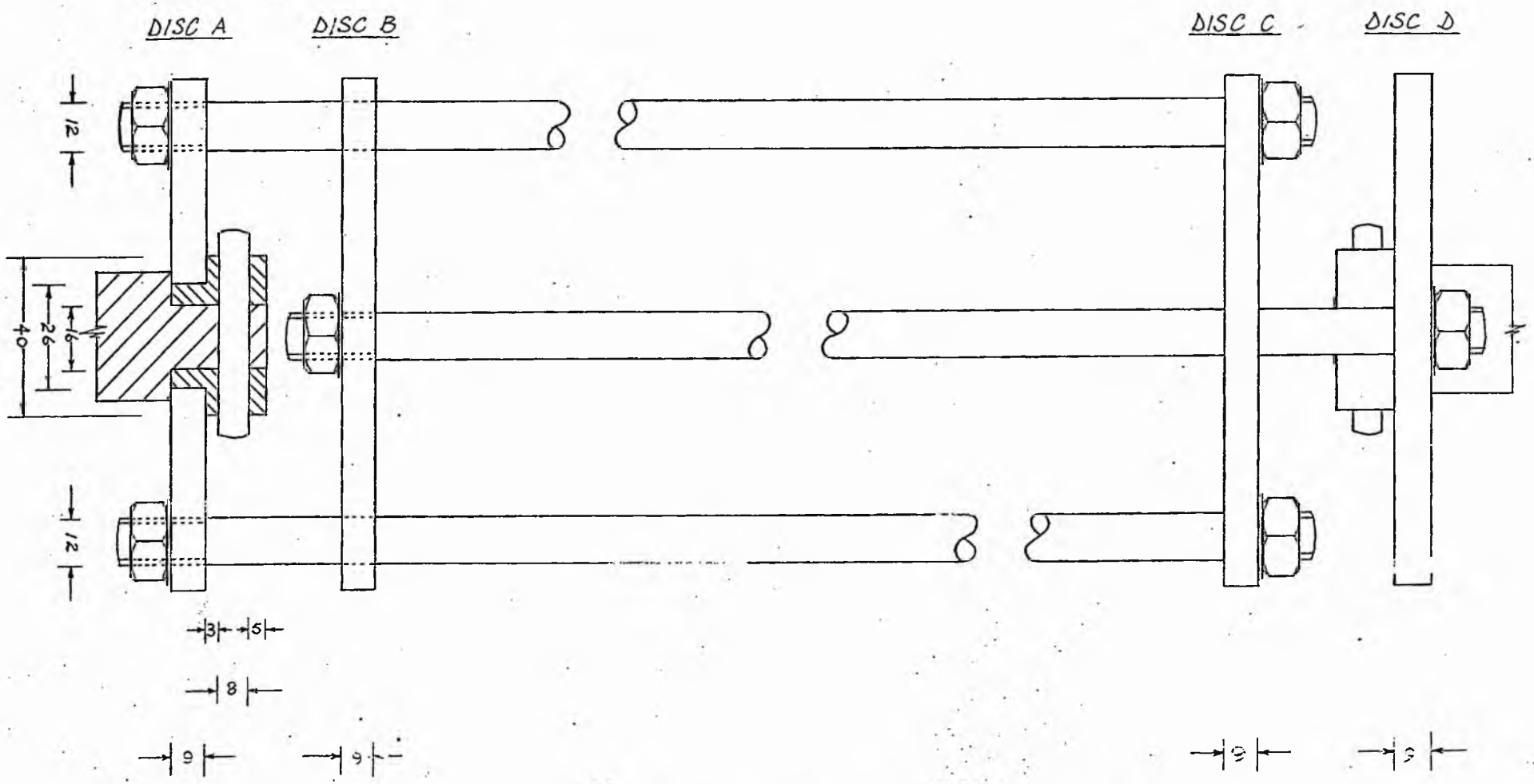

F. M. TURNER BIOMECHANICS

SCALE : FULL SIZE MEASUREMENTS IN M.M.

DRAWING N° 1.

fig 52

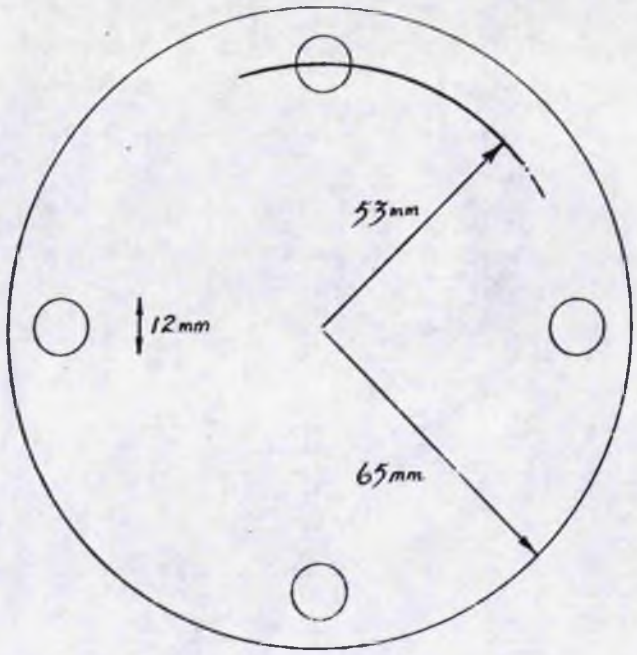

DISCS B & C

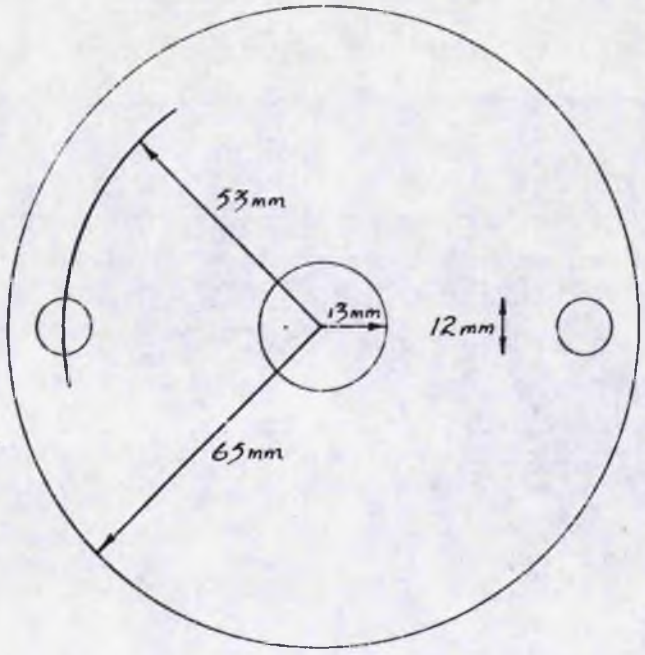

DISCS A & D

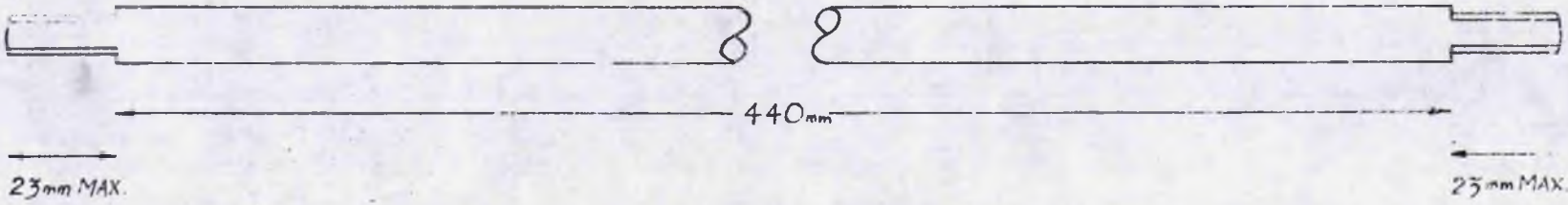

F.M. TURNER BIOMECHANICS

SCALE : FULL SIZE DRAWING N° 2.

fig. 52 cont.

Houndsfield tensometer to determine any hysteresis characteristics of the model. A compression cradle for use in the Hounsfield was designed to accommodate the length of bone, the dimensions of which are given in Figure 52. This cradle consists of four mild steel rods diametrically positioned in four ½" steel discs. As the outer two discs (discs A + D) were drawn apart by the tensometer, the inner two discs moved towards each other, thus applying compression to the "bone" centred between the two inner discs. To ensure pure axial compression of the model, two spigots were designed (Plate E) which inserted into the ends of the bone, and articulated with the centrally placed indentation of the inner two discs (Plate E).

Pretesting of the intact bone specimen

Prior to its attachment to the fixator the intact bone model was placed centrally between the two inner discs of the compression cradle and sufficient compression applied by manual operation of the tensometer to fix the model between the two plates. A 500 kg beam was used and the deflection of the mercury level of the force scale adjusted to zero. The motor was then switched on at an automatic loading speed of .055 in/per minute to a maximum load of 300 kg f (approximately 4 times body weight) and then the switch reversed and unloaded to a zero load condition. This test was repeated three times and no hysteresis was observed. The bone model was therefore assumed to behave in a linearly elastic fashion.

The compression tests on the intact bone model and fixator

The intact bone model with end spigots and attached fixator was positioned centrally between the two inner discs and maintained in

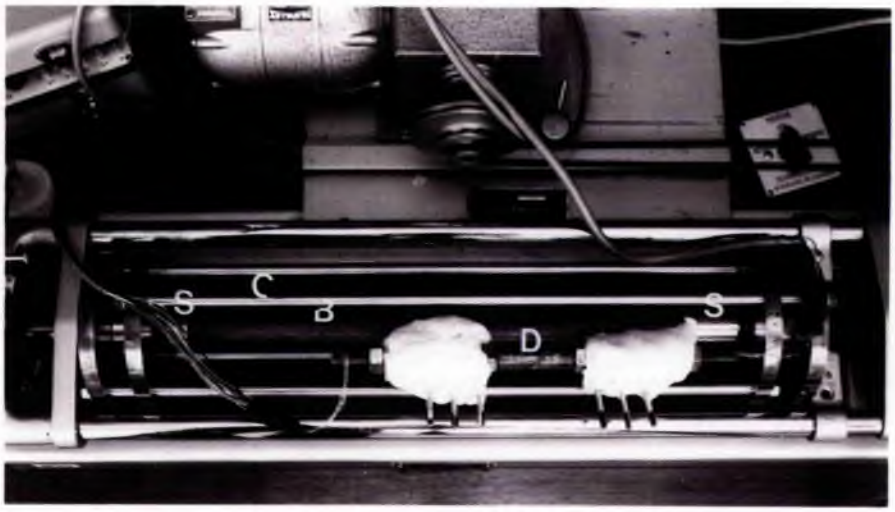

PLATE E

C compression cradle

S attachment spigots

B bone model

D Denham Bar

PLATE F

position according to the technique described in the previous paragraph (Plate E). Care was taken to ensure that the bar, acrylic coated carriages and pins were not resting on the interconnecting rods of the compression cradle so that the only contact between the test rig (bone model, fixator and pins) and the cradle was through the "bone" ends. The tests were conducted on the same day at a temperature of 17.5°C and relative humidity of 44%.

A series of seven tests were carried out with each test defined by the peak load for that test. These were as follows:

Test 1 0 - .5 BW where BW (bodyweight) = 75 kg.
2 0 -1.0 BW
3 0 -1.5 BW
4 0 -2.0 BW
5 0 -3.0 BW
6 0 -4.0 BW
7 0 -5.0 BW

Each test was repeated three times. At the commencement of each test null deflection of the meter (on the Vishay strain indicator) was obtained. The Hounsfield motor was then switched on and the bone axially loaded in compression at a moving crosshead speed of .055 in/min. Just prior to the peak load for each series the motor was switched off and the strain obtained at the peak load recorded. The compressive force was then unloaded automatically to a minimal loading condition determined by the return of the mercury level towards zero. A final reading in the no load condition was then taken.

The results from these tests are tabulated in Appendix 4.3.1 where the strain from the "bending" gauges (1, 2 and 3) and one torsion gauge were recorded (gauge 9). Further difficulty was encountered in obtaining the mutual balance of gauges 7 and 9. The levels of strain that were

recorded from each gauge (1, 2, 3 and 9) were minimal and no significant change in peak strain was noted despite the application of peak loads of 375 kg. From previous tests marked drift was noted in Gauge 4 which was not therefore used in this test.

Bending tests on an intact bone model and attached fixator

Three tests were conducted on an intact bone model to simulate knee extension with an unsupported lower leg and manual resistance applied to the distal limb section. The model was firmly clamped to the edge of the bench to a level of 5 cm from proximal end (which represented the attachment of the ligamentum patellae (Plate F). Gauges 1, 2, 3 and 9 were zeroed under a no-load condition, then incremental loads of 0.9 kg were added to an initial load of 3 kg applied to the distal end of the bone. A maximum load of 8 kg was applied where the final increment was 0.45 kg. Unloading was then carried out by 0.9 kg decrements and the final weights removed. Levels of strain were recorded with each incremental or decremental load, and each test repeated three times.

The results of these tests are tabulated in Appendix 4.3.2 but the levels of strain and random behaviour of the gauges indicated nil detection of load-dependant strain. There was a strong possibility that the remaining gauges had also become disbonded or damaged. They were therefore tested by connection of each gauge to an ohmeter to verify the 120 ohm resistance of each gauge. All gauges 1, 2, 3, and 9 were found to be intact. Although this did not preclude the possibility of disbonding, it was decided that the effects were due to random noise effects associated with non-strain related behaviour.

4.3.1.3 Stage II

Bending tests performed upon a fractured "bone" model supported by the fixator

These experiments simulated an unstable fracture of the lower third of the leg subjected to bending by the application of loads equivalent to the weight of the leg distal to the fracture. A peak load of 2.7 kg was applied at the distal end of the model. This represented the maximum force that may be acting upon a leg under normal post-traumatic conditions, i.e. the weight of the section of limb distal to the fracture and any oedema that may be present.

These tests were carried out before the tests on an intact bone model, but the spatial configuration of bone model, pins and fixator was replicated by the experiments with the intact model. To simulate the fracture a section of wood was removed from the predetermined fracture level of 276 mm.

Four experiments were designed to simulate possible in vivo positions of supine, alternate side lying and prone. In all positions full extension of the "knee" was assumed and an unsupported lower leg. The "bone" was firmly clamped to the edge of the bench by two rectangular blocks. These blocks had an internal diameter equal to the external "bone" diameter and held in position by two G clamps, and clamped to a level of 5 cm from the proximal end of the "bone".

All gauges were then zeroed under a no-load condition. Some difficulty was encountered in obtaining simultaneous balancing of the four torsion gauges. The "bone" was then loaded by incremental point

loads of 0.9 kg to a maximum 2.72kg applied to its distal end. These experiments were conducted on the same day at a temperature of 20°C and a relative humidity of 57% and the moisture content of the wood recorded.

The first experiment was conducted to simulate knee extension in supine lying with the "model" firmly clamped to the bench and the experiment conducted in the same manner as the Bending tests performed on an intact bone model (page 157) To simulate knee extension and the supine position the medially positioned transfixing pins were orientated parallel to the floor. Successive changes in position to 'prone lying' and 'alternate side lying' were obtained by rotating the "bone" and fixator ninety degrees. An initial load of 0.9 kg was applied with subsequent 0.9 kg increments to the peak load of 2.72kg. Unloading was then carried out by 0.9 kg decrements and changes in strain recorded at each successive loading or unloading, respectively.

4.4.1 Analysis of results on the fractured bone model

It had been anticipated that gauges 7 and 8, forming the torsion rosette gauge were likely to produce levels of strain of equal magnitude in each but opposite sign. (see Part A Chapter 2). This was not found to be true and it was hypothesised that the additional effects of bending in the bar (see Chapter 3) accounted for the different levels of strain recorded by these two gauges. Similar behaviour was observed in gauges 9 and 10 which formed the second rosette gauge. The strains recorded by gauges 7 and 8 were summed but the resultant strain was below the theoretical value for microstrain for a given torque, which was calculated using standard formula for torque, i.e. $100\mu\varepsilon$ = 155 mm $D_A N$ (13.9 lb in.)

Lack of repeatability was noted in all gauges (1, 2, 3, 4, 7-10) with slight hysteresis in the unloading phase (pages 163-167). Residual strain was also observed in all gauges on a return to the unloaded state. (For tabulated data see Appendix 4.4.1).

For the "bending" gauges (1,2,3 and 4) the values of strain for a given bending moment were calculated where

$$\frac{M}{I} = \frac{\sigma}{y} \quad \text{and} \quad \frac{\sigma}{\varepsilon} = E$$

These values of microstrain were then compared with the levels of strain obtained experimentally. For the "supine" position gauges 2 and 3 (which were orientated directly opposite) were found to record compressive and tensile strains. The magnitude of strain recorded by gauge 3, however, was greater than the strain recorded by gauge 2. Strain in gauges 4 and 1 was minimal. This was anticipated since these gauges were not subjected to bending in this experimentally simulated position of supine. The level of strain however recorded by gauges 2 and 3 was approximately twice the theoretical value.

Similar results for the torsion and bending gauges were recorded from the "prone" position in which the "bone" was rotated 180°. Consequently reversal of the tensile and compressive strains were recorded by gauges 2 and 3. In all of the four simulated positions of supine, prone and alternate side lying non-linearity was observed below 40 microstrain in all gauges. The torque effects, however, were minimal in the alternate side lying position.

In the simulated left side lying position with the fractured (right leg) abducted and the pins therefore orientated at right angles to the

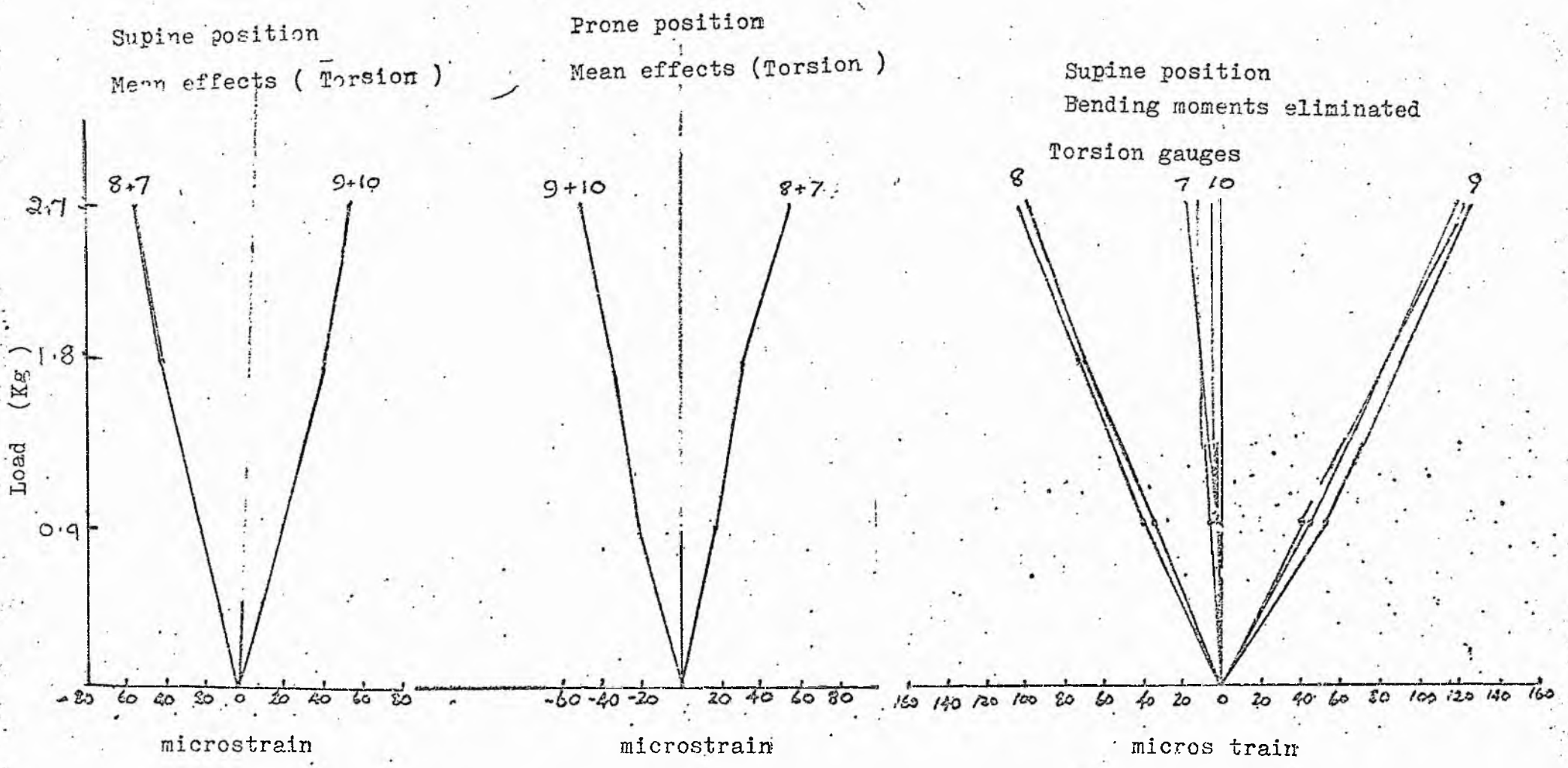
Supine position
Mean effects (Torsion)
Prone position
Mean effects (Torsion)
Supine position
Bending moments eliminated
Torsion gauges
8
7
10
9
8+7
9+10
9+10
8+7
2·7
1·8
0·9
Load (Kg)
-80 -60 -40 -30 0 20 40 60 80
microstrain
-60 -40 -20 20 40 60 80
microstrain
-160 -140 -120 -100 -80 -60 -40 -20 0 20 40 60 80 100 120 140 160
micros train

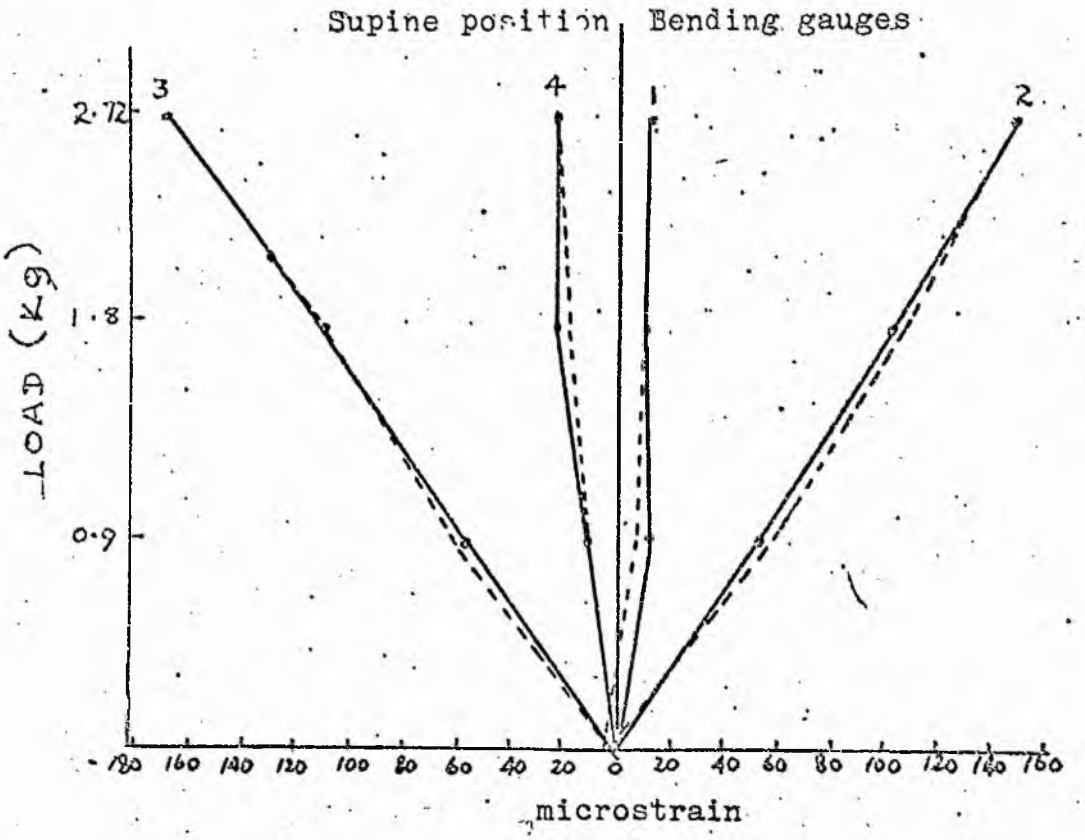
Supine position
Bending gauges
3
4
1
2
2·72
1·8
0·9
LOAD (KG)
180 160 140 120 100 80 60 40 20 0 20 40 60 80 100 120 140 160
microstrain

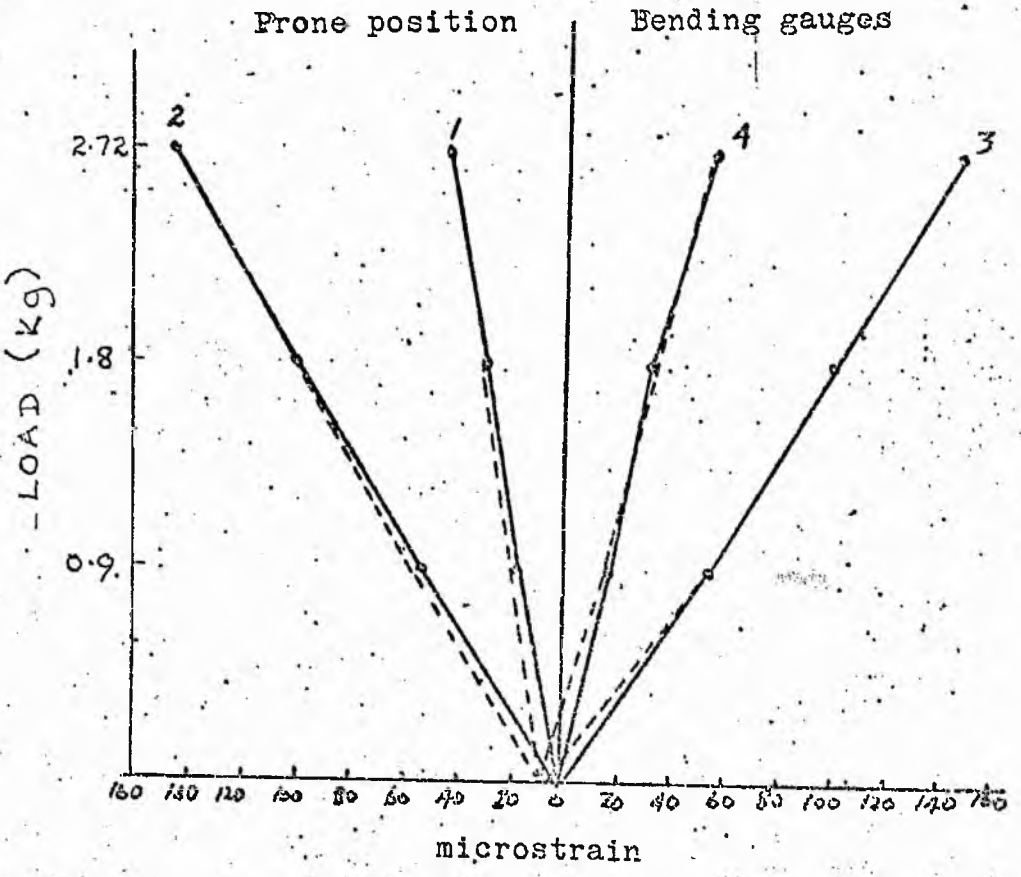
Prone position
Bending gauges
2
1
4
3
2·72
1·8
0·9
LOAD (KG)
160 140 120 100 80 60 40 20 0 20 40 60 80 100 120 140 160
microstrain

Supine position Torsion gauges

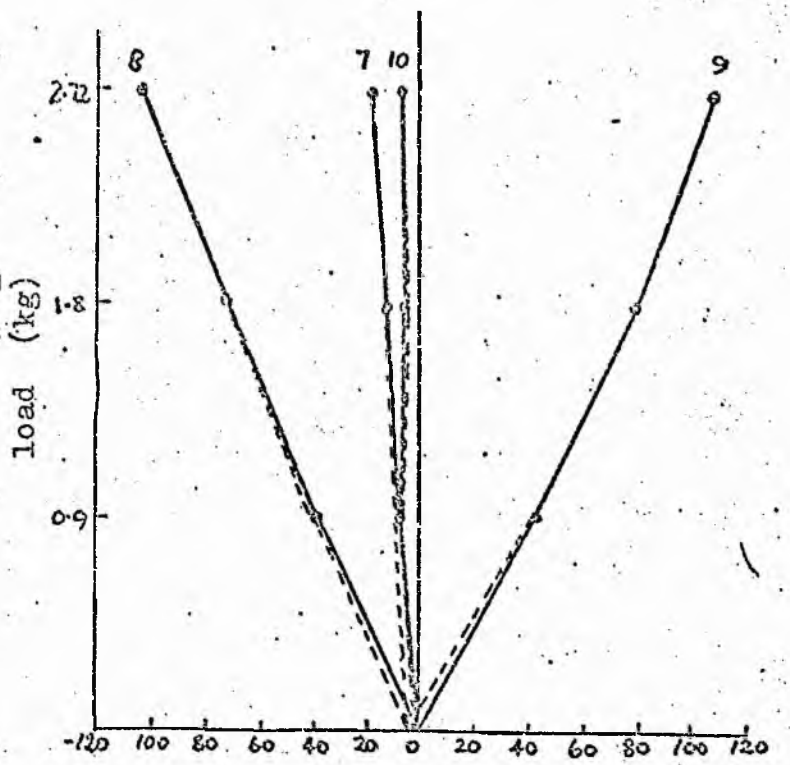

microstrain

Prone position Torsion gauges

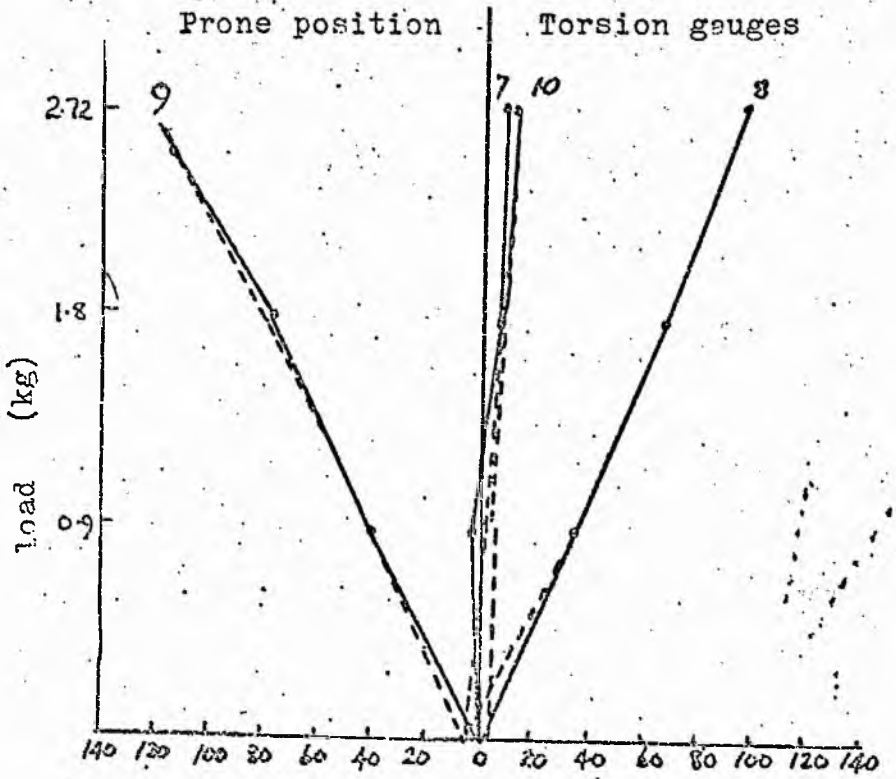

microstrain

RIGHT SIDE LYING. BENDING GAUGES

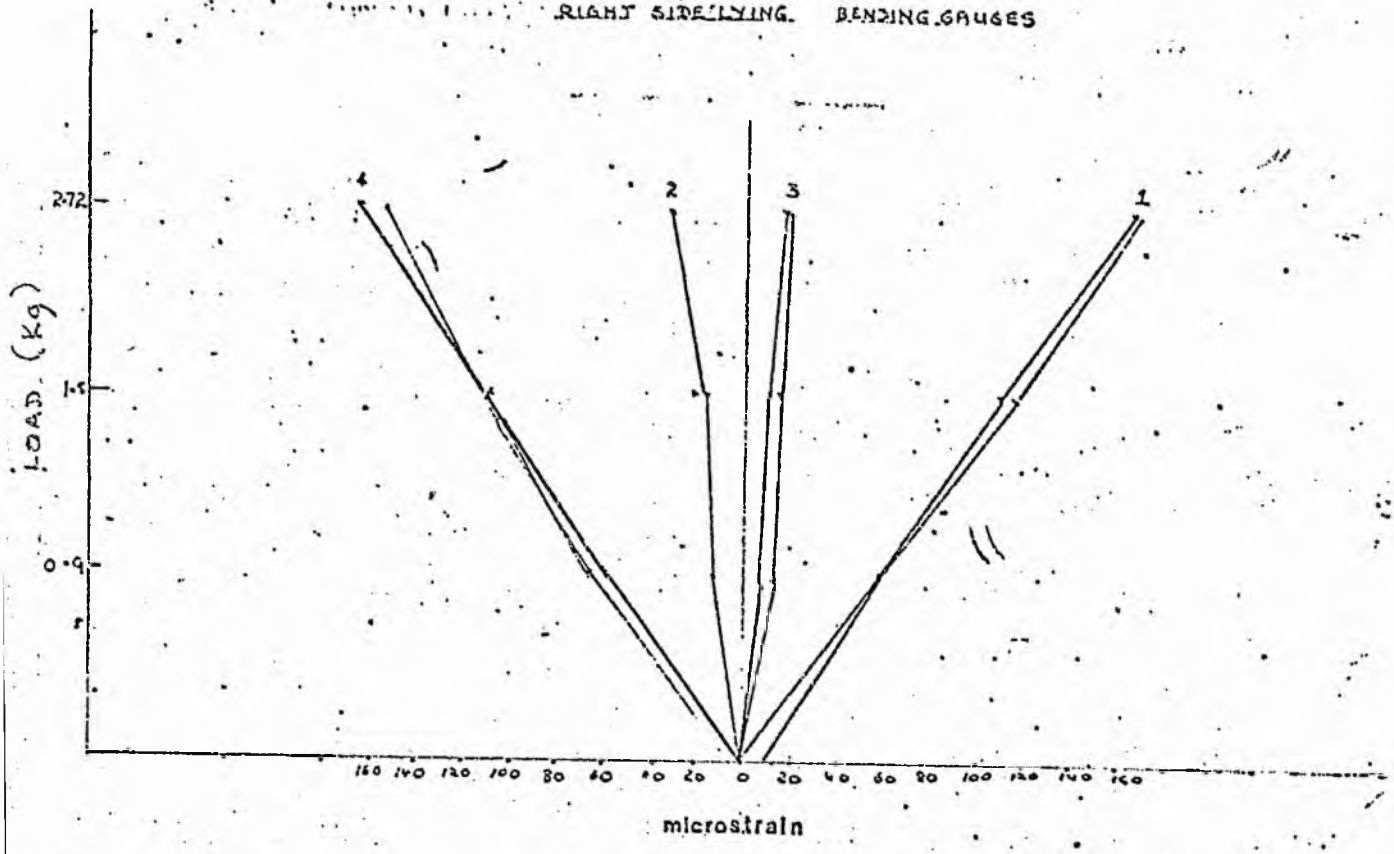

LEFT SIDE LYING BENDING GAUGES

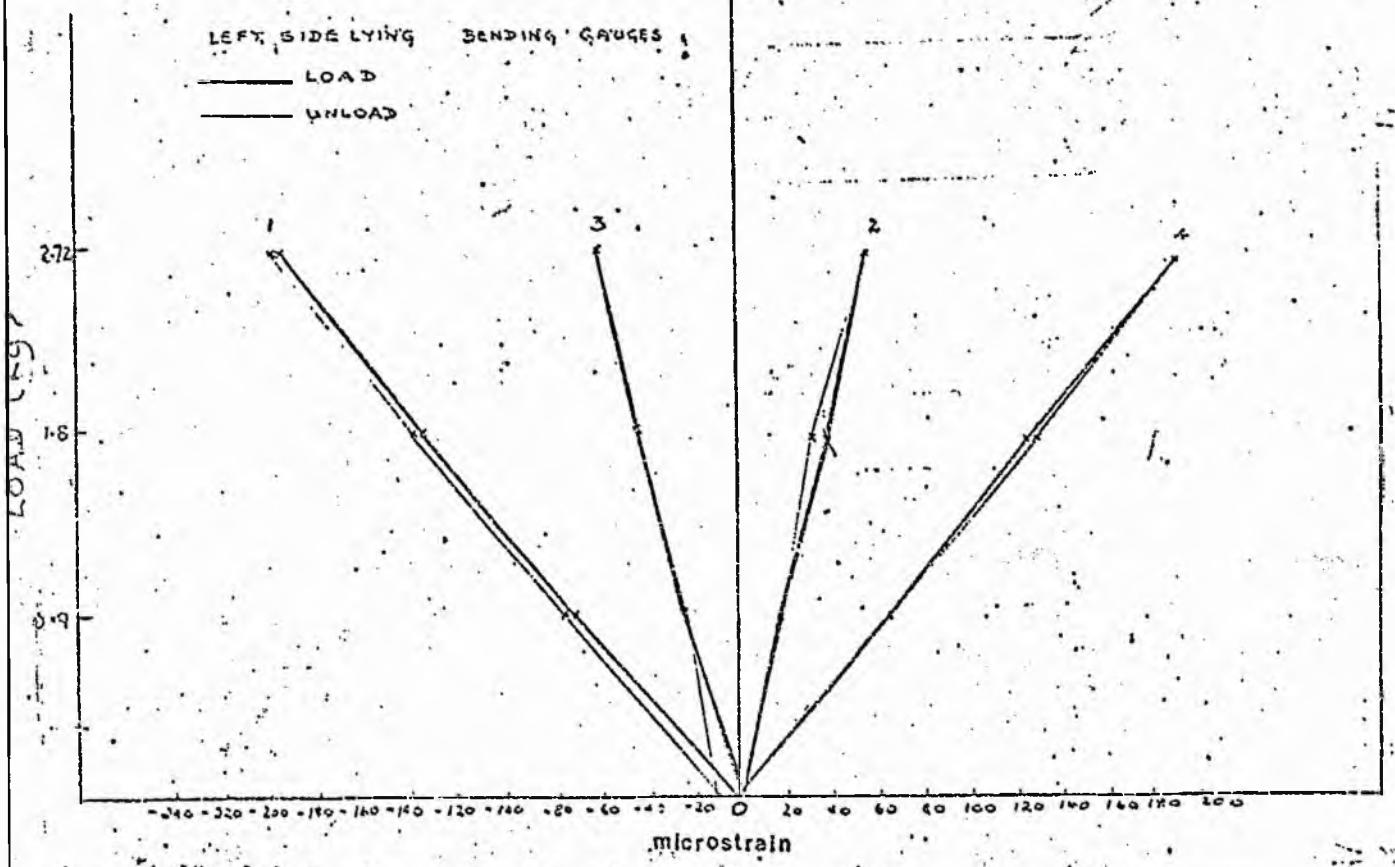

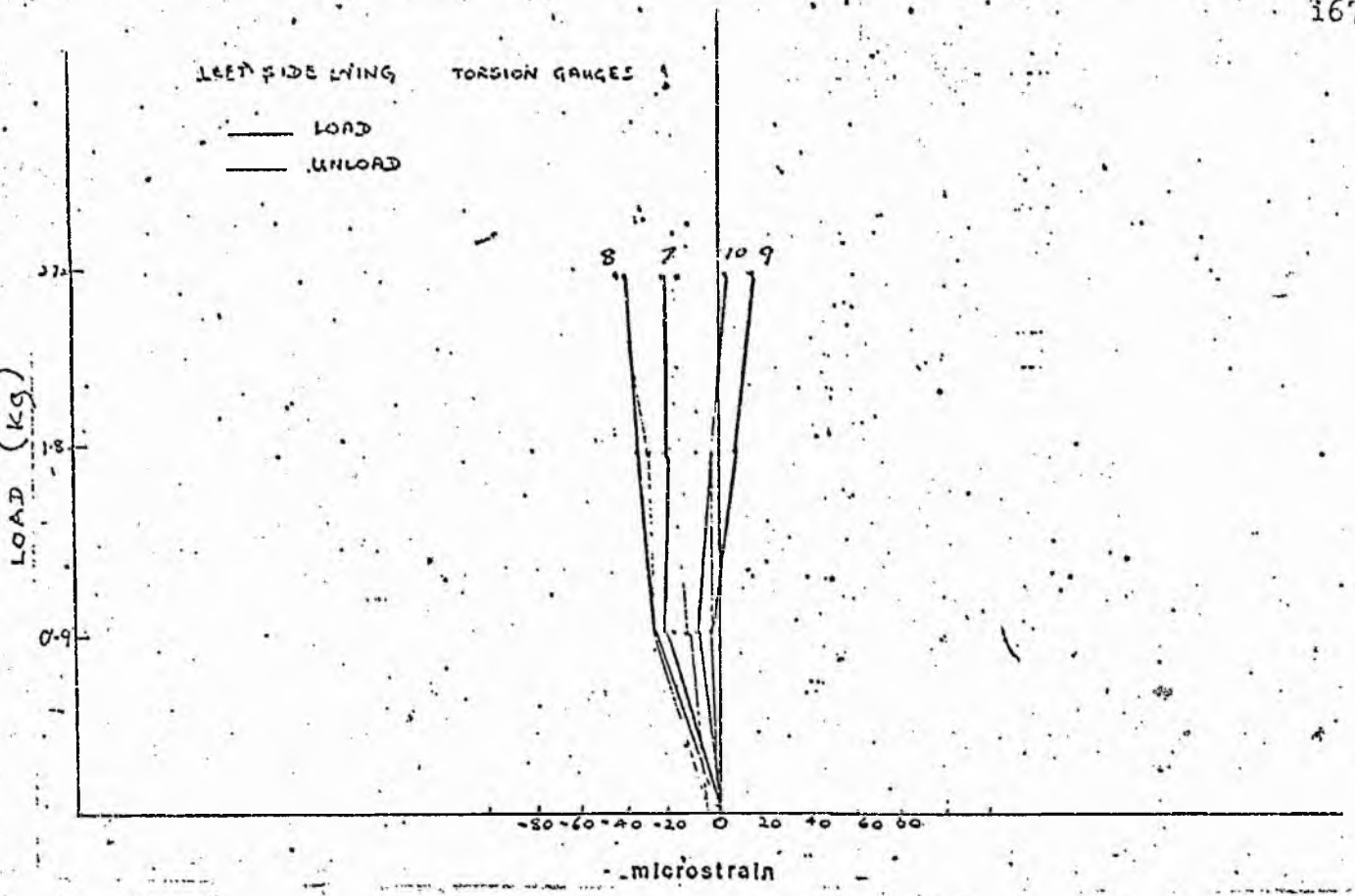
LEFT SIDE LYING TORSION GAUGES
LOAD
UNLOAD
8
7
10
9
LOAD (kg)
0·9
-50 -60 -40 -20 0 20 40 60 80
microstrain

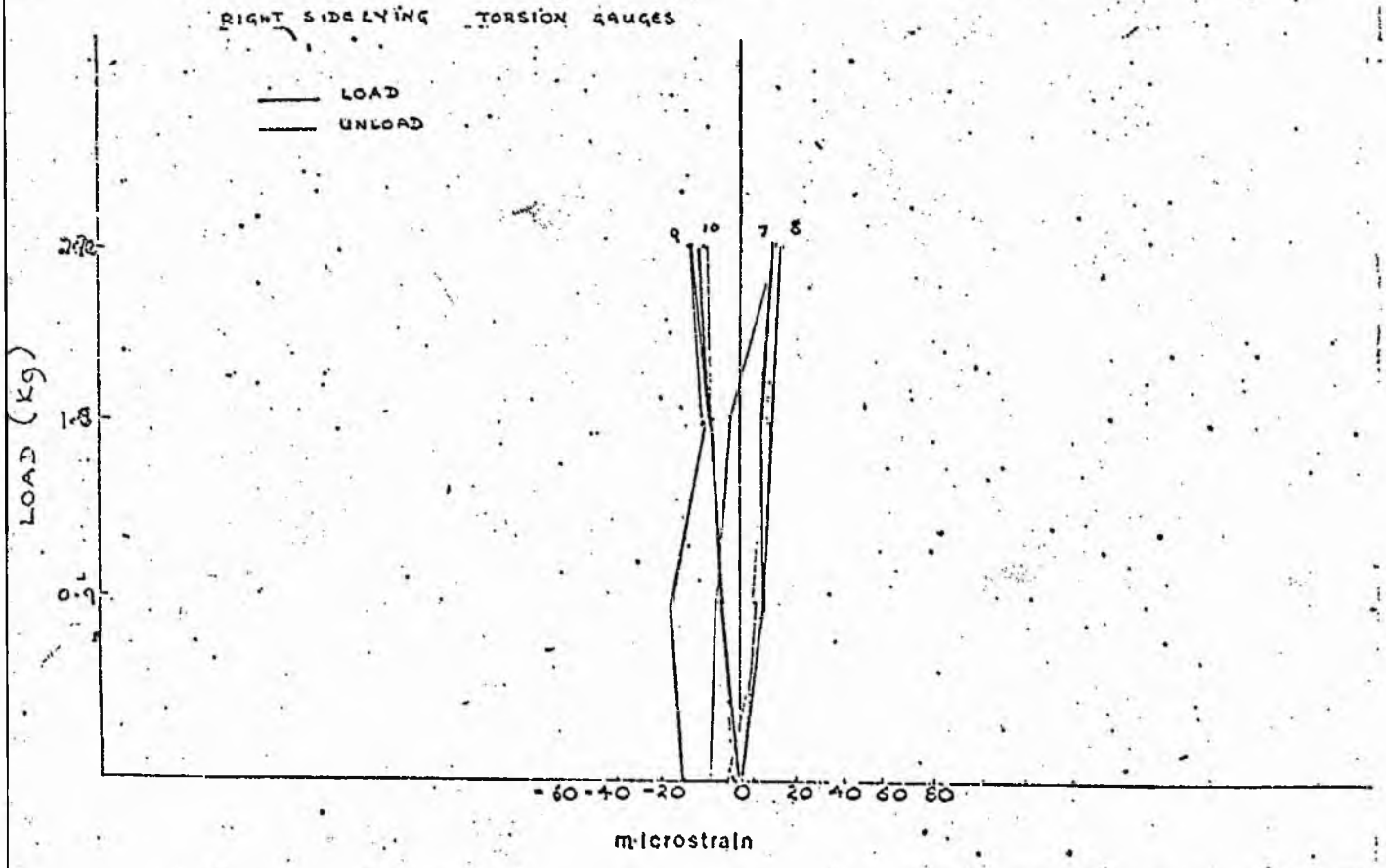
RIGHT SIDE LYING TORSION GAUGES
LOAD
UNLOAD
9
10
7
8
LOAD (kg)
1·8
0·9
-60 -40 -20 0 20 40 60 80
microstrain

to the plane of the floor, greater levels of strain were produced from the bending gauges (1 and 4) than in the supine position. In the latter the torque effects on the bar are considerable. From a theoretical consideration of the direction and point of application of load; in the side lying position, the bar is assumed to be subjected to pure bending. This assumption can be made providing the long axis of the bar and bone are parallel and in the same vertical plane but it is unlikely however, in the clinical situation that this would occur. If this assumption is valid then the response from gauges 3 and 2, which were located in an unstrained position, should have been minimal. Their response however indicated significant bending of the bar for a given load of 2·7 kg and it was concluded that the level of strain recorded is dependant upon the orientation of the limb in space and the relative alignment of the bar and bone.

The sensitivity of the instrumentation as defined by the Vishay instrument guide suggests that adequate sensitivity of the recording instruments is obtained between 80 - 8000 microstrain. The maximum strain recorded from these experiments is below 200 microstrain and the predicted values for strain in the supine position is below 80 microstrain. Absolute levels of detectable strain by direct instrumentation of the device were therefore considered unreliable.

CHAPTER FIVE

The experimental work described in Chapter Four indicated that levels of strain are not detectable when firm union of the bone has occurred. The analysis presented in Chapter Three revealed that changes in the level of strain would not be detectable during the final stages of healing. In a separate analysis, the motion that takes place at the fracture site was determined. This work was however carried out on a single configuration of bone, pins and bar. Variable configurations of the fixator and additional physiological factors had not been taken into account.

The theoretical investigation using the Prime Stress Program considers the effect of these fixator variables and physiological factors upon fracture site motion.

This investigation also includes a study of the effect on fracture site motion when changes in the mechanical properties of callus take place during healing.

5.1.1 The following FIXATOR VARIABLES were identified:

1. Dimensions of the Transfixing Pins

a) Diameter

b) Length

Optimum dimensions of the pins and their effect on strength of bone has been investigated by previous workers (see Chapter Two) but it is evident that a standardized pin size, used in conjunction with different types of single-sided Fixators is not employed in clinical practice.

2. Pin Disposition

a) Spacing between the Pins

b) Angulation of the Pins

3. The Offset of each pin group from the fracture gap

4. Dimensions of the Fixator Bar

a) Diameter

b) Shape of the Bar cross-section

c) The length of the Bar between the two groups of pins.

It is well established that the dimensional factors determining the strength of a structure are the cross-sectional area and second moments of area (see Chapter 2 Part A). If the density of the material remains constant then a dimensional change means a change in weight since

$V = AL$ where V = volume

and $M = V\rho$ A = area

then L = length of member

$M = AL\rho$ ρ = density

M = mass

If L and ρ remain constant then a percentage change in Area gives a percentage change in weight.

Previous workers have suggested that minimal weight of a Fixation Device is important but the relative significance of Bar mass and dimensions upon the fracture site motion has not been fully investigated.

5. The application of Compression across the Fracture Site

Compression may be applied axially through the length of the bone, or by various compressive devices incorporated within the Fixator. (see Chapter 2 Part D).

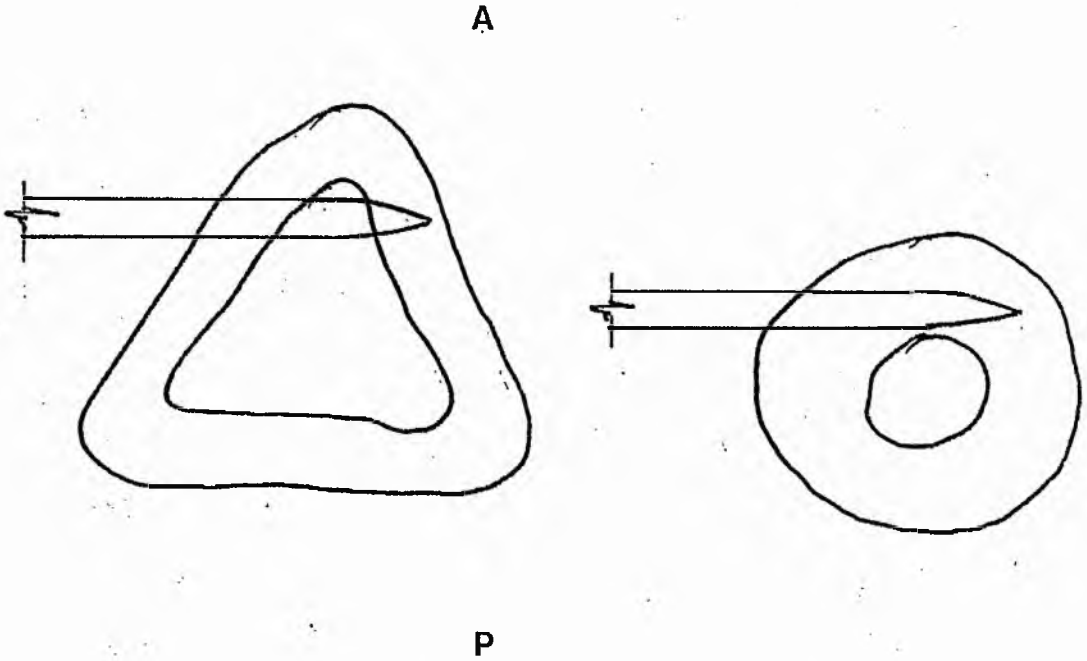

Figure 53: Pin contact area in bone
A. Anterior
P. Posterior

PHYSIOLOGICAL FACTORS

6. Bone and Callus

The transfixing pins, if correctly inserted, normally engage both cortices of the bone, and the area of cortical bone in contact with the pins will be dependant upon the geometry of the cross-section, the angle of insertion and the position of the pins in the antero/posterior plane (Figure 53). The contact area will therefore vary from pin to pin and between each pin group. The dimensional changes with length of cortical bone were therefore considered for analysis.

As callus forms, changes in both the dimensional and elastic properties occur. The representation of callus in a theoretical analysis is however limited by the lack of quantitiable dimensional data. The material properties of callus are dependant upon the type of callus response (see Chapter 2 Part C), and the rate of production of osseous material. As a consequence an estimate of the dimensional and material properties can only be made by considering the processes involved (i.e. the type of callus response) with a particular fixation method, together with a comparison of the data that exists for fibrocartilage, cartilage and bone. This data may, alternatively, be expressed as a percentage of the values for normal bone. The transitional behaviour of callus from plastic to viscelastic behaviour, i.e. time-dependant behaviour, is not however evaluated by this method.

7. Muscle and Soft Tissue

The extent to which soft tissues provide additional support at the fracture site has not been extensively investigated (see Chapter 2 Part B). In addition no work has been carried out which determines the effect of static or dynamic muscle contraction upon fracture site motion in a limb supported by an external fixation device.

8. Functional Loading

The benfits of functional loading of the bone, during healing, are well documented (see Chapter 2 Part C). It is clear that in normal and restricted activity (e.g. crutch walking or periods of bed rest) multi-axial loading of the bone occurs. The direction of the applied load is therefore dependant upon the orientation of the limb in space. For analytical purposes however daily activity may be analysed into four simple activities:

a) straight leg raising with antero-postero bending of the bone.

b) side lying with the leg abducted and lateral bending of the bone.

c) high sitting with tension at the fracture site.

d) standing with axial compressive loading of the leg.

9. Characteristics of the Fracture

The characteristics of the fracture may be defined by the site, type and severity of the break. It was felt intuitively that more distally located fractures would result in smaller bending moments and less motion at the fracture site , i.e. greater stability. The site of the fracture may also determine the number of pins that are used, e.g. if a fracture is located at the ends of the bone, there may be insufficient space to locate more than two pins in the smaller section of bone. The number of pins that are used will also be dependant upon the degree of comminution, since additional pins may be required to secure isolated pieces of bone. During healing, particularly in the early stages, there may be considerable oedema localising in the distal section of the limb. As a result the magnitude of the bending moments acting upon the fracture site and fixator will be correspondingly increased, due to the increase in leg mass distal to the fracture site.

5.2.1 THE PRIME STRESS PROGRAM

When a preliminary investigation into the Prime Stress Program was carried out considerable difficulty was encountered in determining the formula to be used to describe the "Shear Area" of a member. This is referred to in the Prime Stress Manual in the section "Member Properties" which define the cross-sectional shape of a prismatic member and standard formulae are therefore used to define area, polar and second moments of area. In the Prime Stress Program these correspond to:

Area = AX

Polar second moments of Area (J) = 1X

Second Moments of Area (I) = 1Y and IZ

and SHEAR AREA = AY / AZ

The expressions AX, AY / AZ, 1X, 1Y and IZ describe the six vector components which are used in the analysis of a SPACE FRAME. This is a structure in which six degrees of freedom are represented at each joint. It was felt that the bone, fixator, carriages and transfixing pins could be represented as a space frame for which "Shear Area" of each member had to be defined.

Simple beam deflection tests were designed to determine the accuracy of the program and the correct method of inputting data for "Shear Area". In these tests the computed deflections due to bending of the beam were compared with theoretical values which were derived using Strain Energy techniques.

5.2.2 BEAM DEFLECTION TESTS

The formula for total deflection at A (Figure 54) was determined

for a double beam with Cantilever Fixation at C. Four tests were conducted with constant elastic moduli and member lengths for Beams AB and BC.

Test a) A Solid Circular Rod where Diameter = 8 mm

Test b) A Circular Tube where ∂ = 6 mm D = 8 mm

Test c) A Square Beam where L = 8 mm

Test d) A Rectangular Beam where l = 4 mm h = 8 mm

All other input data is listed in Appendix 5.1, and 5.2 together with the Input listing and tabulated results for a Solid Circular Rod (a) in Appendix 5.3.

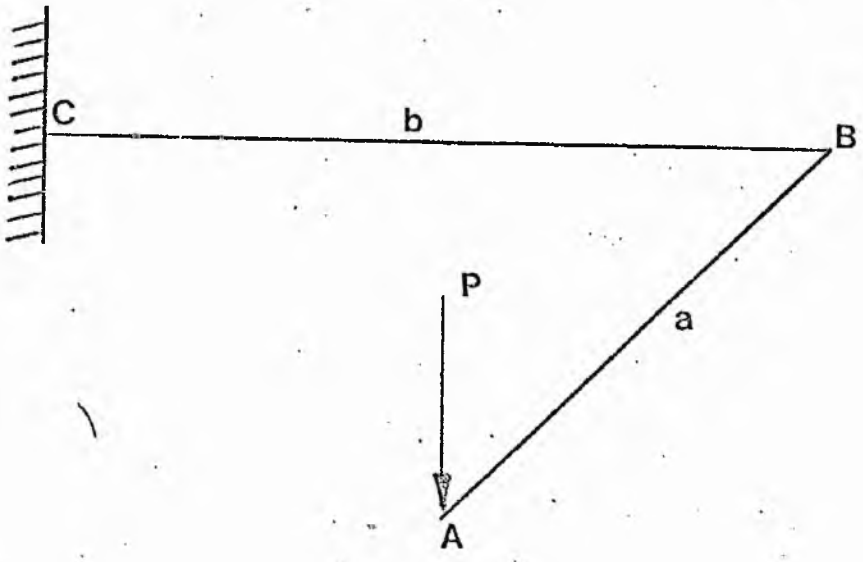

fig 54 Beam deflection

$$\frac{\partial u}{\partial P} = \int_0^a \frac{M_{AB}}{EI}\left(\frac{\partial M_{AB}}{\partial P}\right) dx + \int_0^B \frac{M_{BC}}{EI}\left(\frac{\partial M_{BC}}{\partial P}\right) dz + \int_0^b \frac{T_{BC}}{GI}\left(\frac{\partial T_{BC}}{\partial P}\right) dz$$

$$\frac{\partial u}{\partial P} = V_{AB} = \int_0^a \frac{Px^2}{3EI}\, dx + \int_0^b \frac{Pz^2}{EI}\, dz + \int_0^b \frac{Pa^2}{JG}\, dz$$

$$V = \frac{Pa^3}{3EI} + \frac{Pb^3}{3EI} + \frac{Pa^2 b}{JG} \qquad \text{.....Equation (7)}$$

Results of Beam Deflection Tests

The results from each test are tabulated below (Table 5.1), and the theoretical values for deflection of Beam AB at A are compared with the computed value.

Table 5.1: Results from Double Beam Deflection Tests

Beam AB Test	Deflection mm (theoretical) (V)	Deflection mm (computed)
a)	.4127	.4127
b)	.6080	.6046
c)	.2406	.2432
d)	.3036	.6128

Excellent comparibility was obtained for a Solid Circular Rod, but small errors were noted for a Tube. An error of 0.5% was noted for a Circular Tube and 1.1% error for a Square Tube. A large inconsistency was found for a Solid Rectangular Block. This was thought to be due to the limitations of the formula for Polar Moment of Area for a

Solid Rectangular Block. This was thought to be due to the limitations of the formula for Polar Moment of Area for a Rectangular Block, which was found from Standard Engineering Textbooks (See 'Bibliography'). From additional examples of input data for a Space Frame obtained from PRIME COMPUTERS (MASSACHUSETTS) together with the comparative results obtained from the Beam Deflection Tests, it was concluded that Shear Area (AY / AZ) was a function of cross-sectional Area rather than the length of the Member and that computation of Shear Area was based upon Standard Formula for cross-sectional area.

The Stress Program was however considered to be sufficiently accurate for the Analysis of Variables of the Bone / Fixator Configuration where the detection of trends of behaviour were required rather than absolute values of Displacement.

5.3.1 THE ANALYSIS OF PHYSIOLOGICAL AND FIXATOR VARIABLES BY THE PRIME STRESS PROGRAM

The Base Models

Four configurations of Bone and Fixator formed the basis of this analysis. These are represented by Models 1, 2, 3 and 4, in which the weight of the pins is ignored and all computations are in Newtons and millimetres. Edge and Denham (see Chapter 2 Part D) suggest an interval of 40 mm between the Bar and Bone. This was calculated to give an approximate pin length, for analytical purposes, of 56.58 mm between the central axis of the bone and the central axis of the Bar. The distance between each group of pins and the spacing between the pins represented the configuration used in the experimental work. The pins were assumed to be parallel and in one plane with the central axis of

the bar and bone. To simplify the analysis, it was also assumed that the length of the bar, which protrudes from the remote ends of each carriage, is non load bearing and was therefore excluded from representation in all four models. The mass of the protruding section of bar was however included in the total weight of each carriage. The dimensional data and Elastic Moduli of each component is listed in Appendix 5.4. The data for Models 1, 2 and 3 is in Appendix 5.3 and for Model 4 in Appendix 5.6.

Loading data for Models 1, 2, 3 and 4

Uniformly distributed loading was assumed for the distal section of leg (except Model 1), the two carriage sections and the Bar (Figure 55). The source data from which the total weight of the distal limb section was determined is presented in Chapter 2 Part B. The sum of the forces exerted by each "Member" is equal to the total force exerted by that section of leg. (For definition of "Member" see page 181). The weight of the proximal limb section (p) was ignored, since the investigation was confined to determining the relative displacement of the two bone ends, at the fracture site. The proximal section of bone (p Figure 55) was assumed to be rigidly fixed simulating full extension of the knee, which is maintained by the quadriceps muscle and ligamentous support. Since the unit weight of the fixator bar and the 'bone' used in the experimental model could be easily found, the weight of the carriage sections could be determined by weighing the experimental configuration. (see Chapter 4).

In the subsequent analysis, any change in member lengths due to co-ordinate changes required a change in local member forces. Since the unit length of bone, carriage and bar could be easily calculated, changes in local member forces were made by multiplying the unit length by the new length of each member.

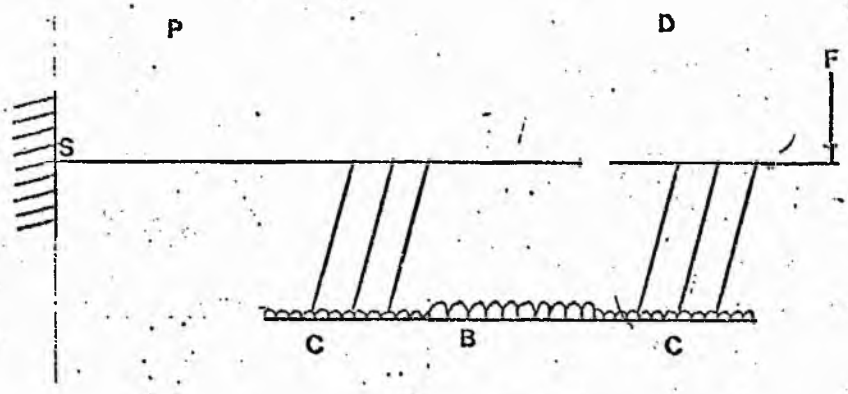

a Model 1.

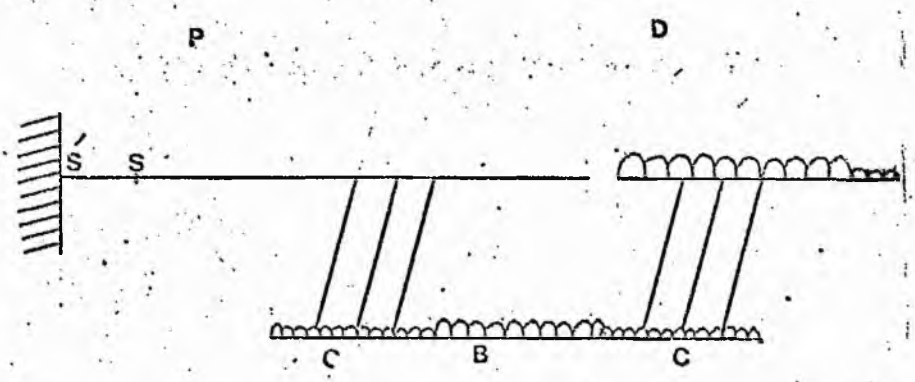

b Models 2, 3 & 4.

S knee — $\overline{S}$ quadriceps attachment

P proximal — D distal

C carriage — B bar

fig 55

LOADING DIAGRAM

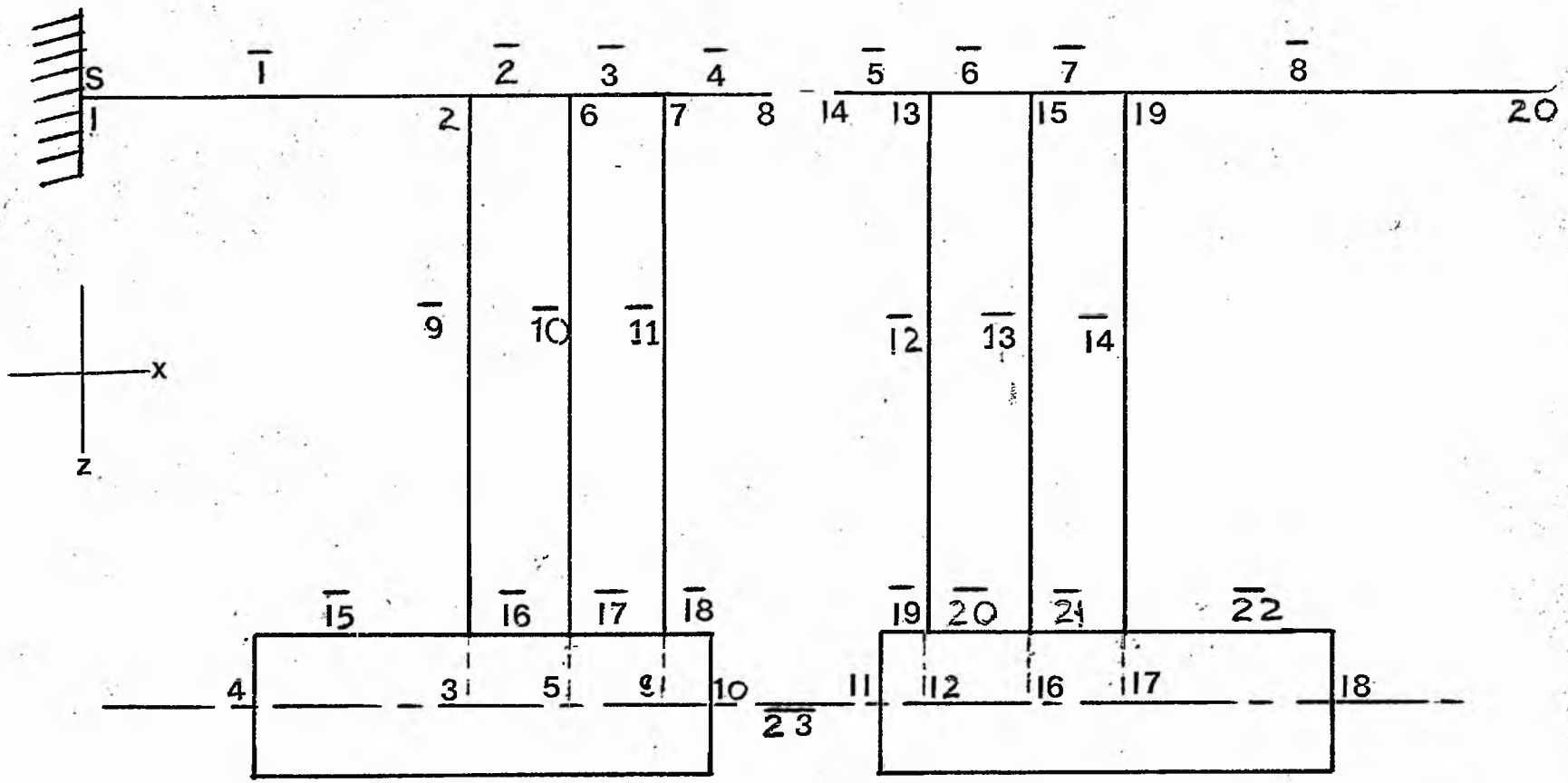

1 member

1 joint

MODEL 1

fig. 56

As the carriage sections included the weight of the protruding end sections of the bar, any increase in central bar length (between the two carriages) necessitated a corresponding reduction in the total weight of the two carriages. For the actual method of calculation and the loading data used in the work the reader is referred to Appendix 5.4.

The length of the foot defined in models 2, 3 and 4 is represented by the fully dorsiflexed position of the foot, where the distance between the ankle joint and the base of the heel pad was found to be 60 mm.

The length of the foot was assumed to be a Beam with a uniformly distributed load.

Description of the Base Models 1, 2, 3 and 4.

Model I

This model simulates the experimental configuration of a distally located unstable fracture of the lower leg (Chapter 4) in which external uniform loads were assumed due to the mass of the foot, the carriage sections and fixator bar. The 'bone' is uniform in cross-section and joint 1 (Figure 56) is identified at 50 mm from the proximal end. This is a support joint (S) in which rigid fixation, representing the mid-point of the insertion of the quadriceps muscle, is assumed. The uniformly distributed loads were represented by point loading at the mid-point of each 'member' where a member is the section between two joints, e.g. member 16 occurs between joints 3 and 5 (Figure 56). The mass of the leg distal to the fracture site was ignored.

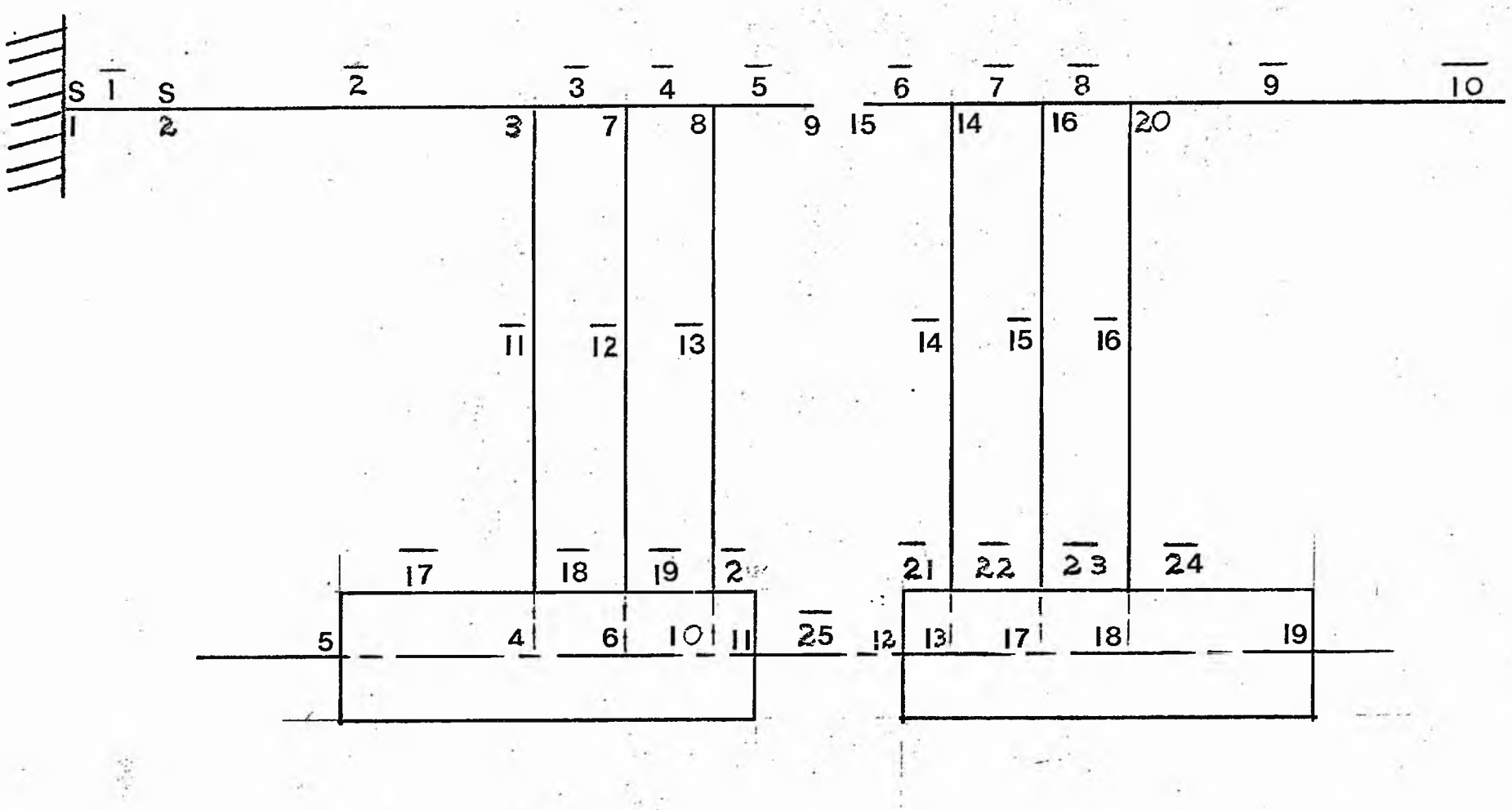

MODELS 2, 3 & 4

fig 57

Model II

Two support joints S_I and S_2 are included in this configuration and represent fixation of the proximal limb section at the knee joint (S_I) (Figure 57). The bone is of uniform cross-section similar to Model I but the Force due to the mass of the leg distal to the Fracture Site is included.

Model III

This model is similar to Model II but the uniform cross-section of bone is replaced by an idealised model of bone derived from tibial dimensional data (see Chapter 2 Part B).

The Prime Stress Program has the facility to analyse straight Prismatic Members of constant cross-section (see Manual: Primes Version of Stress 3.2) and it was felt adequate for this analysis to calculate the mean values for Cortical Area (AX), Polar (IX) and Second Moments of Area 1Y/1Z. These mean values were derived from the data for the cortical profiles presented by Piezali et al (1980) and Miller and Purkey (1980). Their data was replotted and expressed as a percentage of bone length taking care to ensure that the Co-ordinate System presented by these workers matched the Co-ordinate System of the Stress Program where it was found that

$$Ixx = \int_A x^2 \partial A$$

This corresponded to the dimensions in the medial/lateral direction of the bone and the Z axis of the Cartesian Co-ordinate System of Prime Stress so that

$1xx = 1Z$

and $1yy = 1Y$

Various points were then taken along the length of the 'bone' which correspond with landmarks such as the Tibial Tuberosity, the Insertion of the Pins and the level of the Fracture Site. The Area, effective J, and Shear Area were then calculated and expressed in millimetres. The bone was then divided into three zones which were determined by two principle factors.

a) The insertion of the Quadriceps tendon into the Tibial Tubercle, determining the limit of Zone 1.

b) The level of the lowest values for I and J, where fractures are most likely to occur, determining the limit of Zone II.

Zone I

The midpoint of the insertion of the Quadriceps tendon was identified and expressed as a percentage of total bone length. This approximated to 50 mm for a Tibia measuring 420 mm.

Zone II

The limit of Zone II was found to be approximately 272 mm from the proximal end of the bone where total discontinuity and a gap of 4 mm represented the fracture site.

The mean dimensional values were then determined from the data presented in Appendix 5.5 Table a) and the final data used for each zone is presented in Table b) of Appendix 5.5.

The distal section of bone in Model III was therefore in Zone III.

Model IV

This model was represented by a fracture in the middle third of the leg with the fracture site located between joints 9 and 15 at 207 and 211 mm respectively. The middle pin of the distal pin group was therefore loacted at the junction of Zone II and III. (see Figure 57)

5.3.2 INTERPRETATION OF DATA FROM THE PRIME STRESS PROGRAM

The Stress Program calculates individual displacements and rotations which occur at each free joint for each of the six vector components. For example, in the tabulation of FREE JOINT DISPLACEMENTS for Model III, it can be seen for joints 9 and 15, representing the fracture site, the following data is printed (see Appendix 5.6 for complete listing).

JOINT	XDISPL	YDISPL	ZDISPL	X-ROTAT	Y-ROTAT	Z-ROTAT
9	0.0000	-0.5962	0.0000	0.0011	0.0000	-.0039
15	0.0000	-2.4904	0.0000	-0.0099	0.0000	-.0439

The actual movement occurring at the fracture site is then determined by subtracting the displacements and rotations occuring at joint 9 from those at joint 15. Displacements are listed in millimetres and rotations listed in radians. Radians may then be converted to degrees where

$$\frac{x \text{ Rads} \times 180}{\pi} = X \text{ Degrees}$$

Member forces are tabulated for the joints at each end of a member (Appendix 5.6) for which values of shear forces (Y and Z) and moments are given (torsion and bending). Shear force is expressed in Newtons and moments in Newton X millimetres.

Comparison of Motion occurring in the Four Base Models

Maximal deflection occurred at the fracture site in Model IV, which represented a fracture located in the middle of the leg and minimal deflection occurred in Model I. The latter represented the configuration used in the experimental work in which the mass of the foot was included but the mass of the leg distal to the fracture site was ignored. The results from the four base models are tabulated below.

TABLE 5.2

MODEL	DISPLACEMENT mm			ROTATION (Degrees)		
	X	Y	Z	X	Y	Z
I	0	-1.053	0	-.17	0	-1.38
II	0	-1.9	0	-.63	0	-2.29
III	0	-1.89	0	-.63	0	-2.29
IV	0	-2.33	0	-.8	0	-3.5

The deflection occurring in the Y axis represents the vertical deflection at the fracture site (Figure 58).

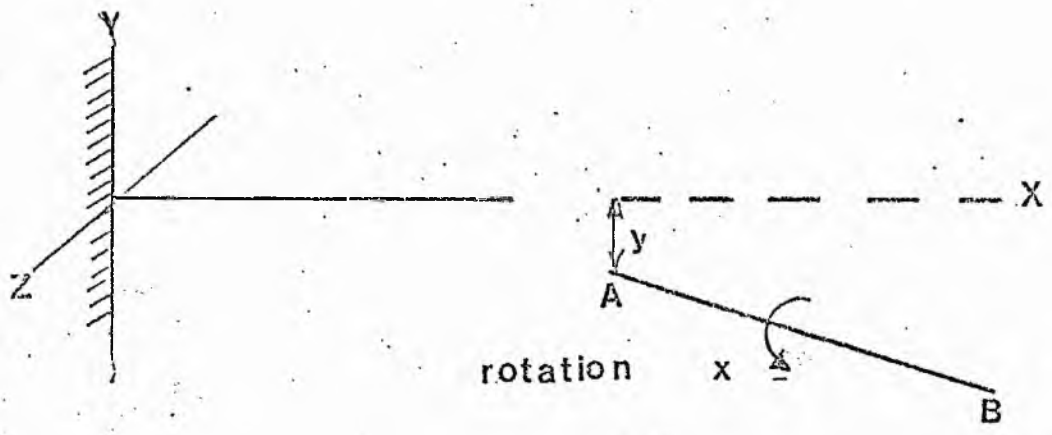

fig. 58.

The deflection obtained from Model I was compared with the measurement of vertical displacement obtained experimentally under similar loading conditions (Table 5.3).

TABLE 5.3

Model I	Vertical Deflection
PRIME STRESS	- 1.053 mm
*EXPERIMENTAL	- .621 mm

* This measurement was obtained using an optical microscope. The computed displacement calculated for Model II was compared with the calculated displacements derived from the analysis of fracture site motion (see Chapter 3 Part A) which are tabulated below.

TABLE 5.4

CALCULATED DISPLACEMENTS		PRIME STRESS Corresponding Joint	
V	3.3 mm	12	3.79 mm
$Y4_B$	3.75 mm	14	4.28 mm
Y_F	1.7 mm	15	1.89 mm
ϕ_2	2.7°	Rotation Z	2.29°
θ	$.4^\circ$	Rotation X	$.63^\circ$

where Y_F (Joint 15) is the deflection occurring at the fracture site. It can be seen from TABLE 5.2 that the dimensional variation of bone (Model III) did not contribute to the overall stability of the bone/fixator configuration when the bone is completely disrupted. This was also observed throughout the subsequent tests on this Model.

5.3.3 METHODOLOGY

Two alternative methods of analysing the variables were considered.

1. MODIFICATION of the existing STRESS Program by the creation of sub-routines for the analysis of each variable, e.g. any change in the spacing of the pins requires an accompanying change in the local member length of the Bone and Carriage Sections. As a result the local member Forces also change. The sequential changes necessary could therefore be written into the existing program.

2. This was the method chosen by the author and considered Models II, III and IV described earlier (see para. 5.3.1). For this second method concurrent tests were carried out on each model, a single variable being modified for each test. The modification of each variable required changes in the data for each base file. Changes in the data were calculated prior to the test and a subfile created from the original base file, then stored in the User File Directory, and subsequently run using the Stress Program.

5.4 DATA MODIFICATION FOR THE FIXATOR VARIABLES AND THE ANALYSIS OF EACH VARIABLE

1a. PIN DIAMETER

The effect of an increase in pin diameter was studied incrementing randomly, in six steps, the core diameter of stainless steel pins from 3.67 mm to 4.8 mm.

The pin length remained constant at 56.58 mm, and for the actual input data for the change in pin member properties, the reader is referred to Appendix 5.6.a.

Since the weight of the pins had been ignored in all Models, a change in force due to the increased dimensions of the pin was not included in the analysis.

Table 5.5, illustrates the percentage change in value of the pin member properties as the diameter is increased.

TABLE 5.5: Percentage change in value of pin member properties - core diamter = 3.67 = 0%.

CORE Ø	Ø	AREA (AX)	SHEAR AREA (AY/AZ)	TORSION CONSTANT (J) (1X)	MOMENT OF INERTIA (I) (1X/1Y)
	% INCREASE				
3.87	5.4	11.25	11.25	23.7	23.7
3.97	8.17	17.0	17.0	37.1	37.0
4.1	11.7	24.9	24.9	55.8	55.8
4.3	17.16	37.2	37.2	88.5	88.5
4.5	22.5	50.43	50.43	126.1	126.1
4.8	30	68.4	68.4	185.4	185.4

RESULTS

These results are presented graphically (Page 190) and the tabulated results (Appendix 5.7.a). From the tabulated results it can be seen that similar deflections and rotations occurred in Models II and III. Plotting motion (deflection and rotation) against an increase in pin diameter, the graphical presentation of the data for Model III demonstrates a gradually diminishing exponential curve and non-linearity. A similar trend is observed for Model IV, but the magnitude of motion is greater. From the slope of the graph in Models III and IV maximal changes in motion occur when the core diameter of the pin is less than 4 mm. From the graph

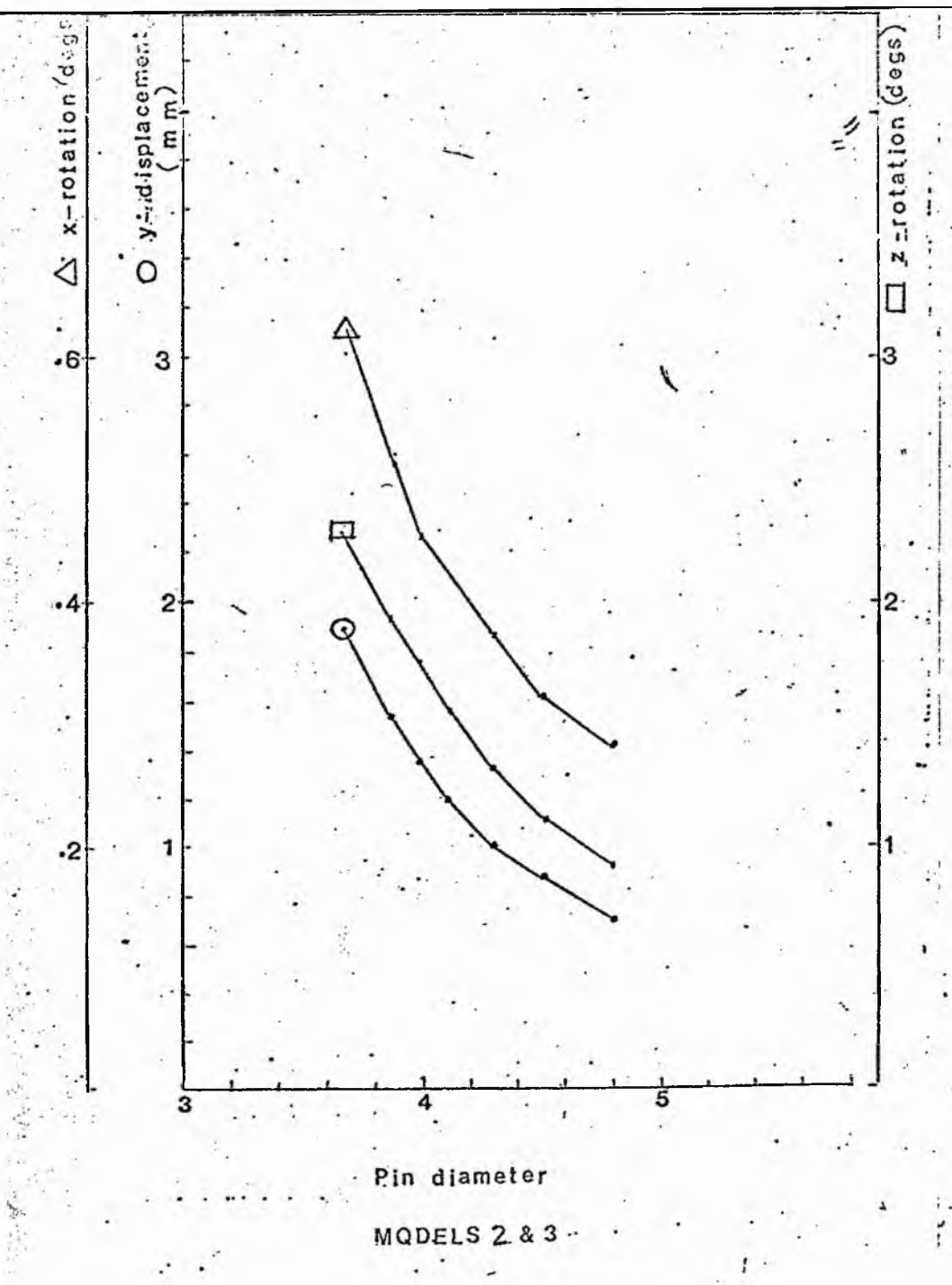

MODELS 2 & 3

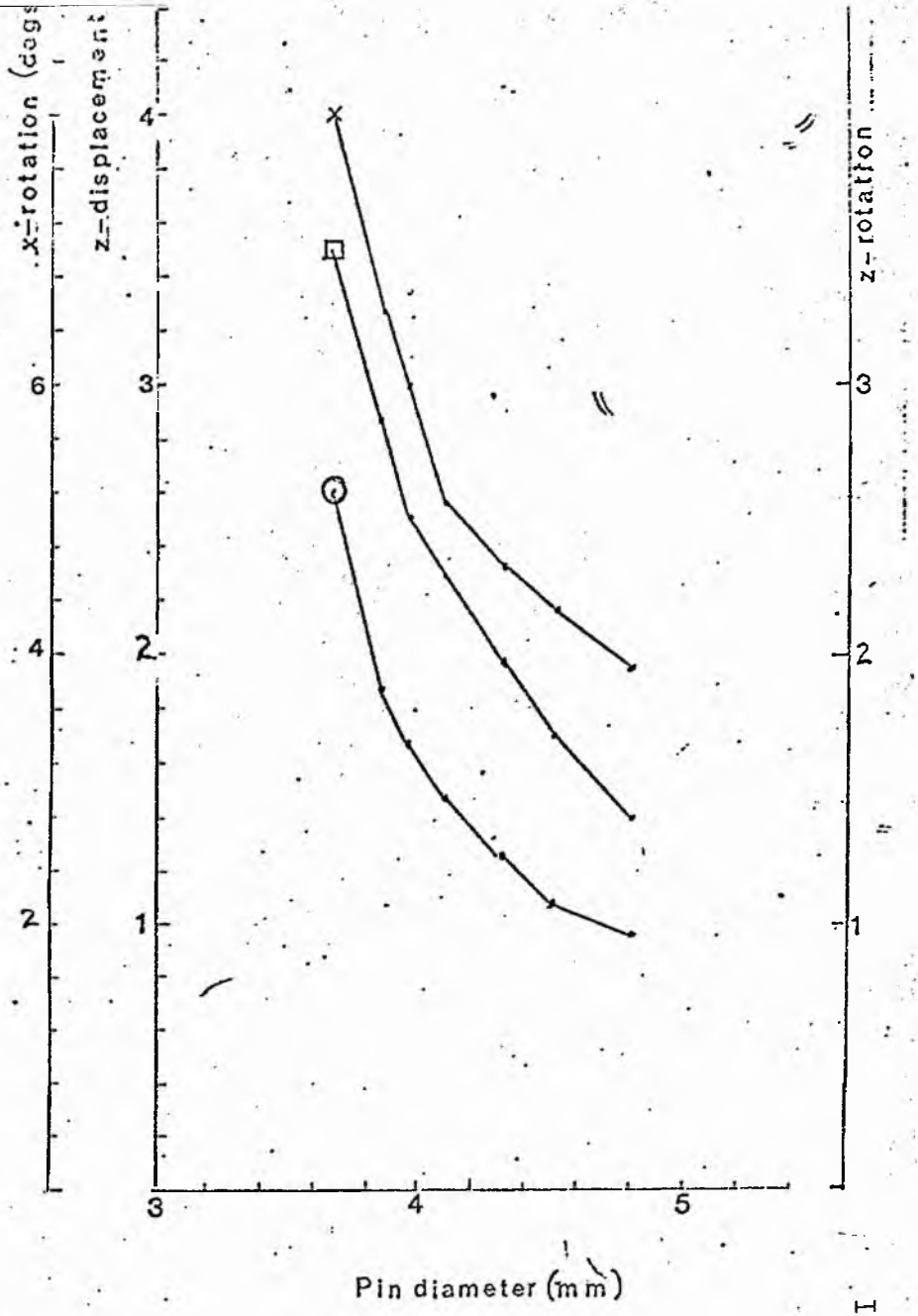

MODEL 4

for Model III it is estimated that vertical deflection at the fracture site may be reduced to .5 mm with a core diameter of 5 mm for each pin and a constant "length" of 56.58. For a fracture in the middle of the leg it is estimated that deflection may be reduced to less than 1 mm with similar pin dimensions.

1b. PIN LENGTH

The offset of the fixator bar from the bone is determined by the "length" of the pins spanning the interval between bone and bar. For analytical purposes this was assumed to be 56.58 mm (see Para. 5.3.1) in the base models. The analysis of fixator stiffness as a function of pin length was determined by random changes in pin length from 40 mm to 73.55 mm. The following values listed below were substituted in Models II, III and IV in the positive Z axis of the Cartesian Co-ordinate System for joints 4 - 6, 10 - 13 and 17 - 19, (Figure 57) in four successive tests:

40 mm, 50 mm, 60 and 73.55 mm

RESULTS of change in pin length :-

Similar results were again obtained between Models II and III (Appendix 5.7.b) and the greatest range of motion occurred in Model IV. The results from Models III and IV are presented graphically on Page. 192 Motion is plotted as a function of pin length and a non-linear response can be observed in both models. From the slope of the graphs, it was concluded that rigid fixation of the fracture site could be obtained by reducing the pin "length" to less than 3 cm. This may, however, be impractical in-vivo.

2. PIN ORIENTATION

Six configurations of pin orientation were considered which were

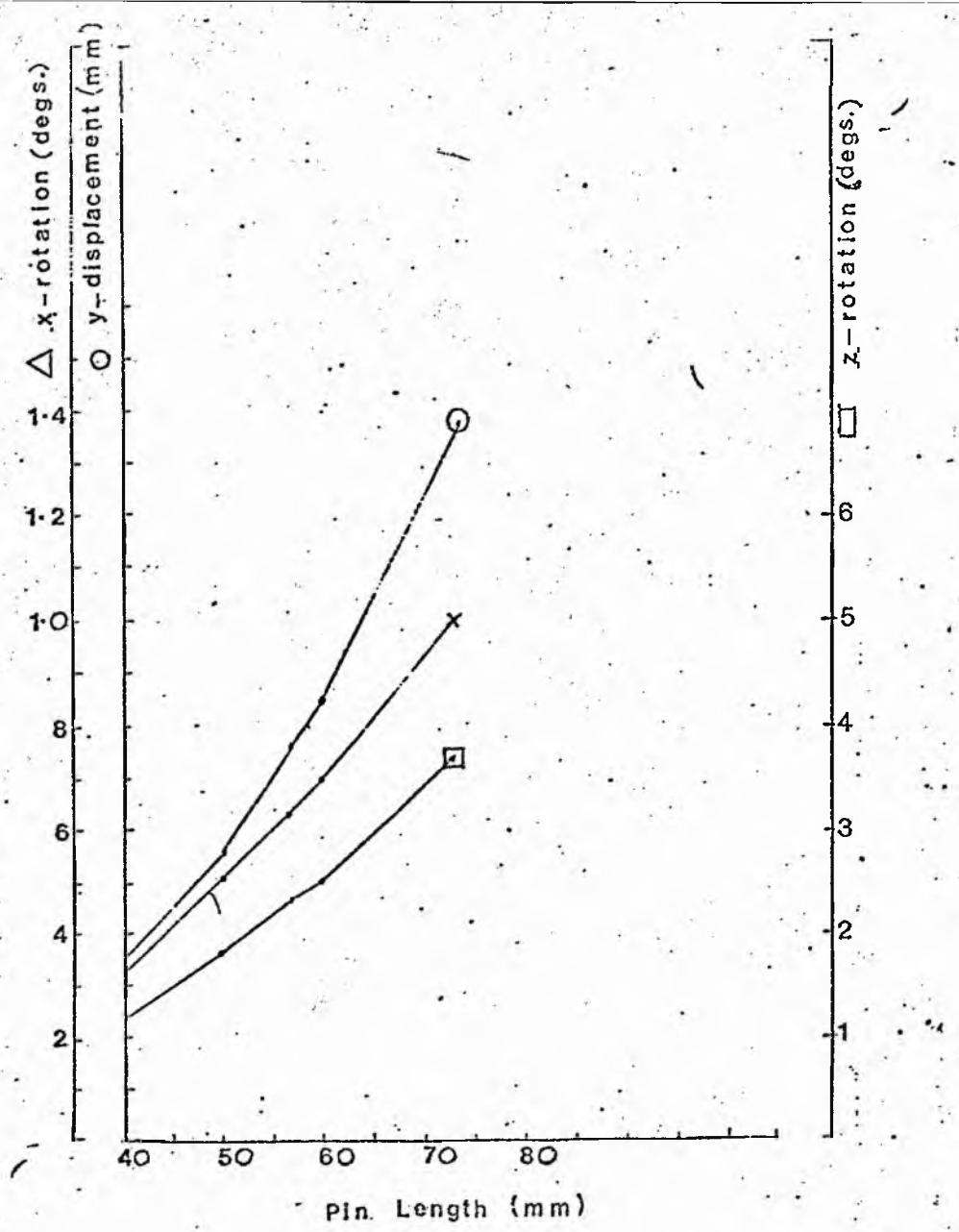

MODELS 2 & 3

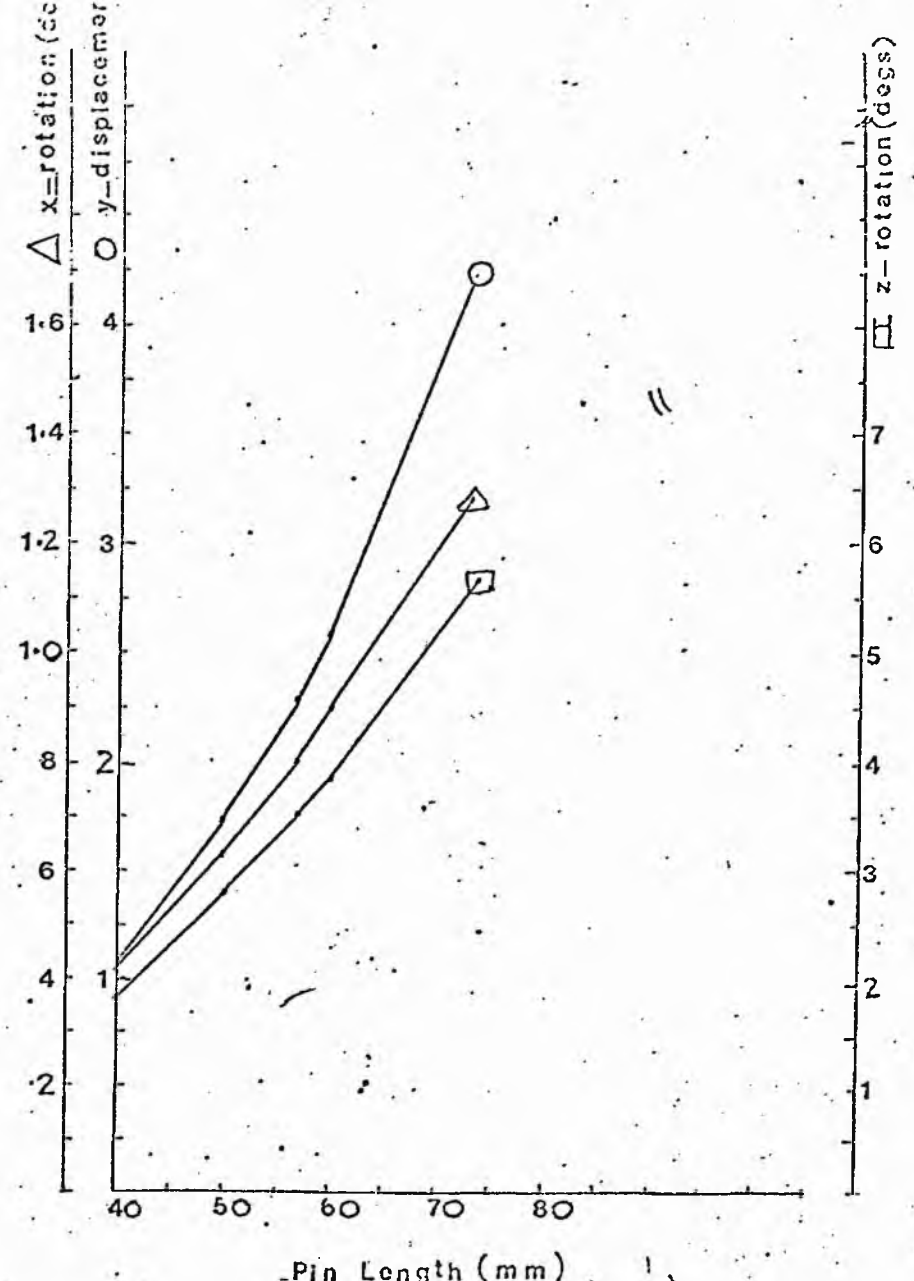

MODEL 4

divided into two groups (see Figures 59)

A. Change in Pin Spacing

The two pin groups were assumed to be parallel and co-planar. Three tests were carried out to determine the effect of a change in width between the first and third pin of each group.

TEST 1 : This was represented by the configuration in the base models with narrow spacing and an interval of 18 mm between adjacent pins. (Figure 59 a).

TEST 2 : Broad spacing between each pin was represented by an interval of 31 mm (Figure 59 b).

TEST 3 : Random spacing of the pins was obtained by an interval of 18 mm and 31 mm in each pin group (Figure 59 c).

B. Angulation of the Pins

The first two tests of this group (Tests 4 and 5) were designed to determine the relative significance of pin spacing at the bone and carriage sections respectively. From the configuration represented by test 6, and comparison with the previous tests (1, 2 and 3), the effect of non-parallelity could be evaluated. In tests 4 and 5, the outer two pins were bilaterally diverged from the middle pin at the bone and carriage sections respectively. In test 6 the inner two sets of pins were convergent at the carriage sections with broad spacing between the pins where they traverse the central axis of the bone.

In all configurations the following constants were maintained: (Figure 59 a).

K_1 - the distance between the inner two pins = 90 mm.

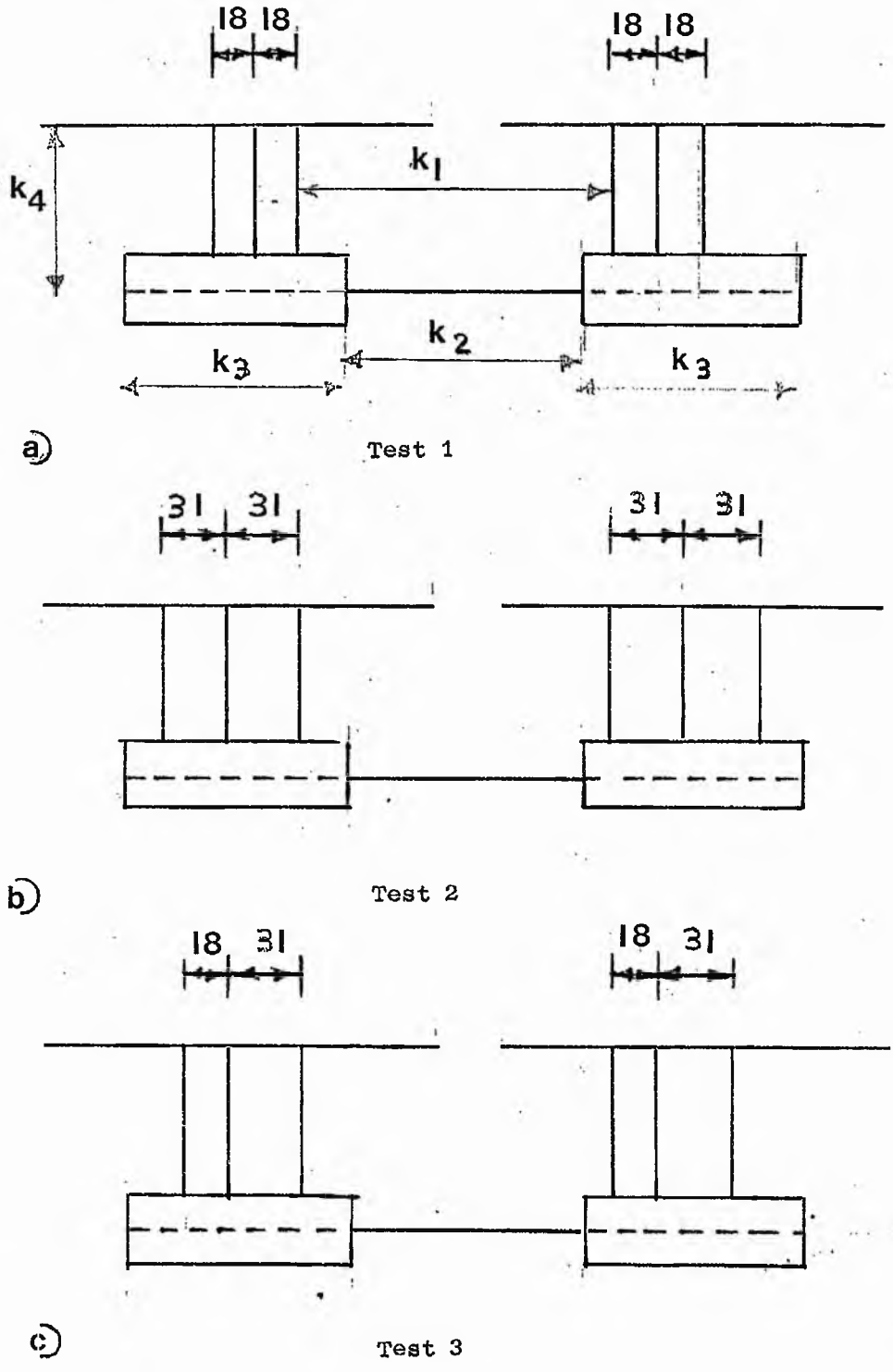

Fig. 59: PIN SPACING (parallel configurations)
Plan view: a) Test one, Base mode, narrow spacing
b) Test two, broad spacing
c) Test three, random spacing

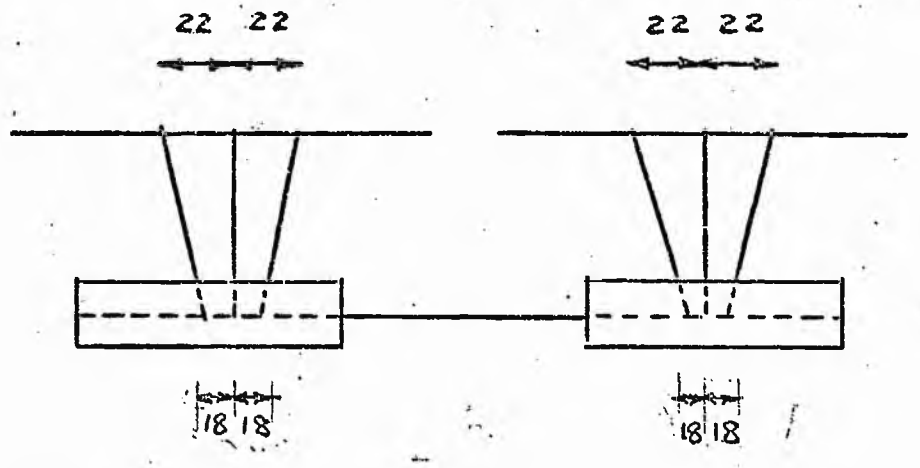

d) Test 4

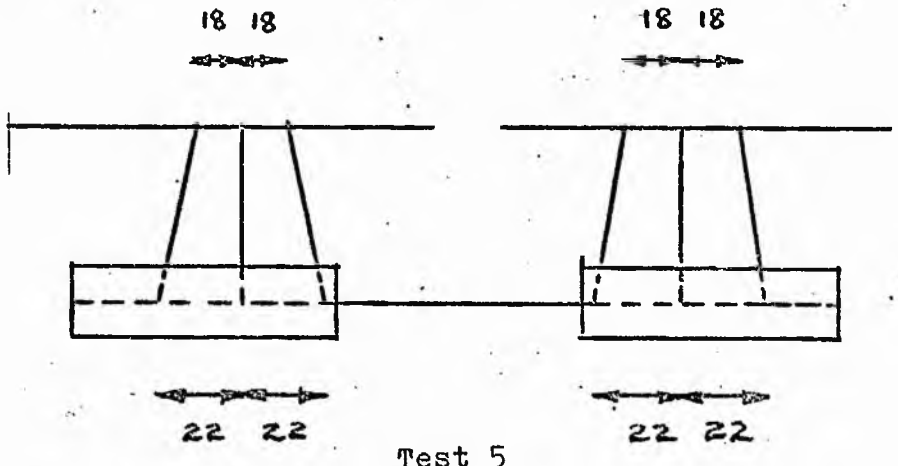

e) Test 5

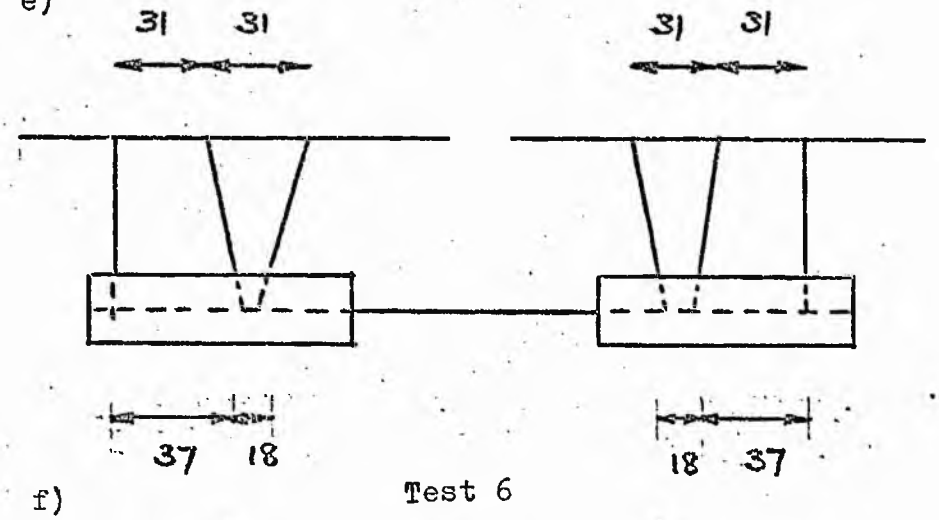

f) Test 6

Fig 59 cont. : PIN ANGULATION

d) Test 4 narrow spacing at the carriage
e) Test 5 narrow spacing at the bone
f) Test 6 narrow spacing with the inner two sets of pins

K_2 - the length of the bar section between joints 11 and 12 = 80 mm.

K_3 - length of the carriage sections = 70 mm.

K_4 - length of the pins = 56.58 mm.

The modifications to the input data resulted from a change in the local 'member' lengths due to axial displacement of the pins. The modifications to the data in the base models for each test may be found in Appendix 5.6.b

RESULTS from a change in Pin Orientation :-

The six tests show comparable behaviour in all three models (pages 196/7) and the greatest fracture site motion occurs in Model IV. The magnitude of the vertical deflection (displacement Y axis) at the fracture site and the slope of the distal portion of bone (Z rotation) is found to be dependant upon the alignment of the pins. The greatest change in Y displacement for the six configurations tested, did not exceed .41 mm in each of the three models. A change in axial rotation (X rotation) of the bone about its own axis did not exceed $.05^{o}$, and in all models total axial rotation was less than $.8^{o}$. The conclusion was drawn that axial rotational stability of the fracture site is not dependant upon pin alignment. (For tabulated results see Appendix 5.7.c).

The most stable configuration was found to occur in test 2, i.e, broad spacing with parallel alignment of the pins. Comparison between tests 4 and 5 demonstrated that vertical stability of the fracture is improved by maintaining wide spacing at the carriage interface.

The deflection occurring in test 6 is however larger than anticipated. This is the only test in which angulation of the middle pins occurs and it is concluded that minimal angulation of this pin in a

PIN ORIENTATION

DISPLACEMENT

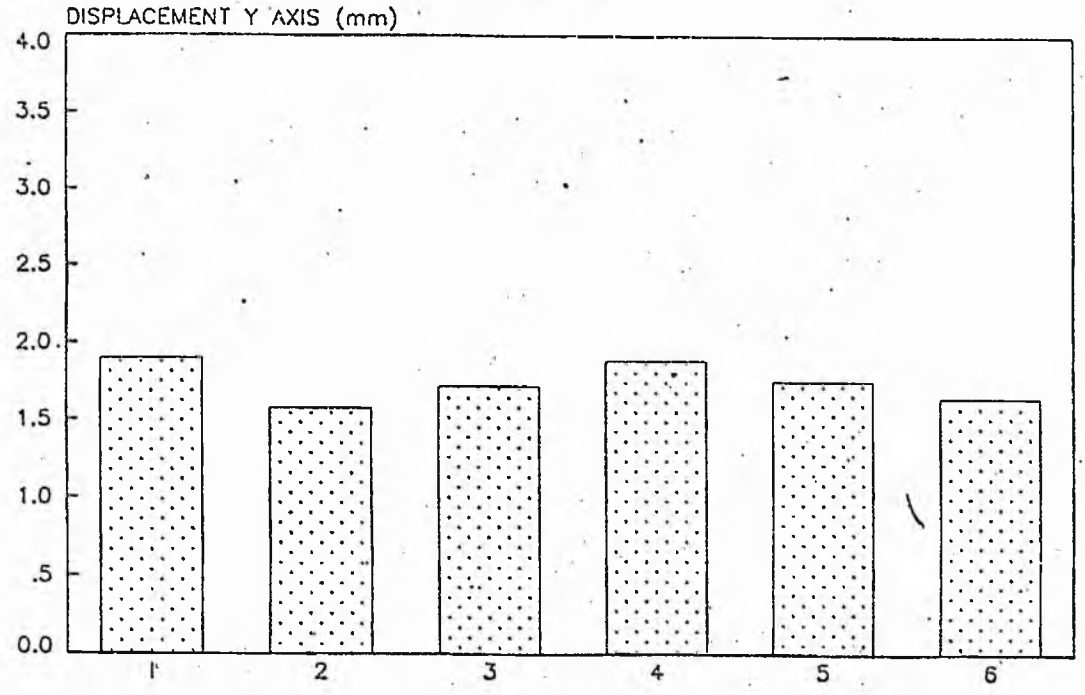

PIN ORIENTATION

X ROTATION

Z ROTATION

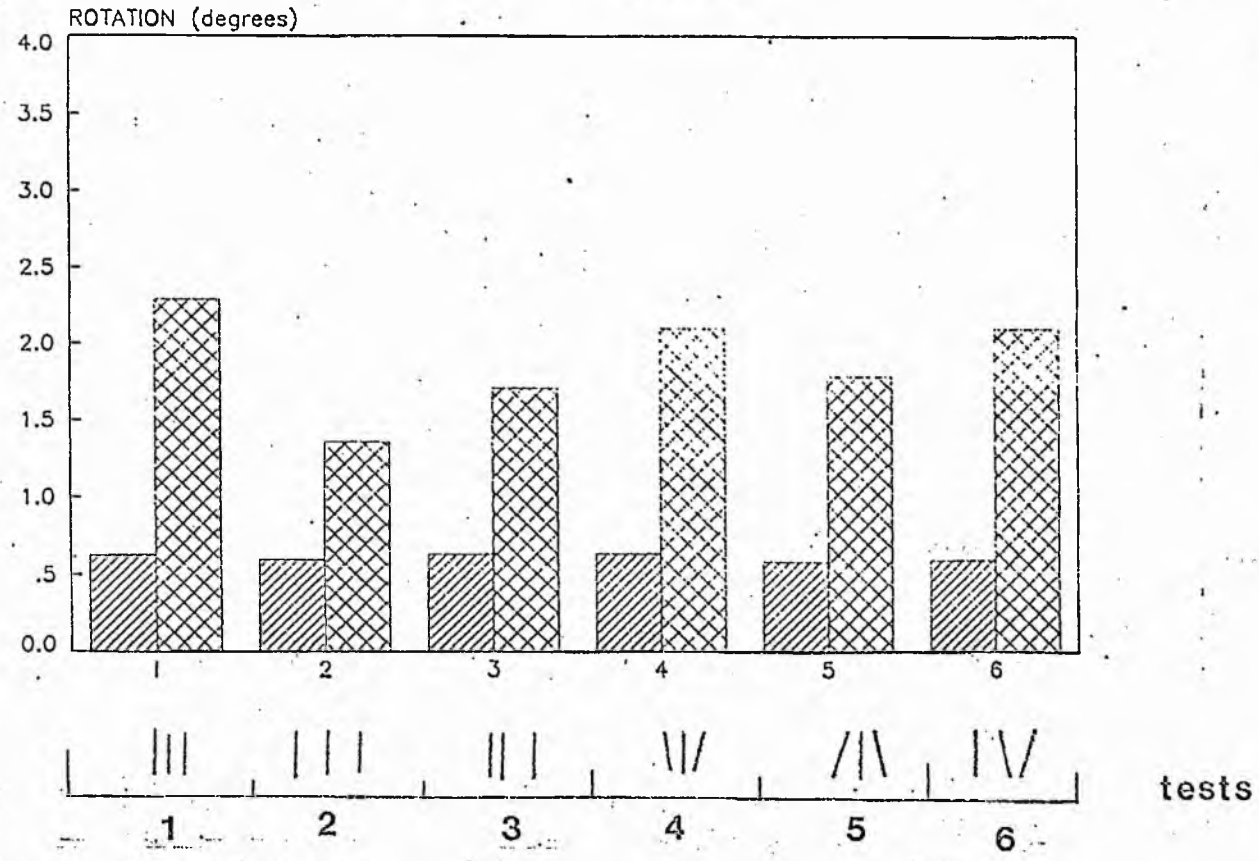

PIN ORIENTATION

DISPLACEMENT

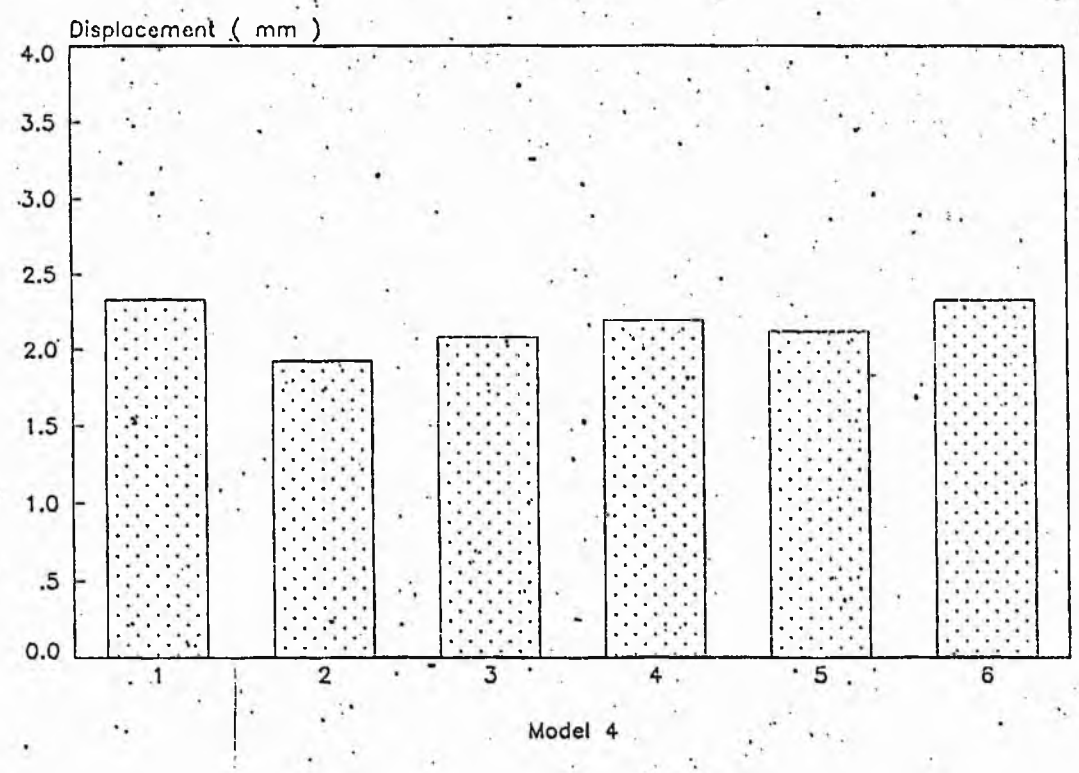

PIN ORIENTATION

X ROTATION Z ROTATION

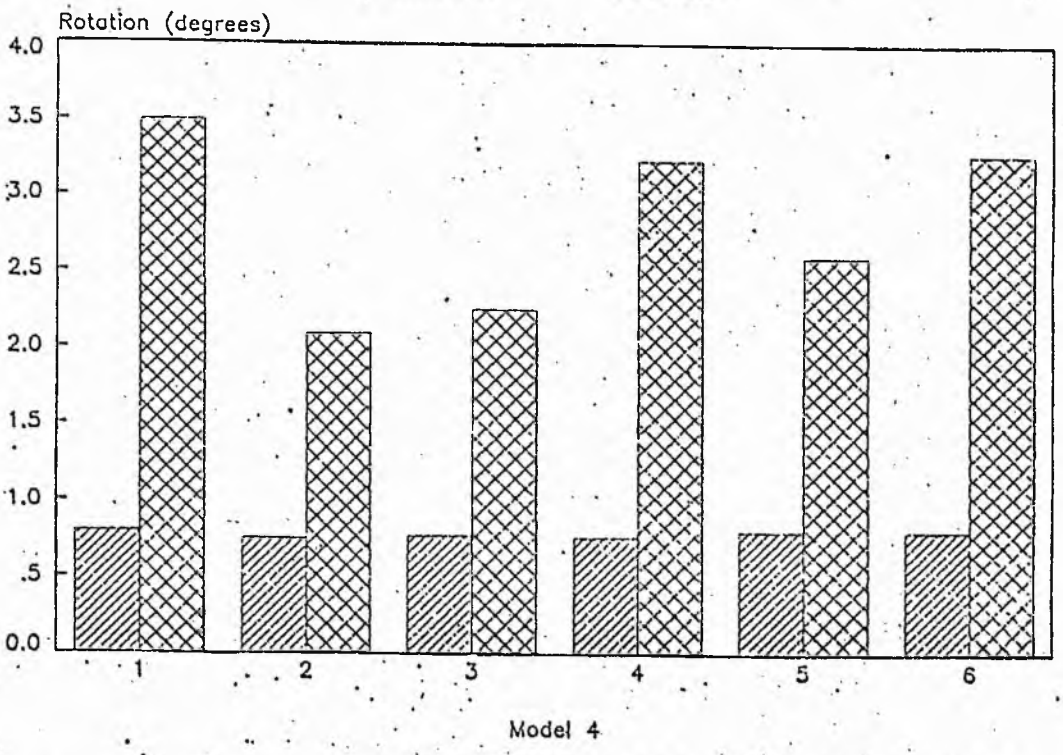

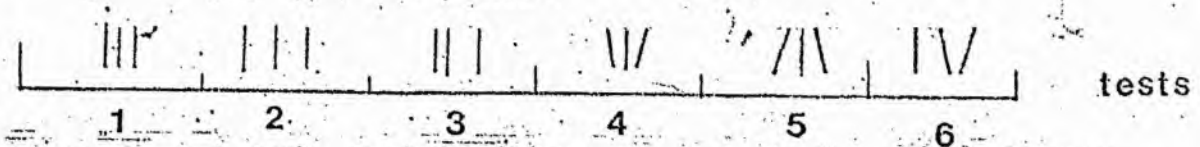

three pin configuration is crucial for maximal stability. This was most marked with non-uniform bone. (Model II).

3. OFFSET OF THE PINS FROM THE FRACTURE SITE

Pin offset is defined as the distance between the inner pin of each pin group and the centre of the fracture site. In the base models the inner two pins (A and D) (Figure 60a) are equidistantly spaced so that the interval between them (L_1) is 90 mm. The distance L_1 was then increased from 90 mm to 124 mm in three successive tests (Tests 2, 3 and 4). This was repeated on each of the three base models. In each of those tests the fracture gap, pin length, and minimal spacing between adjacent pins (18 mm) was maintained.

In test 2 the pins are parallel, and the interval between increased to 124 mm. Corresponding changes in the length of the bar between the carriage sections were made from 80 mm to 114 mm. Local changes in the member forces were made for bone (members 6 and 9) bar (member 25) and the carriage sections (members 17-24). For the method of calculation see Appendix 5.4.

In tests 3 and 4 the offset of only one set of pins was increased to give an overall interval (L_{111})(Figures 60c and d) of 107 mm. In test 3 the offset of the proximal set of pins was increased and in Test 4 only the offset of the distal set of pins was increased. The data for the local member forces was again modified for members 6 and 9, 17 to 25. These modifications are listed in Appendix 5.6.c, along with the changes in local joint co-ordinates for the pins, carriages and bar.

RESULTS of change in Pin Offset :-

From these tests it is again found that the location of the fracture site contributes to the magnitude of relative motion between the fractured

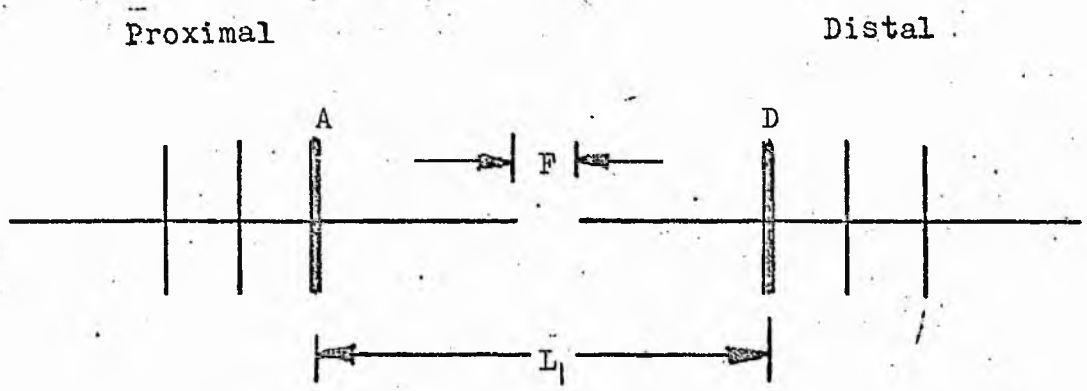

TEST I L_I = 90 mm., F = Fracture gap = 4 mm.

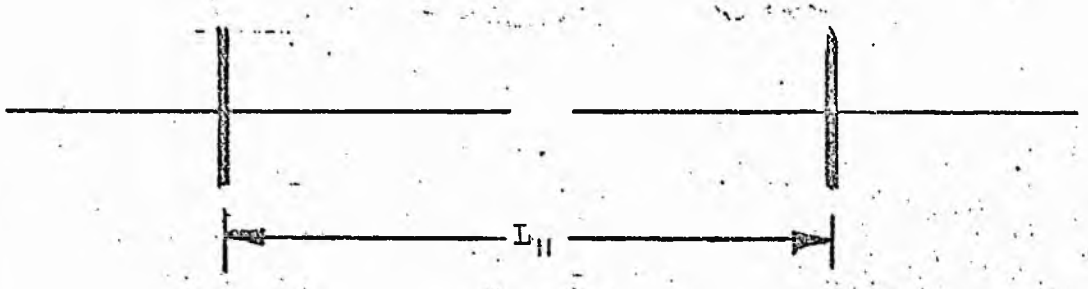

TEST 2 L_{II} = I24 mm.

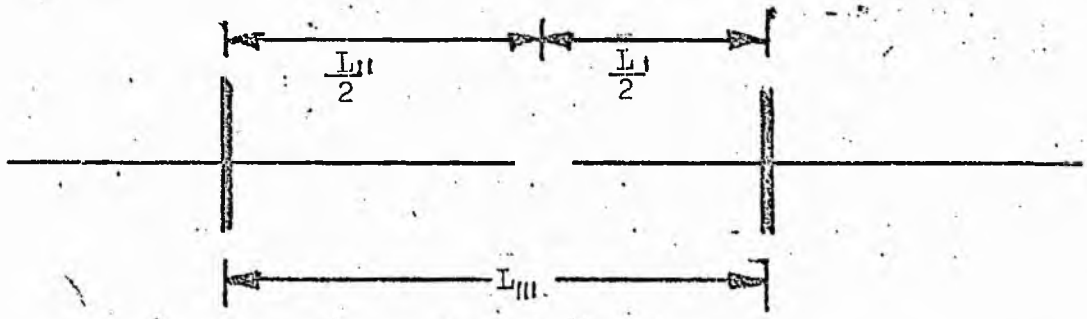

TEST 3 c) L_{III} = I07 mm.

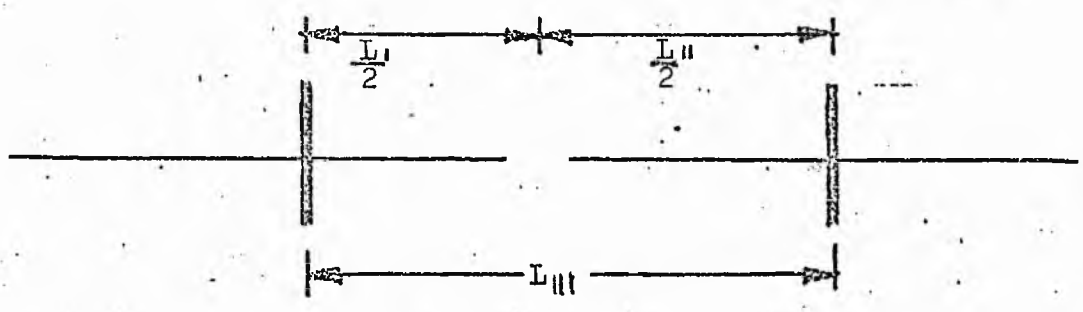

TEST 4

Fig 60 PIN OFFSET

MODELS 2 & 3
PIN OFFSET

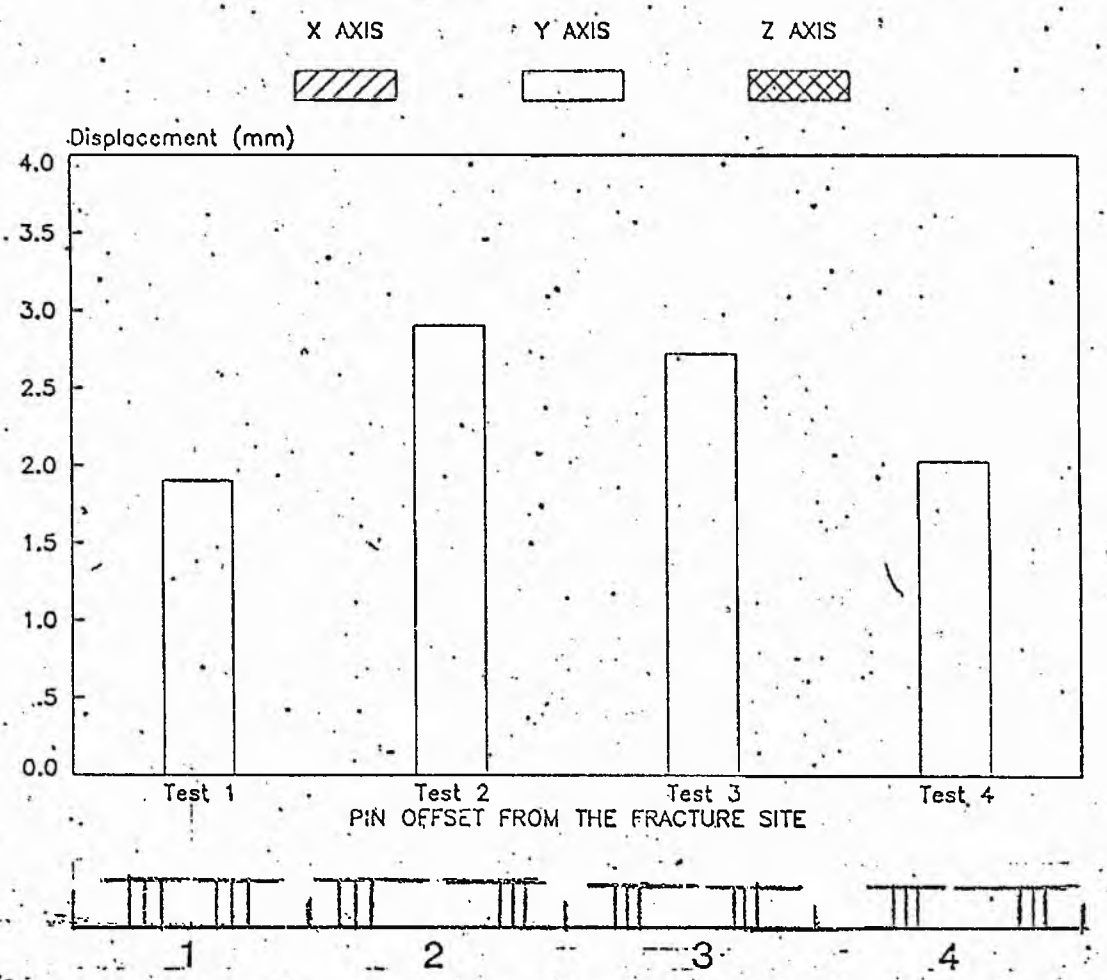

PIN OFFSET

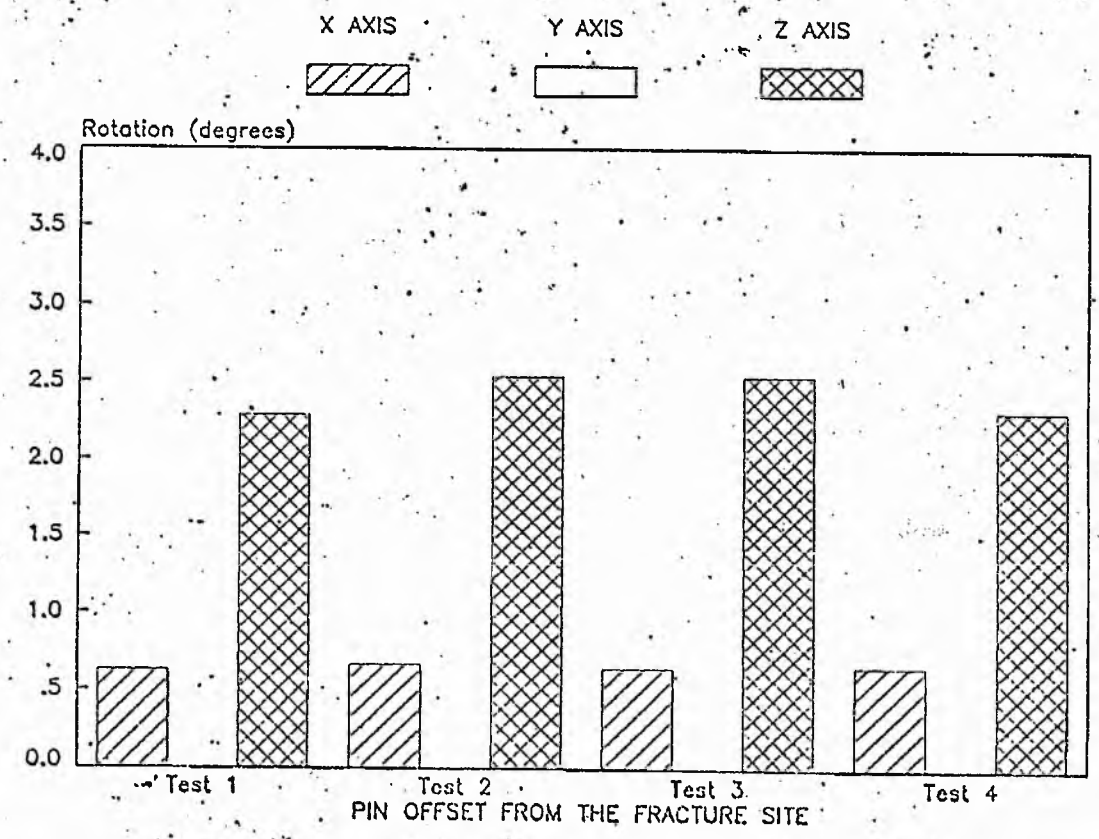

MODEL 4
PIN OFFSET

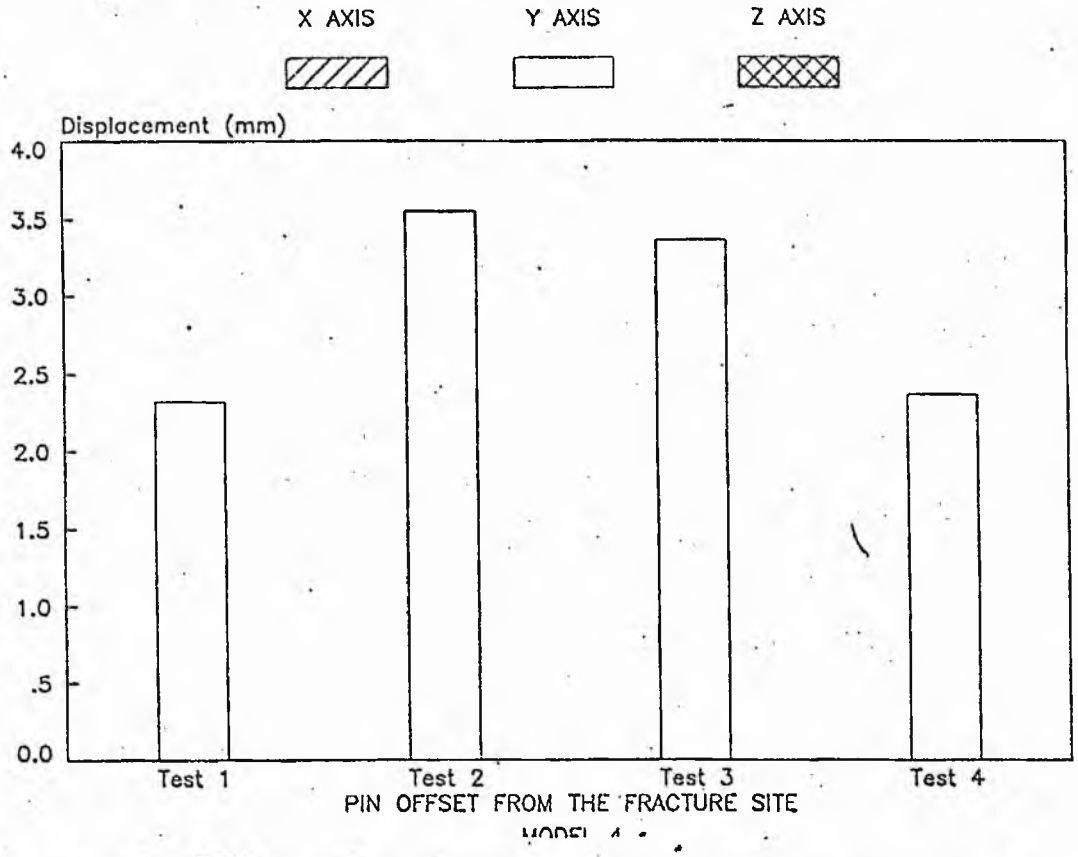

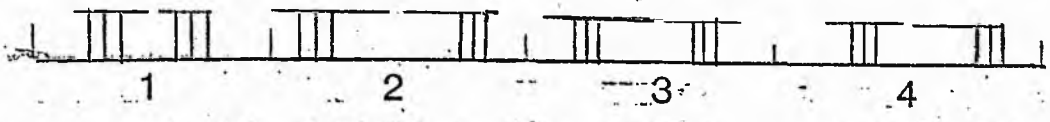

tests.

PIN OFFSET

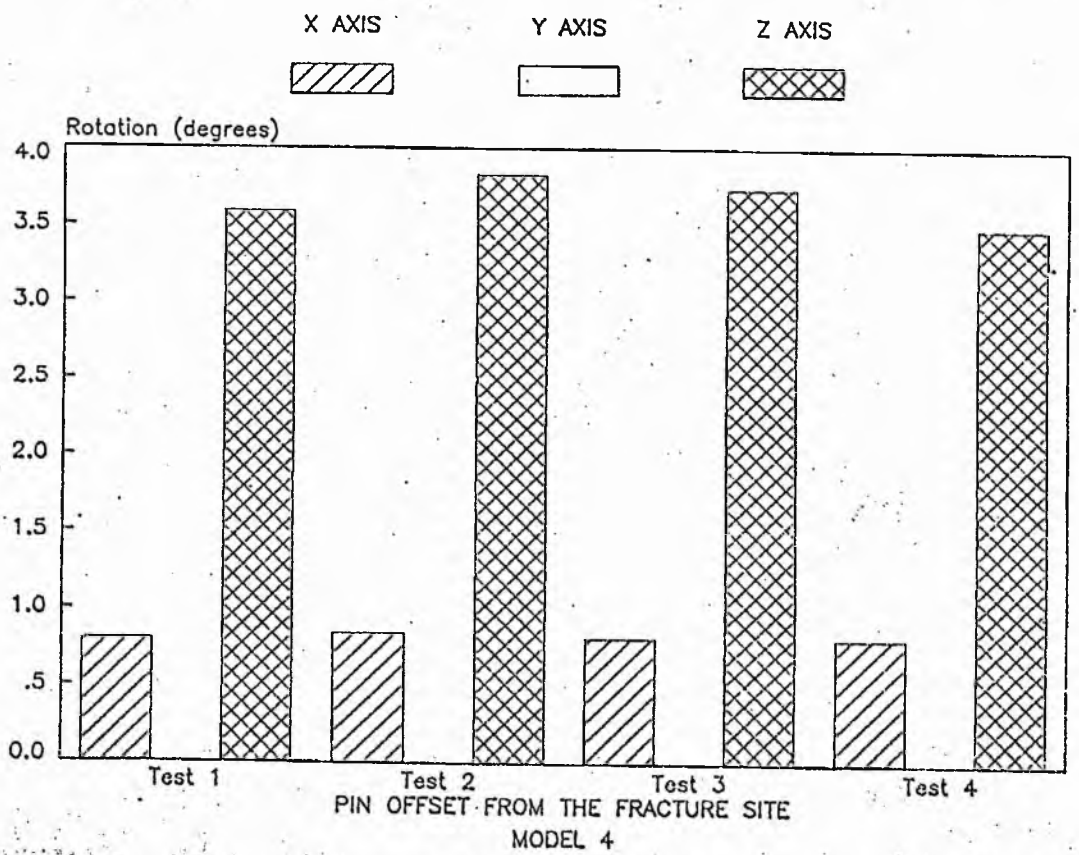

bone ends. (Pages 200/01). Variable magnitudes of vertical deflection (displacement Y) are observed in response to changes in the pin offset in all three models.

An increase in the offset of either pin group magnifies the displacement and fracture site stability is reduced. This effect is most marked when the offset of the proximal pin group is increased (test 3) but the greatest change in displacement occurs when the offset is increased bilaterally (test 2). It is also observed in tests 2 and 3 that a consistent percentage change in displacement occurred in all three models. This suggested that this displacement is directly proportional to a change in pin offset and independant of fracture site location when a change in the interval between the two groups of pins is made.

4. DIMENSIONAL CHANGES OF THE FIXATOR BAR

The effect of alternative Bar design upon Fracture Site motion was considered by conducting three series of tests:

Series A . The core diameter of a solid stainless steel bar was changed in six tests from 9 mm to 15 mm. Corresponding changes in the data were made for the local member properties of the Carriage and Bar sections. (see Appendix 5.6.D). The change in bar diameter was expressed as a percentage of change in area from which a similar percentage in area was made for each carriage section. Since the carriage sections were assumed to be square then L (where L is the length of one side) was derived by

$$L = \sqrt{\%\Delta A + A_1}$$

where $\% \Delta A$ = % change in Area

A_1 = original Area

Corresponding percentage changes in the local Member Forces were made since

$$M = A L_p$$

For all modifications to the input data see Appendix 5.6.D.

Series B. In this series the solid rod with a core diameter of 15 mm was substituted by

a) A circular tube with an outer diameter D = 15 mm and inner diameter of 13 mm.

b) A square tube where the outer length L = 15 mm and the inner length L = 13 mm.

The data were modified for the local member properties of the bar and the local member forces for both the bar and the carriage sections according to the method described for Series A.

Series C. This series of tests were carried out to evaluate the relative importance of the length of bar spanning the two carriages. Four tests were completed in two parts (Figure 61). In Part 1 the pin offset (K_I) remained constant and the bar length then increased in test 2. Conversely in Part 2 the bar length remained constant and the pin offset increased (tests 3 and 4). These tests were carried out as follows:

Part 1: A minimal distance of 18 mm was maintained between each pin and a comparison was made between two central bar lengths of 114 mm (Test 1) and 124 mm (Test II). The distance between the inner two pins (K_I) at the bone remained constant and the change in the length of the

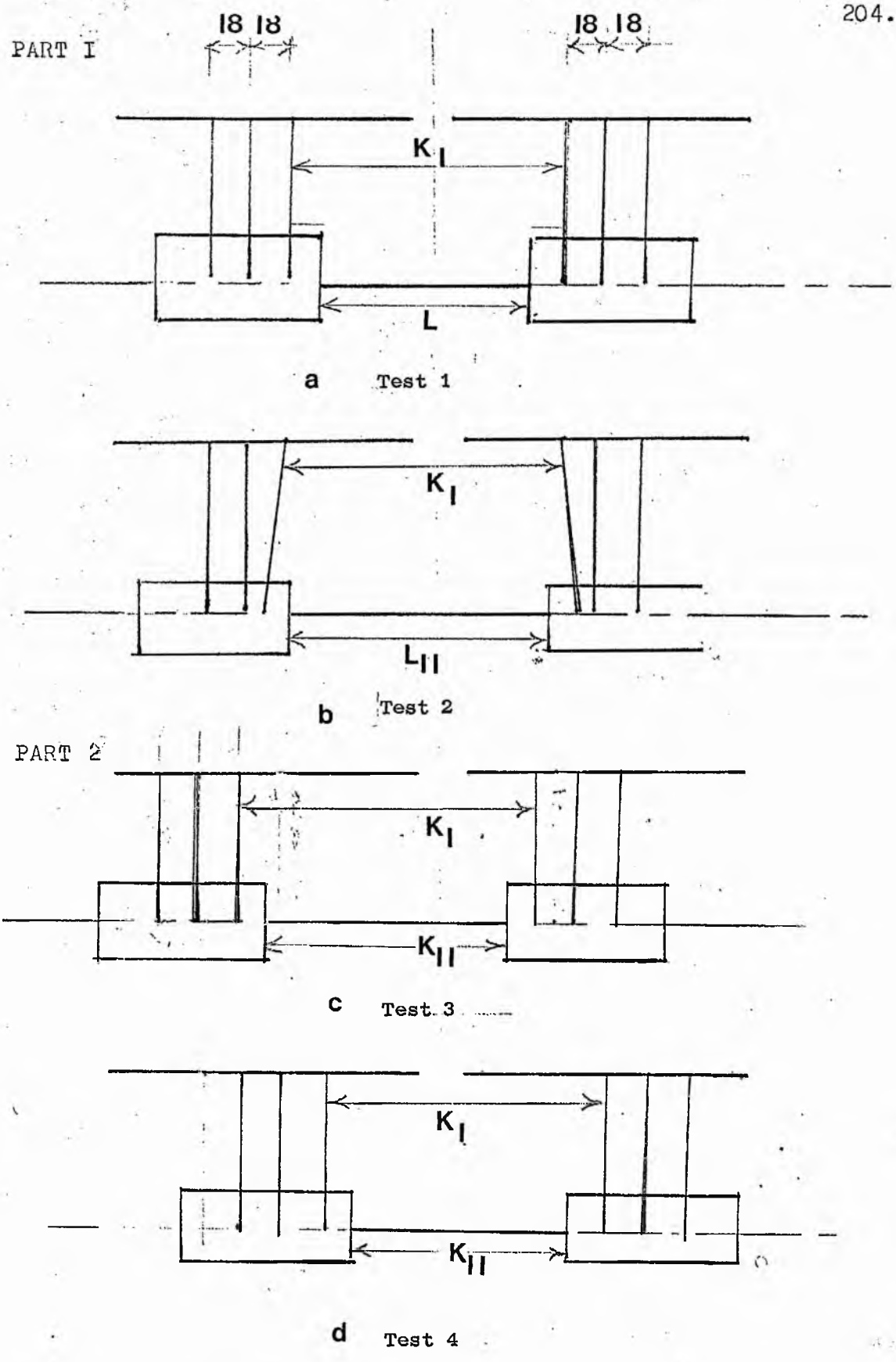

Figure 61 : Variable length of Bar spanning the twin carriages

bar spanning the two carriages in Test 2 was produced by displacement of the inner two pins and carriages in the X direction. The interval between the inner pin and the end of the carriage (K_2) remained constant. The input data for Test 1 is listed in Appendix 5.6.C (Test 2) and the data for Test 2 in Appendix 5.6.D. The core diameter of the bar was maintained at 9.67 mm and the redistribution of force due to the change in the length of the bar was calculated, according to the method described in Appendix 5.

Part 2: These tests had been previously carried out in tests 3 and 4 of "Pin Offset" (Figure 60). In these two tests the length of the bar spanning the two carriages was 97 mm but the pins were unilaterally displaced in each test.

Results of Dimensional Changes in the Fixator Bar

Series A

A slight increase in the vertical displacement at the fracture site occurs as the core diameter of the threaded fixator bar is increased from 9 mm to 15 mm. This is observed in all three models. Axial rotation (X rotation) diminishes and a linear relationship is observed between axial rotation and an increase in bar diameter (pages 206/7) The additional weight of the bar due to the dimensional changes, increases the magnitude of the bending moments at the proximal end of the bar at the bar/carriage junction (Appendix 5.8), and the torsion moments, which are constant along the bar, are virtually unchanged.

From the values of bending moments derived by the Stress Program, at the proximal end of the bar, the level of stress was calculated where

$$\gamma = \frac{My}{I}$$

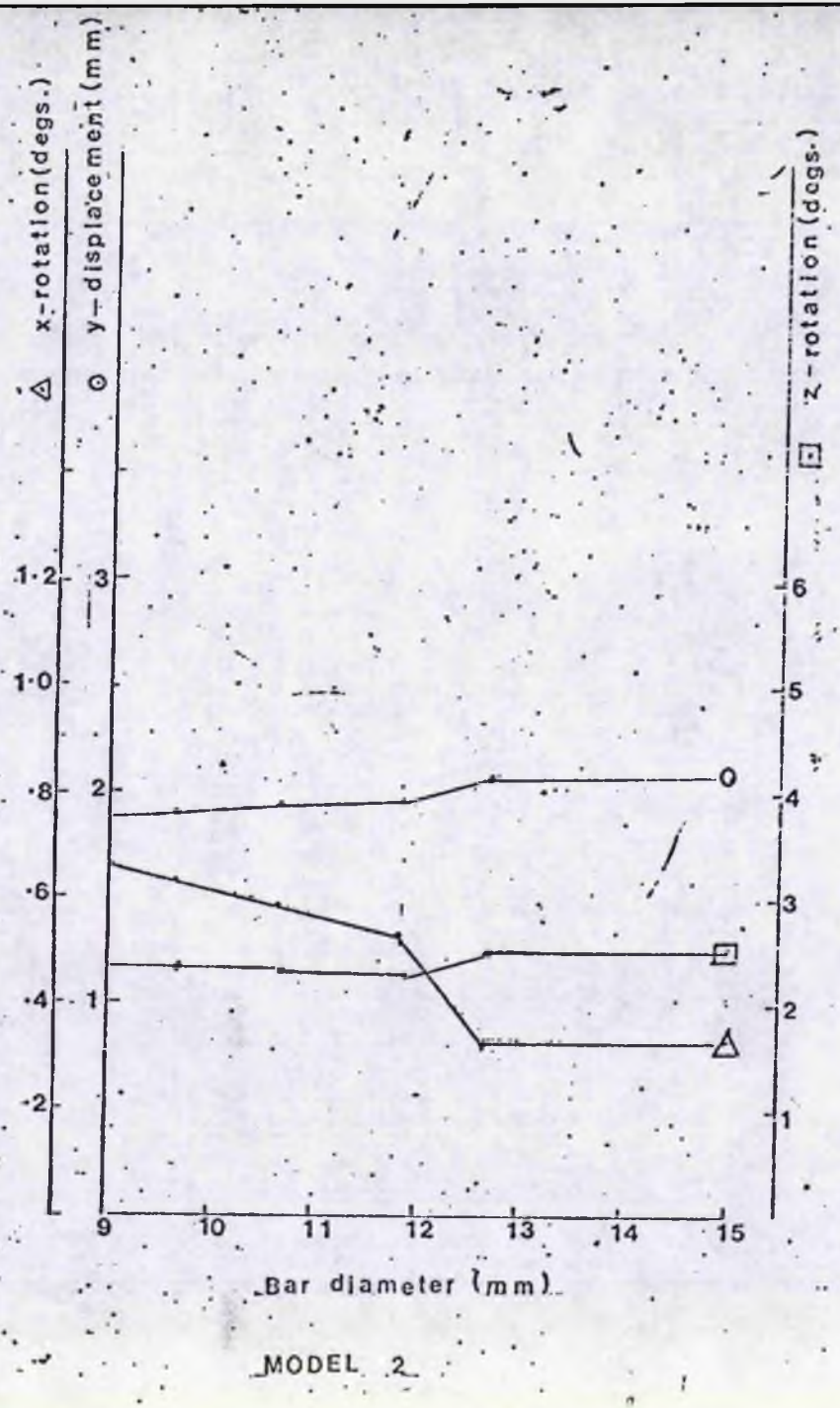

MODEL 2

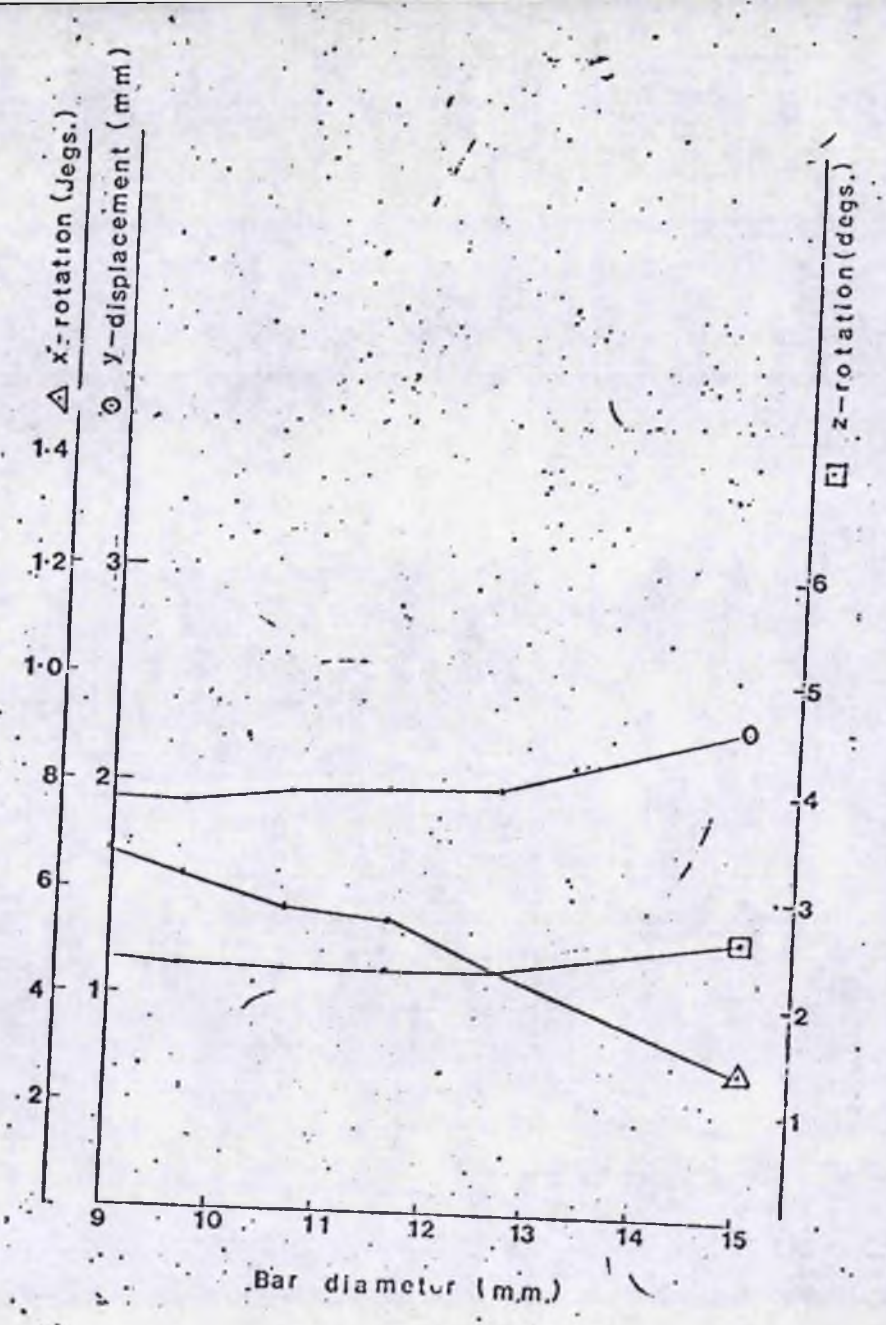

MODEL 3

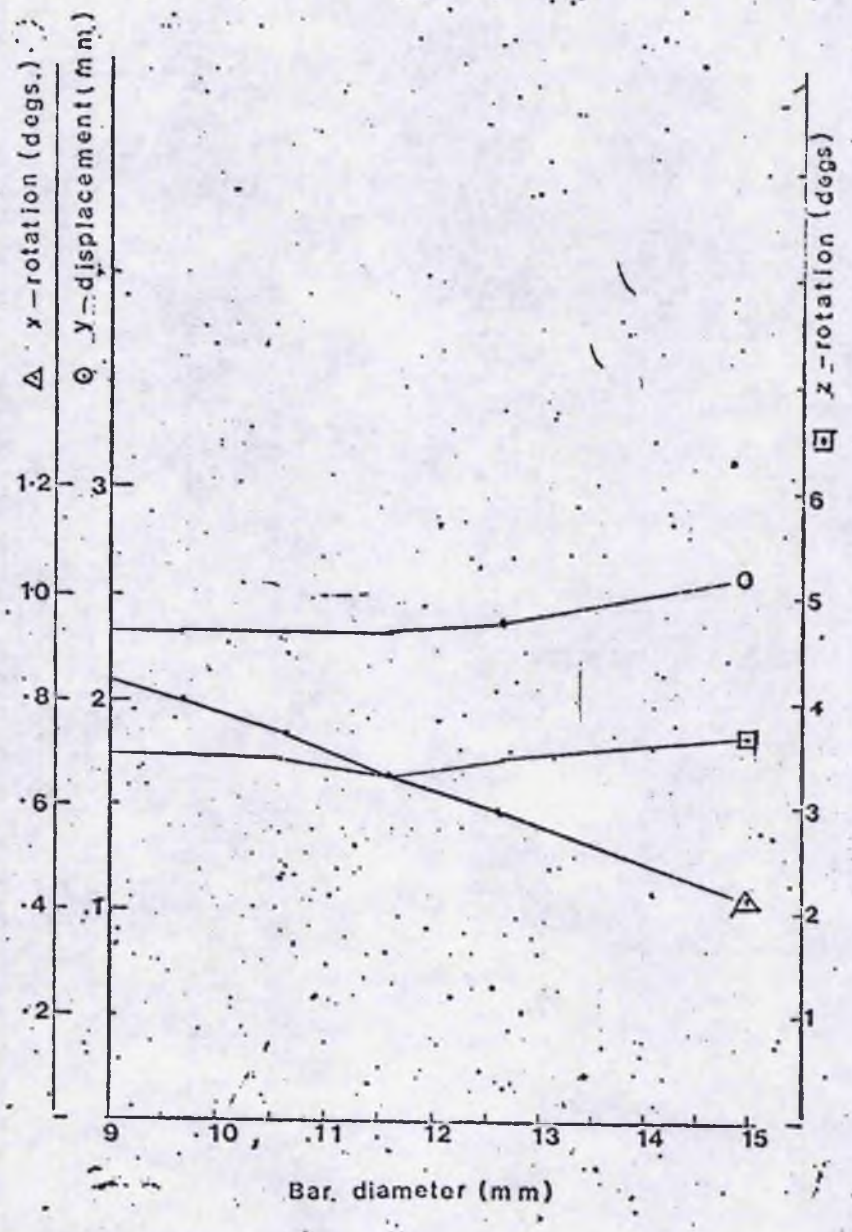
Δ x-rotation (degs.)
○ y-displacement (mm)
□ z-rotation (degs)
1·2
1·0
·8
·6
·4
·2
3
2
1
6
5
4
3
2
1
9
10
11
12
13
14
15
Bar. diameter (mm)
MODEL 4

Stress is found to diminish with an increase in the bar diameter indicating an increase in stiffness. It is concluded that the slight increase in vertical displacement at the fracture site with an increase in bar diameter is due to the increase in the magnitude of the torsional moments (due to the increased weight of the bar) which act upon the proximal set of pins. Angular deformation is increased in the pins (torque) which results in magnification of the vertical deflection at the fracture site.

Since the torque in the bar does not change an increase in the polar second moments of area reduces angular deformation of the bar and rotational stability at the fraxture is improved.

Series B

A comparison of the results from the three bar types, a solid rod and two tubes (circular and square) demonstrated that maximum stability is achieved by the use of a circular tube (pages 209/10). If however a smaller solid rod with a core diameter of 9.67 mm is used a similar displacement occurs. Rotational stability is improved with a large diameter (15 mm) solid rod and axial rotation at the fracture site is reduced to a minimum of $.28^{o}$ and $.43^{o}$ in models III and IV respectively. The Denham Bar appears therefore to provide optimal stability for the configuration in which it is used, although axial roatation may be reduced by replacing the solid rod with a circular tube.

Series C

The tabulated results are presented in Appendix 5.7.f. and graphically on pages 211-212. In tests 1 and 2 the interval between each pin group (K_1) remains constant, but the inner two pins are angled in the latter

to/

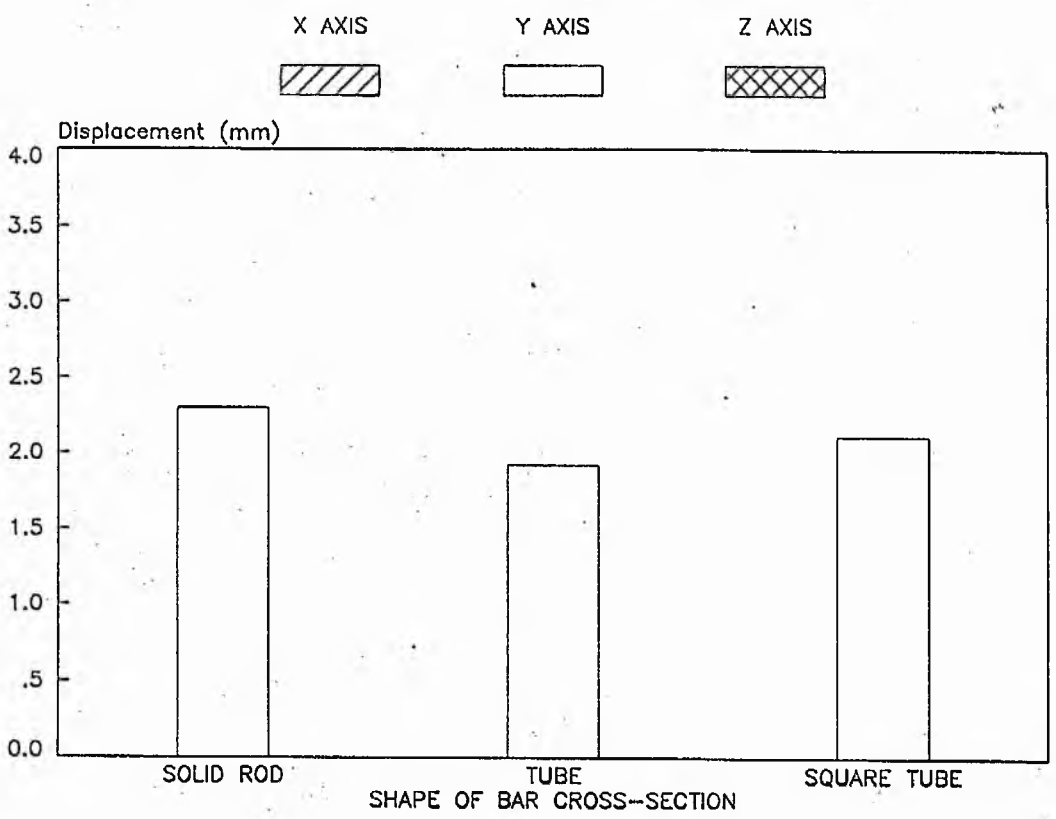
BAR CROSS-SECTION
X AXIS
Y AXIS
Z AXIS
Displacement (mm)
4.0
3.5
3.0
2.5
2.0
1.5
1.0
.5
0.0
SOLID ROD
TUBE
SQUARE TUBE
SHAPE OF BAR CROSS-SECTION

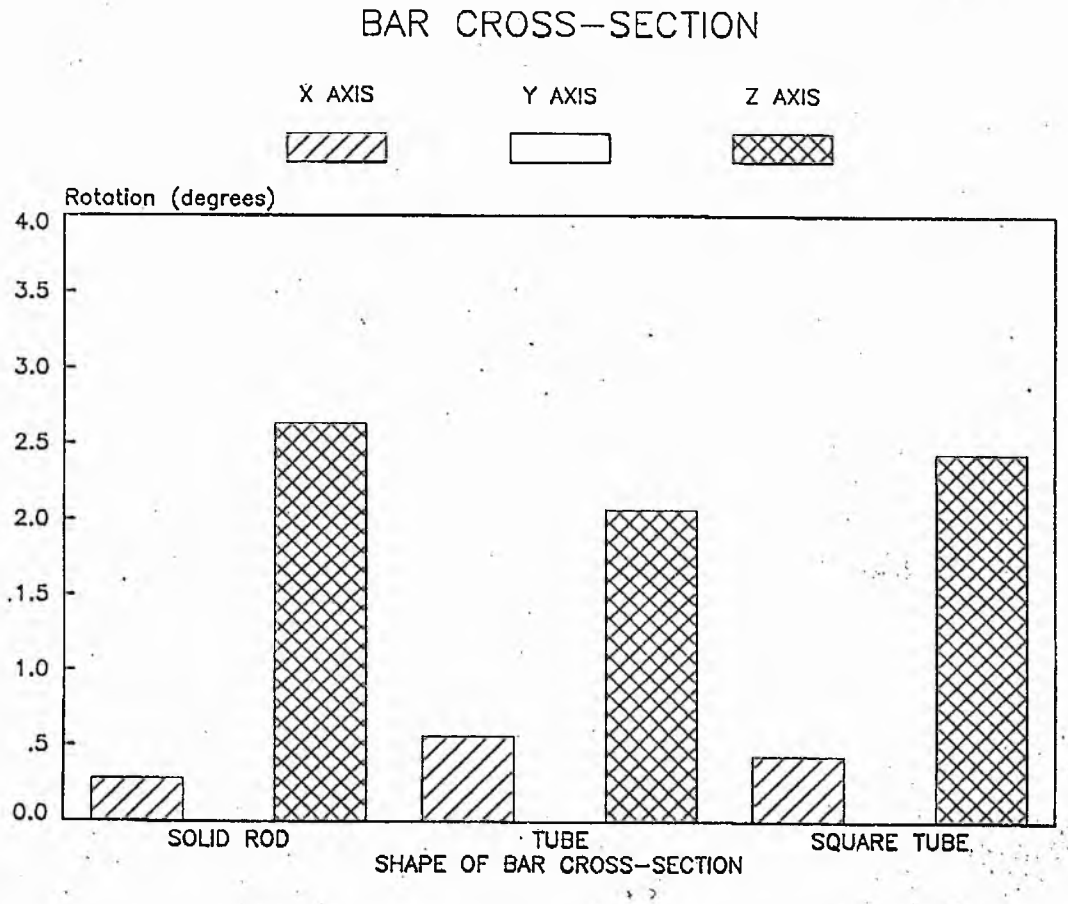
BAR CROSS-SECTION
X AXIS
Y AXIS
Z AXIS
Rotation (degrees)
4.0
3.5
3.0
2.5
2.0
.1.5
1.0
.5
0.0
SOLID ROD
TUBE
SQUARE TUBE
SHAPE OF BAR CROSS-SECTION

MODELS 2 & 3

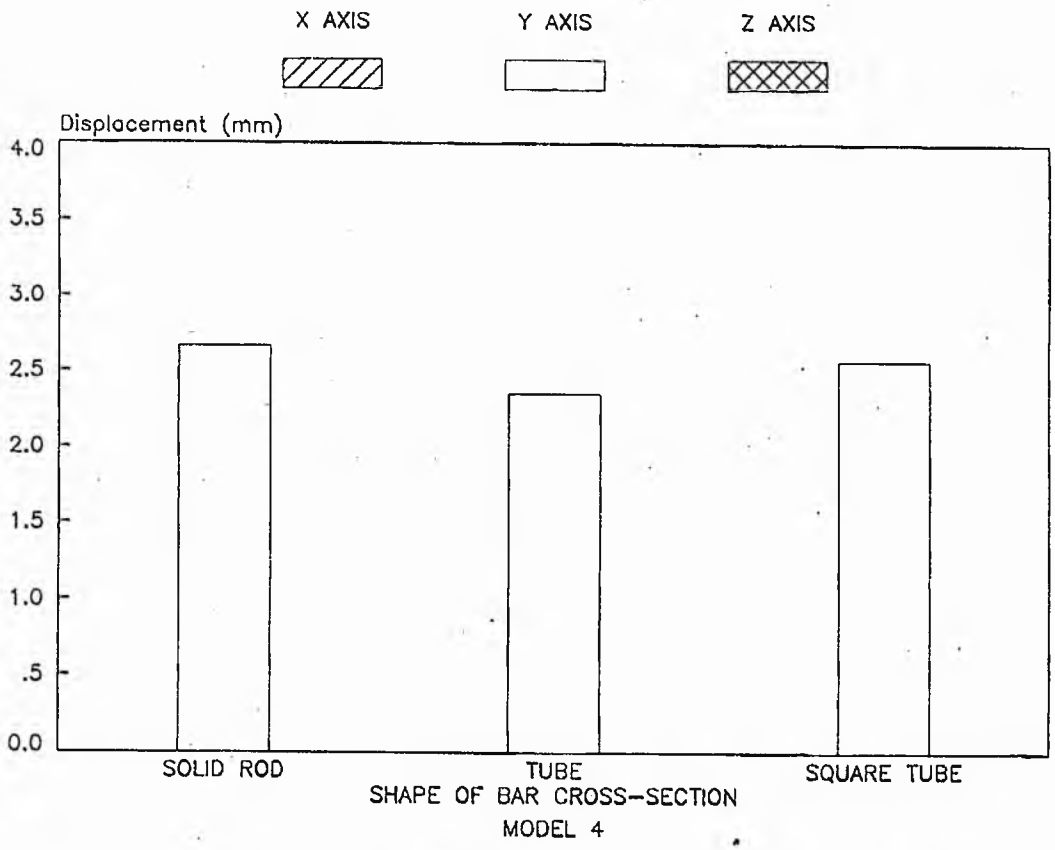
BAR CROSS-SECTION
X AXIS
Y AXIS
Z AXIS
Displacement (mm)
4.0
3.5
3.0
2.5
2.0
1.5
1.0
.5
0.0
SOLID ROD
TUBE
SQUARE TUBE
SHAPE OF BAR CROSS-SECTION
MODEL 4

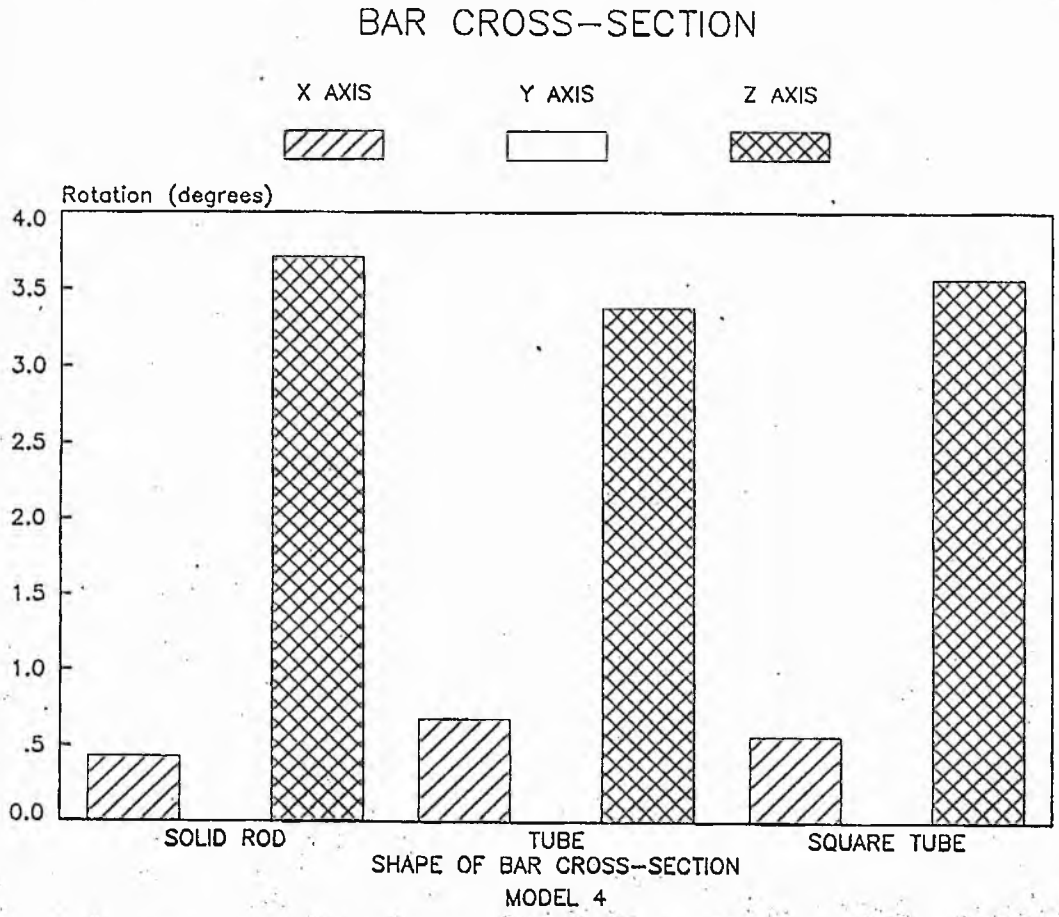
BAR CROSS-SECTION
X AXIS
Y AXIS
Z AXIS
Rotation (degrees)
4.0
3.5
3.0
2.5
2.0
1.5
1.0
.5
0.0
SOLID ROD
TUBE
SQUARE TUBE
SHAPE OF BAR CROSS-SECTION
MODEL 4

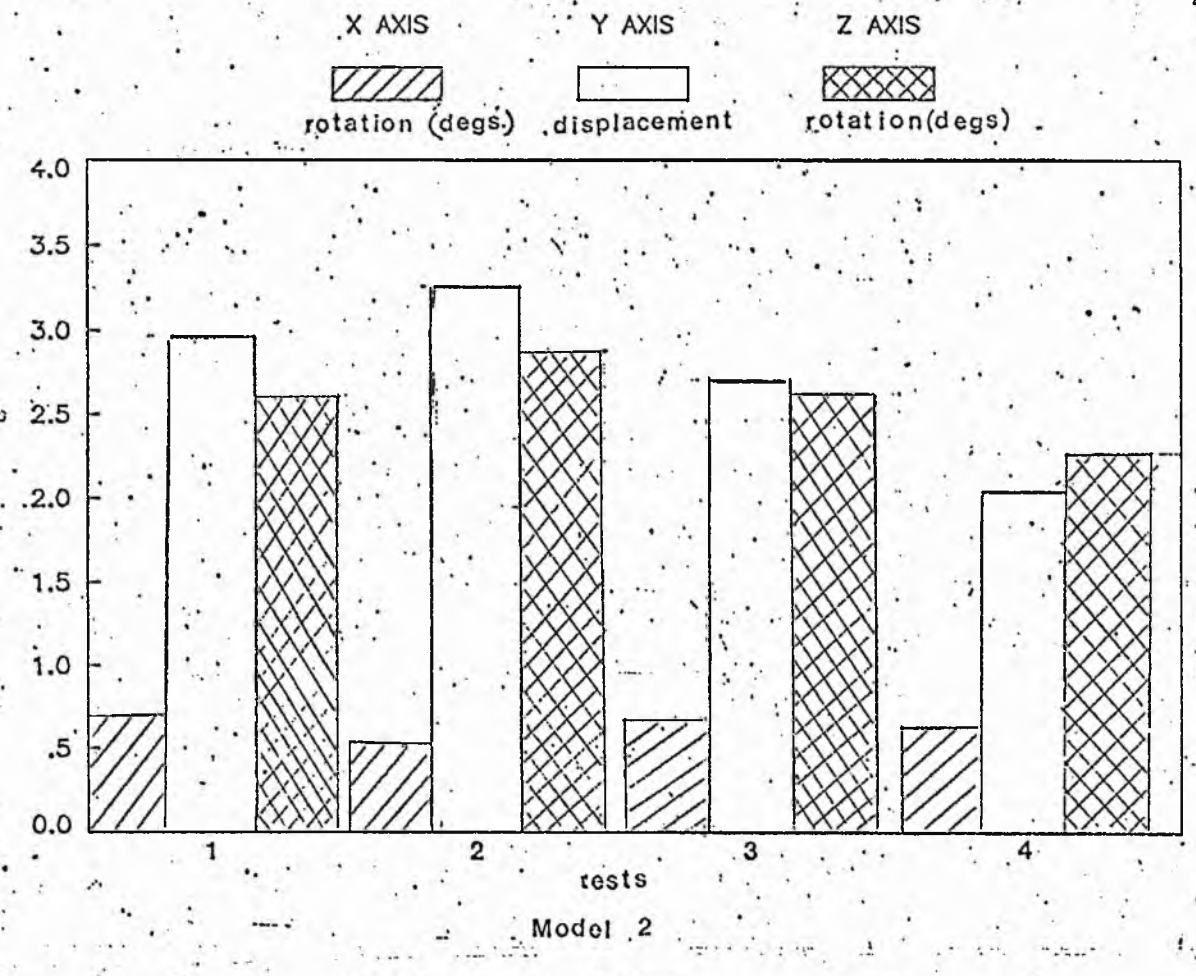

Model 2

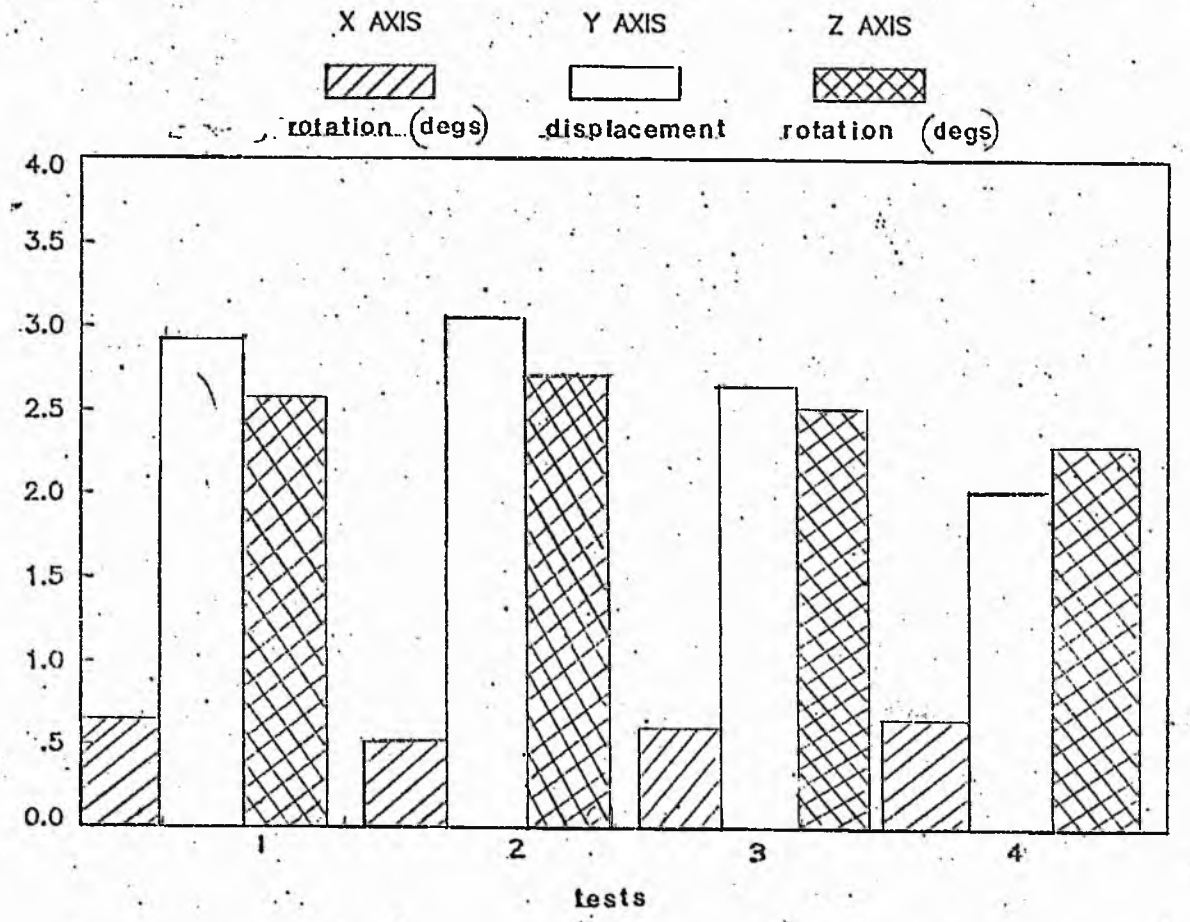

MODEL 3

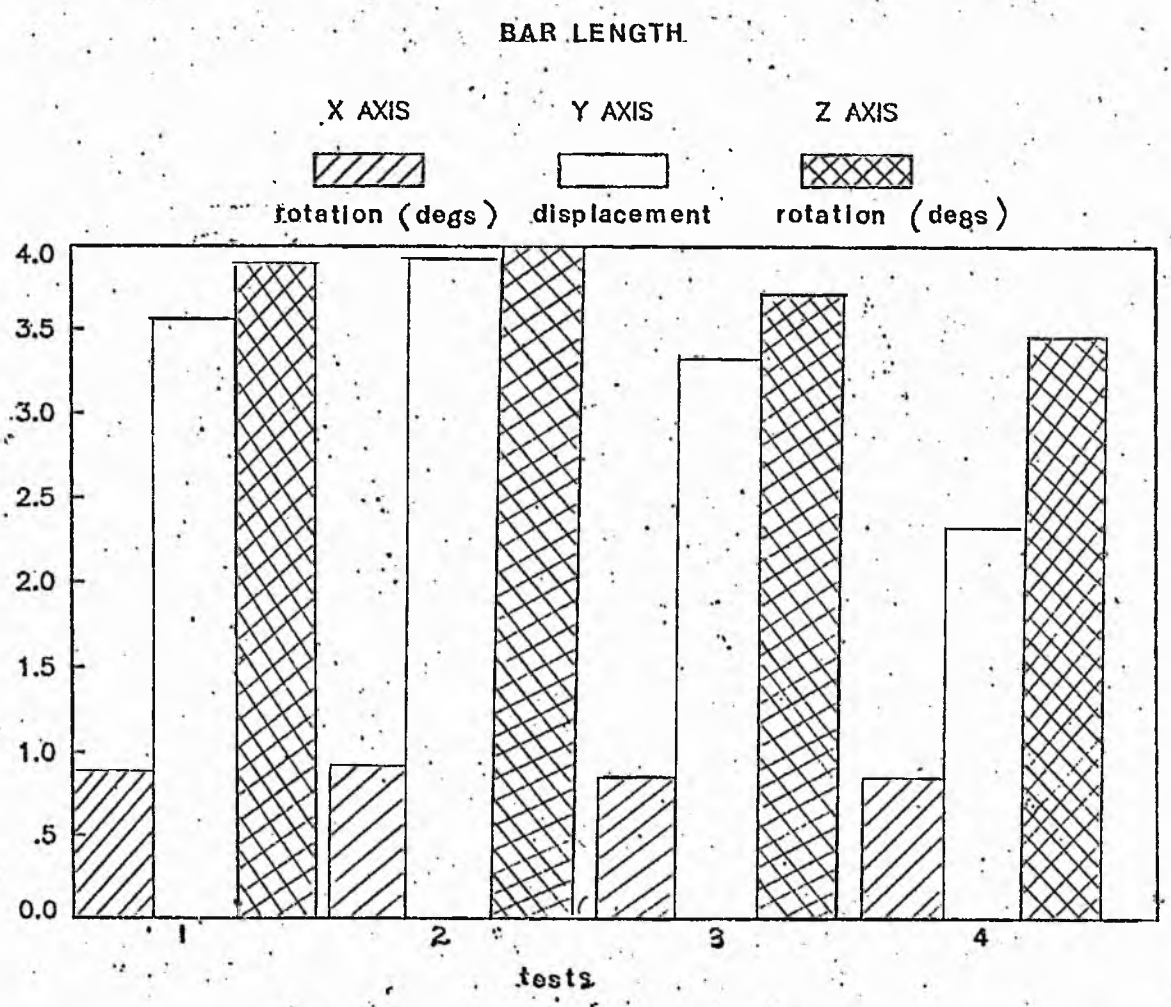
BAR LENGTH
X AXIS
Y AXIS
Z AXIS
rotation (degs)
displacement
rotation (degs)
4.0
3.5
3.0
2.5
2.0
1.5
1.0
.5
0.0
1
2
3
4
tests

MODEL 4

increase the length of the central section of bar. Diminished vertical stability is demonstrated by the configuration in test 2, although rotational stability is improved (Models II and III). In tests 3 and 4 the bar length remains constant and the pins are parallel. In the four configurations tested it is found that vertical displacement at the fracture site is minimal if the interval between the inner pin of the proximal group and the centre of the bar is reduced.

5. COMPRESSION

Alternative methods of applying compression to the fracture site have been reviewed in Chapter 2 Part D. Six methods are considered in this work for their effect upon fracture site stability. A comparison is then made with the displacements at the fracture site in the non-compressed state. (Test 1 Figure 62). The co-ordinate system and loading conditions without compression is represented by Model 3 which is the basis for the five other tests.

Edge and Denham (1979/80 personal communication) utilize two spring washers which are inserted between the locknuts and carriage on either side of one carriage. The force required to fully compress each spring is 1962 Newtons (200 kgs). This was represented in Test 2 Figure 62 by equal and opposite forces of 1962N axially applied along the X axis of the distal carriage at joints 12 and 19.

The effect of a compressive mechanism within the bar was then represented by two forces of equal magnitude but opposite direction at joints 11 and 12 (Test 3 Figure 62). Test 4 represents the application of eccentric forces to the fixator column, by point loading of each pin at 55 mm from the pin bone junctions (Test 4 Figure 62)

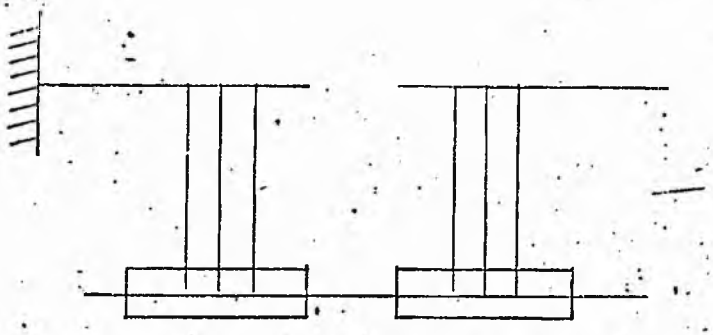

Test I

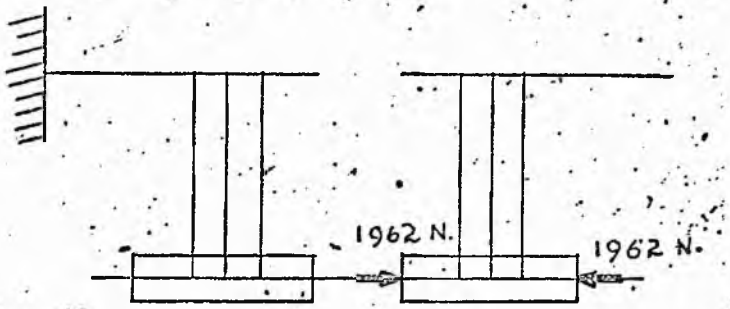

Test 2

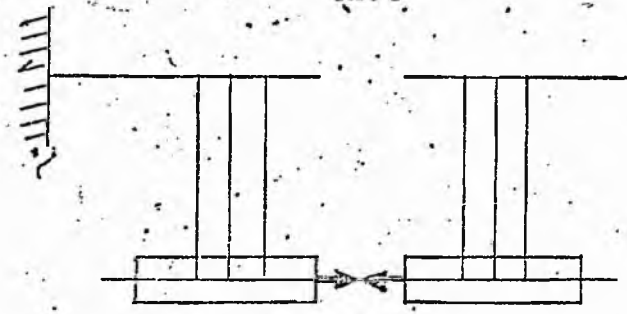

Test 3

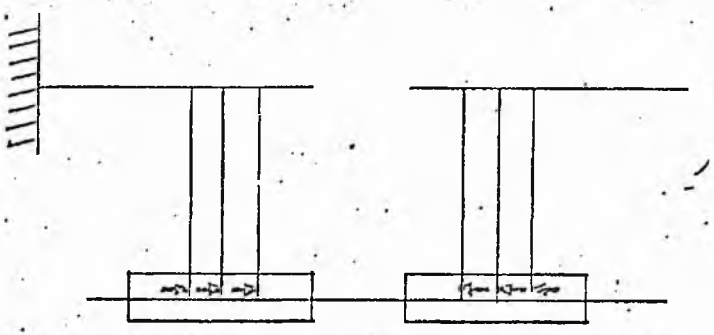

Test 4

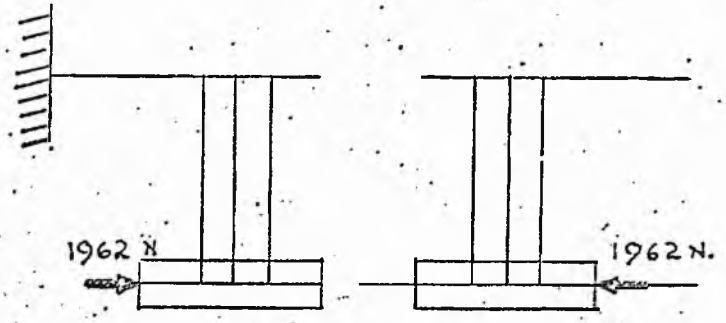

Test 5

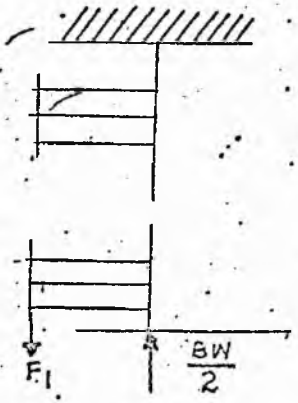

Test 6

fig 62

Each pin is loaded with a vertical force of 654 Newtons so that the total force acting upon each pin group is 1962N. In test 5 an axial load of 1962N is applied to one end of each carriage at joints 5 and 19 and test 6 represents functional loading of the bone during partial weight bearing. In this test an axial load of 367.8N is assumed to represent partial body weight which is applied at joint 19 in the negative X direction. The modified data for each test is listed in Appendix 5.6.E.

RESULTS of Compression Tests :-

The results of these tests are tabulated on page 216 (Table 5.7) Triaxial motion occurred in test 4 with excessive axial displacement and angulation of the distal fragment of bone. The results from tests 2, 3 and 5 indicate that slight approximation of the bone ends takes place and the greatest axial displacement (X displacement) occurs in test 5. Slight lateral displacement (Z displacement) of the bone, distal to the fracture site, occurs in tests 2 and 5 but this small amount of movement would be undetectable clinically using conventional tests. Axial rotation was minimal in all but tests 4 and 6, but significant bending occurs in test 6 (functional loading at partial body weight).

It can be seen in tests 2,3 and 5 that axial displacement of the distal section of bone occurs without any significant change in the initial displacement (Y displacement), which results from the position of the limb in space (i.e. in these tests, straight leg raising). A fracture gap of 4 mm is assumed in these tests and the movement that takes place would not therefore be accompanied by contract of the fragments. It is concluded therefore from these tests that compression across the fracture site occurs if an initial gap of less than .05 mm is present.

TABLE 5.7

MODEL 3. COMPRESSION TESTS: RESULTS

TEST	DISPLACEMENT			ROTATION		
	X	Y	Z	X	Y	Z
1	0	1.89	0	.63°	0	2.29°
2	-.0121	-1.8942	- .0001	.63°	0	2.29°
3	-.0107	-1.8942	0	.63°	0	2.29°
4	-9.0387	-1.8942	-3.67	.63°	9.5°	2.29°
5	.0350	-1.8942	- .0002	.63°	0	2.29°
6	3.54	1.0	.0526	0	1.54°	0

6. THE DIMENSIONAL CHANGES OF BONE

The derivation of data to represent the dimensions of the tibia have been discussed in the design of models 3 and 4. Model 2 represents a uniform section of bone and the effect of the dimensional changes between models 2 and 3 will be discussed in Chapter Six.

7. CHANGES IN THE DIMENSIONAL AND ELASTIC PROPERTIES OF BONE

External fixation tends to produce external bridging callus if motion between the bone ends is permitted (see Chapter 2). A gap of 4 mm was chosen and represents an unstable fracture which, in these tests on the 3 base mdoels, was replaced by a section of callus.

Three series of tests were carried out on Models 2, 3 and 4 with the following "types" of callus substituted in each series:

TYPE 1

External bridging callus with a cross-sectional area less than normal bone, i.e. a thin callus shell.

TYPE 2

This type simulated the dimensions of normal intact bone which is represented by Zone II of the base Models (See Appendix

TYPE 3

External bridging callus with a cross-sectional area greater than normal bone, i.e. a thick callus shell.

Type 1 represents a thin callus shell which has an external diameter (D) of 27.5 mm and an internal diameter (d) of 24.5 mm. The external diameter of type 3 represents a thick callus shell. This is assumed to be 36 mm with an internal diameter of 27.5 mm (Figure 63 The input data for each callus type is listed in Appendix 5.6.F.

Each base file (Models 2, 3 and 4) was then modified by the addition of an intact member, representing the section of callus, between joints 9 and 15. Additional changes to the input data were made to the Member Incidences (each member is "identified" by the adjacent joints) and the local Member Force for Member 26, the section of callus (Appendix 5.6.f) The local member force for the 4 mm section of bone was calculated from the unit weight of the leg section (see Appendix 5.4.) and found to be 0.26N. The assumption was made that the proportion of the force exerted by the small section of callus was considerably less than 0.26N. Any change in the total weight of the section of leg due to a dimensional change of the callus was therefore considered to be negligible, and the local member force for member 26, remained constant throughout all tests.

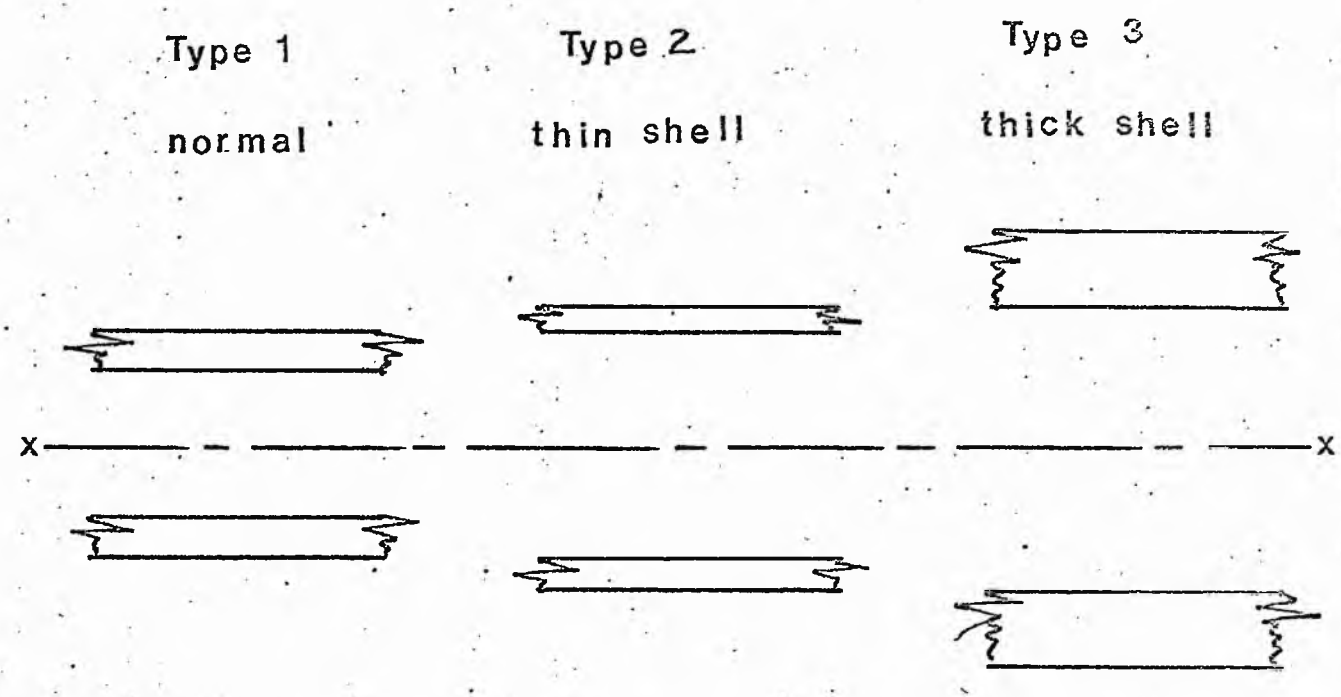

fig. 63 Callus dimensions

The modified base files (described in the previous paragraph) for each callus type, e.g. a thin callus shell, was then subjected to analysis by a sequential percentage change in the values of the Elastic Moduli from N = Normal bone to .01%N (Appendix 5.6.F).

Three series of tests on healing bone were therefore carried out each of which was represented by callus types 1, 2 and 3 (i.e. the three callus dimensions).

The dimensions of callus representing normal bone (type 2 callus) (in Bone Model 2) were however substituted by the data describing in "member properties" for a uniform section of bone (see Apppendix 5.6.f)

The fundamental position of the limb simulated in these tests is a straight leg raising activity with loading conditions similar to those represented in the base models.

RESULTS from the analysis of a change in mechanical properties of callus.

It can be seen from the tabulated results on pages 220-222 for the three types of callus that slight deformation of the bar occurs when the value of the elastic moduli are equivalent to that of normal bone. This remains virtually unchanged until the value of healing bone is approximately 1.0% of normal bone. Between 1% and .1% the callus is unable to adequately support the applied loads, with a consequent reduction in stability at the fracture site.

The magnitude of the bending moment at the proximal end of the bar (Joint 11) also changes in response to diminishing levels of healing and corresponding fluctuations in the levels of strain (ε), detectable in the bar, between 1% and fully healed bone are very small (Page 223) Table 5.8.

RESULTS : SMALL CALLUS (TYPE 1) : VARIABLE ELASTIC MODULI

(% N = Percentage of values for Normal E and G)

MODEL	% N TEST	DISPLACEMENT X	Y	Z	ROTATION X	Y	Z
2	N	0	.015	0	0	0	0
	75	0	.0152	0	0	0	.006
	50	0	.0153	0	.006	0	.006
	25	0	.0157	0	.006	0	.012
	1	0	.0305	0	.017	0	.21
	.1	0	.5988	0	.3	0	1.79
	.01	0	.6585	0	.04	0	2.06
3	N	0	.0176	0	0	0	0
	75	0	.0177	0	0	0	0
	50	0	.0179	0	0	0	0
	25	0	.0183	0	.006	0	.006
	1	0	.0331	0	.008	0	.21
	.1	0	.1388	0	.103	0	1.15
	.01	0	.6665	0	.03	0	2.08
4	N	0	.0146	0	0	0	0
	75	0	.0146	0	0	0	.006
	50	0	.0147	0	0	0	.012
	25	0	.0153	0	0	0	.017
	1	0	.0348	0	.023	0	.31
	.1	0	.1691	0	.1	0	1.7
	.01	0	.8194	0	.063	0	3.15

RESULTS : DIMENSIONS OF CALLUS = NORMAL (TYPE 2) BONE : VARIABLE ELASTIC MODULI

(% N = Percentage of values for Normal E and G).

MODEL	% N TEST	DISPALCEMENT X	Y	Z	ROTATION X	Y	Z
2	N	0	.015	0	0	0	0
	75	0	.015	0	0	0	.006
	50	0	.0152	0	0	0	.006
	25	0	.0153	0	.006	0	.006
	1	0	.0252	0	.017	0	.17
	.1	0	.0932	0	.092	0	1.0
	.01	0	.4416	0	.046	0	2.01
3	N	0	-.0176	0	0	0	0
	75	0	-.0176	0	0	0	0
	50	0	.0177	0	0	0	.006
	25	0	-.0179	0	.006	0	.006
	1	0	-.0269	0	-.023	0	-.2
	.1	0	-.1341	0	-.17	0	-1.67
	.01	0	-.3358	0	-.12	0	-2.04
4	N	0	.0143	0	0	0	.006
	75	0	.0144	0	0	0	.006
	50	0	-.0145	0	0	0	.006
	25	0	.0148	0	0	0	-.017
	1	0	.0275	0	.023	0	-.29
	.1	0	.1045	0	.1089	0	1.66
	.01	0	.4748	0	.1	0	3.08

RESULTS : LARGE CALLUS (TYPE 3) : VARIABLE ELASTIC MODULI

(% N = Percentage of values for Normal E and G)

MODEL	% N TEST	DISPLACEMENT X	Y	Z	ROTATION X	Y	Z
2	N	0	.0151	0	0	0	0
	75	0	.0151	0	0	0	0
	50	0	.015	0	0	0	0
	25	0	.015	0	0	0	.017
	1	0	.0161	0	0	0	.03
	.1	0	.0789	0	.057	0	.42
	.01	0	.4005	0	.58	0	2.9
3	N	0	.0176	0	0	0	0
	75	0	.0176	0	0	0	0
	50	0	.0176	0	0	0	0
	25	0	.0177	0	.006	0	-.017
	1	0	.0214	0	.006	0	-.04
	.1	0	.0871	0	.063	0	-.43
	.01	0	.2848	0	.086	0	1.5
4	N	0	-.0143	0	0	0	0
	75	0	-.0142	0	0	0	0
	50	0	-.0143	0	0	0	-.006
	25	0	-.0145	0	0	0	-.006
	1.	0	-.0194	0	.006	0	-.069
	.1	0	-.0622	0	.034	0	-.56
	.01	0	-.3473	0	.075	0	2.24

TABLE 5.8

LEVELS OF STRAIN IN THE FIXATOR BAR

MODEL	LEVEL OF HEALING	M (TYPE 1)	ε	M (TYPE2)	ε	M (TYPE 3)	ε
2	Fracture	3888	209	3888	209	3888	209
	.01	2963	159	2779	149	1361	73
	.1	1545	83	1371	74	258	13.9
	1.0	359	19	308	16	168	9.1
	25	107	6	104	5.6	97	4.7
	75	99	5.3	98	4.7	96	4.7
	Healed	98	5.3	98	4.7	97	4.7
3	Fracture	3874	208	3874	208	3874	208
	.01	2971	160	2783	150	2081	112
	.1	1577	85	804	43	279	15.0
	1.0	372	20	352	19	181	9.8
	25	122	6.5	121	6.5	113	6.1
	75	114	6.1	114	6.1	110	6.0
	Healed	113	6.0	113	6.0	110	6.0
4	Fracture	5595	300	5595	300	5595	300
	.01	4397	237	4106	221	3058	164
	.1	2320	125	2212	119	858	46
	1.0	545	29	516	28	236	13
	25	170	9.16	169	9.1	156	8.4
	75	159	8.5	158	8.5	154	8.3
	Healed	158	8.5	157	8.4	154	8.3

M = Bending Moment N/mm

ε = microstrain (Bar joint 11)

type 1 = thin callus shell

type 2 = "normal" bone

type 3 = thick callus shell

PREDICTED LEVELS OF MICROSTRAIN WITH CALLUS OF VARYING DIMENSIONS

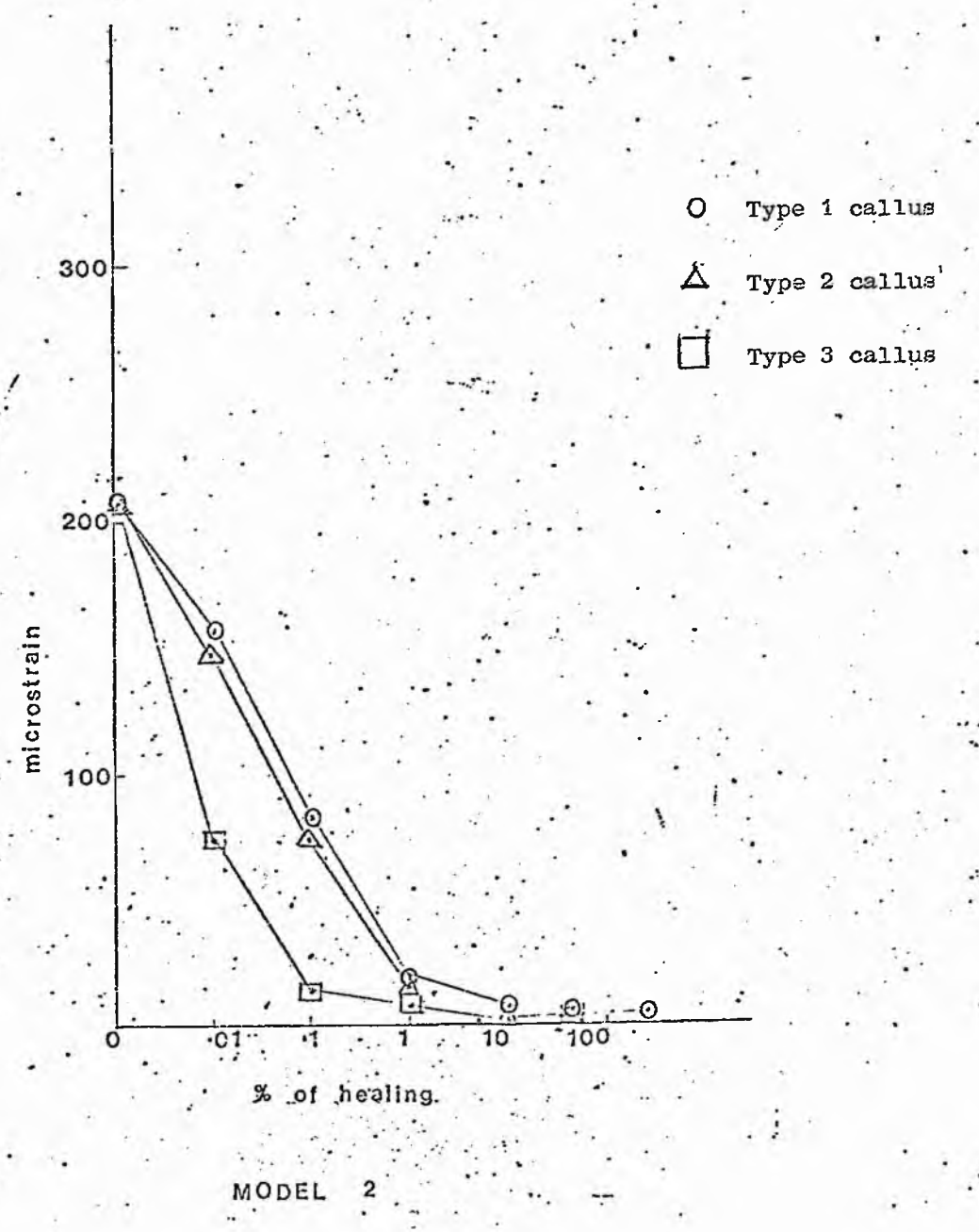

MODEL 2

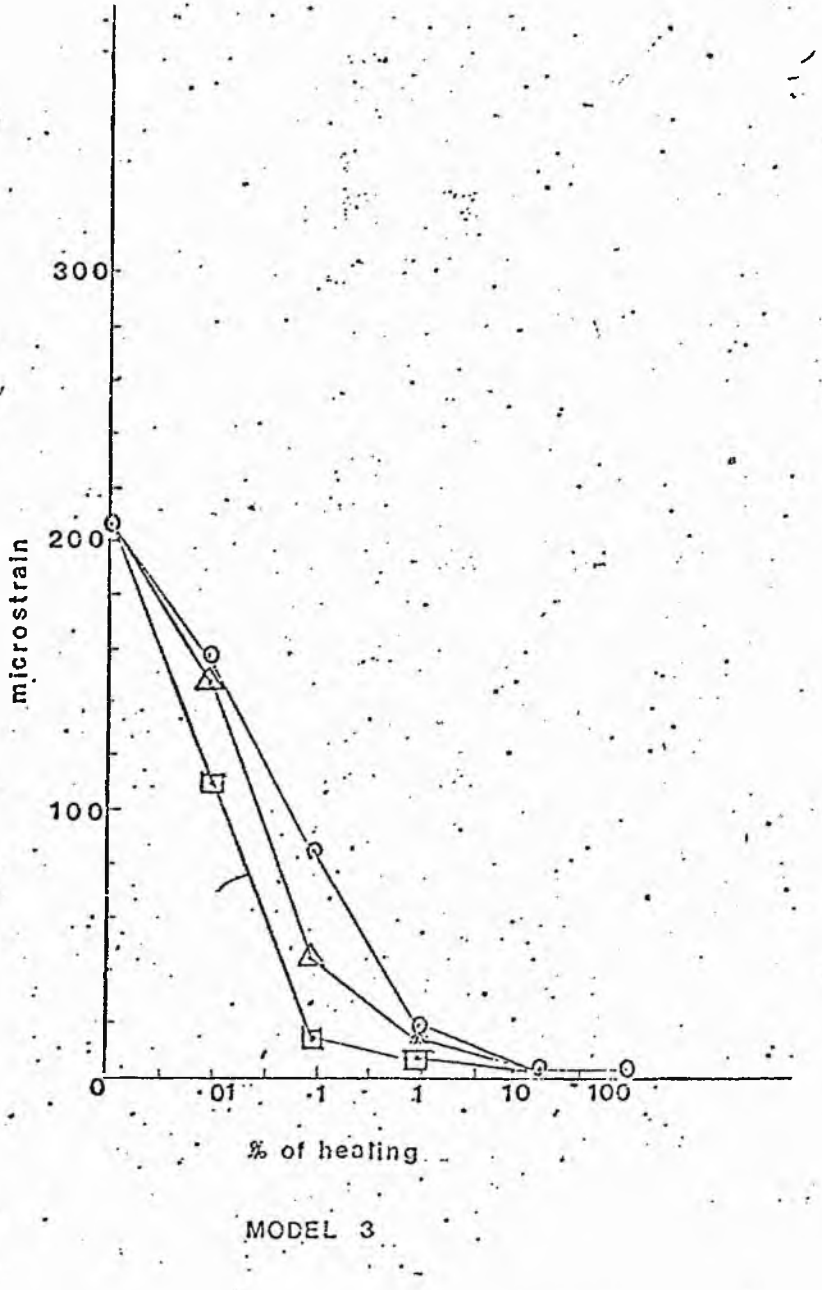

MODEL 3

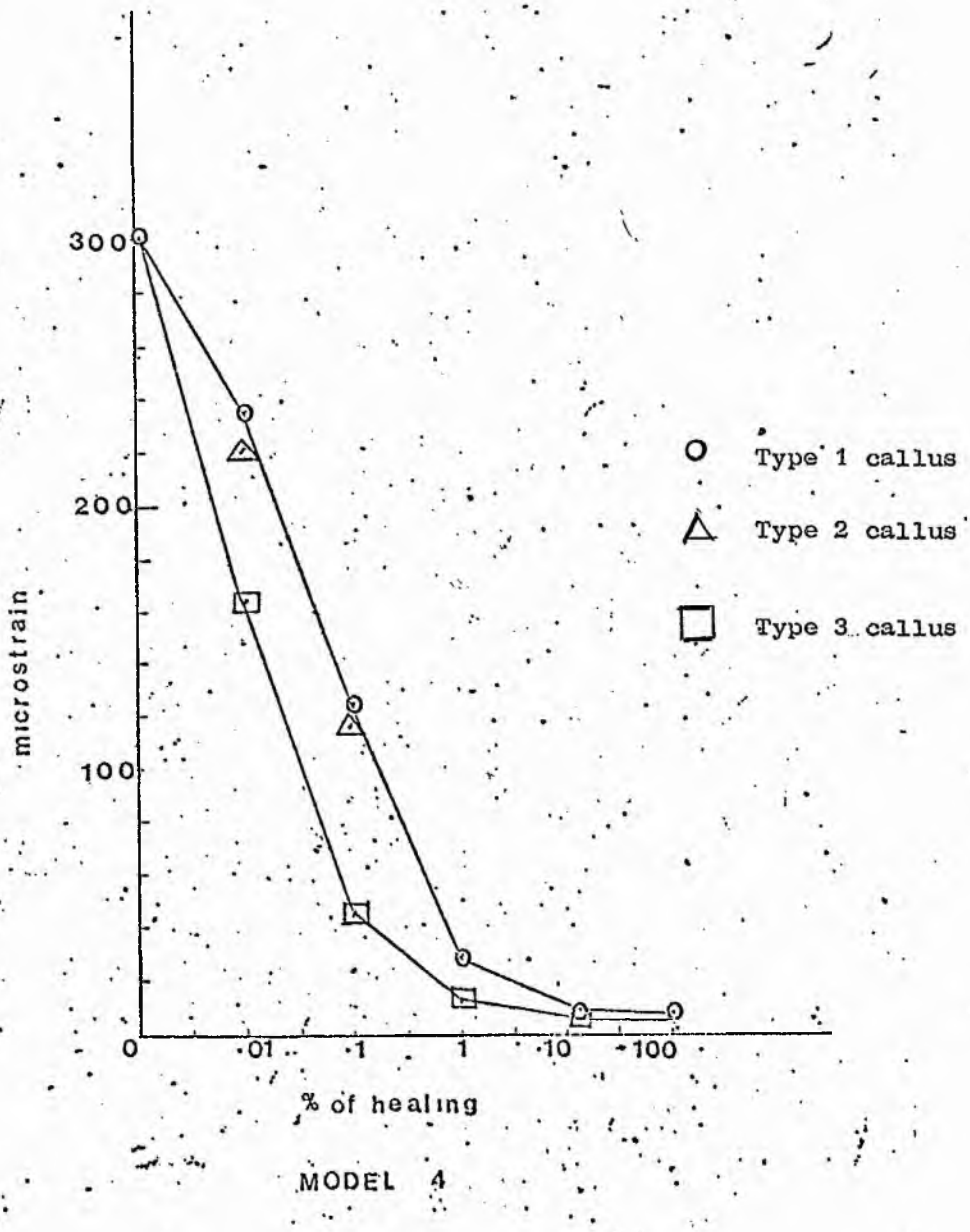

PREDICTED LEVELS OF MICROSTRAIN WITH CALLUS OF VARYING DIMENSIONS

This trend is observed in the three base models but the magnitude of the bending moments and the level of strain are slightly higher in model 4. It is also seen from the graphical presentation of this data (pages 224/5) that levels of strain are smaller for type 3 callus, which represents prolific external bridging callus. For a given level of healing i.e. .01% of normal an average fluctuation of 67$\mu\varepsilon$ in the level of strain between callus types 1 and 3 is observed. This is determined from the individual fluctuations occurring in models 2, 3 and 4.

It is concluded from this study of callus that vertical displacement of the fracture in the early stages of healing may be related to the levels of strain in the fixator bar. The level of strain however decays exponentially and changes in the level of strain are minimal between 1% and 100% of fully healed bone. From the data (presented in Chapter 2 Part A) for the Young's modulus of fibrocartilage and wet hyaline cartilage these values may be expressed as .3% and 2% of the value for fully healed bone respectively. It is suggested therefore that absolute levels of mechanical stability in healing bone may not be determined by strain related potentials in the bar during the intermediary and later stages of healing.

8. FUNCTIONAL LOADING OF THE LIMB

Two series of tests were conducted on (1) A fractured limb and (2) Intact bone.

(1) A fractured limb

Four tests were conducted on each base model to represent the

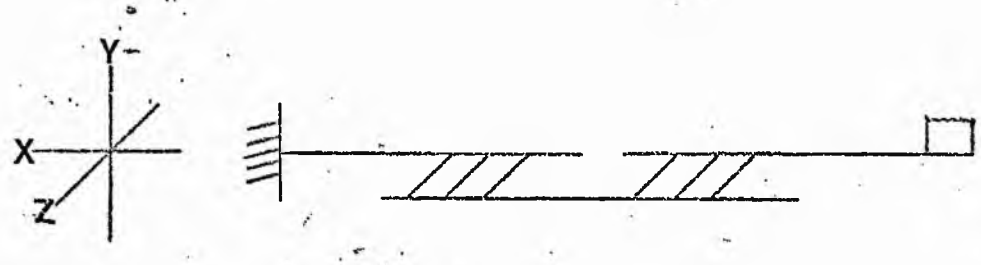

Position A Straight leg raising

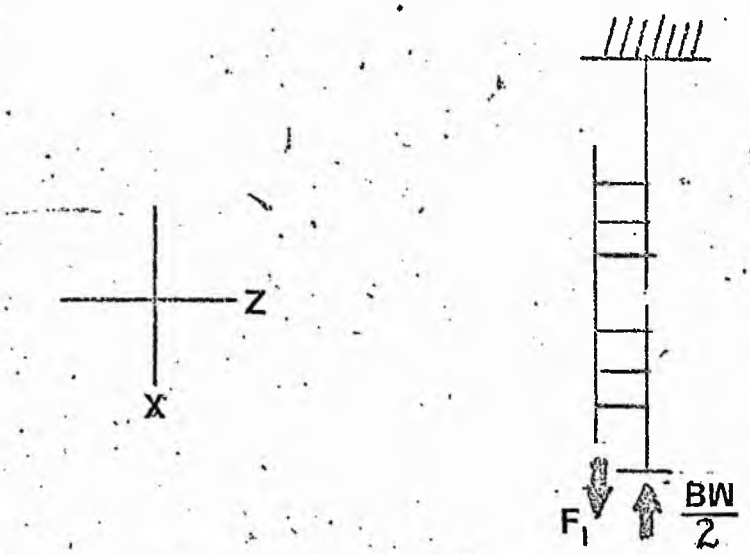

Position B Standing

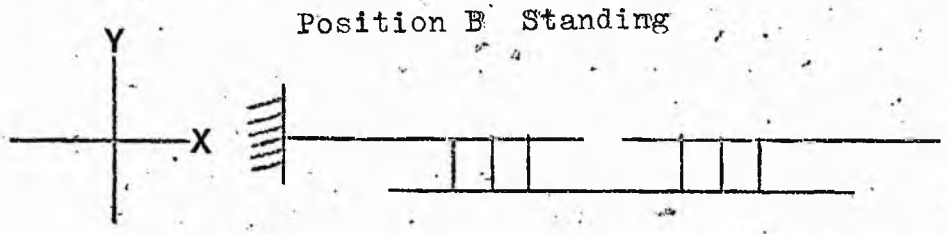

Position C Side lying

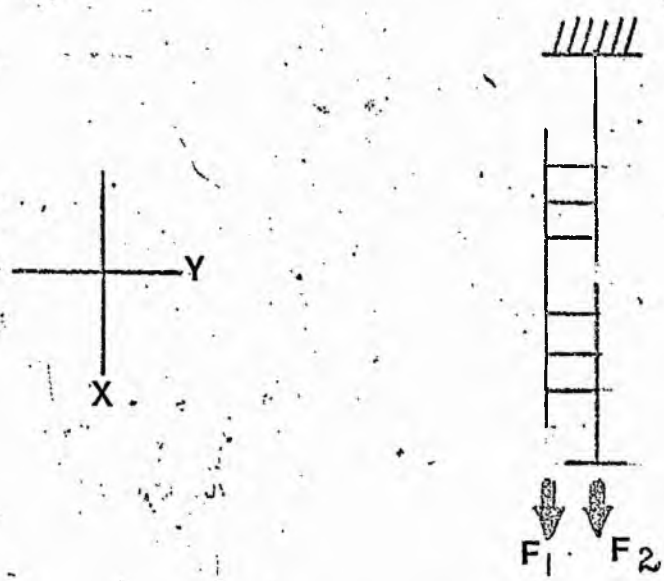

Position D High sitting

Fig. 64

following:

A. Straight leg raising : This position is represented by the fundamental position of each base model.

B. Standing on the fractured limb with partial body weight (BW/z = 367.8N).

C. Side lying with the fractured leg abducted and the bar in the dependent position.

D. High sitting with non-weight healing of the fractured limb.

The modification of data for position B and D was carried out by a change in the loading conditions and the direction of loading. In position B, the force exerted by the Bar and Carriage sections is due to their own weight acting in the positive X direction. A ground reaction force equal to half body weight (367.8N) is applied at joint 22 in the negative X direction (Figure 64). Co-ordinate changes were made for position C (Appendix 5.6.g)

In position D the force due to weight of the distal limb section and Bar (F_2) are presumed to be acting in the positive X direction. The change in limb orientation represented by position C is carried out by a change in the alignment of the pins so that the pin/carriage joints are located vertically along the negative Y axis (see Appendix 5.6.g).

RESULTS from a change in Limb Position :-

The results of these tests are presented graphically on pages 229-230 and tabulated in Appendix 5.7.H. Minimal motion between the bone ends takes place when the limb is in the dependent position or alternatively when the fractured leg is abducted and the patient turns towards the unaffected side. Similar patterns are observed in all 3 models. It is seen that maximum displacement and rotation occurs during standing (position B) (see page 229). It can however be seen from the tabulated data in Appendix 5.7.h that slight separation of the fracture site occurs in

MODELS 2 & 3

CHANGE OF POSITION

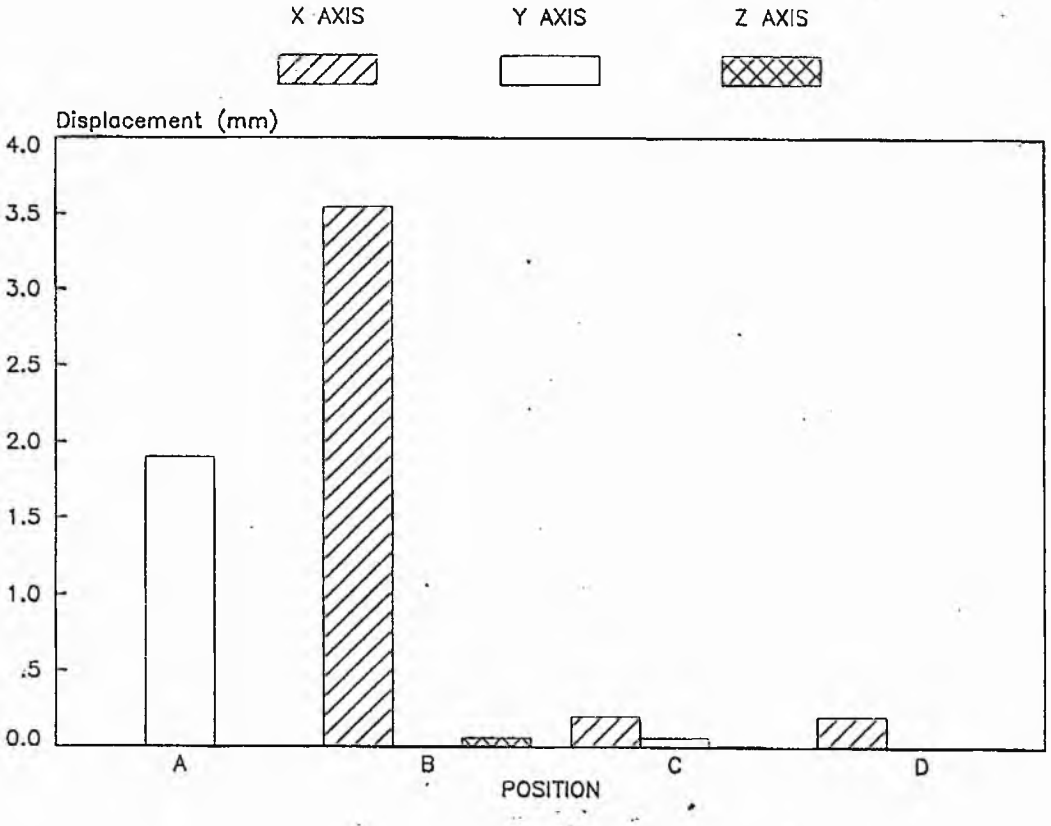

CHANGE OF POSITION

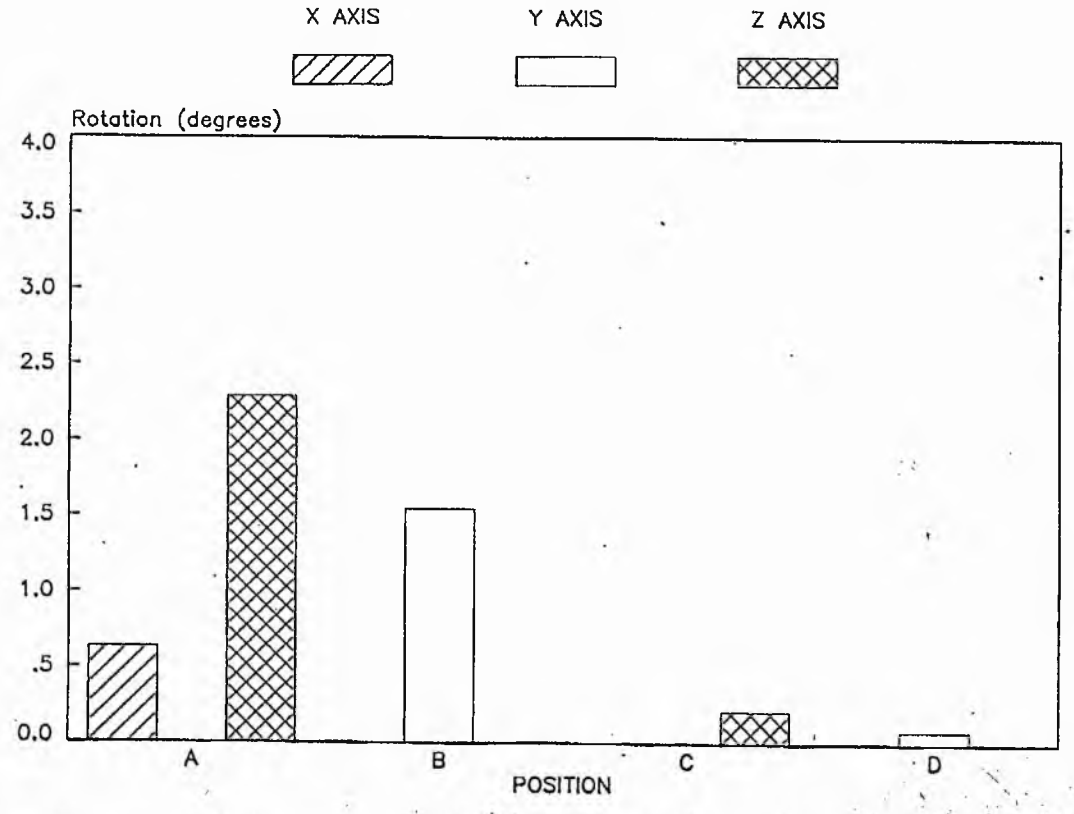

CHANGE OF POSITION

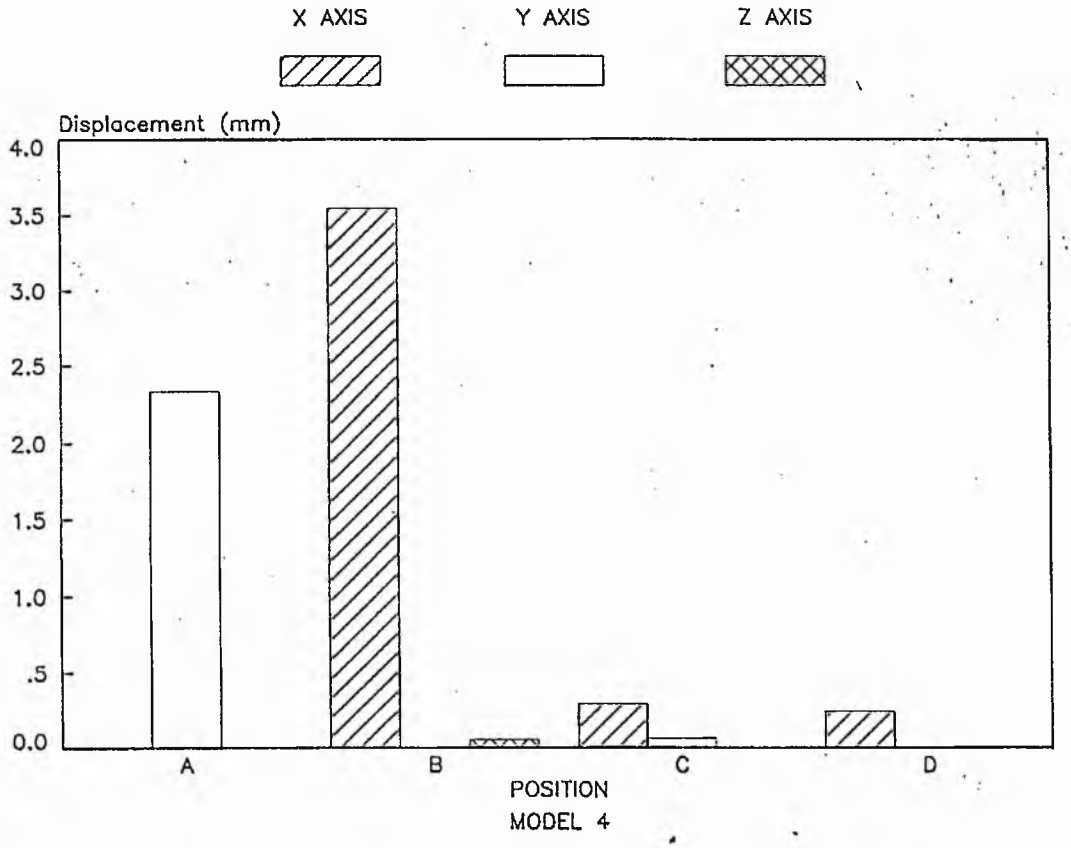

CHANGE OF POSITION

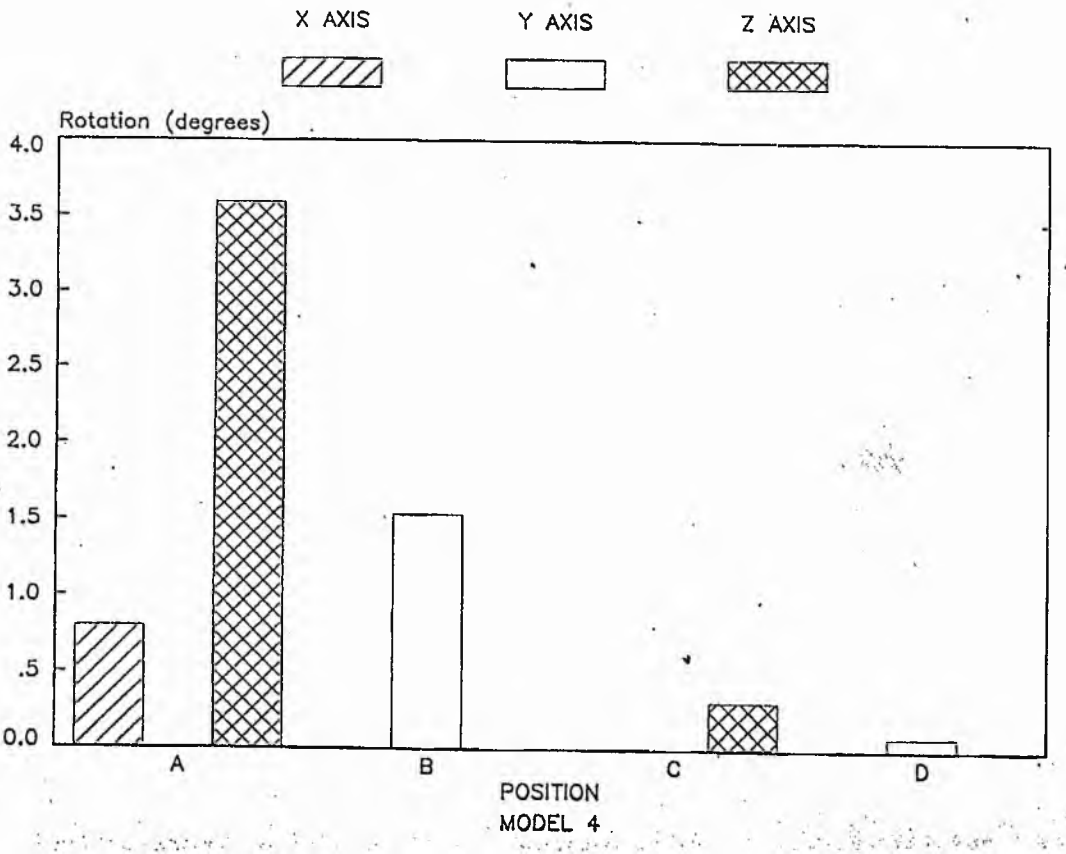

side lying and high sitting (X displacement in the positive direction) so that the fracture gap in side lying for example is increased from 4 mm to 4.2 mm in Model 3 and 4.3 mm in Model 4.

8. (2) FUNCTIONAL LOADING OF INTACT BONE

Intact bone with the fixator attached is subjected to loading firstly in tension then in compression. These two tests are conducted on three base models (2, 3 and 4) in which the fracture gap is replaced by a section of callus. The dimensions of the callus are represented by zone two (Appendix 5.5).

a) Tension

The leg is assumed to be in the dependent position and the loading conditions are similar to the tests on a fractured limb (Figure 64) in a similar position.

b) Compression

This test is similar to the compressive loading of the fractured limb (see Appendix 5.6.E Test 6) in which an axial compressive load is applied through the bone (representing partial weight bearing).

A series of tests is then conducted for each loading mode (compression + tension) and the values of the elastic modulii (E and G) are reduced from 100 per cent to 25 per cent of the values for normal bone. The data modification of the base files (Models 2, 3 and 4) may be found in the Appendices as follows:

Member Forces	Appendix 5.6.g.
Elastic Moduli	Appendix 5.6.f
The Callus	Appendix 5.6.h

From the results tabulated on pages 233-234it is seen that axial displacement in normal bone in tension or compression (due to loading equivalent to partial body weight) is very small (Table 5.9/10 pages 233/4) The magnitude of the movement is unaffected by a change in the level healing (in the later stages) or the fracture site location. From a comparison of these results with the data obtained from the bending of healing bone (page 221)the vertical displacement from anterio-posterior bending is greater than the displacement that occurs when the bone is loaded axially. The magnitude of these displacements during the later stages of healing is however independent of the fracture site location and it is seen that a change does not occur during these later stages (25% to 100% of normal bone).

9. SITE OF THE FRACTURE

The base models (3 and 4) were designed to represent two alternative locations for an unstable fracture. In model 3 a 4 mm fracture gap is located at 272-276 mm from the proximal end of the bone and a similar gap is located, again from the proximal end, at 207-211 mm, for Model 4.

It is found from all the tests carried out that the magnitude of vertical displacement in an unstable fracture is consistently larger in a fracture located in the middle of the leg (22.5%) than a similar fracture located more distally. The patterns of motion (i.e. displacements, axial rotation and angulation of the bone distal to the fracture site) are however similar. It is therefore concluded that the magnitude of motion is proportional to the location of the fracture site from the distal end of the bone.

TABLE 5.9.

RESULTS OF CHANGE IN FRACTURE SITE MOTION DUE TO AXIAL LOADING OF THE CALLUS

MODEL	TEST %N	DISPLACEMENT X	Y	Z	ROTATION (Degrees) X	Y	Z
2	N	.0002	0	.0005	0	0	0
	75	0	0	.0009	0	0	0
	50	.0005	0	.0008	0	0	0
	25	.0010	0	.0009	0	0	0
3	N	.0002	0	.0005	0	0	0
	75	.0002	0	.0005	0	0	0
	50	.0003	0	.0005	0	0	0
	25	.0007	0	.0005	0	0	0
4	N	.0002	0	.0004	0	0	0
	75	.0002	0	.0004	0	0	0
	50	.0004	0	.0004	0	0	0
	25	.0007	0	.0004	0	0	0

Applied Force = Partial Body Weight + Weight of Bar

N = Normal Bone %N = % Reduction in Values for E + G.

TABLE 5.10.

RESULTS FROM APPLICATION OF TENSION TO THE CALLUS

MODEL	TEST %N	DISPLACEMENT X	Y	Z	ROTATION (Degrees) X	Y	Z
2	N	0	0	.0008	0	0	0
	75	0	0	.0009	0	0	0
	50	0	0	.0008	0	0	0
	25	0	0	.0008	0	0	0
3	N	0	0	.0006	0	0	0
	75	0	0	.0006	0	0	0
	50	0	0	.0005	0	0	0
	25	0	0	.0006	0	0	0
4	N	0	0	.0003	0	0	0
	75	0	0	.0003	0	0	0
	50	0	0	.0003	0	0	0
	25	0	0	.0003	0	0	0

Applied Force = Weight of leg below Fracture Site + Weight of the External Fixator.

CHAPTER SIX: DISCUSSION AND FURTHER WORK

The experimental and analytical work suggest that strain related potentials cannot be detected by the bar when the tibia is fully healed or in the later stages of healing (i.e. between 15% - 100% of normal bone strength). The lower limit of healing at which the exponential declining levels of strain are indetectable is found to be lower than the predicted value suggested by Burny (see Chapter 2 Part D). As healing progresses the relative motion between the bone ends at the fracture diminishes and the single-sided fixator becomes a redundant structure. The tibia therefore becomes the principal load-bearing member. Since there is no data for the elastic properties of callus an estimation of these values can only be made. Assuming a mean value of 25 GN/m^2 for human tibial cortical bone then cartilage represents 1% of this value and fibro-cartilage 1% (see Chapter 2).

Cartilage and fibrocartilage are not clearly visible radiologically and it is the clinical practice to remove the bar when radiological evidence of callus formation is evident, i.e. the deposition of osseous material. It is assumed therefore that the bar which becomes redundant at this stage (between 1% - 15% of healing) may be removed and graduated activity begun.

The mechanical tests of stability (See Chapter 2) used in clinical practice do not however define the absolute limits of bone strength at this stage. The need therefore arises for clinical measurements of loads transmitted by the lower leg during the resumption of normal activity i.e. partial weight bearing with a walking aid (crutches or stick) to full weight bearing.

From the analysis using the Prime Stress Program the changes in the level of strain associated with healing bone between 0.1 and 1% of normal values, are small and the magnitude of fracture site motion and consequent changes in the level of detectable strain in the bar are low. This is found to be true for any spatial orientation of the limb. This suggests that a clear distinction between cartilage and fibrocartilage cannot be determined from the instrumented fixator. Furthermore this trend is observed from the three dimensions of callus that were examined. It is observed however that maximum stability is provided by the largest callus. The mechanical advantages of a large callus was observed by Charnley (1970) but it is found from this study that this advantage is most apparent in the very early stage of healing. The conclusion is drawn therefore that the dimensions of callus are less significant for fractures immobilized by external fixations, in the later stages of healing, than a change in the elastic properties of callus. It is also found that the dimensional variations of bone do not contribute to the overall rigidity of the bone fixator system.

The deflection at the fracture site and the levels of strain obtained experimentally from the bending tests were lower than predicted values (Model 1). This discrepancy is thought to be due to the assumptions that were made about the Modulus of Elasticity for the carriage sections (i.e. for aluminium). The peak strain for a maximum "Physiological" load of 2.72 Kg did not exceed 200 microstrain. Non-linearity and hysterêsis is demonstrated (below 40 micro strain) in these tests and in the calibration of the bar. Furthermore the specification of the Vishay recording instruments suggests that reliability is not obtained below 80 micro strain. The practical problems associated with direct bonding of strain gauges to the bar, limits the clinical application of

this technique and any device placed in situ at the time of operation requires sterilization during which mechanical, chemical or thermal damage may be sustained.

The calculated fracture site deflection obtained using Strain Energy techniques were comparable (within 8%) with the deflection obtained using the STRESS program. It is found that an unstable fracture located in the distal third of the leg will displace vertically with a mean value of 1.8 mm during a straight leg raising activity. For a more proximally located fracture the magnitude of the bending and torsion moments is increased with a corresponding increase in motion at the fracture site. For any given configuration of fixator and transfixing pins at the two fracture levels, the displacement at the fracture site is proportional to its location from the distal end.

Other factors which it is found contribute to the loss of vertical stability (tested analytically during a straight leg raising activity) are a reduction in pin diameter, an increase in pin length, an increase in:

a) the weight of the bar

b) the offset of the proximal set of pins from the fracture site

c) the mass of leg distal to the fracture site (e.g. oedema).

Stability is also reduced if the spacing between the pins is reduced, particularly at the junction with the carriages. An axial displacement of 3.5 mm and 1.5° of bending occurs when the bone is axially loaded by partial body weight. This does not assume however any eccentricity of applied load which will occur (see Chapter 2 Part B) in vivo. It is likely therefore that bending at the fracture site would be in excess of 1.5°.

The most significant of the factors defined in the previous paragraph are found to be pin diameter and length, which substantiates the findings of Evans et al (1979). A non-linear relationship is observed between motion and either of these two variables, and it is concluded that absolute rigid fixation cannot be achieved by an increase in pin diameter or conversely a reduction in pin length. The minimal length of pin is determined by the presence of any soft tissue intervening between the bar and bone together with the need to carry out any local nursing care of compound fractures.

Ansell and Scales (1968) demonstrated the minimal loss of bone strength by the use of small diameter screws (less than 3 mm) but stability at the fracture site (with external fixation) is enhanced considerably by the use of large diameter pins. It is suggested that for any given fracture site, vertical displacement of less than 1 mm can be obtained by the use of pins with a core diameter no less than 4.5 mm. This should however be weighted against the loss of bone strength and the local increase in stress at the pin holes. Rotational stability is considerably improved (reduced to 25^{o}) by an increase in bar diameter but this is counteracted by an increase in the vertical displacement, which it is suggested is due to the additional bending moments created by an increase in the mass of the bar.

A marked increase in motion occurs with axial loading of an unstable fracture and it has been observed clinically that premature weight bearing causes bending of the pins, pin loosening and pin tract infections (see Chapter 2 Part D). It has been demonstrated however that intermittent compressive loading in the early stages of healing promotes the formation of external bridging callus (see Chapter 2 Part C). From the author's

work it is suggested that the magnitude of the compressive force across the fracture site is dependant upon apposition of bone ends by callus or early repair tissue, i.e. the resistance of healing bone to deformation (E) compressive techniques used and the effects of muscle contraction. Current methods of applying compression are static, i.e. the compressive force is sustained or increased with the passage of time rather than controlled intermittent loading.

In a six pin configuration the most stable alignment is found with parallel coplanar pins with vertical alignment of the middle pin (of each pin group) between the bar and bone. The maximal spacing between each pin is determined by the length of the carriage section. It is also found that the wide spacing at the carriage section is more significant than at the bone. Rotational stability (about the long axis of the bone) is unchanged for any of the six configurations examined. In this work, however, the effect of biplanar pin orientation was not examined.

The motion at the fracture site is found to be dependant upon the relative position of the limb and fixator in space. Of the three functional positions examined minimal stability occurs during a straight leg raise activity (prone or supine). In this position the fracture deflects 1.89 mm (for a distally located fracture) which is reduced to less than .25 mm when the limb is in the abducted position with the patient lying on the unaffected site. This observation is based upon the assumption that the long axis of the bar and bone are in the same vertical plane and parallel to the floor. Slight distraction (less than .25 mm) at the fracture site occurs when the "high-sitting" position is assumed.

The contribution of bone deflection to overall deflection is found to be very small (.015 mm) and total deflection in a fractured model did not exceed 4 mm in response to the mamipulation of a single variable.

The rigidity or stability of a fracture immobilized by external fixator is therefore dependant upon the fixator configuration, compressive technique and the functional use of the limb.

Further work

1. Determine analytically the forces exerted by contracting muscle and their effect upon fracture site motion in a limb supported by external fixation.

2. The development of a compression device with an integral force transducer.

3. Analysis of the forces transmitted across the fracture site by the various compressive devices.

4. The transfixing pins used in external fixation provide radiographic markers. It is suggested that the photogrammetric method, described in Chapter 2 might be applied to the assessment of fracture healing.

5. A series of clinical trials based upon the development of a graduated exercise program to determine the limits of activity and control of motion in healing bone. These programs could incorporate the use of FORCE plates, a pedobarograph or pressure sensitive insoles to determine the limits of weight bearing.

6. A retrospective radiological study to determine the dimensions of external bridging callus.

REFERENCES

ANDERSON R (1934) "An automatic method of treatment of fracture of the tibia and fibula." Surg. Gynec. and Obst., Vo. 63, pp 639-646.

ANDREWS N (1981) "An introduction to Prime Stress." B.Sc. Thesis, Univ. of Surrey.

ANDERSON R (1945) in Dwyer N.St.J.P. (1973) "A preliminary report upon a new fixation device for fractures of long bones." Injury, 5, p 141.

ANSELL R & Scales J.T. (1968) in Jordon B.A. & Hughes A.N. (1978) "A review of the factors affecting the design, specification and materials of screws for use in orthopaedic surgery." Engineering in Medicine, Vol. 7, No. 2.

ASTM D143 "Tests for small clear specimens."

BANKS A.J. & Dervin E. (1980) "The Salford technique for the treatment of complicated fibial fractures." Eng. in Med., pp 84-86.

BASSETT C.A.L.; PAWLUK R.J. & BECKER R.O. (1964) "The effect of electric currents on bone in vivo." Nature, 204, pp 652-654.

BASSETT C.A.L. (1971) "Biophysical principles affecting bone structure." in the "Biochemistry of bone" 2nd Edition, Vol. 3, pp 1-76. Ed. by Bourne G.H. Academic Press

BOURGOIS R. & Burny F. (1972) "Measurement of the stiffness of fracture callus in vivo." J. Biomech., pp 85-91.

BRADDELEY G.W.; McKenna G.B.; Dunn H.K.; Daniels A.U. & Statton W.O. (1979) "Effects of flexural rigidity of plates on bone healing." Journal of Bone & Joint Surgery, (Sept.).

BROWN S.A. & Mayor M.B. (1976) "Ultra-sonic assessment of early callus formation." Blood. Eng., April, pp 124-125.

BURNY F.; Bourgois R.; Donkerwolke M. & Moullart (1978) "Utilization clinique de jauges de contrainte." Acta. Orthopaedica. Belg., No. 44, Ed. 6.

BURNY F. (1978) "Strain gauge measurement of fracture healing - A study of 350 cases." 6th Int. Conf. on Hoffman E/F, Williams & Williams Co., Baltimore.

BURNY F. & Frank L. (1979) in Brooker A.F. & Edwards (1974) "Current state of the art." Churchill Livingstone.

BURSTEIN A.H. & Reilly D. T. (1976) "Ageing of bone tissue." Mechanical Properties, Journal of Bone & Joint Surgery, (Jan.), No.1.

BERNSTEIN N.A.; Sahrgeber O.A.; Pavlenko P.P. & Gurvich N.A. (1936) in Drillis R.; Contini R.S. & Blustein M.E. (1964) "Body segment parameters - a survey of measurement techniques." Artifical Limbs, Vol. 8, pp 44-46.

BRIGHTON C.T. & Krebs A.G. (1972) "Oxygen tension of healing fracture in the rabbit." Journal of Bone & Joint Surgery, 54A, pp 323-332.

CARTWRIGHT A.G. (1971) "The effects of histological variation on the tensile properties of cortical bone." Ph.D. Thesis, Univ. of Surrey.

CAVENAGH P.R. & Gregor R.J. (1975) "Knee joint torque during the swing phase of normal treadmill walking." J. Biomech., Vol. 8, pp 337-344.

CHAMAY A. & Tschantz, P. (1972) "Mechanical influences in bone remodelling - experimental research on Wolffs Law." J. Biomech., 5.

CHARNLEY J. (1970) "The closed treatment of common fractures." 3rd. Edition, E.S. Livingstone Ltd.

CODIVILLA A. (1978) in Hierholzer G. et al (1978) "External Fixation" - Archives of Orthopaedic & Traumatic Surgery, 92, pp 175-182.

CRILLY (1972) in Houghton G.R. & Rooker G.D. (1979) "The Role of the Periosteum in the Growth of Long Bones." Journal of Bone & Joint Surgery, 61-B.

DEKAL S.; Lenthall G. & Francis M. (1981) "Release of Prostaglandins from bone and muscle after tibial fracture." Journal of Bone & Joint Surgery, 2, 63-B, p 185.

DEMPSTER W.T. (1955) in Drillis R.; Contini R.S. & Bluestein M.E. (1964) "Body segment parameters - a survey of measurement tecniques." Artificial Limb, 8, pp 44-46.

DEMPSTER W.T. & Liddicoat (1952) in Cartwright A.G. (1971) "The effects of histological variation on the tensile properties of cortical bone." Ph.D. Thesis, Univ. of Surrey.

DEMPSTER W.T. & Coleman R.F. (1961) in Da. Fonseca J.C.P. and Da Silva O.L. (1975) "Measurements of stress and strain in live bone by the Electrical Strain Gaugue method." Rev. Bras. de Pesquisas Med. e Biol., 8, (5-6), pp 469-474.

DEN HARTOG J.P. (1952) in Miller G.J. & Purkey W.W. (1980) "The Geometrical Properties of paired human tibia." J. Biomech., Vol. 13, No.1.

DRILLIS R.; Contini R.S. & Bluestein M.E. (1964) "Body segment parameters - a survey of measurement techniques." Artifical Limbs, Vol. 8, pp 44-46.

DUNN A.W. (1976) "Displaced tibial shaft fractures - a comparison of treatment methods." Southern Medical Journal, Vol. 69, pp 37-39.

DWYER N.St.J.P. (1973) "A preliminary report upon a new fixation device for fractures of the long bones." Injury, 5, p 141.

EDGE J. & Denham R. (1977) "The Portsmouth method of External Fixation." Injury, Vol. 11, No. 1.

EVANS M.; Harris J.D.; Kenwright J.; Grew N.D. & Tanner K.E. (1979) "The Oxford External Fixator." The Annual Report of the Oxford Orthopaedic Engineering Centre, Univ. of Oxford.

EVANS M.; Kenwright J. & Tanner K.E. (1979) "Analysis of a single-sided external fracture fixator." Eng. in Medicine, I. Mech.E., Vol. 8, No. 3, pp 133-137.

EVANS M.; Kenwright J. & Harris J.D. (1979) "External fracture fixation - the analysis and design of a new system." Eng. in Medicine, I.Mech. E., Vol. 8, No. 3, pp 138-142.

EVANS M. & Harris D. (1980) "The Oxford External Fixator - fracture monitoring." Report of Oxford Engineering Centre, Univ. of Oxford, pp 74-81.

EVANS F.G. & Lebow M.(1951) "Regional differences in some of the physical properties of the human femur." J. Applied Physiology, 3, pp 563-572.

EVANS F.G. & Lebow M. (1957) "Attempts to show plastic deformation in Bone of circular cross-section." J. Biomechanics, Vol. 5, pp 35-44.

FELLANDER M. (1963) "Treatment of fractures andpseudathrosis of the long bones by Hoffman's transfixation method." Acta Orthop. Scand. Vol.32, pp 132-156.

FISCHER O. (1906) in Drillis R.; Contini R.S. & Bluestein M.E. (1964) "Body segment parameters - a survey of measurement techniques." Artificial Limbs, 8, pp 44-46.

FRANKEL V.H. & Burstein A.H. (1965) in Miller G.W. & Purkey W.W. (1980) "The Geometric properties of paired human tibia." J. Biomech, Vol. 10, pp 569-579.

FRANKEL V.H.; Burstein A.H. & Brooks D.B. (1971) "Biomechnics of Internal Knee Derangement." Journal of Bone & Joint Surgery, 53-A, pp 945-946.

FUKADA E. & Yasuda I. (1957) "On the piezo-electric effect on bone." Journal of the Physical Soc. of Japan, 12, pp 1158-1162.

GARRICK J.G.; Riggins R.S.; Requa R.K. & Lipscomb P.R. (1972) "Fracture of midshaft tibia and fibula - a survey of treatment." Clin. Orthop., Vol. 88, pp 131-137.

GREEN S.A. & Miller E.B. "Complications of external fixation." Lorna Linda University, Lorna Linda, California.

GRIMES D.W. (1979) "Why some fractures do not heal." Med. Trial Tech. Quarterly, Vol. 25, part 7, pp 42-48.

GUZELSI N. & Saha S. (1981) "Electro-mechanical wave propogation in long bones." J. Biomech.,Vol. 14, pp 19-33.

HARLESS E. (1860) in Drillis R.; Contini R.S. & Bluestein M.E. (1964) "Body Segment Parameters - a survey of measurement techniques." 8, pp 44-46.

HARRINGTON I.J. (1976) "A bio-engineering analysis of force actions in the knee in normal and pathological gait." Biomed. Eng., May, pp 167-176.

HASTINGS G.W. (1980) "The nature and origin of the electro-mechanical properties of bone." 3rd. Symposium on methods and materials for fracture fixation. Biol. Eng. Soc., May 9th 1980, Stoke on Trent.

HAYES W.C.; Swenson L.I. & Schurman W. (1978) "Asimetric finite element analysis of the lateral tibial plateau." J. Biomech., Vol. 11, pp 21-23.

HERT J.; Pribylova E & Liskova M. (1972) "Reaction of bone to mechanical stimuli." Acta. Anat., 82, pp 218-230.

HICKS J.H. (1971) "High rigidity in fractures of the tibia." Injury, Vol. 3, pp 121-132.

HIERHOLZER G.; Kleining R; Horster G. & Zemenides P. (1978) "External fixation - classification and indications." Archives of Orthopaedic and Traumatic Surgery, 92, pp 175-182.

HOAGLUND F.T. &States J.D. (1967) "Factors influencing the rate of healing in tibial shaft fractures." Surg. Gynae. and Obst., Jan., pp 71-76.

HOFFMAN R. (1938) in Fellander M. (1963) "Treatment of fractures and Pseudarthroses of the Long bones by Hoffman's transfixation method." Acta. Orthop. Scand., 32, pp 132-150.

HOUGHTON G.R. & Rooker G. (1979) "The role of the periosteum in the growth of long bones." Journal of Bone & Joint Surgery, Vol 61-B.

JANKOVICH J. & Bidmuch (1972) "Effects of mechanical vibration on bone development in the rat." J. Biomech., Vol. 5, pp 241-252.

JERNBERGER (1970) "Measurements of stability of tibial fractures - a mechanical method." Acta. Orthop. Scand., Suppl. 135, p 88.

JOHNSON P.H. (1980) "Fracture Healing." Arkansas Med. Soc., Vol. 76, No. 10, pp 399-402.

JOHNSON & Stowall (1950) in Fellander M. (1963) "Treatment of fractures and Pseudarthrosis of the long bones by Hoffman's transfixation method." Acta. Orthop. Scand., Vol. 32, pp 132-156.

JORDAN B.A. & Hughes A.N. (1978) "A review of the factors affecting the design, specification and materials of screws for use in Orthopaedic surgery." Eng. in Med., Vol.7, No. 2.

JORGENSON T.F. (1972) "Measurements of stability of crucial fractures treated with Hoffman osteotaxis." Act. Orthop. Scand. (43), pp 207-210.

KARLSTRÖM G. & Olerud S. (1977) "Stable externalfixation of open tibial fractures - a report of five years experience." Orthop. Review, Vol. 6, No.8.

KAUFER H. (1971) "Mechanical function of the patella." Journal of Bone & Joint Surgery, 53-A, Vol. 8, pp 551-556.

KETENIJAN A.V. & Arsenis C. (1978) "Studies on the mechanism of callus cartilage differentiation and calcification during fracture healing." Orthopaedic Times of N.A., Vol. 9, No. 1, Jan.

KETTELKAMP D.B.; Johnson R.J.;Schmidt G.L.;ChaoE.Y.S. & Walker M. (1970) "An electro-goniometric study of knee motion in normal gait." Journal of Bone & Joint Surgery, Vol. 52-A, No. 4, pp 775-790.

KIMURA "Mechanical characteristics of human lower leg bones." Journal of the Faculty of Science, Univ. of Tokyo, Section V (Anthrop) Vol iv, part 4.

KLIP E.J. & Bosma R. (1978) "Investigations into the mechanical behaviour of pin-bone connections." Eng. in Medecine, Vol. 7, pp 43-46.

LAKE F.T.; Solomon D.V.M.; Davis R.W.; Pace N. & Morgan J.R. "Biolectric potentials associated with growing deer antler." Dept. of Oral Biol. & Anat. School of Dentistry and Medicine. Medical College of Georgia, Georgia 309112.

LAMBERT (1971) in Minns et al (1977) "A Biomechanical study of Internal fixation of the Tibial Shaft." J. Biomech., 10, pp 569-579.

LAMBOTTE (1907) in Brooker A.F. & Edwards (1979) "External Fixation - Current state of the art." Churchill Livingstone.

LANYON L.E. & Bourn S. (1979) "The influence of mechanical function on the development and remodelling of the tibia." Journal of Bone & Joint Surgery, Vol. 61-A, No. 2, March.

LINDHOLM R.; Lindholm S.; Liukko P.; Paastuaki J.; Isokaanta S.; Rossi R.; Autio E. & Tahminens E. (1909) in McGibbon R. (1980) "The Biology of fracture healing in Long bones." Journal of Bone and Joint Surgery, 60-B, No. 2.

LIPPERT F.G. & Hirsch C. (1974) "The three-dimensional measurements of tibial fracture motion by photogrammetry." Clinic Orthop. Vol. 105, pp 130-143.

LJUNGGREN A.E. (1980) "The human tibia with regard to principles of functional anatomy of long bones." Journal of Anthropology, 70, 3, 251-257.

MATTACH B. (1980) "Design of a cross-country wheelchair." B.Sc. Thesis, Univ. of Surrey.

MATTHEWS L.S.; Kaufer H. & Sonstegard D.A. (1974) "Manual sensing of fracture stability - a biomechanical study." Acta.. Orthop. Scand. 1974, 45, (3), pp 373-381.

McKIBBIN B. (1978) "The Biology of fracture healing in long bones." Journal of Bone & Joint Surgery, Vol. 60-B, No. 2.

MILLER G.J. & Purkey W.W. (1980) "The Geometric properties of paired human tibia." J. Biomech., Vol. 13, No.1.

MINNS R.J. Bremble G.R. & Campbell J. (1977) "A Biomechanical study of internal fixation of the tibial shaft." J. Biomech., Vol. 10, pp 569-579.

MORRISON J.B. (1968) "Bioengineering analysis of force actions transmitted by the knee joint." Biomed. Eng. pp 164-170.

MULHOLLAND M.C. & Pritchard J.J. (1959) "The Fracture Gap" Journal of Anatomy, 93, p. 590.

MUHEIM G. (1973) "Assessment of fracture healing in man by serial 87^{m} strontium semtimetry." Acta. Orthop. Scand., 44, pp 621-623.

MULLER M.E. (1955) "Kompressionsosteosynthesis inter besondere Berucksichtigung die Kinearthrodes." Helv. Chin. Acta., 22, 474-844.

NADAN J.R. (1949) "External Skeletal Fixation in the treatment of fractures of the tibia." Journal of Bone and Joint Surgery, 31-A, pp 586-598.

NICHOLLS, P.J.; Berg E.; Bliuen E.E. & Kling M.J. (1979) "X-Ray diagnosis of healing fractures in rabbits." Clinical Orthopaedics and Related Research, No. 142, (July-Aug.)

NISSAN M. (1980) "Review of some basic assumptions of knee biomechanics." J. Biomech. Vol. B, pp 375-381.

PATRIARCO A.G.; Mann R.W.; Simon S.R. & Mansour J.M. (1981) "An evaluation of the approaches of optimization models in the prediction of muscle forces during human gait." J. Biomech., Vol. 14, No. 8, pp 513-525.

PAUL J.P. (1967) "Forces at the human hip joint." Ph.D. Thesis, Univ. of Glasgow.

PAUL J.P. (1974) "Force actions transmitted in the knee in normal subjects and by Prosthetic Joint replacements." in "Total Knee Replacement (Conference) Mechanical Engineering Publications Ltd., London, New York.

PHILLIPS G. & McGibbin R. (1976) in McGibbin R. (1978) "The Biology of Fracture healing." Journal of Bone & Joint Surgery, 60-B, No.2.

PIETROWSKI G. & Kellerman G.I. (1973, 1978) in Miller G.J. & Purkey W.W. (1980) "The Geometric Properties of paired human tibia." J. Biomechanics, 13, pp 1-8.

PIEZALI R.L.; Hight T.K. & Nagal D.A. (1976) "An extended structural analysis of long bones." J. Biomech., Vol. 9, pp 695-701.

PIEZALI R.I.; Hight T.K. & Nagal D.A. (1980) "Geometric properties of human leg bones." J. Biomech., Vol. 13, pp 881-885.

PIEZALI R.I.; Seering W.P.; Nagel D.A.; Schurman D.J. (1978) "The function of the primary ligaments of the knee in anterio-posterio or medio-lateral motions." J. Biomech., Vol. 13, pp 777-784.

PRITCHARD J.J. in McGibbon R. (1978) "The Biology of fracture healing." Journal of Bone & Joint Surgery, 60-B, 2.

RAUBER (1876) in Evans F.G. (1973) "Mechanical Properties of Bone." Charles C. Thomas, Springfield, Illinois.

REZAIN S.M. (1971) "The effect of a new external bone-fixator on treatment of fractures of long bones." Ann. Royal College of Surgeons, 48, p 336.

REZAIN S.M. (1975) "A new external fixator device for treatment of complicated fractures of the leg." Injury, 9, p.17.

REZAIN S.M. (1976) "Tibial lengthening using a new extension device." Journal of Bone & Joint Surgery, Vol. 58-A, No. 2.

REZAIN S.M. (1978) "A new External fixation device for treatment of complicated fractures of the leg." Injury, 9, pp 17-22.

RHINELNADER F.W. (1974) "Tibial blood supply in relation to healing." Clinical Orthopaedics and Related Research, Vol. 105, pp 34-81.

RYBICKI E.F. (1977) "Studies on the effect of mechanical stress on bone healing in growth and remodelling." Bull. Hosp. for Joint Disease, N.Y., Vol. 38, Pt. 1, pp 21-22.

RYDELL N. (1965) "Forces in the hip joint. Intravital studies in Biomechanics and related Engineering topics." (Kennedi R.M.) Pergamon Press, London.

SARMIENTO A.; Latta L.; Zilioli A.; Sinclair W. (1974) "Role of the Sort Tissues in the Stabilization of Tibial Fractures." Clin. Orthop., Vol. 105, pp 116-129.

SAYEGH A. (1979) "A study of External Fixation Devices for fractures of the tibia and fibula." M.Sc. Thesis, Univ. of Surrey.

SCHENK R. & Willeneger R. in McGibbin R. (1978) "The Biology of fracture healing in long bones." Journal of Bone & Joint Surgery, 60-B, 2.

SCHUROV V.A. (1979) "The Volkov Organesian Device for tibial fractures." Ortop. Traumatologia Pro. 6, 44-45.

SEEDHOLM B.B. & Tereyama K. (1976) "Knee forces during the activity of getting out of a chair with and without the aid of arms." Biomed. Eng., (Aug.), pp 278-282.

SEIREG A. & Arvikar R.J. (1975) "The prediction of muscular load sharing and joint forces in the lower extremities during walking." J. Biomech., Vol. 18, pp 89-102.

STADER V.; Lewis K. & Breidenbach L. (1942), "The Stader Reduction Splint." Ann. Surg., Vol. 116, pp 628-636.

THOMSON G.A. (1971) in Piezali R.L.; Hight T.K. & Nagal D.A. (1980) J. Biomechanics. Vol. 13, pp 881-885.

TRUETA J. (1968) "Studies of the development and decay of the human frame." London, William Heineman Ltd.

TRUETA J. (1963) "The role of vessels in osteogenisis." Journal of Bone & Joint Surgery, 45-B, pp 402-418.

UNSWORTH A. & Shannon F.T. (1979) "A Biomechanical study of the treatment of tibial shaft fractures using plaster casts." Eng. in Medicine, Vol. 8.

UTHOFF H.K. & Dubue F.L. (1971) "Bone structure changes in the dog under rigid E/F." Clinical Orthop. and Related Research, 81, pp 165-170.

VIDAL J. & Buscayret C. in Brooker A.F. &Edwards (1979). "External fixation - current state of the art." Churchill-Livingstone.

WEINMANN J.P. & Sicher H. (1955) "Healing of Bone in Bone and Bones." Fundamentals of Bone Biology, Ed. 2., The C.V. Mosby Co.

WEISER C. (1964) in Muheim G. (1973) "Assessment of Fractures in man by serial 87^{m} Strontium Semtimetry." Acta. Orthop. Scand. 44, pp 621-627.

WHITE A.A. (1975) "Fracture treatment - the still unsolved problem." Clin. Orthop., Vol. 106, pp 279-284.

WINDOW A.L. (1982) "An introduction to strain gauges." Welwyn Strain Measurements Ltd. 6th Edition, March, 1982.

WINTER D. (1980) "Overall principle of lower limb support during stance phase of gait." J. Biomech., Vol. 13, pp 923-927.

WYN-JONES C. (1978) "Wrinkle corner - External Skeletal." Injury, Vol. 9, p. 329.

YAMAGISHI M. & Yoshimura Y. (1955) "The Biomechanics of fracture healing." Journal of Bone & Joint Surgery, 37-A, pp 1035-1068.

YOUNG R.W. (1972) in McGibbin (1978) "The Biology of Fracture Healing." Journal of Bone & Joint Surgery, Vol. 60-B, No.2. pp 158-162.

ZIMMER "Denham External Fixation Compression" Leaflet No. 2008, London.

BIBLIOGRAPHY

BASMAIJAN J.V. (1967) "Muscles Alive." Williams & Wilkins Co. Ltd., Baltimore, 2nd. Edition.

BIOLOGICAL ENGINEERING SOCIETY (1978) - 1st Symposium on Recent Developments in methods and materials for fracture fixation.

BLOOM & Fawcett "A textbook of histology." 10th Edition.

BRAILSFORD J.F. (1948) "Radiology of Bones and Joints." Churchill Ltd., London.

BROOKER A.F. & Edwards (1979) "External Fixation - Current State of the Art." Churchill-Livingstone.

CAUSTON J.R. (1977) "A Biologist's Mathematics." Publ. by Edward Arnold.

EVANS F.G. (1957) "Stress and Strain in Bones." C.C. Thomas, Springfield, Illinois, U.S.A.

FRANKEL V.H. & Burstein (1970) "Orthpaedic Biomechanics." Lea & Febiger, Philadelphia, U.S.A.

FRANKEL V.H. & Nordin M. (1980) "Basic Biomechanics of the Skeletal System." Lea & Febiger, Philadelphia, U.S.A.

FROST H.M. & Charles, C. (1967) "An Introduction to Biomechanics." Thomas, Illinois, U.S.A.

HAM A.W. & Harris W.R. (1971) "Repair Transplantation on Bone" in the "Biochemistry and Physiology of Bone." Second Edition, 3, 337-339. Ed. by Bourne G.H., N.Y., London, Academic Press.

HAMILTON W.J. & Simon G. (1980) "Surface & Radiological Anatomy." McMillan Press Ltd., London, 5th Edition.

HOLES K.A. (1962) "Experimental strength of materials." English Universities Press Ltd.

I.B.M. (1981) Application Program "STRESS" for the IBM 1130 Model 2B, Version 2 available from PRIME Computer Inc., Prime Park, Natick, Massachusetts C1760.

JOHNSON M.B.; Davies D.V. & Davies F. (1958) "Grays Anatomy" 32nd. Edition Longmans Green & Co., London, New York, Toronto.

PERRY C.C. & Lissner H.R. (1955) "The Strain Gauge Primer." 2nd. Edition, McGraw-Hill, New York, London.

SHIGLEY J.E. (1976) "Applied Mechanics of Materials." McGraw-Hill, Kogakusha Ltd., London.

STEVEN J. (1964) "STRESS" - a User's Manual. M.I.T. Press, Cambridge, Massachusetts.

SWANSON S.A.V. & Freeman N.A.R. "The Scientific Basis of Joint Replacement." Pitman Medical, London.

TIMOSHENKO S. (1965) "Strength of Materials" Parts I and II. Van Nostrand Co.

WILLIAMS P.L. & Warwick R. (1980) "Grays Anatomy" Churchill-Livingstone, Edinburgh, London.

YAMADA H. (1970) "Strength of Biological materials." Ed. by F. Gayner-Evans. Williams & Wilkins Co. Baltimore.

APPENDIX 3.1.1

DIMENSIONAL AND LOADING DATA USED IN THE ANALYSIS OF FRACTURE SITE MOTION

L^1 = length of Fixator Bar between Carriages = .08 m

m/unit = Fixator Bar = .0012N

L_A = distance between centre of fracture site and the pin = .045 m

L = distance between each pin axis = .018 m

L* = length of distal part of leg and foot = .176 m

$\bar{L}$ = length of distal part of leg = .146 m

C = length of pins from central axis of bone to central axis of fixator bar = .057 m

w/unit = distal part of leg = .062N

F = force due to mass of the foot = 9.81N

L_E = distance between end of carriage and inner pin = .005 m

I pin = $8.9^{-12} m^4$

J pin = $1.78^{-1} m^4$

I Bar = $4.3^{-10} m^4$

E of Stainless Steel = 200 GN/M^2

Force exerted by 1 carriage section = 2.8N

APPENDIX 3.1.2

RESULTS FROM THE ANALYSIS OF FRACTURE SITE MOTION

EQUATION	SOLVING FOR:	RESULTS
31	$\bar{F}$	1.27
32	U	.01189 RADS
30	Y_4	-.000127
27	F_c	-7.49
29	T_c	.429
	M*	3.8 Nm
18	Y_1	-9.2^{-4}
17	$\emptyset$	.035
20	V	.0033
28	Mc	.597
	Y_5	8.7^{-5}
16	Θ	-.0068 RADS
	Y_{4B}	.00375
	$\emptyset_2$	.046

NOTE: M* = $\leftarrow$M acting about pin 1.

Results in Nm and metres

APPENDIX 3.2

DATA FOR THE ANALYSIS OF HEALING BONE

I_1 pins = 6.9×10^{-9} M^4

E pins = 200×10^9 GN/M^2

E BAR = 200×10^9 GN/M^2

I_{II} BAR = 4.3×10^{-10} M^4

A^1 BAR = $.0003$ M^2

a = 57 mm

b = 63 mm

F = PARTIAL BODY WEIGHT = 363N

M = 3.1 NM

I_o = 1.2×10^{-8} M^4

E_o = 25×10^9 GN/M^2

APPENDIX 4.1.1 : Torsion Test 1 : Calibration of the Bar

(Temperature 20°C)

Load (mm $D_A N$)	Displacement	Revs.	GAUGES Microstrain					
			3	4	2	1	7	9
0	.5	0	0	0	0	0	0	0
40	.73	0	0	0	0	0	+ 14	+ 15
80	1	0	0	+ 8	1	0	+ 27	+ 28
120	1.23	0	+ 3	+ 8	+ 2	+ 4	+ 41	+ 43
160	1.5	0	+ 3	+ 12	+ 1	+ 5	+ 56	+ 57
200	1.7	0	- 5	+ 10	- 7	- 4	+ 63	+ 70
240	1.98	0	- 4	+ 16	- 7	- 4	+ 76	+ 80
280	2.2	0	- 14	+ 6	- 19	- 12	+ 75	+ 90
320	2.41	0	52	- 52	- 58	- 48	+ 32	+ 52
360	2.69	0	- 47	- 45	- 62	- 52	+ 64	+ 67
400	2.9	0	- 46	- 38	- 60	- 43	+ 77	+ 88
440	3.11	0	- 42	- 42	- 47	- 46	+ 93	+ 97
480	3.4	0	- 40	- 38	- 52	- 38	+ 115	+ 131
520	3.65	0	- 30	- 28	- 43	- 32	+ 129	+ 146
560	3.9		- 28	- 28	- 40	- 25	+ 150	+ 168
600	4.11		- 28	- 28	- 38	- 24	+ 163	+ 168
640	4.39	0	- 26	- 26	- 28	- 28	+ 175	+ 182
680	4.59		- 26	- 32	- 28	- 28	+ 188	+ 196
720	4.81		- 25	- 25	- 27	- 27	+ 204	+ 214
740	5.00		- 23	- 34	- 25	- 24	+ 208	+ 218
780	5.29	0	- 22	- 32	- 23	- 23	+ 245	+ 235
820	5.5	0	- 29	- 36	- 20	- 19	+ 238	+ 249
860	5.8		- 18	- 38	- 17	- 15	+ 255	+ 266
900	6.2	1	- 16	- 28	- 16	- 14	266	278
800	5.61		- 16	- 30	- 16	- 15	+ 335	243
720	4.99		- 28	- 33	- 17	- 17	+ 218	228
620	4.4		- 19	- 33	- 16	- 18	+ 181	+ 190
520	3.78		- 18	34	15	19	+ 149	+ 156
420	3.25		- 21	- 32	- 14	- 20	+ 128	+ 124
320	2.6		- 18	- 25	- 11	- 20	+ 90	+ 94
220			- 20	- 18	- 10	- 23	+ 58	+ 60
120	1.43		- 20	- 15	- 10	- 23	+ 27	+ 26
0			- 20	+ 16	- 10	- 26	- 21	- 22

APPENDIX 4.1.1 : Torsion Test 2 : Calibration of the Bar

(Temperature 20°C)

(mm D_AN) Load	Displacement	Revs.	GAUGES Microstrain 3	4	2	1	7	9
0	.5	0	0	0	0	0	0	0
40	.9	0	- 6	- 8	- 6	- 6	+ 17	+ 17
80	1.14	0	- 6	- 7	- 6	- 5	+ 26	+ 26
120	1.4	0	- 4	- 8	- 5	- 4	+ 40	+ 41
160	1.6	0	- 4	- 8	- 5	- 2	+ 52	+ 54
200	1.87	0	- 3	- 10	- 5	- 1	+ 66	+ 68
240	2.11	0	- 1	- 7	- 5	+ 5	+ 80	+ 83
280	2.35	0	+ 5	- 5	- 5	+ 6	+ 90	+ 96
320	2.58	0	+ 5	+ 6	+ 2	+ 6	+ 104	+ 112
360	2.82	0	+ 6	- 5	- 4	+ 7	+ 116	+ 125
400	3.8	0	+ 6	+ 4	+ 2	+ 8	+ 128	+ 138
440	3.31	0	+ 6	- 8	+ 1	+ 8	+ 141	+ 152
480	3.55	0	+ 6	- 6	- 4	+ 10	+ 155	+ 165
520	3.78	0	+ 8	- 5	+ 2	+ 12	+ 168	+ 177
560	4.1	0	+ 8	+ 4	+ 2	+ 12	+ 180	+ 192
600	4.38	0	+ 8	+ 3	+ 1	+ 12	+ 193	+ 205
640	4.5	0	+ 8	+ 5	+ 2	+ 14	+ 206	+ 218
680	4.74	0	+ 9	+ 3	+ 1	+ 14	+ 217	+ 231
720	4.99	0	+ 10	+ 8	+ 2	+ 15	+ 231	+ 241
760	5.22	0	+ 10	+ 4	+ 2	+ 16	+ 244	+ 258
800	5.47	0	+ 10	+ 3	+ 2	+ 16	+ 252	+ 276
840	5.69	0	+ 10	- 6	+ 2	+ 17	+ 268	+ 283
860	5.59	0	+ 12	- 10	+ 3	+ 20	+ 278	+ 294
900	6.2	1	+ 12	- 9	+ 3	+ 20	+ 293	+ 310
800	5.49	0	+ 11	- 12	+ 4	+ 18	+ 254	+ 277
720	5.1	0	+ 9	- 21	+ 4	+ 16	+ 231	+ 252
620	4.44	0	+ 11	- 23	+ 4	+ 16	+ 201	+ 221
520	3.81	0	+ 7	- 28	+ 4	+ 16	+ 169	+ 186
420	3.38	0	+ 6	- 26	+ 4	+ 12	+ 140	+ 158
320	2.68	0	+ 6	- 20	+ 5	+ 10	+ 108	+ 122
220	2.8	0	+ 15	- 13	+ 5	+ 10	+ 78	+ 88
120	.7		+ 5	+ 8	+ 6	+ 6	+ 23	+ 26
0	0	0	+ 5	+ 7	3	3	16	12

APPENDIX 4.1.1 : Torsion Test 3 : Calibration of the Bar

(Temperature 20°C)

(mm D_AN) Load	Displacement	Revs.	GAUGES Microstrain 3	4	2	1	7	9
0	.2	0	0	0	0	0	0	0
40	.6	0	3	- 11	- 3	+ 5	+ 12	+ 12
82	.8	0	+ 3	+ 7	+ 2	+ 4	+ 28	+ 28
120	1.1	0	+ 4	- 7	- 3	+ 5	+ 42	+ 43
162	1.38	0	- 2	- 5	- 5	+ 4	+ 56	+ 56
200	1.5	0	+ 4	- 13	- 5	+ 5	+ 65	+ 65
240	1.71	0	+ 5	+ 23	0	+ 6	+ 78	+ 80
280		0	+ 5	+ 33	0	+ 7	+ 92	+ 106
320	2.2	0	+ 5	- 3	- 5	+ 7	+ 102	+ 108
360	2.43	0	6	14	- 5	+ 8	+ 115	+ 115
400		0	+ 10	- 13	+ 5	+ 15	+ 132	+ 131
440	2.95	0	+ 12	+ 16	+ 5	+ 14	+ 148	+ 148
480	3.19	0	+ 12	- 27	+ 5	+ 15	+ 160	+ 160
520	3.4	0	+ 9	- 30	+ 3	+ 14	+ 168	+ 168
560	3.62	0	+ 9	+ 10	- 4	+ 14	+ 180	+ 178
600	3.88	0	+ 15	- 15	- 5	+ 17	+ 195	+ 181
640	4.15	0	+ 15	+ 3	+ 17	+ 20	+ 213	+ 201
680	4.4	1	+ 18	+ 36	+ 10	+ 22	+ 226	+ 214
720	4.6	0	+ 18	+ 63	+ 8	+ 23	+ 239	+ 228
760	4.79	0	+ 22	+ 40	+ 12	+ 28	+ 250	+ 240
800	5.09	0	+ 23	+ 4	+ 12	+ 27	+ 235	+ 266
840	5.3	0	+ 24	+ 13	+ 14	+ 30	+ 278	+ 248
880	5.56	0	+ 24	+ 5	+ 13	+ 31	+ 291	+ 221
920	5.78	0	+ 23	- 30	+ 13	+ 29	+ 301	+ 231
820	5.18	0	+ 22	- 30	+ 12	+ 28	+ 270	+ 180
720	4.58	0	+ 21	- 38	+ 14	+ 28	+ 248	+ 150
620	4.00	0	+ 20	- 46	+ 13	+ 25	+ 208	+ 120
520	3.42	0	+ 20	- 58	+ 13	+ 24	+ 180	+ 90
420	2.83	0	+ 20	- 58	+ 14	+ 22	+ 149	+ 52
320	2.21	0	+ 17	- 78	+ 14	+ 20	+ 116	+ 18
220	1.62	0	+ 18	- 51	+ 15	+ 18	+ 86	- 25
120	.35	0	+ 16	- 32	+ 16	+ 18	+ 56	- 61
0	0	0	+ 16	+ 11	+ 18	+ 18	+ 20	- 94

APPENDIX 4.1.1 : Torsion Test 4 : Calibration of the Bar

(Temperature 20°C)

(mm $D_A N_i$) Load	Displacement	Revs.	GAUGES Microstrain 3	4	2	1	7	9
0	.35	0	0	0	0	0	0	0
40	.55	0	- 4	- 6	+ 2	+ 2	+ 16	+ 16
100	.95	0	- 3	- 13	- 16	- 2	+ 34	+ 38
130	1.2	0	- 3	- 18	- 5	+ 4	+ 49	+ 52
160	1.32	0	- 5	- 18	- 6	- 1	+ 56	+ 59
200	1.61	0	- 5	- 18	- 5	+ 5	+ 70	+ 73
240	1.9	0	- 1	- 20	- 8	+ 6	+ 84	+ 90
280	2.1	0	0	- 23	- 5	+ 5	+ 94	+ 98
320	2.51	0	0	- 23	- 6	+ 6	+ 108	+ 114
360	2.58	0	0	- 25	- 7	+ 7	+ 120	+ 126
440	2.9	0	+ 5	- 21	- 6	+ 7	+ 135	+ 145
480	3.18	0	+ 6	- 20	- 6	+ 8	+ 152	+ 160
520	3.4	0	+ 5	- 18	- 8	+ 8	+ 163	+ 177
560	3.62	0	+ 7	- 24	- 7	+ 9	+ 175	+ 190
600	3.85	0	+ 14	- 20	- 8	+ 9	+ 185	+ 201
640	4.15	0	+ 6	- 19	- 6	+ 11	+ 201	+ 216
680	4.49	0	+ 6	- 16	- 7	+ 12	+ 214	+ 225
720	4.59	0	+ 7	- 13	- 7	+ 15	+ 227	+ 226
760	4.8	0	+ 7	- 13	- 15	+ 15	+ 238	+ 249
800	5.99	0	+ 7	- 13	- 8	+ 15	+ 252	+ 263
840	5.3	0	+ 10	- 9	- 9	+ 15	+ 263	+ 272
880	5.55	0	+ 13	- 16	- 6	+ 16	+ 275	+ 283
920	5.78	0	+ 6	- 16	- 6	+ 16	+ 286	+ 275
820	5.15	0	+ 6	- 16	- 6	+ 14	+ 254	+ 242
720	4.6	0	+ 7	- 15	- 5	+ 12	+ 225	+ 201
620	4.0	0	+ 5	- 22	- 8	+ 10	+ 193	+ 168
520	3.45	0	+ 5	- 28	- 7	+ 9	+ 165	+ 135
420	2.85	0	- 7	- 33	- 9	+ 6	+ 133	+ 104
320	2.35	0	- 5	- 8	+ 30	+ 6	+ 100	+ 86
220	1.65	0	- 5	- 20	- 6	+ 4	+ 72	+ 2
120	.6	0	- 6	- 16	- 36	- 4	+ 12	- 66
0	0	0	- 14	+ 6	- 6	- 6	- 6	- 76

APPENDIX 4.2.1 : Tension Test 1 (Houndsfield) : Calibration of the Bar

	GAUGE NUMBERS					
Load Kg.	3	4	2	1	7	9
20	+ 8	- 10	+ 17	+ 10	- 2	+ 6
40	+ 18	+ 17	+ 35	+ 20	0	+ 10
60	+ 25	+ 100	+ 53	+ 33	+ 5	+ 17
80	+ 34	+ 183	+ 70	+ 43	+ 6	+ 22
100	+ 42	+ 142	+ 87	+ 57	+ 8	+ 27
120	+ 48	+ 185	+ 102	+ 64	+ 10	+ 33
140	+ 56	+ 235	+ 121	+ 73	+ 14	+ 40
160	+ 64	+ 234	+ 140	+ 84	+ 16	+ 47
180	+ 70	+ 272	+ 156	+ 93	+ 20	+ 53
200	+ 77	+ 301	+ 174	+ 103	+ 23	+ 61
220	+ 83	+ 327	+ 195	+ 115	+ 28	+ 69
240	+ 92	+ 388	+ 210	+ 126	+ 32	+ 117
260	+ 101	+ 361	+ 227	+ 138	+ 37	+ 124
280	+ 109	+ 433	+ 240	+ 148	+ 38	+ 135
300	+ 114	+ 427	+ 257	+ 160	+ 43	+ 140
260	+ 98	+ 390	+ 228	+ 136	+ 35	+ 128
220	+ 76	+ 330	+ 188	+ 106	+ 24	+ 112
180	+ 87	+ 248	+ 154	+ 86	+ 17	+ 98
140	+ 45	+ 304	+ 120	+ 67	+ 10	+ 88
100	+ 25	+ 503	+ 84	+ 46	+ 3	+ 73
60	+ 8	+ 603	+ 50	+ 25	- 5	+ 11
20	- 8	+ 520	+ 6	- 2	- 4	+ 54
0	- 7	+ 152	- 18	- 13	+ 6	+ 48

APPENDIX 4.2.1 : Tension Test 2 (Houndsfield) : Calibration of the Bar

	GAUGE NUMBERS					
Load Kg.	3	4	2	1	7	9
20	- 3	+ 23	+ 44	+ 15	- 6	+ 18
40	+ 8	+ 38	+ 61	+ 22	0	+ 22
60	+ 18	+ 48	+ 77	+ 30	+ 6	+ 30
80	+ 27	+ 46	+ 92	+ 38	+ 10	+ 37
100	+ 35	+ 35	+ 108	+ 48	+ 13	+ 42
120	+ 43	- 8	+ 125	+ 57	+ 16	+ 49
140	+ 53	- 8	+ 142	+ 68	+ 20	+ 55
160	+ 60	+ 4	+ 158	+ 77	+ 24	+ 63
180	+ 68	+ 50	+ 174	+ 88	+ 28	+ 68
200	+ 77	+ 82	+ 90	+ 96	+ 32	+ 74
220	+ 85	+ 117	+ 207	+ 108	+ 36	+ 80
240	+ 92	+ 153	+ 222	+ 120	+ 40	+ 88
260	+ 101	+ 182	+ 240	+ 134	+ 44	+ 93
280	+ 110	+ 218	+ 256	+ 144	+ 48	+ 102
300	+ 120	+ 252	+ 272	+ 154	+ 53	+ 108
260	+ 94	+ 207	+ 234	+ 127	+ 40	+ 90
220	+ 76	+ 172	+ 198	+ 102	+ 32	+ 78
180	+ 58	+ 135	+ 167	+ 83	+ 24	+ 65
140	+ 42	+ 96	+ 133	+ 65	+ 17	+ 52
100	+ 25	+ 13	+ 100	+ 47	+ 10	+ 39
60	+ 7	- 67	+ 67	+ 28	+ 6	+ 25
20	- 8	- 112	+ 25	+ 8	- 5	+ 14
0	+ 1	- 35	- 4	- 1	0	0

APPENDIX 4.2.1 : Tension Test 3 (Houndsfield) : Calibration of the Bar

	GAUGE NUMBERS					
Load Kg.	3	4	2	1	7	9
20	+ 10	+ 20	+ 20	+ 7	+ 16	+ 8
40	+ 20	+ 38	+ 37	+ 15	+ 7	+ 15
60	+ 38	+ 44	+ 54	+ 24	+ 12	+ 22
80	+ 38	+ 37	+ 70	+ 34	+ 16	+ 29
100	+ 45	+ 3	+ 88	+ 42	+ 20	+ 36
120	+ 56	- 8	+ 106	+ 54	+ 23	+ 43
140	+ 63	- 6	+ 120	+ 63	+ 28	+ 51
160	+ 73	+ 17	+ 139	+ 72	+ 32	+ 58
180	+ 78	+ 58	+ 153	+ 84	+ 36	+ 62
200	+ 87	+ 93	+ 170	+ 95	+ 40	+ 70
220	+ 95	+ 126	+ 187	+ 105	+ 44	+ 76
240	+ 105	+ 194	+ 204	+ 117	+ 48	+ 84
260	+ 114	+ 205	+ 220	+ 127	+ 55	+ 90
280	+ 124	+ 258	+ 235	+ 142	+ 55	+ 94
300	+ 131	+ 274	+ 250	+ 154	+ 58	+ 100
264	+ 108	+ 248	+ 214	+ 123	+ 48	+ 95
220	+ 88	+ 208	+ 180	+ 98	+ 38	+ 72
180	+ 71	+ 177	+ 149	+ 80	+ 31	+ 60
140	+ 50	+ 128	+ 107	+ 56	+ 22	+ 44
100	+ 36	+ 97	+ 83	+ 44	+ 14	+ 34
60	+ 25	+ 14	+ 58	+ 29	+ 10	+ 23
20	+ 5	+ 25	+ 15	+ 6	+ 5	+ 8
0	+ 13	+ 190	- 34	- 10	+ 8	- 12

APPENDIX 4.2.1. : Tension Test 4 (Houndsfield) : Calibration of the Bar

	GAUGE NUMBERS					
Load Kg.	3	4	2	1	7	9
20	+ 8	+ 20	+ 20	+ 6	+ 4	+ 7
40	+ 18	+ 26	+ 36	+ 14	+ 8	+ 15
60	+ 26	+ 22	+ 54	+ 22	+ 10	+ 22
80	+ 34	+ 90	+ 72	+ 31	+ 16	+ 28
100	+ 44	- 86	+ 88	+ 40	+ 18	+ 36
120	+ 52	- 60	+ 104	+ 52	+ 22	+ 42
140	+ 61	- 58	+ 120	+ 60	+ 28	+ 48
160	+ 68	- 10	+ 136	+ 72	+ 32	+ 56
180	+ 78	+ 23	+ 152	+ 80	+ 34	+ 61
200	+ 84	+ 73	+ 170	+ 92	+ 38	+ 68
220	+ 94	+ 98	+ 188	+ 102	+ 42	+ 75
240	+ 102	+ 133	+ 203	+ 114	+ 47	+ 84
260	+ 111	+ 183	+ 220	+ 126	+ 50	+ 88
280	+ 118	+ 275	+ 235	+ 140	+ 54	+ 93
300	+ 127	+ 287	+ 257	+ 150	+ 58	+ 101
260	+ 114	+ 248	+ 214	+ 122	+ 66	+ 84
220	+ 86	+ 210	+ 180	+ 100	+ 38	+ 73
180	+ 70	+ 176	+ 150	+ 80	+ 32	+ 60
140	+ 52	+ 140	+ 117	+ 58	+ 24	+ 47
100	+ 35	+ 80	+ 82	+ 40	+ 16	+ 34
60	+ 19	+ 88	+ 50	+ 23	+ 8	+ 21
20	+ 6	- 104	+ 13	+ 5	+ 5	+ 13
0	+ 10	+ 16	- 28	- 10	+ 12	- 10

APPENDIX 4.3.1 : Compression Tests : Intact Bone Model + Denham Bar

Load Kg.	Test No.	GAUGE NUMBERS (MICROSTRAIN) 1	2	4	3	7	9
37	1	0	+ 5	-	0	-	+ 3
0		- 3	+ 5		0		0
37	2	0	+ 5		- 4		1
0		- 5	+ 3		0		0
37	3	- 3	+ 4		- 3		0
0		- 5	+ 3		- 3		- 3
75	1	- 5	0		- 3		- 3
0		- 5	+ 5		- 3		- 3
75	2	- 3	- 3		- 3		0
0		- 4	+ 3		- 3		0
75	3	- 1	0		0		0
0		- 4	+ 3		0		0
112	1	- 5	0		0		0
0		- 5	+ 5		- 3		0
112	2	- 3	0		0		0
0		- 5	+ 5		+ 4		- 5
112	3	- 3	+ 4		0		0
0		- 5	+ 6		- 4		0
150	1	- 5	- 3		- 4		- 2
0		- 3	- 3		- 5		+ 2
150	2	- 5	- 4		- 4		0
0		- 5	- 1		- 5		- 9
150	3	- 5	- 5		- 5		- 9
0		- 5	- 5		- 5		+57
225	1	- 4	- 5		- 5		+55
0		- 4	- 1		- 5		+56
225	2	- 4	- 5		0		- 5
0		+ 2	- 4		- 4		- 4
225	3	+ 4	- 9		+ 3		- 6
0		0	- 4		- 4		- 4
225	4	+ 5	- 8		+16		- 5
0		0	- 2		- 4		- 2
300	1	+ 4	- 8		+ 4		- 6
0		0	- 4		- 4		- 4

Appendix 4.3.1 continued

		GAUGE NUMBERS (MICROSTRAIN)					
Load Kg.	Test No.	1	2	4	3	7	9
300	2	+ 4	- 8		+ 6		- 8
0		0	- 5		- 5		- 6
300	3	+ 4	- 8		+ 5		- 7
0		0	- 4		- 3		- 6
375	1	0	- 8		+ 6		- 8
0		+ 3	- 4		- 4		- 6
375	2	+ 3	- 8		+ 5		- 8
0		0	- 4		- 3		- 6
375	3	0	- 8		+ 5		- 8
0		+ 3	- 3		- 4		- 8

APPENDIX 4.3.2 : Bending : Intact Bone + Fixator

TEST 1					TEST 2 (microstrain)			
	GAUGE NUMBER				GAUGE NUMBER			
Load	1	2	3	9	1	2	3	9
6.6	- 14	0	+ 14	- 7	+ 18	+ 16	+ 21	- 8
8.6	+ 12	+ 6	+ 18	+ 23	+ 18	+ 14	+ 19	- 35
10.6	+ 23	+ 14	+ 33	+ 18	- 14	+ 79	- 9	- 36
12.6	+ 22	+ 11	+ 28	+ 22	- 12	- 21	- 7	- 21
14.6	+ 15	+ 13	+ 35	+ 15	- 9	+ 79	+ 12	- 24
16.6	+ 22	+ 13	+ 39	+ 24	- 9	- 12	+ 10	- 26
17.6	+ 5	+ 5	+ 35	+ 22	- 7	- 21	+ 4	- 31
14.6	0	- 12	+ 8	- 10	- 9	- 22	- 6	- 35
12.6	- 14	- 13	+ 8	- 8	- 16	- 23	- 11	- 34
10.6	- 7	- 11	- 7	- 8	- 14	- 20	- 13	- 7
8.6	- 7	- 9	- 6	- 8	+ 7	0	+ 10	- 11
6.6	- 8	- 8	- 7	+ 35	+ 6	+ 3	+ 5	- 60
0	- 34	+ 31	+ 31	+ 35	- 46	- 42	- 49	- 60

TEST 3				
6.6	0	- 8	+ 8	+ 3
8.6	+ 4	- 8	+ 10	+ 3
10.6	+ 5	- 10	+ 12	+ 15
12.6	+ 4	- 11	+ 13	+ 13
14.6	+ 5	- 12	+ 14	+ 12
16.6	+ 7	- 14	+ 17	+ 11
17.6	+ 7	- 14	+ 17	+ 12
14.6	+ 6	- 11	+ 17	+ 12
12.6	+ 7	- 9	+ 13	+ 13
10.6	+ 5	- 7	+ 11	+ 13
8.6	+ 5	- 7	+ 10	+ 13
6.6	+ 5	- 6	+ 8	+ 13
0	+ 2	+ 2	+ 2	+ 18

APPENDIX 4.4.1 : Bending - fractured bone model and fixator

Position Prone

	TORSION GAUGES			(microstrain)		BENDING GAUGES		
Load Kg.	7	8	9	10	1	2	3	4
.9	- 1	+ 35	- 42	- 1	- 17	- 53	+ 54	+ 17
1.8	- 6	+ 67	- 78	+ 7	- 28	- 99	+ 102	+ 32
2.72	+ 8	+ 98	- 116	+ 100	- 43	- 146	+ 151	+ 49
1.8	+ 6	+ 67	- 80	+ 7	- 29	- 99	+ 102	+ 35
.9	+ 3	+ 35	- 43	+ 5	- 18	- 55	+ 55	+ 18
0	- 5	- 5	- 5	+ 2	- 6	- 6	- 4	- 4

Right Side Lying

	TORSION GAUGES			(microstrain)		BENDING GAUGES		
Load Kg.	7	8	9	10	1	2	3	4
.9	+ 6	+ 8	- 8	- 9	+ 58	- 12	+ 8	- 58
1.8	+ 10	+ 14	- 13	- 14	+ 110	- 18	+ 14	- 110
2.72	+ 14	+ 18	- 18	- 20	+ 164	- 26	+ 18	- 163
1.8	- 7	+ 12	- 12	- 15	+ 112	- 20	+ 13	- 113
.9	- 11	+ 16	- 30	- 8	+ 59	- 13	+ 12	- 62
0	- 14	+ 5	- 25	- 4	+ 6	- 6	+ 7	- 7

Left Side Lying

.9	- 18	- 24	- 7	- 12	- 70	+ 20	- 22	+ 67
1.8	- 20	- 33	+ 8	- 8	- 131	+ 40	- 40	+ 128
2.72	- 22	- 40	+ 17	+ 3	- 193	+ 56	- 58	+ 191
1.8	- 20	- 34	+ 8	- 7	- 133	+ 37	- 41	+ 130
.9	- 19	- 24	- 6	- 12	- 71	+ 20	- 23	+ 68
0	- 6	- 6	- 6	- 7	- 6	0	- 6	- 2

APPENDIX 4.4.1 : Posture Supine : Bending - fractured bone model and fixator

Test No. 1	TORSION GAUGES				(microstrain)		BENDING GAUGES		
Load Kg.	7	8	9	10	1		2	3	4
.9	- 7	- 37	+ 41	- 4	+ 13		+ 54	- 57	- 11
1.8	- 11	- 70	+ 79	- 6	+ 11		+ 103	- 108	- 22
2.72	- 19	- 102	+ 107	- 7	+ 13		+ 153	- 169	- 23
1.8	- 12	- 72	+ 80	- 6	+ 11		+ 104	- 110	- 17
.9	- 8	- 38	+ 42	- 5	+ 8		+ 57	- 61	- 10
0	- 4	- 5	- 5	- 5	- 5		- 4	- 4	- 4
Test No. 2									
.9	- 6	- 34	+ 43	- 3	- 4		+ 53	- 56	- 6
1.8	- 8	- 67	+ 79	- 4	- 6		+ 100	- 106	- 7
2.72	- 15	- 98	+ 113	- 5	- 8		+ 152	- 160	- 7
1.8	- 11	- 68	+ 81	- 4	- 7		+ 102	- 109	- 7
.9	- 8	- 36	+ 50	- 3	- 6		+ 52	- 57	- 6
0	- 6	- 3	+ 11	+ 4	- 4		- 4	- 6	- 3

NOTE:

100 $\mu\varepsilon$ = 1.5 N/m (13.9 lb inch T)

76 $\mu\varepsilon$ = 1.5 N/m in Bending

APPENDIX 5.1

INPUT DATA FOR BEAM DEFLECTION TESTS

E	Young's modulus of elasticity	$200\ 10^3\ N/mm^2$
G	Torsional modulus of elasticity	$87\ 10^3\ N/mm^2$
P	25 N	
a	100 mm	
b	50 mm	

Input data for Member properties:

Test	Area ax mm^2	Shear Area ay/az mm^2	J Ix mm^4	I Iy mm^4	I Iz mm^4
a)	50.2	50.2	402.12	201.06	201.06
b)	21.9	21.99	274.8	137.4	137.4
c)	64	64	682.66	241.33	341.33
d)	32	32	213.3	42.66	170.66

NOTE: a) Solid circular rod Ø = 8 mm

b) Circular tube d = 6 mm D = 8 mm

c) Square beam L = 8 mm

d) Rectangular beam b = 4 mm h = 8 mm

APPENDIX 5.2

The following standard formulae were used in the analysis of

a) Solid circular rod
b) Circular tube
c) Square beam
d) Rectangular beam

a) Solid circular rod

$\emptyset = 8$ mm

$$I = \frac{\pi D^4}{64}$$

$$J = \frac{\pi D^4}{32}$$

b) Circular tube

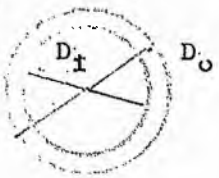

$D_o = 8$ mm

$D_i = 6$ mm

$$I = \frac{\pi (D^4 - d^4)}{64}$$

$$J = \frac{\pi (D^4 - d^4)}{32}$$

c) Square beam

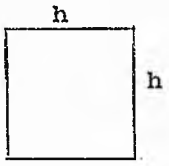

$h = 8$ mm

$$I = \frac{h^4}{12}$$

$$J = \frac{h^4}{6}$$

d) Rectangular beam

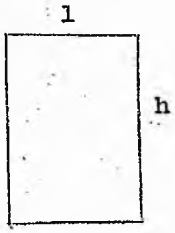

$l = 4$ mm

$h = 8$ mm

$$I = \frac{l h^3}{12}$$

$$J = \frac{l h (h^2 + l^2)}{12}$$

PRIME VERSION OF STRESS(3.2) 18/03/1978

==========

INPUT LISTING OF STRESS PROBLEM

==========

```
STRUCTURE DEN BAR LAB SIMULATION MODEL1
NUMBER OF JOINTS 20
NUMBER OF MEMBERS 23
NUMBER OF SUPPORTS 1
NUMBER OF LOADINGS 1
TYPE SPACE FRAME
JOINT COORDINATES
1 X 50  Y 0  Z 0  S
2 X 193  Y 0  Z 0.
3 X 193  Y 0. Z 56 58
4 X 164. Y 0  Z 56 58
5 X 211  Y 0. Z 56.58
6 X 211  Y 0. Z 0.
7 X 229  Y 0  Z 0.
8 X 272  Y 0. Z 0.
9 X 229. Y 0. Z 56 58
10 X 234. Y 0. Z 56 58
11 X 314  Y 0  Z 56 58
12 X 319  Y 0. Z 56 58
13 X 319  Y 0. Z 0.
14 X 276  Y 0  Z 0.
15 X 337  Y 0  Z 0.
16 X 337  Y 0  Z 56.58
17 X 355  Y 0  Z 56 58
18 X 384  Y 0. Z 56 58
19 X 355. Y 0  Z 0
20 X 420  Y 0  Z 0.
MEMBER INCIDENCES
1 1 2
2 2 6
3 6 7
4 7 8
5 14 13
6 13 15
7 15 19
8 19 20
9 2 3
10 6 5
11 7 9
12 13 12
13 15 16
14 19 17
15 4 3
16 3 5
17 5 9
18 9 10
19 11 12
20 12 16
21 16 17
22 17 18
23 10 11
MEMBER PROPERTIES PRISMATIC
1 THRU 8 AX 230 9 AY 230 9 AZ 230 9 IX 26164.7 IY 13082 3 IZ 13082 3
```

```
9 THRU 14 AX 10 57 AY 10 57 AZ 10 57 IX 17 8 IY 8 9 IZ 8 9
15 THRU 22 AX 362 9 AY 362.9 AZ 362.9 IX 21949.7 IY 10974.9 IZ 10974.9
23 AX 73 44 AY 73 44 AZ 73.44 IX 858 4 IY 429 2 IZ 429.2
CONSTANTS E 200000. ALL BUT 25000. 1 2 3 4 5 6 7 8
CONSTANTS E 10000. 15 16 17 18 19 20 21 22
CONSTANTS G 87000. ALL BUT 5500. 1 2 3 4 5 6 7 8
CONSTANTS G 3745. 15 16 17 18 19 20 21 22
TABULATE ALL
LOADING 1
MEMBER LOADS
8 FORCE Y CONCENTRATED P  9 8 L 60.
15 FORCE Y CONCENTRATED P -1.16 L 14.5
16 FORCE Y CONCENTRATED P  0 72 L 9.
17 FORCE Y CONCENTRATED P  0.72 L 9.
18 FORCE Y CONCENTRATED P  0 2 L 2 5
19 FORCE Y CONCENTRATED P  0 2 L 2 5
20 FORCE Y CONCENTRATED P  0 72 L 9
21 FORCE Y CONCENTRATED P  0.72 L 9
22 FORCE Y CONCENTRATED P  1.16 L 14.5
23 FORCE Y CONCENTRATED P  0.99 L 40
SOLVE
1
1
```

PRIME VERSION OF STRESS(3.2) 18/03/1978

INPUT LISTING OF STRESS PROBLEM

STRUCTURE DEN BAR MODEL2
NUMBER OF JOINTS 22
NUMBER OF MEMBERS 25
NUMBER OF SUPPORTS 2
NUMBER OF LOADINGS 1
TYPE SPACE FRAME
JOINT COORDINATES
1 X 0. Y 0. Z 0. S
2 X 50. Y 0. Z 0. S
3 X 193. Y 0. Z 0.
4 X 193. Y 0. Z 56.58
5 X 164. Y 0. Z 56.58
6 X 211. Y 0. Z 56.58
7 X 211. Y 0. Z 0.
8 X 229. Y 0. Z 0.
9 X 272. Y 0. Z 0.
10 X 229. Y 0. Z 56.58
11 X 234. Y 0. Z 56.58
12 X 314. Y 0. Z 56.58
13 X 319. Y 0. Z 56.58
14 X 319. Y 0. Z 0.
15 X 276. Y 0. Z 0.
16 X 337. Y 0. Z 0.
17 X 337. Y 0. Z 56.58
18 X 355. Y 0. Z 56.58
19 X 384. Y 0. Z 56.58
20 X 355. Y 0. Z 0.
21 X 420. Y 0. Z 0.
22 X 480. Y 0. Z 0.
MEMBER INCIDENCES
1 1 2
2 2 3
3 3 7
4 7 8
5 8 9
6 15 14
7 14 16
8 16 20
9 20 21
10 21 22
11 3 4
12 7 6
13 8 10
14 14 13
15 16 17
16 20 18
17 5 4
18 4 6
19 6 10
20 10 11
21 12 13
22 13 17
23 17 18

```
24 18 19
25 11 12
MEMBER PROPERTIES PRISMATIC
1 THRU 10 AX 230.9 AY 230.9 AZ 230.9 IX 26164.7 IY 13082.3 IZ 13082.3
11 THRU 16 AX 10.57 AY 10.57 AZ 10.57 IX 17.8 IY 8.9 IZ 8.9
17 THRU 24 AX 362.9 AY 362.9 AZ 362.9 IX 21949.7 IY 10974.9 IZ 10974.9
25 AX 73.44 AY 73.44 AZ 73.44 IX 858.4 IY 429.2 IZ 429.2
CONSTANTS E 200000. ALL BUT 25000. 1 2 3 4 5 6 7 8 9 10
CONSTANTS E 10000. 17 18 19 20 21 22 23 24
CONSTANTS G 87000. ALL BUT 5500. 1 2 3 4 5 6 7 8 9 10
CONSTANTS G 3745. 17 18 19 20 21 22 23 24
TABULATE ALL
LOADING 1
MEMBER LOADS
6 FORCE Y CONCENTRATED P -2.78 L 21.5
7 FORCE Y CONCENTRATED P -1.16 L 9.
8 FORCE Y CONCENTRATED P -1.16 L 9.
9 FORCE Y CONCENTRATED P -4.18 L 32.5
10 FORCE Y CONCENTRATED P -9.81 L 30.
17 FORCE Y CONCENGTRATED P -1.16 L 14.5
18 FORCE Y CONCENTRATED P -0.72 L 9.
19 FORCE Y CONCENTRATED P -0.72 L 9.
20 FORCE Y CONCENTRATED P -0.2 L 2.5
21 FORCE Y CONCENTRATED P -0.2 L 2.5
22 FORCE Y CONCENTRATED P -0.72 L 9.
23 FORCE Y CONCENTRATED P -0.72 L 9.
24 FORCE Y CONCENTRATED P -1.16 L 14.5
25 FORCE Y CONCENTRATED P -0.99 L 40.
SOLVE
1
1
```

PRIME VERSION OF STRESS(3,2) 18/03/1978 **Appendix 5.3.**

INPUT LISTING OF STRESS PROBLEM

```
STRUCTURE DEN BAR MODEL 4
 NUMBER OF JOINTS 22
 NUMBER OF MEMBERS 25
 NUMBER OF SUPPORTS 2
 NUMBER OF LOADINGS 1
 TYPE SPACE FRAME
 JOINT COORDINATES
 1 X 0. Y 0. Z 0. S
 2 X 50. Y 0. Z 0. S
 3 X 128. Y 0. Z 0.
 4 X 128. Y 0. Z 56.58
 5 X 99. Y 0. Z 56.58
 6 X 146. Y 0. Z 56.58
 7 X 146. Y 0. Z 0.
 8 X 164. Y 0. Z 0.
 9 X 207. Y 0. Z 0.
 10 X 164. Y 0. Z 56.58
 11 X 169. Y 0. Z 56.58
 12 X 249  Y 0. Z 56.58
 13 X 254. Y 0. Z 56.58
 14 X 254. Y 0. Z 0.
 15 X 211. Y 0. Z 0.
 16 X 272. Y 0. Z 0.
 17 X 272. Y 0. Z 56.58
 18 X 290. Y 0. Z 56.58
 19 X 319. Y 0. Z 56.58
 20 X 290. Y 0. Z 0.
 21 X 420. Y 0. Z 0.
 22 X 480. Y 0. Z 0.
 MEMBER INCIDENCES
 1 1 2
 2 2 3
 3 3 7
 4 7 8
 5 8 9
 6 15 14
 7 14 16
 8 16 20
 9 20 21
 10 21 22
 11 3 4
 12 7 6
 13 8 10
 14 14 13
 15 16 17
 16 20 18
 17 5 4
 18 4 6
 19 6 10
 20 10 11
 21 12 13
 22 13 17
 23 17 18
```

```
24 18 19
25 11 12
MEMBER PROPERTIES PRISMATIC
1 AX 450. AY 450. AZ 450. IX 108683. IY 47978.5 IZ 19387.8
2 THRU 7 AX 365. AY 365. AZ 365. IX 22931.3 IY 21073.5 IZ 11153.9
8 THRU 10 AX 252. AY 252. AZ 252. IX 19076. IY 12140.2 IZ 10251.5
11 THRU 16 AX 10.57 AY 10.57 AZ 10.57 IX 17.8 IY 8.9 IZ 8.9
17 THRU 24 AX 362.9 AY 362.9 AZ 362.9 IX 21949.7 IY 10974.9 IZ 10974.9
25 AX 73.44 AY 73.44 AZ 73.44 IX 858.4 IY 429.2 IZ 429.2
CONSTANTS E 200000. ALL BUT 25000. 1 2 3 4 5 6 7 8 9 10
CONSTANTS E 10000. 17 18 19 20 21 22 23 24
CONSTANTS G 87000. ALL BUT 5500. 1 2 3 4 5 6 7 8 9 10
CONSTANTS G 3745. 17 18 19 20 21 22 23 24
TABULATE ALL
LOADING 1
MEMBER LOADS
6 FORCE Y CONCENTRATED P -2.78 L 21.5
7 FORCE Y CONCENTRATED P -1.16 L 9.
8 FORCE Y CONCENTRATED P -1.16 L 9.
9 FORCE Y CONCENTRATED P  8.38 L 65.
10 FORCE Y CONCENTRATED P -9.81 L 30.
17 FORCE Y CONCENTRATED P -1.16 L 14.5
18 FORCE Y CONCENTRATED P -0.72 L 9.
19 FORCE Y CONCENTRATED P -0.72 L 9.
20 FORCE Y CONCENTRATED P -0.2 L 2.5
21 FORCE Y CONCENTRATED P -0.2 L 2.5
22 FORCE Y CONCENTRATED P -0.72 L 9.
23 FORCE Y CONCENTRATED P -0.72 L 9.
24 FORCE Y CONCENTRATED P -1.16 L 14.5
25 FORCE Y CONCENTRATED P -0.99 L 40.
SOLVE
1
1
```

APPENDIX 5.4

INPUT LISTING OF CONSTANTS FOR THE ANALYSIS OF FRACTURE SITE STABILITY

All data is in Newtons and millimetres.

Stainless Steel	E	=	200 000 N/mm^2
	G	=	87 000 N/mm^2
Aluminium	E	=	10 000 N/mm^2
	G	=	3 745 N/mm^2
Tibial Cortical Bone	E	=	25 000 N/mm^2
	G	=	55 000 N/mm^2

Dimensions:

Transfixing Pins

Core Diameter	3.67	mm
Length	56.58	mm
Interval between pins	18	mm

Aluminium Carriages (square)

Length	70	mm
Breadth	18.4	mm

Fixator Bar

Core Diameter	9.67	mm
Length between Carriages	80	mm

LOADING DATA and method of calculation for Bone, Bar and Carriage Sections.

Bone

Weight of leg distal to its centre of gravity = W_B

Length of leg distal to its centre of gravity = L_B

Local "member" length = L_1

Therefore Total Force exerted by each member = $\left[\frac{W_B L_1}{L_B}\right]$ 9.81

F = x Newtons

Similarly for Bar and Carriage Sections:

W_{BAR} = Weight of Bar W_C = Weight of Carriage

Therefore $F = \frac{W_B L_1}{L_B} \cdot x \cdot 9.81$ = x Newtons

LOADING DATA:

Force exerted by:

1. Length of bone distal to centre of gravity = 16.8 N
2. The mass of the foot = 9.81N
3. One carriage section = 2.8 N
4. Length of central bar section = .99N

APPENDIX 5.5

DATA DERIVED FOR BONE MODELS THREE AND FOUR (table A)

% bone length	Area mm^2 AX	Effective J IX	Iyy mm^4 IY	Ixx mm^4 IZ
11.9	450	108683.5	47978.5	19387.8
45.95	375	25204.7	22888.7	11255.1
50.23	366	22153.35	20944.1	11211.4
54.5	354	21435.8	19387.7	10995.1
64.76	330	16889.6	14963.1	10000.0
65.7	300	16771.4	13858.6	9528.6
75.9	240	16478.6	11879.6	10080.2
80.2	210	16478.6	10000.0	10824.3
84.5	180	28762.4	10000.0	10824.3
98.8	600.25	79270.0	10000.0	10824.3

Data source: Piezali et al, Miller and Purkey.

DATA FOR 3 ZONES IN MODELS III AND IV (table B)

ZONE	AX	1X	1Y	1Z
1 (0-50 mm)	450	108683.5	47978.5	19387.8
2 (50-272 mm)	365	22931.28	21073.5	11153.9
3 (272-470 mm)	252	19076.0	12140.2	10251.5

PRIME VERSION OF STRESS(3.2) 18/03/1978

INPUT LISTING OF STRESS PROBLEM

STRUCTURE DEN BAR MODEL3
NUMBER OF JOINTS 22
NUMBER OF MEMBERS 25
NUMBER OF SUPPORTS 2
NUMBER OF LOADINGS 1
TYPE SPACE FRAME
JOINT COORDINATES
1 X 0. Y 0. Z 0. S
2 X 50. Y 0. Z 0. S
3 X 193. Y 0. Z 0.
4 X 193. Y 0. Z 56.58
5 X 164. Y 0. Z 56.58
6 X 211. Y 0. Z 56.58
7 X 211. Y 0. Z 0.
8 X 229. Y 0. Z 0.
9 X 272. Y 0. Z 0.
10 X 229. Y 0. Z 56.58
11 X 234. Y 0. Z 56.58
12 X 314. Y 0. Z 56.58
13 X 319. Y 0. Z 56.58
14 X 319. Y 0. Z 0.
15 X 276. Y 0. Z 0.
16 X 337. Y 0. Z 0.
17 X 337. Y 0. Z 56.58
18 X 355. Y 0. Z 56.58
19 X 384. Y 0. Z 56.58
20 X 355. Y 0. Z 0.
21 X 420. Y 0. Z 0.
22 X 480. Y 0. Z 0.
MEMBER INCIDENCES
1 1 2
2 2 3
3 3 7
4 7 8
5 8 9
6 15 14
7 14 16
8 16 20
9 20 21
10 21 22
11 3 4
12 7 6
13 8 10
14 14 13
15 16 17
16 20 18
17 5 4
18 4 6
19 6 10
20 10 11
21 12 13
22 13 17
23 17 18

```
24 18 19
25 11 12
MEMBER PROPERTIES PRISMATIC
1 AX 450. AY 450. AZ 450. IX 108683.5 IY 47978.5 IZ 19387.8
2 THRU 5 AX 365. AY 365. AZ 365. IX 22931.28 IY 21073.5 IZ 11153.9
6 THRU 10 AX 252. AY 252. AZ 252. IX 19076. IY 12140.2 IZ 10251.5
11 THRU 16 AX 10.57 AY 10.57 AZ 10.57 IX 17.8 IY 8.9 IZ 8.9
17 THRU 24 AX 362.9 AY 362.9 AZ 362.9 IX 21949.7 IY 10974.9 IZ 10974.9
25 AX 73.44 AY 73.44 AZ 73.44 IX 858.4 IY 429.2 IZ 429.2
CONSTANTS E 200000. ALL BUT 25000. 1 2 3 4 5 6 7 8 9 10
CONSTANTS E 10000. 17 18 19 20 21 22 23 24
CONSTANTS G 87000. ALL BUT 5500. 1 2 3 4 5 6 7 8 9 10
CONSTANTS G 3745. 17 18 19 20 21 22 23 24
TABULATE ALL
LOADING 1
MEMBER LOADS
6 FORCE Y CONCENTRATED P -2.78 L 21.5
7 FORCE Y CONCENTRATED P -1.16 L 9.
8 FORCE Y CONCENTRATED P -1.16 L 9.
9 FORCE Y CONCENTRATED P -4.18 L 32.5
10 FORCE Y CONCENTRATED P -9.81 L 30.
17 FORCE Y CONCENTRATED P -1.16 L 14.5
18 FORCE Y CONCENTRATED P -0.72 L 9.
19 FORCE Y CONCENTRATED P -0.72 L 9.
20 FORCE Y CONCENTRATED P -0.2 L 2.5
21 FORCE Y CONCENTRATED P -0.2 L 2.5
22 FORCE Y CONCENTRATED P -0.72 L 9.
23 FORCE Y CONCENTRATED P -0.72 L 9.
24 FORCE Y CONCENTRATED P -1.16 L 14.5
25 FORCE Y CONCENTRATED P -0.99 L 40.
SOLVE
1
1
```

STRUCTURE DEN BAR MODEL3

==========

LOADING 1

==========

MEMBER FORCES

MEMB	JOINT	AXIAL FORCE	SHEAR FORCE Y	SHEAR FORCE Z	TORSION MOMENT	MOMENT Y	MOMENT Z
1	1	0.000	0.000	0.000	0.00	0.00	0.00
1	2	0.000	0.000	0.000	0.00	0.00	0.00
2	2	0.000	29.428	0.000	-514.38	0.00	9182.92
2	3	0.000	-29.428	0.000	514.38	0.00	-4974.78
3	3	0.000	77.794	0.000	-1987.45	0.00	4195.67
3	7	0.000	-77.794	0.000	1987.45	0.00	-2795.37
4	7	0.000	68.213	0.000	-1822.49	0.00	2016.62
4	8	0.000	-68.213	0.000	1822.49	0.00	-788.80

5	8	0.000	-0.008	0.000	0.00	0.00	-0.28
5	9	0.000	0.008	0.000	0.00	0.00	-0.06
6	15	0.000	0.154	0.000	0.01	0.00	0.59
6	14	0.000	2.626	0.000	-0.01	0.00	-53.72
7	14	0.000	-12.315	0.000	455.52	0.00	277.68
7	16	0.000	13.475	0.000	-455.52	0.00	-509.79
8	16	0.000	-7.169	0.000	455.66	0.00	726.37
8	20	0.000	8.329	0.000	-455.66	0.00	-865.85
9	20	0.000	14.122	0.000	-0.01	0.00	1082.95
9	21	0.000	-9.942	0.000	0.01	0.00	-300.88
10	21	0.000	9.810	0.000	-0.01	0.00	295.97
10	22	0.000	-0.000	0.000	0.01	0.00	-1.65
11	3	0.000	-48.380	0.000	779.13	0.00	-1473.07
11	4	0.000	48.380	0.000	-779.13	0.00	-1264.25
12	7	0.000	9.530	0.000	778.54	0.00	164.98
12	6	0.000	-9.530	0.000	-778.54	0.00	374.23
13	8	0.000	68.193	0.000	788.82	0.00	1822.49
13	10	0.000	-68.193	0.000	-788.82	0.00	2035.85
14	14	0.000	9.180	0.000	-224.63	0.00	455.61
14	13	0.000	-9.180	0.000	224.63	0.00	63.80
15	16	0.000	-6.712	0.000	-220.01	0.00	0.15
15	17	0.000	6.712	0.000	220.01	0.00	-379.92
16	20	0.000	-22.706	0.000	-219.47	0.00	-455.57
16	18	0.000	22.706	0.000	219.47	0.00	-829.13
17	5	0.000	0.025	0.000	0.00	0.00	0.19
17	4	0.000	1.135	0.000	-0.00	0.00	-16.29
18	4	0.000	-49.661	0.000	-1264.24	0.00	795.32
18	6	0.000	50.381	0.000	1264.24	0.00	-1695.70
19	6	0.000	-40.882	0.000	-890.02	0.00	2474.25
19	10	0.000	41.602	0.000	890.02	0.00	-3216.60
20	10	0.000	26.020	0.000	1145.79	0.00	4003.92
20	11	0.000	-25.820	0.000	-1145.79	0.00	-3874.32
21	12	0.000	23.744	0.000	1145.74	0.00	1833.79
21	13	0.000	-23.544	0.000	-1145.74	0.00	-1715.57
22	13	0.000	32.829	0.000	1209.52	0.00	1490.58
22	17	0.000	-32.109	0.000	-1209.52	0.00	-906.14
23	17	0.000	24.973	0.000	829.63	0.00	683.72
23	18	0.000	-24.253	0.000	-829.63	0.00	-240.69
24	18	0.000	1.172	0.000	0.29	0.00	17.83
24	19	0.000	-0.012	0.000	-0.29	0.00	-0.67
25	11	0.000	25.964	0.000	1145.76	0.00	3874.16
25	12	0.000	-24.974	0.000	-1145.76	0.00	-1836.66

APPLIED JOINT LOADS, FREE JOINTS

JOINT	FORCE X	FORCE Y	FORCE Z	MOMENT X	MOMENT Y	MOMENT Z
3	0.000	-0.013	0.000	-0.00	0.00	0.02
4	0.000	-0.147	0.000	0.00	0.00	-0.09
5	0.000	0.025	0.000	0.00	0.00	0.19
6	0.000	-0.031	0.000	-0.02	0.00	0.00
7	0.000	-0.051	0.000	-0.01	0.00	-0.21
8	0.000	-0.028	0.000	-0.00	0.00	-0.25
9	0.000	0.008	0.000	0.00	0.00	-0.06
10	0.000	-0.571	0.000	-0.03	0.00	-1.50
11	0.000	0.144	0.000	-0.03	0.00	-0.16
12	0.000	-1.229	0.000	-0.02	0.00	-2.87
13	0.000	0.104	0.000	-0.02	0.00	-0.36
14	0.000	-0.509	0.000	-0.10	0.00	-0.67

15	0.000	0.154	0.000	0.01	0.00	0.59
16	0.000	-0.406	0.000	-0.02	0.00	-3.44
17	0.000	-0.424	0.000	0.03	0.00	-2.41
18	0.000	-0.375	0.000	-0.22	0.00	-3.40
19	0.000	-0.012	0.000	-0.29	0.00	-0.67
20	0.000	-0.255	0.000	-0.09	0.00	-2.37
21	0.000	-0.131	0.000	0.00	0.00	-4.91
22	0.000	-0.000	0.000	0.01	0.00	-1.65

REACTIONS,APPLIED LOADS SUPPORT JOINTS

JOINT	FORCE X	FORCE Y	FORCE Z	MOMENT X	MOMENT Y	MOMENT Z
1	0.000	0.000	0.000	0.00	0.00	0.00
2	0.000	29.428	0.000	-514.38	0.00	9182.92

FREE JOINT DISPLACEMENTS

JOINT	X DISPL	Y DISPL	Z DISPL	X-ROTAT	Y-ROTAT	Z-ROTAT
3	0.0000	-0.2874	0.0000	0.0006	0.0000	-0.0036
4	0.0000	0.1867	0.0000	-0.0027	0.0000	-0.0321
5	0.0000	1.1175	0.0000	-0.0027	0.0000	-0.0321
6	0.0000	-0.3919	0.0000	-0.0025	0.0000	-0.0323
7	0.0000	-0.3556	0.0000	0.0009	0.0000	-0.0039
8	0.0000	-0.4265	0.0000	0.0011	0.0000	-0.0039
9	0.0000	-0.5962	0.0000	0.0011	0.0000	-0.0039
10	0.0000	-0.9768	0.0000	-0.0023	0.0000	-0.0328
11	0.0000	-1.1412	0.0000	-0.0023	0.0000	-0.0329
12	0.0000	-3.8960	0.0000	-0.0036	0.0000	-0.0356
13	0.0000	-4.0743	0.0000	-0.0036	0.0000	-0.0357
14	0.0000	-4.3774	0.0000	-0.0099	0.0000	-0.0439
15	0.0000	-2.4904	0.0000	-0.0099	0.0000	-0.0439
16	0.0000	-5.1675	0.0000	-0.0099	0.0000	-0.0439
17	0.0000	-4.7188	0.0000	-0.0039	0.0000	-0.0359
18	0.0000	-5.3657	0.0000	-0.0041	0.0000	-0.0360
19	0.0000	-6.4083	0.0000	-0.0041	0.0000	-0.0360
20	0.0000	-5.9583	0.0000	-0.0100	0.0000	-0.0440
21	0.0000	-8.8234	0.0000	-0.0100	0.0000	-0.0441
22	0.0000	-11.4727	0.0000	-0.0100	0.0000	-0.0442

1

STRUCTURE DEN BAR MODEL3

MEMBER FORCES FOR MEMBER 1

LOAD	JOINT	AXIAL FORCE	SHEAR FORCE Y	SHEAR FORCE Z	TORSION MOMENT	MOMENT Y	MOMENT Z
1	1	0.000	0.000	0.000	0.00	0.00	0.00
1	2	0.000	0.000	0.000	0.00	0.00	0.00

MEMBER FORCES FOR MEMBER 2

LOAD	JOINT	AXIAL FORCE	SHEAR FORCE Y	SHEAR FORCE Z	TORSION MOMENT	MOMENT Y	MOMENT Z
1	2	0.000	29.428	0.000	-514.38	0.00	9182.92
1	3	0.000	-29.428	0.000	514.38	0.00	-4974.78

MEMBER FORCES FOR MEMBER 3

LOAD	JOINT	AXIAL FORCE	SHEAR FORCE Y	SHEAR FORCE Z	TORSION MOMENT	MOMENT Y	MOMENT Z
1	3	0.000	77.794	0.000	-1987.45	0.00	4195.67
1	7	0.000	-77.794	0.000	1987.45	0.00	-2795.37

MEMBER FORCES FOR MEMBER 4

LOAD	JOINT	AXIAL FORCE	SHEAR FORCE Y	SHEAR FORCE Z	TORSION MOMENT	MOMENT Y	MOMENT Z
1	7	0.000	68.213	0.000	-1822.49	0.00	2016.62
1	8	0.000	-68.213	0.000	1822.49	0.00	-788.80

MEMBER FORCES FOR MEMBER 5

LOAD	JOINT	AXIAL FORCE	SHEAR FORCE Y	SHEAR FORCE Z	TORSION MOMENT	MOMENT Y	MOMENT Z
1	8	0.000	-0.008	0.000	0.00	0.00	-0.28
1	9	0.000	0.008	0.000	0.00	0.00	-0.06

MEMBER FORCES FOR MEMBER 6

LOAD	JOINT	AXIAL FORCE	SHEAR FORCE Y	SHEAR FORCE Z	TORSION MOMENT	MOMENT Y	MOMENT Z
1	15	0.000	0.154	0.000	0.01	0.00	0.59
1	14	0.000	2.626	0.000	-0.01	0.00	-53.72

MEMBER FORCES FOR MEMBER 7

LOAD	JOINT	AXIAL FORCE	SHEAR FORCE Y	SHEAR FORCE Z	TORSION MOMENT	MOMENT Y	MOMENT Z
1	14	0.000	-12.315	0.000	455.52	0.00	277.68
1	16	0.000	13.475	0.000	-455.52	0.00	-509.79

MEMBER FORCES FOR MEMBER 8

LOAD	JOINT	AXIAL FORCE	SHEAR FORCE Y	SHEAR FORCE Z	TORSION MOMENT	MOMENT Y	MOMENT Z
1	16	0.000	-7.169	0.000	455.66	0.00	726.37
1	20	0.000	8.329	0.000	-455.66	0.00	-865.85

MEMBER FORCES FOR MEMBER 9

LOAD	JOINT	AXIAL FORCE	SHEAR FORCE Y	SHEAR FORCE Z	TORSION MOMENT	MOMENT Y	MOMENT Z
1	20	0.000	14.122	0.000	-0.01	0.00	1082.95
1	21	0.000	-9.942	0.000	0.01	0.00	-300.88

MEMBER FORCES FOR MEMBER 10

LOAD	JOINT	AXIAL FORCE	SHEAR FORCE Y	SHEAR FORCE Z	TORSION MOMENT	MOMENT Y	MOMENT Z
1	21	0.000	9.810	0.000	-0.01	0.00	295.97
1	22	0.000	-0.000	0.000	0.01	0.00	-1.65

MEMBER FORCES FOR MEMBER 11

LOAD	JOINT	AXIAL FORCE	SHEAR FORCE Y	SHEAR FORCE Z	TORSION MOMENT	MOMENT Y	MOMENT Z
1	3	0.000	-48.380	0.000	779.13	0.00	-1473.07
1	4	0.000	48.380	0.000	-779.13	0.00	-1264.25

MEMBER FORCES FOR MEMBER 12

LOAD	JOINT	AXIAL FORCE	SHEAR FORCE Y	SHEAR FORCE Z	TORSION MOMENT	MOMENT Y	MOMENT Z
1	7	0.000	9.530	0.000	778.54	0.00	164.98
1	6	0.000	-9.530	0.000	-778.54	0.00	374.23

MEMBER FORCES FOR MEMBER 13

LOAD	JOINT	AXIAL FORCE	SHEAR FORCE Y	SHEAR FORCE Z	TORSION MOMENT	MOMENT Y	MOMENT Z
1	8	0.000	68.193	0.000	788.82	0.00	1822.49
1	10	0.000	-68.193	0.000	-788.82	0.00	2035.85

MEMBER FORCES FOR MEMBER 14

LOAD	JOINT	AXIAL FORCE	SHEAR FORCE Y	SHEAR FORCE Z	TORSION MOMENT	MOMENT Y	MOMENT Z
1	14	0.000	9.180	0.000	-224.63	0.00	455.61
1	13	0.000	-9.180	0.000	224.63	0.00	63.80

MEMBER FORCES FOR MEMBER 15

LOAD	JOINT	AXIAL FORCE	SHEAR FORCE Y	SHEAR FORCE Z	TORSION MOMENT	MOMENT Y	MOMENT Z
1	16	0.000	-6.712	0.000	-220.01	0.00	0.15
1	17	0.000	6.712	0.000	220.01	0.00	-379.92

MEMBER FORCES FOR MEMBER 16

LOAD	JOINT	AXIAL FORCE	SHEAR FORCE Y	SHEAR FORCE Z	TORSION MOMENT	MOMENT Y	MOMENT Z
1	20	0.000	-22.706	0.000	-219.47	0.00	-455.57
1	18	0.000	22.706	0.000	219.47	0.00	-829.13

MEMBER FORCES FOR MEMBER 17

LOAD	JOINT	AXIAL FORCE	SHEAR FORCE Y	SHEAR FORCE Z	TORSION MOMENT	MOMENT Y	MOMENT Z
1	5	0.000	0.025	0.000	0.00	0.00	0.19
1	4	0.000	1.135	0.000	-0.00	0.00	-16.29

MEMBER FORCES FOR MEMBER 18

LOAD	JOINT	AXIAL FORCE	SHEAR FORCE Y	SHEAR FORCE Z	TORSION MOMENT	MOMENT Y	MOMENT Z
1	4	0.000	-49.661	0.000	-1264.24	0.00	795.32
1	6	0.000	50.381	0.000	1264.24	0.00	-1695.70

MEMBER FORCES FOR MEMBER 19

LOAD	JOINT	AXIAL FORCE	SHEAR FORCE Y	SHEAR FORCE Z	TORSION MOMENT	MOMENT Y	MOMENT Z
1	6	0.000	-40.882	0.000	-890.02	0.00	2474.25
1	10	0.000	41.602	0.000	890.02	0.00	-3216.60

MEMBER FORCES FOR MEMBER 20

LOAD	JOINT	AXIAL FORCE	SHEAR FORCE Y	SHEAR FORCE Z	TORSION MOMENT	MOMENT Y	MOMENT Z
1	10	0.000	26.020	0.000	1145.79	0.00	4003.92
1	11	0.000	-25.820	0.000	-1145.79	0.00	-3874.32

MEMBER FORCES FOR MEMBER 21

LOAD	JOINT	AXIAL FORCE	SHEAR FORCE Y	SHEAR FORCE Z	TORSION MOMENT	MOMENT Y	MOMENT Z
1	12	0.000	23.744	0.000	1145.74	0.00	1833.79
1	13	0.000	-23.544	0.000	-1145.74	0.00	-1715.57

MEMBER FORCES FOR MEMBER 22

LOAD	JOINT	AXIAL FORCE	SHEAR FORCE Y	SHEAR FORCE Z	TORSION MOMENT	MOMENT Y	MOMENT Z
1	13	0.000	32.829	0.000	1209.52	0.00	1490.58
1	17	0.000	-32.109	0.000	-1209.52	0.00	-906.14

MEMBER FORCES FOR MEMBER 23

LOAD	JOINT	AXIAL FORCE	SHEAR FORCE Y	SHEAR FORCE Z	TORSION MOMENT	MOMENT Y	MOMENT Z
1	17	0.000	24.973	0.000	829.63	0.00	683.72
1	18	0.000	-24.253	0.000	-829.63	0.00	-240.69

MEMBER FORCES FOR MEMBER 24

LOAD	JOINT	AXIAL FORCE	SHEAR FORCE Y	SHEAR FORCE Z	TORSION MOMENT	MOMENT Y	MOMENT Z
1	18	0.000	1.172	0.000	0.29	0.00	17.83
1	19	0.000	-0.012	0.000	-0.29	0.00	-0.67

MEMBER FORCES FOR MEMBER 25

LOAD	JOINT	AXIAL FORCE	SHEAR FORCE Y	SHEAR FORCE Z	TORSION MOMENT	MOMENT Y	MOMENT Z
1	11	0.000	25.964	0.000	1145.76	0.00	3874.16
1	12	0.000	-24.974	0.000	-1145.76	0.00	-1836.66

APPENDIX 5.6.a

INPUT DATA FOR PIN DIAMETER

CORE DIAMETER	X - SECTIONAL AREA	SHEAR AREA		TORSIONAL CONSTANT J	MOMENT OF INERTIA	MOMENT OF INERTIA
	AX	AY	AZ	1X	1X	1Y
3.67	10.57	10.57	10.57	17.8	8.9	8.9
3.87	11.76	11.76	11.76	22.02	11.0	11.0
3.97	12.37	12.37	12.37	24.4	12.19	12.19
4.1	13.2	13.2	13.2	27.74	13.9	13.9
4.3	14.5	14.5	14.5	33.56	16.78	16.78
4.5	15.9	15.9	15.9	40.25	20.12	20.12
4.8	17.8	17.8	17.8	50.8	25.4	25.4

Pin Diamter Changes for Models II, III, and IV.

APPENDIX 5.6.b

PIN ORIENTATION DATA MODIFICATION FOR TEST 2

Co-ordinate Changes Models II and III

3	x	167	YO:	ZO
4	x	167	YO.	Z56.58
5	x	164	YO.	Z56.58
6	x	198	YO.	Z56.58
7	x	198	YO.	ZO
8	x	229	YO.	ZO
9	x	272	YO.	ZO
10	x	229	YO.	Z56.58
11	x	234	YO.	Z56.58
12	x	314	YO.	Z56.58
13	x	319	YO.	Z56.58
14	x	319	YO.	ZO
15	x	276	YO.	ZO
16	x	350	YO.	ZO
17	x	350	YO.	Z56.58
18	x	381	YO.	Z56.58
19	x	384	YO.	Z56.58
20	x	381	YO.	ZO

Model IV

3	x	102	YO.	ZO
4	x	102	YO.	Z56.58
5	x	99	YO.	Z56.58
6	x	133	YO.	Z56.58
7	x	133	YO.	ZO
8	x	164	YO.	ZO
9	x	207	YO.	ZO
10	x	164	YO.	Z56.58
11	x	169	YO.	Z56.58
12	x	249	YO.	Z56.58
13	x	254	YO.	Z56.58
14	x	254	YO.	ZO
15	x	211	YO.	ZO

APPENDIX 5.6.b continued

Model IV

16 x 285 YO. ZO
17 x 285 YO. Z56.58
18 x 316 YO. Z56.58
19 x 319 YO. Z56.58
20 x 316 YO. ZO

Revised data for local member forces Models II, III and IV, Test 2

7	FORCE	Y	CONCENTRATED	P - 2.	L 15.5
8	FORCE	Y	CONCENTRATED	P - 2.	L 15.5
*9	FORCE	Y	CONCENTRATED	P - 2.52	L 19.5
17	FORCE	Y	CONCENTRATED	P - 0.13	L 1.5
18	FORCE	Y	CONCENTRATED	P - 1.23	L 15.5
19	FORCE	Y	CONCENTRATED	P - 1.23	L 15.5
20	FORCE	Y	CONCENTRATED	P - .16	L 2.5
21	FORCE	Y	CONCENTRATED	P - .16	L 2.5
22	FORCE	Y	CONCENTRATED	P - 1.23	L 15.5
23	FORCE	Y	CONCENTRATED	P - 1.23	L 15.5
24	FORCE	Y	CONCENTRATED	P - 0.13	L 1.5

* Models II and III only. Model IV 9 FORCE Y CONCENTRATED P - 6.9 L 52

APPENDIX 5.6.b

PIN ORIENTATION DATA MODIFICATION FOR TEST 3

Co-ordinate Changes Models II and III

3	x	180	YO.	ZO
4	x	180	YO.	Z56.58
6	x	198	YO.	Z56.58
7	x	198	YO.	ZO
18	x	368	YO.	Z56.58
20	x	368	YO.	ZO

Model IV

3	x	115	YO.	ZO
4	x	115	YO.	Z56.58
6	x	133	YO.	Z56.58
7	x	133	YO.	ZO
18	x	303	YO.	Z56.58
20	x	303	YO.	ZO

Local Member Forces

8	FORCE	Y	CONCENTRATED	P - 2.	L	15.5
*9	FORCE	Y	CONCENTRATED	P - 3.35	L	26.
17	FORCE	Y	CONCENTRATED	P - 0.64	L	8.
19	FORCE	Y	CONCENTRATED	P - 1.23	L	15.5
23	FORCE	Y	CONCENTRATED	P - 1.23	L	15.5
24	FORCE	Y	CONCENTRATED	P - 0.64	L	8.

* Models II and III only. Model IV 9 FORCE Y CONCENTRATED P - 7.6 L 58.5

APPENDIX 5.6.b.

PIN ORIENTATION DATA MODIFICATION FOR TEST 4

Co-ordinate Changes : Models II and III

3	x	185	YO.	ZO
4	x	189	YO.	Z56.58
5	x	164	YO.	Z56.58
6	x	207	YO.	Z56.58
7	x	207	YO.	ZO
10	x	225	YO.	Z56.58
13	x	323	YO.	Z56.58
16	x	341	YO.	ZO
17	x	341	YO.	Z56.58
18	x	359	YO.	Z56.58
19	x	384	YO.	Z56.58
20	x	363	YO.	ZO

Model IV

3	x	120	YO.	ZO
4	x	124	YO.	Z56.58
5	x	99	YO.	Z56.58
6	x	142	YO.	Z56.58
7	x	142	YO.	ZO
10	x	160	YO.	Z56.58
13	x	258	YO.	Z56.58
16	x	276	YO.	ZO
17	x	276	YO.	Z56.58
18	x	294	YO.	Z56.58
19	x	319	YO.	Z56.58
20	x	298	YO.	ZO

APPENDIX 5.6.b.

PIN ORIENTATION DATA MODIFICATION FOR TEST 4

Local Member Forces : Models II, III and IV

7	FORCE	Y	CONCENTRATED	P - 1.42	L 11.
8	FORCE	Y	CONCENTRATED	P - 1.42	L 11.
*9	FORCE	Y	CONCENTRATED	P - 3.7	L 28.5
17	FORCE	Y	CONCENTRATED	P - 1.1	L 12.5
20	FORCE	Y	CONCENTRATED	P - 0.4	L 4.5
21	FORCE	Y	CONCENTRATED	P - 0.4	L 4.5
24	FORCE	Y	CONCENTRATED	P - 1.1	L 12.5

* Models II and III only. Model IV 9 FORCE Y CONCENTRATED P - 7.9 L 61.

APPENDIX 5.6.b.

PIN ORIENTATION DATA MODIFICATION FOR TEST 5

Models II and III

4 x 189 YO. Z56.58
5 x 154 YO. Z56.58
6 x 211 YO. Z56.58
10 x 233 YO. Z56.58
11 x 234 YO. Z56.58
12 x 314 YO. Z56.58
13 x 315 YO. Z56.58
18 x 359 YO. Z56.58
19 x 384 YO. Z56.58
20 x 355 YO. ZO

Model IV

4 x 124 YO. Z56.58
5 x 99 YO. Z56.58
6 x 146 YO. Z56.58
10 x 168 YO. Z56.58
11 x 169 YO. Z56.58
12 x 249 YO. Z56.58
13 x 250 YO. Z56.58
18 x 294 YO. Z56.58
19 x 319 YO. Z56.58
20 x 290 YO. ZO

APPENDIX 5.6.b.

PIN ORIENTATION DATA MODIFICATION FOR TEST 5

Local member forces : Models II, III and IV

17	FORCE	Y	CONCENTRATED	P	-	1.1	L 12.5
18	FORCE	Y	CONCENTRATED	P	-	0.9	L 11.
19	FORCE	Y	CONCENTRATED	P	-	0.9	L 11.
20	FORCE	Y	CONCENTRATED	P	-	0.04	L 0.5
21	FORCE	Y	CONCENTRATED	P	-	0.04	L 0.5
22	FORCE	Y	CONCENTRATED	P	-	0.9	L 11.
23	FORCE	Y	CONCENTRATED	P	-	0.9	L 11.
24	FORCE	Y	CONCENTRATED	P	-	1.1	L 12.5

APPENDIX 5.6.b.

PIN ORIENTATION DATA MODIFICATION FOR TEST 6

Co-ordinate changes - Models II and III

3	x	167	YO.	ZO
4	x	167	YO.	Z56.58
5	x	164	YO.	Z56.58
6	x	204	YO.	Z56.58
7	x	198	YO.	ZO
8	x	229	YO.	ZO
10	x	204	YO.	Z56.58
11	x	222	YO.	Z56.58
13	x	326	YO.	Z56.58
14	x	319	YO.	ZO
16	x	350	YO.	ZO
17	x	344	YO.	Z56.58
18	x	381	YO.	Z56.58
19	x	384	YO.	Z56.58
20	x	381	YO.	Z56.58

Model IV

3	x	102	YO.	ZO
4	x	102	YO.	Z56.58
5	x	99	YO.	Z56.58
6	x	139	YO.	Z56.58
7	x	133	YO.	ZO
8	x	164	YO.	ZO
9	x	207	YO.	ZO
10	x	157	YO.	ZO
11	x	169	YO.	Z56.58
12	x	249	YO.	Z56.58
13	x	261	YO.	Z56.58
14	x	254	YO.	ZO
15	x	211	YO.	ZO
16	x	285	YO.	ZO
17	x	279	YO.	Z56.58
18	x	316	YO.	Z56.58
19	x	319	YO.	Z56.58
20	x	316	YO.	ZO

APPENDIX 5.6.*b*.

PIN ORIENTATION DATA MODIFICATION TEST 6

Local member forces : Models II, III and IV

7	FORCE	Y	CONCENTRATED	P	-	2.0	L 15.5
8	FORCE	Y	CONCENTRATED	P	-	2.0	L 15.5
*9	FORCE	Y	CONCENTRATED	P	-	2.52	L 19.5
17	FORCE	Y	CONCENTRATED	P	-	0.1	L 1.5
18	FORCE	Y	CONCENTRATED	P	-	1.48	L 18.5
19	FORCE	Y	CONCENTRATED	P	-	0.72	L 9.
20	FORCE	Y	CONCENTRATED	P	-	0.48	L 6.
21	FORCE	Y	CONCENTRATED	P	-	0.48	L 6.
22	FORCE	Y	CONCENTRATED	P	-	0.72	L 9.
23	FORCE	Y	CONCENTRATED	P	-	1.48	L 18.5
24	FORCE	Y	CONCENTRATED	P	-	0.1	L 1.5

* Models II and III only. Model IV 9 FORCE Y CONCENTRATED P - 6.71 L 52

APPENDIX 5.6.C

INPUT DATA : PIN OFFSET FROM FRACTURE SITE

Co-ordinate Changes for Test 2 - Models II and III

3	x	176	YO.	ZO
4	x	176	YO.	Z56.58
5	x	147	YO.	Z56.58
6	x	194	YO.	Z56.58
7	x	194	YO.	ZO
8	x	212	YO.	ZO
9	x	272	YO.	ZO
10	x	212	YO.	Z56.58
11	x	217	YO.	Z56.58
12	x	331	YO.	Z56.58
13	x	336	YO.	Z56.58
14	x	336	YO.	ZO
15	x	276	YO.	ZO
16	x	354	YO.	ZO
17	x	354	YO.	Z56.58
18	x	372	YO.	Z56.58
19	x	401	YO.	Z56.58
20	x	372	YO.	ZO

Model IV

3	x	111	YO.	ZO
4	x	111	YO.	Z56.58
5	x	82	YO.	Z56.58
6	x	129	YO.	Z56.58
7	x	129	YO.	ZO
8	x	147	YO.	ZO
9	x	207	YO.	ZO
10	x	147	YO.	Z56.58
11	x	152	YO.	Z56.58
12	x	266	YO.	Z56.58
13	x	271	YO.	Z56.58
14	x	271	YO.	ZO
15	x	211	YO.	ZO
16	x	289	YO.	ZO
17	x	289	YO.	Z56.58
18	x	307	YO.	Z56.58
19	x	336	YO.	Z56.58
20	x	307	YO.	ZO

APPENDIX 5.6.c

INPUT DATA : PIN OFFSET FROM FRACTURE SITE

Co-ordinate Changes for Test 3 - Models II and III

3	x	176	YO.	ZO
4	x	176	YO.	Z56.58
5	x	147	YO.	Z56.58
6	x	194	YO.	Z56.58
7	x	194	YO.	ZO
8	x	212	YO.	ZO
9	x	272	YO.	ZO
10	x	212	YO.	Z56.58
11	x	217	YO.	Z56.58

Model IV

3	x	128	YO.	ZO
4	x	128	YO.	Z56.58
5	x	99	YO.	Z56.58
6	x	146	YO.	Z56.58
7	x	146	YO.	ZO
8	x	164	YO.	ZO
9	x	207	YO.	ZO
10	x	164	YO.	Z56.58
11	x	169	YO.	Z56.58

APPENDIX 5.6.c

INPUT DATA : PIN OFFSET FROM FRACTURE SITE

Co-ordinate Changes for Test 4 - Models II and III

12 x 331 YO. Z56.58
13 x 336 YO. Z56.58
14 x 336 YO. ZO
15 x 276 YO. ZO
16 x 354 YO. ZO
17 x 354 YO. Z56.58
18 x 372 YO. Z56.58
19 x 401 YO. Z56.58
20 x 372 YO. ZO
21 x 420 YO. ZO
22 x 480 YO. ZO

Model IV

12 x 266 YO. Z56.58
13 x 271 YO. Z56.58
14 x 271 YO. ZO
15 x 211 YO. ZO
16 x 289 YO. ZO
17 x 289 YO. Z56.58
18 x 307 YO. Z56.58
19 x 336 YO. Z56.58
20 x 307 YO. ZO
21 x 420 YO. ZO
22 x 480 YO. ZO

APPENDIX 5.6.c

INPUT DATA : PIN OFFSET FROM FRACTURE SITE

Change in local member forces, Tests 2 and 3.

TEST 2 : MODELS II, III and IV

6	FORCE	Y	CONCENTRATED	P - 3.88	L 30.
*9	FORCE	Y	CONCENTRATED	P - 3.10	L 24.
17	FORCE	Y	CONCENTRATED	P - 1.07	L 14.5
18	FORCE	Y	CONCENTRATED	P - 0.66	L 9.
19	FORCE	Y	CONCENTRATED	P - 0.66	L 9.
20	FORCE	Y	CONCENTRATED	P - 0.18	L 2.5
21	FORCE	Y	CONCENTRATED	P - 0.18	L 2.5
22	FORCE	Y	CONCENTRATED	P - 0.66	L 9.
23	FORCE	Y	CONCENTRATED	P - 0.66	L 9.
24	FORCE	Y	CONCENTRATED	P - 1.07	L 14.5
25	FORCE	Y	CONCENTRATED	P - 1.4	L 57.

* Models II and III only. Model IV 9 FORCE Y CONCENTRATED P - 4.59 L 58.5

TEST 3 : MODELS II, III and IV

6	FORCE	Y	CONCENTRATED	P - 2.78	L 21.5
*9	FORCE	Y	CONCENTRATED	P - 1.18	L 32.5
17	FORCE	Y	CONCENTRATED	P - 1.11	L 14.5
18	FORCE	Y	CONCENTRATED	P - 0.69	L 9.
19	FORCE	Y	CONCENTRATED	P - 0.69	L 9.
20	FORCE	Y	CONCENTRATED	P - 0.19	L 2.5
21	FORCE	Y	CONCENTRATED	P - 0.19	L 2.5
22	FORCE	Y	CONCENTRATED	P - 0.69	L 9.
23	FORCE	Y	CONCENTRATED	P - 0.69	L 9.
24	FORCE	Y	CONCENTRATED	P - 1.11	L 14.5
25	FORCE	Y	CONCENTRATED	P - 1.2	L 48.5

*Models II and III only. Model IV 9 FORCE Y CONCENTRATED P - 8.38 L 65.

APPENDIX 5.6.c

INPUT DATA : PIN OFFSET FROM FRACTURE SITE

Change in local member forces , Test 4

MODELS II, III and IV

6	FORCE	Y	CONCENTRATED	P - 3.88	L	30.
*9	FORCE	Y	CONCENTRATED	P - 3.10	L	24.
17	FORCE	Y	CONCENTRATED	P - 1.11	L	14.5
18	FORCE	Y	CONCENTRATED	P - 0.69	L	9.
19	FORCE	Y	CONCENTRATED	P - 0.69	L	9.
20	FORCE	Y	CONCENTRATED	P - 0.19	L	2.5
21	FORCE	Y	CONCENTRATED	P - 0.19	L	2.5
22	FORCE	Y	CONCENTRATED	P - 0.69	L	9.
23	FORCE	Y	CONCENTRATED	P - 0.69	L	9.
24	FORCE	Y	CONCENTRATED	P - 1.11	L	14.5
25	FORCE	Y	CONCENTRATED	P - 1.2	L	48.5

* Models II and III only. Model IV 9 FORCE Y CONCENTRATED P - 4.59 L 65.

APPENDIX 5.6.d.

INPUT DATA FOR THE CHANGE IN MEMBER PROPERTIES OF THE FIXATOR BAR - SERIES A

a) The Fixator Bar

b) The Acrylic Sections

a) The Fixator Bar

Test No.	Bar Ø mm	Area ax_2 mm^2	Shear Area ay/az mm^2	J IX_4 mm^4	I IY/IZ mm^4
1	9.0	63.6	63.6	644.12	322.1
2	9.67	73.44	73.44	585.4	429.2
3	10.63	88.7	88.7	1253.5	626.8
4	11.6	105.7	105.7	1777.6	888.8
5	12.6	124.1	124.1	2451.0	1225.0
6	15.0	176.7	176.7	4970.1	2485.1

b) Carriage Sections

Test No.	1 mm	Area ax mm^2	Shear Area ay/az mm^2	J IX mm^4	I IY/IZ mm^4
1	17.7	314.6	314.6	16498.7	8249.3
2	19.0	362.9	362.9	21949.7	10974.9
3	20.9	438.4	438.4	32029.9	16015.0
4	22.8	522.2	522.2	45451.1	22725.5
5	24.7	613.3	613.3	62689.7	31344.8
6	29.5	870.96	870.96	126428.0	63214.3

APPENDIX 5.6.d.

INPUT DATA FOR VARIABLE CROSS-SECTION OF FIXATOR BAR - SERIES C

1) Solid circular cross section Ø 15 mm.

2) Circular tube D 15 mm d 13 mm

3) Square tube L 15 mm l 13 mm

Table x : Member forces - Acrylic and Bar sections Nm.

Test No.	17	18	19	20	21	22	23	24	25
1	2.8	1.73	1.73	0.48	0.48	1.73	1.73	2.8	2.4
2	0.7	0.43	0.43	0.12	0.12	0.43	0.43	0.7	0.59
3	0.88	0.55	0.55	0.15	0.15	0.55	0.55	0.88	0.75

Table y : Member Properties for Acrylic and Bar sections

Test No.	Bar Dimensions	Area Ax mm^2	Shear Area Ay/Az mm^2	J Ix mm^4	I Iy/Iz mm^4
1	Ø = 15 mm	176.7	176.7	4970.1	2485.1
2	D=15mm d=13mm	43.98	43.98	2166.1	1083.1
3	L=15mm l=15mm	56.0	56.0	3677.3	1838.7
	Dimensions of Acrylic				
1	29.5	871.0	871.0	126428.0	63214.3
2	29.5	871.0	871.0	126428.0	63214.3
3	33.3	1112.0	1112.0	206053.0	103026.0

APPENDIX 5.6.d.

INPUT DATA FOR CHANGES IN LENGTH OF FIXATOR BAR (SERIES C)

Test 2 : Co-ordinate changes Models II and III

10 x 207 YO. Z56.58
11 x 212 YO. Z56.58
12 x 336 YO. Z56.58
13 x 341 YO. Z56.58

Model IV

10 x 142 YO. Z56.58
11 x 147 YO. Z56.58
12 x 271 YO. Z56.58
13 x 276 YO. Z56.58

Changes in local forces of acrylic and bar sections

Models II, III and IV

17 FORCE Y CONCENTRATED P - 0.84 L 14.5
18 FORCE Y CONCENTRATED P - 0.52 L 9.
19 FORCE Y CONCENTRATED P - 0.38 L 6.5
20 FORCE Y CONCENTRATED P - 0.15 L 2.5
21 FORCE Y CONCENTRATED P - 0.15 L 2.5
22 FORCE Y CONCENTRATED P - 0.38 L 6.5
23 FORCE Y CONCENTRATED P - 0.52 L 9.
24 FORCE Y CONCENTRATED P - 0.84 L 14.5
25 FORCE Y CONCENTRATED P - 1.54 L 62

APPENDIX 5.6.d.

INPUT DATA FOR LENGTH OF BAR : TEST 2

(Data modified from Test 1 Appendix

Co-ordinate Changes - Models II and III

10 x 207 YO. Z56.58
11 x 212 YO. Z56.58
12 x 336 YO. Z56.58
13 x 341 YO. Z56.58

Model IV

10 x 142 YO. Z56.58
11 x 147 YO. Z56.58
12 x 271 YO. Z56.58
13 x 276 YO. Z56.58

Member Forces

17 FORCE Y CONCENTRATED P - 0.84 L 14.5
18 FORCE Y CONCENTRATED P - 0.52 L 9.
19 FORCE Y CONCENTRATED P - 0.38 L 6.5
20 FORCE Y CONCENTRATED P - 0.15 L 2.5
21 FORCE Y CONCENTRATED P - 0.15 L 2.5
22 FORCE Y CONCENTRATED P - 0.38 L 6.5
23 FORCE Y CONCENTRATED P - 0.52 L 9.
24 FORCE Y CONCENTRATED P - 0.84 L 14.5
25 FORCE Y CONCENTRATED P - 1.54 L 62.

APPENDIX 5.6.d.

INPUT DATA FOR THE CHANGES IN MEMBER FORCES DUE TO THE INCREASE IN FIXATOR BAR LENGTH

Change in force for members 17 - 25 - carriage and bar sections .

Test No.	17	18	19	20	21	22	23	24	25
1	1.0	0.62	0.62	0.17	0.17	0.62	0.62	1.0	0.86
2	1.16	0.72	0.72	0.20	0.20	0.72	0.72	1.16	0.99
3	1.40	0.87	0.87	0.24	0.24	0.87	0.87	1.4	1.2
4	1.67	1.04	1.04	0.29	0.29	1.04	1.04	1.67	1.43
5	1.96	1.22	1.22	0.34	0.34	1.22	1.22	1.96	1.67
6	2.8	1.73	1.73	0.48	0.48	1.73	1.73	2.8	2.4

APPENDIX 5.6.e.

MODIFIED INPUT DATA

Model III. Compression Tests

Test 2 : Joint Loads

```
12  FORCE  X  1962
19  FORCE  X  1962
```

Test 3 : Joint Loads

```
11  FORCE  X  1962
12  FORCE  X  1962
```

Test 4 : Member Loads

```
11  FORCE  X  CONCENTRATED  P - 6.54  L 55.
12  FORCE  X  CONCENTRATED  P - 6.54  L 55.
13  FORCE  X  CONCENTRATED  P - 6.54  L 55.
14  FORCE  X  CONCENTRATED  P - 6.54  L 55.
15  FORCE  X  CONCENTRATED  P - 6.54  L 55.
16  FORCE  X  CONCENTRATED  P - 6.54  L 55.
```

Test 5 : Joint Loads

```
 5  FORCE  X  1962
19  FORCE  X  1962
```

Test 6 : Functional Loading

```
22  FORCE  X  367.8
```

APPENDIX 5.6.F

INPUT DATA : PERCENTAGE CHANGES IN THE VALUES OF THE ELASTIC MODULI FOR HEALING BONE

N	E_{N/mm^2}	G_{N/mm^2}
100.0 %	25000	5700
75.0 %	18750	4125
50.0 %	12500	2750
25.0 %	6250	1375
1.0 %	250	55
.1 %	25	5.5
.01%	2.5	.55

NB: E = Fibrocartilage 72.5 N/mm^2

E = Wet Hyaline Cartilage 490 N/mm^2

APPENDIX 5.6.f.

INPUT DATA FOR CALLUS TYPES 1, 2 and 3

Table

Type	D mm	d mm	Ax/Ay/Az mm^2	1X mm^4	1Y mm^4	1Z mm^4
1	27.5	24.5	122.7	20775	10387.6	10387.6
2	-	-	365	2293128	21073.5	11153.9
3	36	27.5	419.6	107927	53963	53963

xx Models 3 and 4 only

Modifications to the heading statements for callus types 1, 2 and 3

Number of members 26

Member incidences

26 9 15

Member forces

26 FORCE Y CONCENTRATED P - 0.26 L 2

Member Properties

CONSTANTS E 25000 26

CONSTANTS G 5700 26

Model 2

26 AX 230.9 AY 230.9 AZ 230.9 1X 26164.0 1Y 13082.3 1Z 13082.3

APPENDIX 5.6.g.

DATA MODIFICATION FOR A CHANGE IN POSITION OF THE LIMB MEMBER FORCES

Position B : Standing

17 FORCE X CONCENTRATED P 1.16 L 14.5
18 FORCE X CONCENTRATED P 0.72 L 9.
19 FORCE X CONCENTRATED P 0.72 L 9.
20 FORCE X CONCENTRATED P 0.2 L 2.5
21 FORCE X CONCENTRATED P 0.2 L 2.5
22 FORCE X CONCENTRATED P 0.72 L 9.
23 FORCE X CONCENTRATED P 0.72 L 9.
24 FORCE X CONCENTRATED P 1.16 L 14.5
25 FORCE X CONCENTRATED P 0.99 L 40

JOINT LOADS

22 FORCE X - 367.8

Position D : High sitting

6 FORCE X CONCENTRATED P 2.78 L 21.5
7 FORCE X CONCENTRATED P 1.16 L 9.
8 FORCE X CONCENTRATED P 1.16 L 9.
*9 FORCE X CONCENTRATED P 4.18 L 32.3
10 FORCE X CONCENTRATED P 9.81 L 30.
17 FORCE X CONCENTRATED P 1.16 L 14.5
18 FORCE X CONCENTRATED P 0.72 L 9.
19 FORCE X CONCENTRATED P 0.72 L 9.
20 FORCE X CONCENTRATED P 0.2 L 2.5
21 FORCE X CONCENTRATED P 0.2 L 2.5
22 FORCE X CONCENTRATED P 0.72 L 9.
23 FORCE X CONCENTRATED P 0.72 L 9.
24 FORCE X CONCENTRATED P 1.16 L 14.5
25 FORCE X CONCENTRATED P 0.99 L 40.

* Models 2 and 3 only. Model 4 9 FORCE X CONCENTRATED P 8.38 L 65

APPENDIX 5.6.g.

DATA MODIFICATION FOR A CHANGE IN THE POSITION OF THE LIMB

Position C. Side Lying

Models II and III

4	x	193.	Y -	56.58	ZO.
5	x	164.	Y -	56.58	ZO.
6	x	211.	Y -	56.58	ZO.
10	x	229.	Y -	56.58	ZO.
11	x	234.	Y -	56.58	ZO.
12	x	314.	Y -	56.58	ZO.
13	x	319.	Y -	56.58	ZO.
17	x	337.	Y -	56.58	ZO.
18	x	355.	Y -	56.58	ZO.
19	x	384.	Y -	56.58	ZO.

Model IV

4	x	128.	Y -	56.58	ZO.
5	x	99.	Y -	56.58	ZO.
6	x	146.	Y -	56.58	ZO.
10	x	164.	Y -	56.58	ZO.
11	x	169.	Y -	56.58	ZO.
12	x	249.	Y -	56.58	ZO.
13	x	254.	Y -	56.58	ZO.
17	x	272.	Y -	56.58	ZO.
18	x	290.	Y -	56.58	ZO.
19	x	319.	Y -	56.58	ZO.

APPENDIX 5.6.h.

DATA MODIFICATION FOR INTACT BONE SUBJECT TO AXIAL LOADING IN TENSION AND COMPRESSION

Number of Members: 26

Member incidences:

26 9 15

Member properties (Model II only):

26 AX 230.9 AY 230.9 AZ 230.9 1X 26164.7 1Y 13082.3 1Z 13082.3

Models III and IV:

26 AX 365.0 AY 365.0 AZ 365.0 1X 2293128 1Y 21073.5 1Z 11153.9

APPENDIX 5.7.a.

RESULTS: THE ANALYSIS OF FRACTURE SITE MOTION WITH VARIABLE PIN DIAMETER

(* Relative rotation and displacement between fracture ends)

MODEL	PIN CORE Ø mm	DISPLACEMENT (mm)* X	Y	Z	ROTATION (degress) * X axis	Y axis	Z axis
2	3.67	0	-1.9	0	- .63	0	-2.29
	3.87	0	-1.53	0	- .52	0	-1.87
	3.97	0	-1.37	0	- .47	0	-1.68
	4.10	0	-1.2	0	- .43	0	-1.5
	4.30	0	-1.0	0	- .37	0	-1.26
	4.50	0	- .88	0	- .33	0	-1.1
	4.80	0	- .7	0	- .28	0	- .91
3	3.67	0	-1.89	0	- .63	0	-2.29
	3.87	0	-1.5476	0	- .52	0	-1.89
	3.97	0	-1.3785	0	- .48	0	-1.69
	4.10	0	-1.2278	0	- .44	0	-1.5
	4.30	0	1.027	0	.36	0	1.28
	4.50	0	-0.8788	0	- .32	0	-1.1
	4.80	0	.716	0	- .28	0	- .91
4	3.67	0	-2.32	0	- .8	0	-3.5
	3.87	0	-1.8689	0	- .66	0	-2.84
	3.97	0	-1.6851	0	- .60	0	2.5
	4.10	0	-1.4704	0	- .56	0	-2.28
	4.30	0	1.26	0	.49	0	2.0
	4.50	0	1.08	0	.43	0	1.7
	4.80	0	.87	0	.37	0	1.4

APPENDIX 5.7.b.

RESULTS: THE ANALYSIS OF FRACTURE SITE MOTION WITH VARIABLE PIN LENGTH

MODEL	PIN LENGTH mm	DISPLACEMENT (mm) X	Y	Z	ROTATION (degrees) X	Y	Z
2	40	0	- .84	0	- .33	0	-1.16
	50	0	-1.42	0	- .55	0	-1.8
	56.58	0	-1.9	0	- .63	0	-2.29
	60	0	-2.1	0	- .7	0	-2.52
	73.55	0	-3.3	0	-1.05	0	-3.6
3	40	0	- .8512	0	.33	0	-1.18
	50	0	-1.4185	0	- .51	0	1.8
	56.58	0	-1.89	0	- .63	0	-2.29
	60	0	-2.11	0	- .7	0	-2.52
	73.55	0	3.45	0	-1.01	0	3.73
4	40	0	-1.02	0	.42	0	1.77
	50	0	-1.74	0	- .63	0	-2.76
	56.58	0	2.32	0	- .80	0	-3.5
	60	0	2.58	0	- .91	0	3.79
	73.55	0	4.26	0	1.28	0	5.65

APPENDIX 5.7.c.

RESULTS: VARIABLE PIN ANGULATION

MODEL	PIN ANGLE TEST NO.	DISPLACEMENT (mm) X	Y	Z	ROTATION (degrees) X	Y	Z
2	1	0	-1.9	0	- .63	0	-2.29
	2	0	-1.57	0	- .60	0	-1.36
	3	0	-1.72	0	- .64	0	-1.71
	4	0	-1.89	0	- .64	0	-2.1
	5	0	-1.76	0	- .59	0	-1.79
	6	0	-1.65	0	- .60	0	-2.1
3	1	0	-1.89	0	- .63	0	2.29
	2	0	1.6	0	- .59	0	1.42
	3	0	1.69	0	- .62	0	1.5
	4	0	1.76	0	- .61	0	2.1
	5	0	1.71	0	- .64	0	1.7
	6	0	1.89	0	- .64	0	2.08
4	1	0	-2.33	0	- .8	0	3.5
	2	0	-1.92	0	- .75	0	2.09
	3	0	-2.08	0	- .77	0	2.25
	4	0	2.19	0	- .76	0	3.23
	5	0	2.12	0	- .8	0	2.6
	6	0	2.33	0	- .8	0	3.2

APPENDIX 5.7.d.

RESULTS: OFFSET OF THE PINS FROM THE FRACTURE SITE

MODEL	Test No.	Distance between inner two pins L	DISPLACEMENT (mm) X	Y	Z	ROTATION (Degrees) X	Y	Z
2	I	90	0	-1.9	0	- .63	0	-2.2
	II	124	0	-2.9	0	-..67	0	-2.5
	*III	107	0	-2.72	0	- .65	0	-2.5
	* IV	107	0	-2.03	0	- .66	0	-2.3
3	I	90	0	-1.89	0	- .63	0	-2.2
	II	124	0	-2.91	0	- .66	0	-2.5
	*III	107	0	-2.71	0	- .64	0	-2.5
	* IV	107	0	-1.99	0	- .65	0	-2.2
4	I	90	0	-2.32	0	- .80	0	-3.5
	II	124	0	-3.55	0	- .84	0	-3.8
	*III	107	0	-3.36	0	- .81	0	-3.7
	* IV	107	0	-2.3688	0	- .81	0	-3.4

APPENDIX 5.7.e.

RESULTS: SERIES A. VARIABLE DIAMETER OF STAINLESS STEEL FIXATOR BAR

MODEL	BAR Ø (mm)	DISPLACEMENT (mm) X	Y	Z	ROTATION (degrees) X	Y	Z
2	9	0	-1.91	0	- .67	0	-2.35
	9.67	0	-1.9	0	- .63	0	-2.29
	10.63	0	-1.94	0	- .58	0	-2.3
	11.6	0	-1.93	0	- .52	0	-2.27
	12.67	0	-2.15	0	- .33	0	-2.48
	15.0	0	-2.15	0	- .33	0	-2.5
3	9	0	-1.92	0	- .67	0	-2.35
	9.67	0	-1.89	0	- .63	0	-2.29
	10.63	0	-1.93	0	- .57	0	-2.31
	11.6	0	-1.97	0	- .5	0	-2.33
	12.67	0	-1.98	0	- .46	0	-2.33
	15.0	0	-2.3	0	- .28	0	-2.63
4	9	0	-2.30	0	- .84	0	3.5
	9.67	0	-2.32	0	- .8	0	3.5
	10.63	0	-2.31	0	.74	0	3.45
	11.6	0	-2.3346	0	- .66	0	-3.34
	12.67	0	-2.395	0	- .60	0	-3.46
	15.0	0	-2.66	0	.43	0	-3.71

APPENDIX 5.7.e.

RESULTS: B. VARIABLE SECOND MOMENT OF AREA FOR A STAINLESS STEEL FIXATOR BAR

MODEL	BAR TYPE	DISPLACEMENT (mm) X	Y	Z	ROTATION (Degrees) X	Y	Z
2	Solid Rod	0	-2.15	0	- .33	0	-2.5
	Tube	0	-1.93	0	- .54	0	-2.24
	Square Tube	0	-2.05	0	- .44	0	-2.37
3	Solid Rod	0	-2.3	0	- .28	0	-2.63
	Tube	0	-1.92	0	- .56	0	-2.07
	Square Tube	0	-2.116	0	- .43	0	-2.44
4	Solid Rod	0	-2.66	0	- .43	0	-3.71
	Tube	0	-2.3509	0	- .68	0	-3.38
	Square Tube	0	-2.5693	0	- .57	0	-3.57

Dimension of Bar Type

Circle $\emptyset = 15$ mm

Circular Tube $D_O = 15$ mm $D_I = 13$ mm

Square Tube $L_O = 15$ mm $L_I = 13$ mm

APPENDIX 5.7.f : RESULTS

Changes in fracture size motion due to s variable bar length

		Displacement mm.			Rotation (Degrees)		
Model	Test	X	Y	Z	X	Y	Z
2	1	0	2.9	0	.67	0	2.54
	2	0	3.26	0	.56	0	2.82
	3	0	2.72	0	.65	0	2.54
	4	0	2.03	0	.66	0	2.3
3	1	0	2.91	0	.66	0	2.56
	2	0	3.13	0	.53	0	2.73
	3	0	2.71	0	.64	0	2.53
	4	0	1.99	0	.65	0	2.25
4	1	0	3.55	0	.84	0	3.83
	2	0	3.86	0	.87	0	4.09
	3	0	3.36	0	.81	0	3.74
	4	0	2.37	0	.81	0	3.49

Central Bar length

Test 1 114 mm

Test 2 124 mm

Test 3 97 mm

Test 4 97 mm

APPENDIX 5.7.h.

RESULTS : THE EFFECT OF CHANGE IN POSITION OF THE FRACTURED LIMB

MODEL	POSITION	DISPLACEMENT (mm) X	Y	Z	ROTATION (Degrees) X	Y	Z
2	A	0	-1.9	0	-.63	0	2.29
	B	-3.55	0	- .06	0	+1.54	0
	C	+ .2	- .06	0	0	0	- .21
	D	+ .2	0	+ .002	0	- .08	0
3	A	0	-1.89	0	-.63	0	2.29
	B	3.54	0	.0526	0	1.54	0
	C	+ .1965	- .0563	0	0	0	.21
	D	.2029	0	.0015	0	- .08	0
4	A	0	-2.33	0	-.8	0	-3.5
	B	3.54	0	- .055	0	1.53	0
	C	+ .2984	- .0618	0	0	0	- .31
	D	+ .2434	0	+ .002	0	.086	0

A Supine lying - straight leg raise

B Standing on leg with an unstable fracture

$$F = \frac{B.W.}{2}$$

C Side lying - fractured leg abducted

D High sitting - non wieght bearing

APPENDIX 5.8

VARIABLE BAR DIAMETER

Values of torsion and bending moments at the proximal end of the bar.

MODEL	BAR DIAMETER	TORSION MOMENT N/mm	BENDING MOMENT N/mm
2	9	1144.5	+3835.22
	9.67	1152.78	+3888.42
	10.63	1146.79	+4049.23
	11.6	1149.26	+4096.2
	12.6	1152.23	+4364.34
	15.0	1152.23	+4680.84
3	9	1141.09	3848.49
	9.67	1145.76	3874.16
	10.63	1151.68	4041.83
	11.6	1142.82	4196.74
	12.6	1146.87	4259.14
	15.0	1154.53	5017.75
4	9	1384.33	5432.88
	9.67	1405.92	5595.31
	10.63	1394.21	5592.25
	11.6	1397.19	5765.33
	12.6	1394.08	5979.5
	15.0	1410.46	6635.88